Philosophiae Doctor (PhD)
Thesis 2020:60

Dietary influence on intestinal microbiota and immune responses in mice - roles of high-fat diet and reactive oxygen species (ROS)

Effekter av kosthold på tarmmikrobiota og immunrespons i mus – hva er rollene til høy fettdiett og reaktive oksygenforbindelsen (ROS)?

Sérgio Domingos Cardoso da Rocha

Dietary influence on intestinal microbiota and immune responses in mice - roles of high-fat diet and reactive oxygen species (ROS)
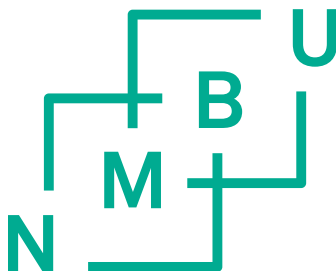
Effekter av kosthold på tarmmikrobiota og immunrespons i mus – hva er rollene til høy fettdiett og reaktive oksygenforbindelsen (ROS)?

Philosophiae Doctor (PhD) Thesis

Sérgio Domingos Cardoso da Rocha

Norwegian University of Life Sciences
Faculty of Chemistry, Biotechnology and Food Science

Ås 2020

PhD Supervisors

Professor Harald Carlsen
Faculty of Chemistry, Biotechnology and Food Science
Norwegian University of Life Sciences
Ås, Norway

Doctor Anders Kielland
Faculty of Chemistry, Biotechnology and Food Science
Norwegian University of Life Sciences
Ås, Norway

Evaluation committee

Head of research, Dr. philos, Lise Madsen
IMR, Institute of Marine Research
Bergen, Norway

Associate professor, PhD Robert Caesar
University of Gothenburg,
Gothenburg, Sweden

Associate professor, PhD, Bjørge Westereng
Faculty of Chemistry, Biotechnology and Food Science,
NMBU, Ås, Norway

"What makes the desert beautiful,
said the little prince,
is that somewhere it hides a well"

- Antoine de Saint-Exupéry

Table of Contents

Acknowledgments

First of all, I want to thank my supervisors **Harald Carlsen** and **Anders Kielland.** Thanks for guiding me and showing me a new version of real science, full of obstacles, fights, struggles and achievements. I learned a lot during these years and I believe I equipped myself with the best of each of you to tackle my future work. With you, I learned way more than what is written in this thesis.

I want to give a warm thanks to all the people at NMBU that helped me in one way or the other during my endless hours in the lab. Thanks for all the coffee breaks, nice talks and for all the tips and tricks to solve my problems. Thanks to my colleagues, especially to **Chrysa**, **Henrietta**, **Kasia**, **Silje**, **Stine, Navreet, Vladana** and **Yke** for all the help and support when I really needed it. A special thanks to **Anne Mari**, **Dimitris** and **Lars Fredrik** for being there every day, to discuss science or simply listen to my frustrations and complains. Thanks for all the good moments! Anne Mari and Dimitris: thanks for being there during the writing process, a tough period when I sometimes lacked creativity and confidence. I am sorry in advance if I am not there to support you as much as you supported me. Of course, I could not forget to mention all my colleagues from SoDoC. It was a great opportunity to meet people from around the world, different fields and backgrounds during the four years I was on the board. A special thanks to **Conny**, **Pablo**, **Sara** and **Victoria** for being such a good inspiration, help and kind of a family at NMBU. I hope this friendship holds for many many years.

I am also glad that several people outside NMBU helped me to get here. Thanks to my **good old friends from Portugal** that, even after being apart for 10 years, were always there supporting me and constantly asking "Are you finished yet?". Thanks for making my forced home-office much easier. Thanks also to my friends in Norway that were always there, and I am sure will still be in the future. Special thanks to **Alina**, **Bojan**, **Ingrid**, **Marta**, **Milan**, **Mari Elisa** and **Telma** for the nice talks about life, parties, trips and random things. Thanks for asking me all the time how I am doing in the PhD progress and then change the topic, because our friendship is more than that.

Last but not least, a HUGE thanks to my partner in crime and best friend **Ronnie.** Thanks for being there since day 1. Thanks for keeping up with my mood and grumpiness. You made me relativize all problems and realize that they were not "that big". Thanks for listening to my complaints, even the nonsensical ones - but you knew I just needed to put them out there! Thanks for rooting for me all the time, making me smile and believing in myself. I hope after you "read" this thesis you realize that my work was not just sacrificing mice. I did way more than that!

Finally, Obrigado to my family and especially to my **parents**, **sister** and **Rita**! Thanks for all the love and support. Thanks for believing in me and for the simple things, like asking about my day. Thanks for everything! I mean it! Rita, if you ever consider taking a PhD, speak with me first. I have some grownup stuff to tell you.

Thank you all!

Summary

The gastrointestinal tract harbors trillions of bacteria. Host and microbiota co-evolved in a mutualism relationship with a certain degree of dependency, where the host provides a nutrient-rich environment and benefits from microbiota metabolism. While the intestinal epithelial layer needs to be thin enough to allow the passage of nutrients, it is also the primary defense barrier in the intestine to prevent the passage of undesired material, such as pathogens.

The immune system has evolved in the direction to tolerate beneficial bacteria and avoid the overgrowth of harmful ones. A balanced and diverse microbiota, and a continuous interaction with the immune system, are the key to the intestinal homeostasis. Although host genetics and environment are relevant, diet is an obvious modulating factor for microbiota composition and by consequence in regulating the immune response and host metabolism.

This thesis presents studies where diet proves to have a relevant effect on microbiota modulation and how microbiota-dependent mechanism affects the host.

In paper I, we fed mice with a low-fat diet (LFD) and a high-fat diet (HFD). We performed a long-term experiment; both diets were lacking soluble fibers, to avoid it as a cofounder; we analyzed the small intestine in the different sections, and not as a whole; and we included microbiota sequencing associated with reactive oxygen species (ROS) as part of ours analysis. The microbiota in mice fed HFD shifted towards dysbiosis and the affected gut barrier allowed the passage of bacteria into the lamina propria. We also observed the activation of immune response pathways related to the presence of pathogens, increased production of pro-inflammatory cytokines and increased ROS production along the intestine.

Paper II was an extension of the previous study, where mice fed HFD received different dosages of coffee representing low and moderate coffee consumption by humans. Results suggested that coffee attenuates the microbial dysbiosis caused by HFD in a dose-depended matter for some bacterial groups. In fact, moderate coffee group presented a microbiota profile more similar to mice fed LFD. Immune response and ROS production were also ameliorated by coffee, indicating the restoring of the gut barrier.

In paper III, we demonstrated that the production of ROS by epithelial cells in ileum plays an important role in the intestinal homeostasis. The number of microbiota in the ileum is larger than in the rest of the small intestine, possibly due to its proximity to the large intestine. In mice deficient in iNOS and NOX1, peroxynitrite production in the ileum was diminished and the bacterial load was increased, with a composition resembling cecum. The ROS production in ileum may therefore be of relevance to prevent bacterial reflux from the large intestine and regulate bacterial community.

Lastly, in paper IV, we sought to understand in more detail the role of NOX1 in the colon. Under infection, pro-inflammatory cytokines activate NOX2 to enhance the production of peroxynitrite. However, during low-grade inflammation, it is plausible that NOX1 is the primary source of peroxynitrite. We used a low dose of DSS to induce low-grade inflammation in the colon of wild type mice and mice deficient in NOX1. In the absence of NOX1, we observed a reduced peroxynitrite production, a mildly increased inflammatory response and a microbial profile characteristic of pro-inflammation. We therefore propose that NOX1 has a role in shaping the colonic microbiota, which may have a consequence for intestinal health.

Sammendrag

Tarmen er vert for trillioner av bakterier. Gjennom evolusjonen har vert og bakterier utviklet seg i et mutualistisk samliv hvor verten bidrar med et næringsrikt miljø og drar nytte av bakterienes metabolisme. Mens tarmepitellaget må være tynt nok til at næringsstoffer kan passere, virker det også som en primær forsvarsbarriere i tarmen for å forhindre passasje av uønskede molekyler og for eksempel patogene bakterier.

Immunsystemet har utviklet seg til å tåle gunstige bakterier og unngå overvekst av skadelige. Et balansert og mangfoldig mikrobielt miljø, og en kontinuerlig interaksjon med immunforsvaret, er nøkkelen til en sunn tarm og homeostase. Selv om vertsgenetikk og miljø er relevant, er kosthold en åpenbar modulerende faktor for mikrobiotasammensetning og en utløsende faktor for å regulere immunresponsen og vertsmetabolismen.

Denne oppgaven presenterer studier der kosthold viser seg å ha en relevant effekt på mikrobiota-modulering og hvordan mikrobiota-avhengig mekanisme påvirker verten.

I artikkel I ble mus matet med en lav-fett diett (LFD) og en høy-fett diett (HFD). Dette var et fôringsforsøk som pågikk i 18 uker; begge diettene manglet løselige fibre for å unngå inklusjon av konfunderende faktorer; vi analyserte tynntarmen i de forskjellige seksjonene, og ikke som en helhet; og vi inkluderte mikrobiotasekvensering assosiert med reaktive oksygenarter (ROS) som en del av vår analyse. Mikrobiotaen hos mus som ble gitt HFD ble forskjøvet mot dysbiose, og den berørte tarmbarrieren tillot passasje av bakterier inn i lamina propria. Det ble også observert aktivering av immunresponsveier relatert til tilstedeværelse av patogen, økt produksjon av pro-inflammatoriske cytokiner og økt ROS-produksjon langs tarmen.

Artikkel II var en forlengelse av det studiet beskrevet i artikkel I, der mus som ble fôret med HFD fikk forskjellige doser kaffe som representerte lavt og moderat kaffeforbruk av mennesker. Resultatet antydet at kaffe demper mikrobiell dysbiose forårsaket av HFD noen bakteriegrupper. Gruppen som ble gitt moderat doser resulterte i en mikrobiota-profil mer lik mus på en LFD. Immunrespons og ROS-produksjon ble også forbedret med kaffe, noe som indikerte gjenoppretting av tarmbarrieren.

I artikkel III demonstrerte vi at produksjon av ROS epitelceller i ileum spiller en viktig rolle i tarmhomeostasen. Antallet mikrobiota i ileum er større enn i resten av

tynntarmen, trolig på grunn av dens nærhet til tykktarmen. Hos mus med mangel på iNOS og NOX1, ble peroksynitrittproduksjonen i ileum redusert og bakteriebelastningen ble økt, med en bakteriell sammensetning som lignet det vi fant i cøkum. ROS-produksjonen i ileum kan derfor være av relevans for å forhindre refluks fra tykktarmen og regulere bakteriesamfunnet.

Til slutt, i artikkel IV, prøvde vi å forstå rollen til NOX1 i tykktarm i en tilstand vi karakteriserte som en lavgradig betennelse. Under infeksjon aktiverer pro-inflammatoriske cytokiner NOX2 for å øke produksjonen av peroksynitritt. Ved svak betennelse er det imidlertid sannsynlig at NOX1 er den primære kilden til peroksynitritt. Vi brukte en lav dose med DSS for å indusere lavgradig betennelse i tykktarmen hos villtype-mus og hos mus som var mangelfulle for NOX1. Vi Det ble observerte en endring i peroksynitrittproduksjonen og mangel på en kompensasjonsmekanisme i fravær av NOX1. Mus som manglet NOX1 viste en liten, men økt betennelsesrespons og dysbiotisk mikrobiota-profil.

Abbreviations

AMPs	Antimicrobial peptides
APCs	Antigen presenting cells
CD	Cluster of differentiation
CGA	Chlorogenic acid
CONV	Conventionalized germ-free (mice)
DSS	Dextran sodium sulfate
F:B	*Firmicutes/Bacteroidetes*
GI	Gastrointestinal
GF	Germ-free
HFD	High-fat diet
IECs	Intestinal epithelial cells
IgA	Immunoglobulin A
KO	Knock-out
LFD	Low-fat diet
LP	Lamina propria
LPL	Lipoprotein lipase
LPS	Lipopolysaccharides
PGNs	Peptidoglycans
PPs	Peyer's patches
PRRs	Pattern recognition receptor
PUFAs	Polyunsaturated fatty acids
ROS	Reactive oxygen species
SI	Small intestine
SFAs	Saturated fatty acids
SCFAs	Short chain fatty acids
Th	T helper cell
TJs	Tight junctions
WAT	White adipose tissue
WT	Wild type

List of papers

PAPER I

Small intestine microbiota and immune status in high-fat dieting mice.

Rocha S.D.C., Kielland C., Harvei S., Carlsen H., Kielland, A.

Manuscript

PAPER II

Coffee consumption in moderate doses attenuates microbial dysbiosis and inflammation induced by high-fat feeding in mice.

Rocha S.D.C.*, Kielland C.*, Harvei S., Carlsen H., Kielland, A.

Manuscript

PAPER III

iNOS-and NOX1-dependent ROS production maintains bacterial homeostasis in the ileum of mice.

Matziouridou C., **Rocha S.D.C.**, Haabeth O.A., Rudi K., Carlsen H., Kielland, A.

Published in Mucosal Immunology (2018)

doi: 10.1038/mi.2017.106

PAPER IV

NOX1 regulates colonic microbiota and gut defense following DSS-induced low-grade inflammation in mice

Herfindal A.M.*, **Rocha S.D.C.***, Papoutsis D., Bøhn S.K. Carlsen H.

Manuscript

*Shared first author

x

Introduction

A plethora of studies has demonstrated the importance of microbiota for host health. Food intake and dietary habits have proven to manipulate the intestinal microbiota, which is associated with metabolism and the immune system. An unbalanced microbiota can prompt the development of metabolic-related diseases and initiate an immune response. In fact, some disorders could be earlier diagnosticated based on characteristic microbiota profiles. However, such mechanisms are not yet fully understood. In this regard, it is important to scrutinize the interaction between diet and diseases, by taking into consideration the interaction between microbiota and immune system as a relevant factor for the development and prevalence of non-communicable diseases.

This introductory chapter situates the present thesis in current scientific development. It is presented the motivation for this research, based on the interaction between diet, microbiota and immune system. Paper I and II present the effect of diet in the microbiota community and consequent immune response, associated with the host health; paper III and IV seek to understand the role of reactive oxygen species produced by the host and its interaction with microbiota and contribution for intestinal homeostasis.

The Gastrointestinal system

The main function of the Gastrointestinal system (GI system) is to digest and absorb nutrients, water and electrolytes from ingested food and discard undigested material, bacterial debris and other undesired products. The GI system is composed of the GI tract, a group of hollow organs spanning from the mouth to the anus, and accessory organs such as the liver, pancreas and gall bladder. The small and large intestine compose most of the GI tract's length and they are located intraperitoneally in the abdominal cavity. Its extensive length and luminal contact surface provide the necessary transit time and approximation for effective digestion and absorption of nutrients. In addition, the several accessory organs, such as the liver, gall bladder and pancreas contribute to the regulation and execution of the digestive process. The GI system also interacts with other systems such as the circulatory and lymphatic systems. They ensure that absorbed

compounds from the gut reach the rest of the body [1]. In this work, when mentioning the GI tract, I will focus on the small intestine and colon.

The small and large intestine

The small intestine is responsible for digestion and uptake of nutrients and is divided into three regions: duodenum, jejunum and ileum. Following the first part of digestion in the mouth and stomach, food in the form of chyme reaches the duodenum through the pyloric sphincter. Here, bile from the gall bladder, and digestive enzymes from the pancreas are mixed with the chyme to form a suspension of small particles available for further enzymatic degradation. The pH is increased by bicarbonates produced by the pancreatic ducts, which activate several pro-enzymes involved in the hydrolysis of long and complex molecules made small enough to be absorbed by epithelial cells, such as monosaccharides, amino acids and fatty acids. [1].

Absorption occurs mostly in the jejunum, where surface folds, villi and microvilli increase the surface area. Lining microvilli in the villi tips, there are several membrane-bounded hydrolases, known as brush border enzymes and also specialized transporters for the uptake of nutrients. The last part of the SI, ileum, has fewer folds and less frequent and shorter villi. The ileum is less involved in the absorption of nutrients but more engaged in selective absorption of specific compounds, such as vitamin B12 and bile acids [1].

Absorbed nutrients in the small intestine are transported through blood or lymphatic system, depending on its size and solubility. Commonly, water-soluble nutrients are transported directly to the liver via the portal vein, whereas lipids and lipid-soluble vitamins are transported in lymphatic vessels using chylomicrons as vehicles and later drained into the blood at the thoracic duct [1].

Between ileum and the large intestine, the ileocecal valve contributes to the unidirectional movement of the chyme into the colon and has an important role in avoiding the flow of colonic bacteria back into the ileum [1].

The large intestine includes the cecum, appendix, colon, rectum and anus. The appendix has been considered an evolutionary remnant, and it is suggested that it works

as a harbor for symbiotic gut microbiota and can re-inoculate the gut with normal gut-flora following e.g. gastrointestinal infections [2].

The colon is less involved in nutrient absorption than the small intestine. There are no villi on its surface and the colon wall is thicker. Once in the colon, water is absorbed from the indigestible material and other debris to form harder stools. At the end of the colon, rectum and anus are responsible for controlling the release of feces [1].

Gastrointestinal wall structure

Along the GI tract, from the stomach to the rectum, the GI wall has an overall similar structure. It is formed by three distinct layers: mucosa, submucosa and the serosa, each with specialized functions (**figure 1**). The mucosa is facing the lumen and consists of a thin sheet of epithelium and the underlying lamina propria (LP). The epithelium is a single layer of columnar epithelial cells, with an apical side facing the lumen and a basolateral side in contact with the underlying LP. This orientation keeps the polarity of the cells which is important for the absorption and secretion processes. The LP is composed of loose connective tissue rich in immune cells, myofibroblasts, nerve endings and blood vessels. Further, the mucosa also contains a layer of smooth muscle cells named muscularis mucosa primarily involved in moving villi in the small intestine. Below the mucosa is the submucosa, composed of connective tissue and a complex network of neurons forming the enteric nervous system. Next, we have two layers of smooth muscle cells (muscularis propria) with enteric neurons (myenteric nerve plexus) in between to secure regulation and coordination of the intestine. The muscular layer closer to the lumen is formed by circular muscle fibers and in the second layer fibers are organized longitudinally. Together, they are able to produce complex motility patterns such as chyme mixing, to allow absorption of nutrients, and synchronized contractions to move intestinal content in the proximal to distal direction.

The most external layer, serosa, is formed by loose connective tissue and coated by mucus to prevent any mechanical injury when in contact with other organs. Finally, the abdominal cavity is enclosed by the peritoneum which folds around the organs forming the mesentery. Together, they support the GI tract and adjacent organs and supply the tissues with blood, lymph and nerves [1].

Small intestine   *Colon*

Enterocyes   Paneth cell
Goblet cell   Stem cell

Mucus layer

Epithelium

Mucosa

Lamina propria

Muscularis mucosa

Submucosa — Submousal nerve plexus

Muscularis propria

Circular muscle

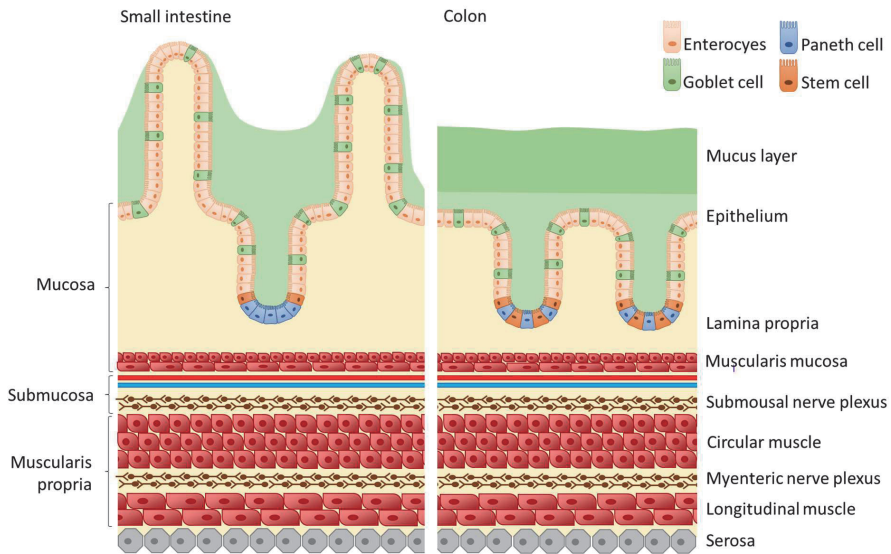Myenteric nerve plexus

Longitudinal muscle

Serosa

Figure 1 – Representation of the main epithelial cells and structure of the gastrointestinal wall in the small intestine and colon. Main layers names on the left and sub-divisions on the right. Inspired by illustrations in Barret 2007 [1] and Peterson et al. *2014 [4].*

The epithelium

The organization of the intestinal epithelial cells (IECs) layer varies between the small intestine and colon (**figure 1**). The small intestine surface is composed of both crypts and villi, finger-like structures that extend into the lumen, while in colon there are only crypts. The epithelium surface in both segments is mostly composed of enterocytes and goblet cells, involved in the absorption of nutrients and secretion of mucus, respectively. At the apical side of epithelial cells, there are membrane protrusions formed by actin filaments, making the microvilli, which increase the contact surface with the lumen. Additionally, Paneth cells, stem cells and enteroendocrine cells make up the epithelial cell layer, but with specialized functions. Both Paneth cells and stem cells are located at the bottom of the crypts. Paneth cells produce and secrete antimicrobial peptides and stem cells are undifferentiated epithelial cells that will divide, migrate upwards towards the lumen and differentiate into all the different epithelial cells. Enteroendocrine cells produce and secrete hormones involved in the

regulation of digestion, creating a link between the central and enteric neuroendocrine systems [3, 4].

Adjacent IECs are kept close to each other by several anchoring structures such as tight junctions (TJ), desmosomes and gap junctions. TJs are a complex of proteins located in the apex of the epithelial cells and form a seal in order to regulate and restrict paracellular movement of water, solutes and bacteria or bacterial products. Therefore, these protein complexes have a crucial contribution to the intestinal barrier function [5, 6]. The four types of TJs (occludin, claudins, junctional adhesion molecule and tricellulin) are linked to an intracellular macromolecular complex known as zonula occludens, which work as a bridge between TJs and the actin cytoskeleton of the cells and other signaling proteins. Factors that promote the disruption of the TJs seal such as inflammation or pathological conditions, increase the permeability of the TJs and facilitate the passage of microbiota and other undesired material into the lamina propria triggering an immune response [5, 6].

In both the SI and colon, IECs are covered by mucus produced by goblet cells. Mucus is formed by glycoproteins, called mucins, organized in a dense net-like insoluble structure. There are several types of mucins and they are classified depending on their function. Transmembrane mucins lay on the top of the enterocytes and are involved in intracellular signaling. Gel-forming mucins build up the skeleton of mucus and prevent bacteria to reach the IECs. In fact, 80% of the mucin biomass is composed mostly of O-linked glycans [7]. MUC2 is the main mucin produced in the intestine and it is stored in vesicles inside of the goblet cell [8]. Mucus is continuously secreted into the lumen by exocytosis through the apical part of the cell. However, in a stressful situation, most of the vesicles fuse with each other in tandem and large amounts of mucus are released, leaving the goblet cell empty and with its cytoplasm exposed, a process known as compound exocytosis [8, 9].

The mucus composition and thickness differ significantly between the SI and the colon. The SI has a single mucus layer with a rather porous structure. The porous structure in the SI allows nutrient uptake, however, it increases the vulnerability of the IECs for bacterial infiltration. In the colon, the mucus layer is 200μm thick [10] and divided into two different layers. The outer mucus layer is loose and harbors most of the commensal bacteria. The inner layer is dense and compact to prevent bacterial

penetration. Its constant renewing is important to keep the intestinal homeostasis. It avoids bacterial overgrowth and reduces the proximity between IECs and bacteria, which are removed by distal transport. Johansson *et al.* observed that the complete regeneration of the 50μm thick inner mucus layer in the distal colon in mice takes only one hour [11]. Moreover, in the opening of colonic crypts, there are specialized Goblet cells known as sentinel goblet cells. In the presence of pathogens, these cells can initiate an inflammatory response to the adjacent goblet cells in order to increase mucus release and flush out a possible invader [12].

Gut Microbiota

The human gastrointestinal (GI) tract holds a diverse microbiota composed of an array of bacteria, viruses, fungi and archaea, where bacteria dominate. It is estimated that ~30-40 trillion bacteria reside in the colon [13]. Colonization of the GI-tract starts at birth, and the exposure of bacteria is dependent on whether the new-born is vaginally delivered or born by cesarean section. Vaginal delivery exposes the baby to both fecal and vaginal bacteria, including *Lactobacillus, Bifidobacterium* and *Enterobacteriaceae* [14] whereas caeserean delivered babies are exposed to skin microbiota and hospital environment [15]. After birth breast milk is the major factor for determining colonization until weaning by providing bacteria, nutrients and immune modulators. Breast milk bacteria include facultative anaerobes of the genus *Streptococcus* and *Staphylococcus*, which also create a favorable environment for the colonization of strict anaerobes, such as, *Bacteroides*, *Clostridium* and *Bifidobacterium* [16]. Moreover, breast milk is abundant in complex oligosaccharides, with prebiotic properties for the bacteria already present. Breast milk is also rich in immunoglobulin A (IgA) specific for the environment in which the mother and baby live, and finally, it contains proteins that can exclude potentially pathogenic bacteria (e.g. lactoferrin). Therefore, the duration of lactation or the use of formula is a key factor for the microbiota composition in the first months [17]. After weaning microbiota diversity increases particularly due to the introduction of solid diet. Thus, by the end of the first year, the microbiota of an infant becomes relatively stable and it is more or less similar to an adult. Later on, not only the diet but host genetics and environment are relevant factors for gut microbiota modulation. Simple factors as the number of close family members or the geographical location can shape the microbiota into an individual profile. [16, 18].

The GI tract of an adult contains bacteria from at least 1000 species, where the average number in humans is approximately 150-200 species per person [19]. The dominant phyla are *Bacteroidetes* and *Firmicutes*, followed by *Proteobacteria*, *Actinobacteria* and *Verrucomicrobia* [18, 20]. The amount of gut microbes increases dramatically throughout the GI tract from only a few bacteria per mL in the stomach to 10^{11-12} bacteria/mL in the colon. The SI experiences a gradual increase from the duodenum into the ileum [21]. The diversity of the microbiota also increases along the GI tract and its composition is region-specific (**figure 2**) [18, 20, 22].
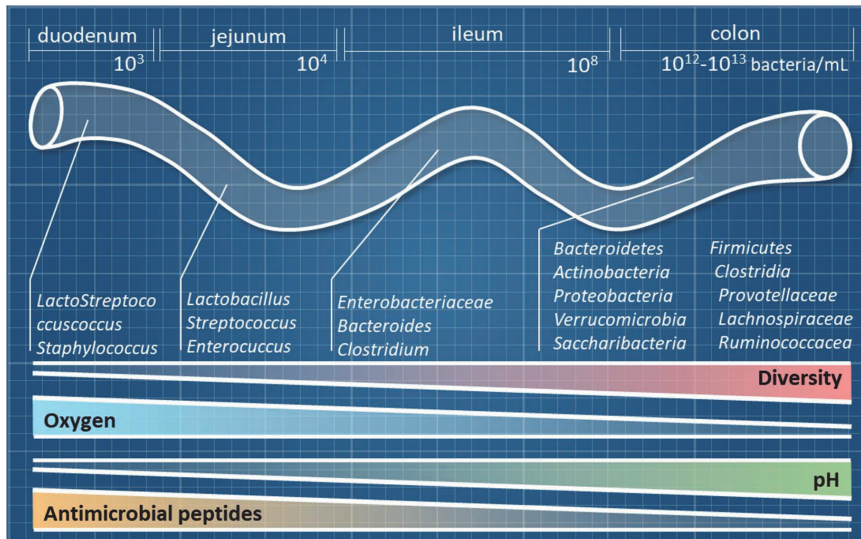
Factors such as oxygen concentration, the transit time of lumen content, mucus layer thickness and composition, pH and antimicrobial peptides determine the number and the bacterial profile in each section (**figure 2**). The SI has higher concentrations of oxygen in the proximal part, more production of antimicrobial peptides (AMPs) and the environment is more acidic. These conditions favor the growth of facultative anaerobic bacteria and shape the bacterial content in different parts of the SI. Cecum and colon are very low in oxygen content, have a more basic environment, contain more undigestible nutrients and have a longer transit time and a thicker mucus layer. These factors favor the growth of a large number of obligate anaerobic bacteria [20]

The microbiota composition differs between individuals and between regions and countries. It has been proposed that gut microbiota be classified according to their enterotypes; *Prevotella*, *Ruminococcus* and *Bacteroides*, which can form a stable group of bacteria shared by humans [23]. These enterotypes might be driven by diet and are able to use different routes of energy to preserve their stability. However, Turnbaugh *et al.* suggest that the idea of a "core gut microbiota" or the term enterotypes might not exist [24]. Instead, they suggest the existence of the "core microbiome", a conserved set

of microbial genes involved in metabolic functions that we all share. By analyzing the metagenome, they found functional groups consistently present across samples. Those groups include relevant metabolic pathways and intestinal secretion systems. The conservation of such genes, rather than bacterial groups as such, suggests that there is a redundancy of the gut microbiome and their importance might be based on their function rather than the species *per se* [24].

Microbiota and relation to disease and health

A balanced and diverse bacterial community is important to keep its own stability as well as keeping the host healthy. Such a community will decrease the chances of colonization of pathogenic microorganisms by competing for space and nutrients [25]. The total number of bacterial cells in the human body is roughly similar to the total number of host cells [21] but the commensal genome can be 10-fold higher, increasing the metabolic flexibility to the host [24, 26]. In fact, there is a correlation between individuals with low bacterial gene richness and the incidence of metabolic diseases [27].

When it comes to microbiota exposition during early life, there are indications that new-borns and young children either deprived or a less exposed have higher risks of developing chronic inflammatory diseases and allergies [28]. Although germ-free mice born and raised in sterile conditions are apparently healthy and able to grow and reproduce without obvious problems, the absence of microbiota affects negatively the proliferation and differentiation rate of IECs. And animals in sterile conditions present an underdeveloped mucosal immune system [1, 29].

Microbiota supports the host metabolism through the production of essential nutrients such as vitamin K and most of B-vitamin group [30]. Secreted bile acids by the liver can be metabolized by colonic microbiota into secondary bile acids before return to the liver [31]. Microbiota is also essential for the production of the short-chain fatty acids (SCFA), acetate, propionate and butyrate, through the fermentation of complex carbohydrates indigestible to the host, like dietary fibers [32]. In a situation with reduced dietary fiber, some microbiota can indeed switch their energy source and degrade the colonic mucus layer instead, inducing colonic inflammation and enhanced

susceptibility to pathogen colonization [33, 34]. Moreover, SCFA produced by microbiota influences food intake by the host, energy homeostasis, regulates immune system response [32, 35] and the integrity of the intestinal barrier [25].

Dysbiosis

In the situation of a large shift in microbial composition with concurrent imbalance in community structure, a condition known as dysbiosis can arise. Diet, antibiotic usage, presence of pathogens, low fiber intake or inflammation are potential causes for dysbiosis [36]. Microbiota analysis consistently reports the change of the relative amounts of the two dominant phyla *Bacteroidetes* and *Firmicutes* connected to metabolic disorders [37, 38]. These analyses also reveal a bloom of *Proteobacteria.* There are indications that *Proteobacteria* are involved in glucose homeostasis as Fei *et al.* observed obesity and insulin resistance in germ-free mice that were monocolonized with *Enterobacter cloacae B29* isolated from obese humans [39], but its role in the gut is still uncertain. In a healthy state, members of this phylum are commonly found [18, 20] and between the dominant phyla, *Proteobacteria* is the most unstable, even without showing clinical signs [40]. Thus, Shin *et al.* suggest that the increased abundance of *Proteobacteria* can reflect an unstable structure of the gut microbial community and it should be considered an active mark of disturbance and not a passive consequence [36].

Defense mechanisms in the GI tract

The GI tract is constantly exposed to external factors such as ingested food and pathogens. However, there is only a single layer of IECs separating the external environment and the inside body. This represents a potential entrance for pathogenic microorganisms. At the same time, the GI tract harbors the largest bacterial community in the human body, which have co-evolved in a mutual relationship with the host. Therefore, the immune system has developed several strategies at the GI tract to allow the presence of beneficial bacteria and at the same time preventing the passage of pathogenic organisms or other harmful compounds into the body. In fact, the gut contains approximately 60% of the immune cells present in the human body [22, 41].

Depending on the promptness of the response, duration and specificity, the immune system is categorized in innate and adaptative. The innate immune system serves as first line of defense against foreign agents providing a quick and non-specific immune response, and consists of physical and chemical barriers (mucus, epithelial cells, antimicrobial peptides and proteins) and cellular component including phagocytic and antigen-presenting cells (APCs, dendritic cells and macrophages) and cells with cytotoxic activity (e.g. NK cells). On the other hand, the adaptative immune system is very specific and long-lasting (although slower) with the ability to recognize and remember a foreign material by developing an immunologic memory. The adaptative immunity is mediated by T cells (cellular immunity) and B lymphocytes (antibody-mediated immunity).

The low pH in the stomach is one of the first strategies to decrease the number of viable microorganisms to reach the intestine. In the intestine, the mucus layer and TJs create a physical barrier to reduce the proximity of pathogens with the IECs and avoid the paracellular transport into the lamina propria. Mucus production is regulated by commensal bacteria. Germ-free mice have for instance reduced quality and production of mucus, and it takes up to up to eight weeks to reach a normal mucus structure in the colon after bacterial colonization of germ-free mice [29]. However, some pathogens have developed mechanisms to counteract the mucus barrier and reach the epithelial cell layer, such as the use of flagella (*Salmonella enterica*) or the secretion of mucin-degrading proteases (*Citrobacter rodentium; mouse specific*) [42, 43].

To enhance the mucus barrier and compensate for the lower production of mucus in the SI, production of antimicrobial peptides (AMPs) and immunoglobulin A (IgA) are essential, both with a broad range of actions, creating another challenge for pathogens to reach the epithelium. AMPs such as defensins, cathelicidins and lysozyme-C, are produced by Paneth cells to promote a pathogen-free environment near the epithelial cells [22]. IgA is secreted by plasma cells in the lamina propria and it is transported to the apical surface by transcytosis. Once in the gut, IgA can bind to bacteria both with its variable Fab region of the antibody (canonical binding) or to glycans in the bacteria via its constant region of the antibody (non-canonical binding) [44]. The latter creates bacterial agglutination thus preventing pathogenic bacteria from getting too close to the IECs.

When pathogens come closer to the epithelium, they are recognized by Pattern recognition receptors (PRRs). They are present in both IECs and immune cells in the lamina propria. These receptors recognize essential molecular structures present in microorganisms, known as pathogen-associated molecular patterns (PAMPs). They can be components of the cell wall, such as lipopolysaccharide (LPS) of Gram-negative bacteria or peptidoglycans (PGN), flagellar components or products of pathways that are exclusive to microorganisms, such as fungal B-glucan or viral RNA and DNA [45, 46].

Toll-like receptors (TLRs) and NOD-like receptors (NLRs) are well known PRRs [47]. TLRs are on the cell surface and intracellularly in vesicles or other organelles. The majority of TLRs are involved in signaling and recruiting pro-inflammatory cytokines most commonly via NF-κB activation, but recent research has demonstrated that TLR10 is the only TLR family member that inhibits the inflammation process [48-51]. Perhaps the best studied TLR in the gut innate immune system is TLR4. When activated by a ligand such as LPS, TLR4 activates intracellular signaling events that in most cases lead to an induction of the NF-κB family of transcriptional activators. NF-κB in turn activate gene expression of pro-inflammatory cytokines exemplified by IL-1, TNF-α and IL-6 [48] [49]. Mice with a TLR4 mutation develop an inadequate response to LPS and become highly susceptible to gram-negative sepsis [52].

Nucleotide-binding oligomerization domain-containing protein 1 (NOD1) and NOD2 are present in the cytosol of Paneth cells and macrophages and they are both able to detect PGNs or parts of their degradation products [53-55]. Regarding their sensitivity,

NOD1 is more sensitive to PGN of gram-negative bacteria while NOD2 detects the presence of both gram-negative and gram-positive bacteria [56]. NOD2 expression is regulated by TNF-α and augmented by interferon-gamma (INF-γ), where NOD1 is regulated only by INF-γ and is indifferent to TNF-α [57]. A defect form of NOD1 and NOD2 are linked to inflammatory bowel diseases and increase the vulnerability toward pathogens [58, 59]. NODs and TLRs response systems are parallels and largely independent. However, some synergy between these two families has been observed to provide a larger and more efficient response, most likely in sepsis or overstimulation of the innate immune system [60, 61].

Finally, different populations of cells produce cytokines, peptides involved in intracellular signaling and regulator of the immune response. Cytokines such as tumor necrosis factor-alpha (TNF-α), interleukin (IL) -1, IL-6, IL-18 interferon-gamma (IFNγ) and prostaglandin-endoperoxide synthase 2 (Ptgs2) are classified as pro-inflammatory as they act as triggers for the immune response; whereas IL-10, transforming growth factor-beta (TGF-β) and IL-27 are regarded as anti-inflammatory since they act as repressors. Cytokines can interact in a synergistic or antagonist manner. However, their actions vary with location, concentration, timing and target. The balance between them guarantees an efficient immune response as disruption of this balance could be deleterious to the host [62].

Activation of Immune cells in the gut

The intestinal immune system is strictly organized and regulated to ensure a swift and controlled response towards foreign material. The gut immune system contains both inductive sites and effector sites. The inductive sites are located at the mucosal-luminal interphase, where the initial contact between the gut luminal content and the host immune system takes place. The effector sites are in fact LP, to which antigen-specific immune cells migrate after antigen priming to exert their effector functions. The inductive sites consist of lymphoid tissues and aggregates of immune cells known as gut-associated lymphoid tissues (GALT) including Peyer's patches (PPs), isolated lymphoid follicles (ILFs) and mesenteric lymph nodes (MLNs) [63, 64]. PPs are aggregates of lymphoid follicles, forming a protrusion into the mucosa and present with increasing

density from jejunum to the ileum (fig.3), but are not present in the colon. The sampling of luminal content is carried out by several routes. Specialized enterocytes without microvilli, known as microfold cells (M cells), are located at the epithelial surface of PPs. Their function is to transport substances, such as intact bacteria and antigens, from the lumen to the underlying antigen-presenting and -processing cells (lymphocytes and mononuclear phagocytes) [63-65]. Also dendritic cells residing in the LP are important for sampling luminal antigens by extending dendritic processes into the lumen through the epithelial layer and sample material into the lamina propria without disturbing the epithelium structure [66, 67].

Although not yet fully understood, a goblet cell that is actively secreting mucus can also take-up antigenic material from the lumen and present to dendritic cells in the LP [8]. This route is known as goblet cell-associated antigen passage (GAPs) [68]. Finally, bacteria or other material can also reach the lamina propria through other routes such as paracellular leakage.

After a bacterium or antigen have crossed the epithelium, phagocytic cells, such as dendritic cells and macrophages recognize the threat and can initiate the phagocytosis. Phagosomes resulting from the phaocytosis fuse with other vesicles that reduce its pH and contain reactive oxygen and nitrogen species, antimicrobial proteins and peptides, creating a mature phagolysosome where the destruction of microorganism takes place [69]. However, antigenic peptides can also be preserved and presented on the surface of the phagocytic cell which then becomes an antigen-presenting cell (APC).

The APCs can then migrate from the inductive site, through lymphatic vessels that drain different regions of the intestine, into specific mesenteric lymph nodes. There, antigens are presented to naïve T- and B- cells which can be primed and differentiate into effector cells. These cells are then drained through the lymphatic system and enter the bloodstream through the thoracic duct to return to their effector site (homing) [70] (**figure 3**).
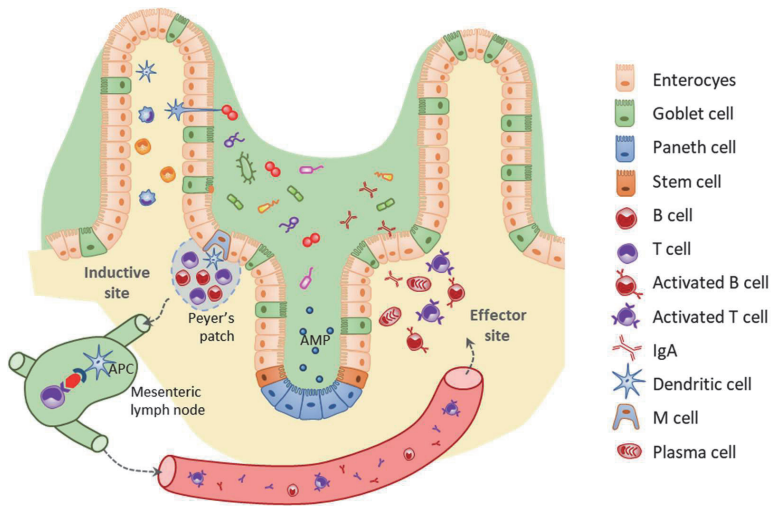
Figure 3. *Activation of immune cells in the gut and homing pathway. Inspired by illustrations in Brandtzaeg* et al. *2008 [64] and Brown* et al. 2013 [22]*.

Activated B cells can differentiate into effector plasma cells producing specific antibodies with the most abundance isotype produced being IgA. B cells call also differentiate into memory cells and remain in circulation, supporting a faster response in the next encounter with the specific antigen. Moreover, antibodies produced by B cells can also mediate the activity of natural killer cells, which are able to destroy microbes or other particles that have been coated with antibodies [70].

Naïve T cells can differentiate into T helper cells, regulatory T cells (Treg) and cytotoxic T cells. The first produces alarm cytokines involved in the activation macrophages, B cells and production of antibodies. Treg cells, as its name indicate, regulate the inflammatory response by suppressing the activity of other T cells through the production of anti-inflammatory cytokines. Cytotoxic T cells, when activated by T helper cells, are also involved in the production of cytokines and capable of creating an immune synapse with a phagocyte cell and release molecules that promote programmed apoptosis [71]. Moreover, there are intraepithelial lymphocytes (T cells) located at the tip of the villi. Although their function is not certain, they may be involved in surveillance and protection against pathogens and supporting healing after injury [72].

Reactive oxygen species

Reactive oxygen species (ROS) are oxygen-derived compounds. Commonly they have a short life span depending on their reactiveness and stability. Hydroxyl radical (HO$^\bullet$) is very reactive and its half-life is 10^{-9}s, and superoxide anion radical (O$_2^{\bullet-}$) has a half-life of 10^{-5}s. On the other side, hydrogen peroxide (H_2O_2), which is less reactive and relatively stable, has a half-life of 10^{-2}-10^{-3}s [73].

Superoxide anion radical is the start-point of several ROS (**figure 4**). In mitochondria, there is a constant production of O$_2^{\bullet-}$ due to incomplete reduction of oxygen to water. To avoid the accumulation of O$_2^{\bullet-}$, both the mitochondria and cytosolic compartment have enzymes that convert O$_2^{\bullet-}$ to less reactive molecules such as H_2O_2 by superoxide dismutase (SOD) and later converted to water by catalase or glutathione peroxidase [73, 74]. However, the production of ROS can also be regulated in order to create an intentional response, such as the respiratory burst in phagocytic cells. In this situation, NADPH-oxidase is crucial as it can reduce O$_2$ to O$_2^{\bullet-}$ that can further react with nitric oxide (NO$^\bullet$) and form peroxynitrite (ONOO$^-$). Alternatively, H_2O_2 formed by SOD can be converted to HO$^\bullet$ in the presence of ferrous ion through the Fenton reaction or converted to hypochlorous acid (HOCl) by myeloperoxidase (MPO) in the presence of chloride [73, 74].
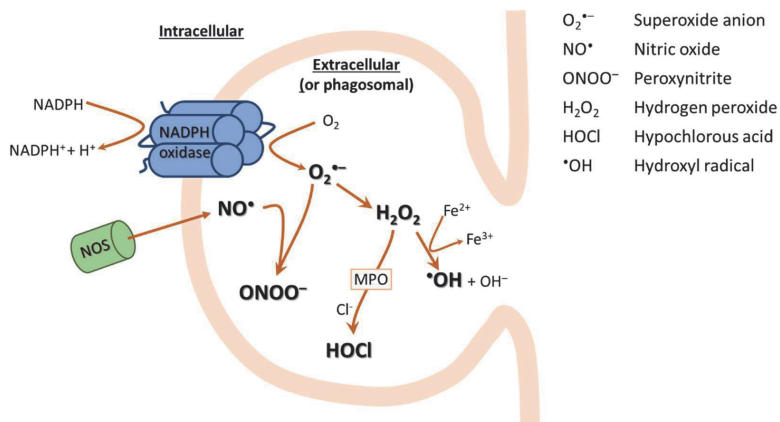

Figure 4 - Reactive oxygen species produced during the oxidative burst.; NOS: nitric oxide (NO) synthase; MPO: myeloperoxidase. Inspired by illustration in Hart et al. [75].

ROS production and their role in GI tract

As mentioned above, besides the electron transport chain, ROS can be also synthesized by transmembrane NADPH oxidases (NOX1-5, DUOX1-2) and nitric oxide synthases (NOSes). NOX1-5 reduces oxygen to $O_2^{\bullet-}$, DUOX1-2 synthesize H_2O_2 and oxidation of L-arginine by NOS produces $NO^{\bullet}$. ROS is in close interaction with the immune system and microbiota [74]. After antibiotic treatment, it was observed a significant decrease of ROS production in the ileum [76] and with complete NOX1-4 KO, mice present much less protective microbiota in the GI tract [73].

NOX1 and DUOX2 are both produced in the epithelium of the GI tract. NOX1 is mostly synthesized in epithelial cells, particularly in ileum, cecum and colon, while DUOX2 is produced along all intestine. NOX2 is expressed by phagocytic cells in the LP, such as macrophages and neutrophils, after engulfing a microorganism [77]. Furthermore, inducible NOS (iNOS) is expressed in epithelial cells of the small intestine, in association with bacterial content, and immune cells such as macrophages and neutrophils. Its synthesis occurs after activation by microbial products [78] or pro-inflammatory cytokines such as TNF-α, IL-1β and INF-γ.

ROS are versatile, they can react with different molecules and their action can change with their location. In the LP, activated phagocytic cells by the presence of pathogens, will produce ROS and kill the invader microorganisms inside of phagosomes, a process known as oxidative burst f. However, also secreted ROS from epithelial cells can affect bacterial viability such as DUOX mediated bacterial killing in Drosophila. In a study from 2005, Ha and coworkers showed that DUOX indeed was crucial for host defence against pathogenic bacteria [79]. In *Caenorhabditis elegans* DUOX-dependent ROS revealed to improve survival during bacterial infections, but no direct antimicrobial property was determined [80]. In mammals, DUOX2 is also reported to act against bacteria as demonstrated during *Helicobacter felis* infection in gastric epithelium with H_2O_2 as a substrate for lactoperoxidase and later formation of hypothiocyanous acid with bactericidal action [81]. NOX1 plays a relevant role in the proliferation of IECs in colonic crypts as a signaling factor [82] or promoting cell growth in the healing process after injury [83]. NOX1 also participate in the defense mechanism, being activated by INF-γ, LPS and flagellin [77]. However, its role in microbiota regulation is uncertain. Pircalabioru *et al.* observed that NOX1 specifically deleted in IECs offered protection

against *Citrobacter rodentium* infection. Further investigation revealed that the absence of NOX1 favored the bloom of probiotics strains such as *Lactobacilli* in comparison to wild type mice with intact NOX1. *Lactobacilli* are known to produce H_2O_2, and the authors hypothesize that lower amounts of these lactobacilli in NOX1 intact mice will offer less antimicrobial protection against pathogenic infections [84].

In an inflammation environment, NOX2 express higher amounts of $O_2^{\bullet-}$ by phagocytic cells to fight invading microorganisms, exceeding the production by NOX1. At the same time, $NO^{\bullet}$ synthesis by iNOS is also increased, that together with $O_2^{\bullet-}$, produce large amounts of the reactive and stable ONOO. Botteaux *et al.* showed that elevated amounts of NOXs decreased the adherence and invasion of pathogenic microbiota [85]. When endogenous ROS was diminished by pharmacological inhibitors, such benefits were canceled [86].

Microbiota and metabolic syndrome

Change of lifestyle in the last decades and the great abundance of energy-rich processed food, together with less fiber consumption, has likely contributed to the increase of diet-related diseases. Obesity, type two diabetes (T2D), cardiovascular diseases and several cancers are chronic diseases related to poor nutrition choices.

Obesity has reached epidemic proportions. In 2016 1.9 billion adults were overweight worldwide, and 650 million were obese (WHO). Obesity is one of the hallmarks of metabolic syndrome, which has a high prevalence in affluent societies. Metabolic syndrome is characterized by a cluster of interrelated disorders associated with obesity, cardiovascular diseases and T2D. Due to the misuse of the term and not applicable to all ethnicities, in 2009 it was developed a set of criteria to determine the metabolic syndrome. It is considered metabolic syndrome when an adult has at least three of following: elevated waist circumferences (country-specific); ≥150 mg/dl triglycerides; < 40 mg/dl HDL-cholesterol in men and <50 mg/dl in women; ≥130/85 mmHg of blood pressure; fasting glucose ≥ 100 mg/dl [87].

In 2004, Bäckhed *et al.* demonstrated a relationship between gut microbiota and fat storage [88]. Germ-free (GF) mice and conventionally raised wild type (WT) mice were both fed with standard chow diet for two weeks. GF mice had significantly less body fat (42%) compared with the other group, even though GF mice had significantly higher food consumption. They then transferred microbiota from conventionally raised mice to GF mice (CONV mice) to see whether this impacted weight gain. After two weeks, CONV mice had similar body fat and food consumption as the conventionally raised mice and also significantly different than the GF mice [88]. Both fasting glucose and insulin levels were increased in CONV mice compared to GF mice, and they observed increased levels of triglycerides, increased expression of genes related to fatty acids *de novo* synthesis and increased uptake of monosaturated fat from the gut in CONV mice than their GF counterpart [88]. Crucially, the team observed that CONV mice had higher levels of lipoprotein lipase (LPL), which is involved in the fatty-acids uptake and storage in adipocytes. At the same time, they found that expression of fasting-induced adipocyte factor (Fiaf), an inhibitor of LPL, was present in much lower values in CONV mice when compared to GF mice. Interestingly, the suppression of Fiaf was observed in the ileal

epithelium, suggesting a direct role by microbiota to suppress Fiaf, with a subsequent increase of LPL and promotion of adiposity [88].

Later, Ley *et al.* studied cecal microbiota in genetically obese (*ob/ob*) mice, lacking functional leptin [37]. Both WT and *ob/ob* mice received the same diet but *ob/ob* mice had a significantly increased weight, associated with higher food intake. Although lean and obese mice have *Bacteroidetes* and Firmicutes as the dominant phyla they observed a significant increase in the *Firmicutes/Bacteroides* (F:B) ratio. Obese mice displayed a 50% decrease of *Bacteroidetes* and a proportional increase of *Firmicutes* [37].

Turnbaugh *et al.* also studied *ob/ob* and WT mice [89]. Mutant mice had higher amounts of *Firmicutes*, increased concentration of butyrate and acetate in their feces as well as less energy in their feces when compared to the lean group. Together, this suggests more energy retention and it could explain the increased body mass in the *ob/ob* mice. The group went further and transplanted cecal microbiota from both mutant and wild type mice to GF mice. Both colonized groups were fed chow diet and had no difference in initial weight and body fat percentage. After two weeks, no differences in food consumption were observed but *ob/ob* recipient mice had a significantly increased percentage in body fat than the WT recipient mice. These results corroborate the hypothesis of Bäckhed regarding the role of microbiota in energy harvest from the diet [88, 90]. Together with host genotype, microbiota contributes to the pathophysiology of obesity, without necessarily changing the food consumption, and such effects were proven to be transmittable through microbiota transplantation [89].

HFD and the effect on gut immunity and gut microbiota

Numerous studies have demonstrated a dramatic effect of a high-fat diet on metabolic syndrome markers, microbiota and gut health. In 2009 Kennedy *et al.* demonstrated that a diet rich in saturated fatty acids (SFA) leads to adipocytes hypertrophy, accumulation of diacylglycerol and ceramide, NF-κB activation and associated inflammation response, decreased PPAR-γ activation and the consequent decrease in oxidation of fatty acids and glucose followed by the recruitment of immune cells to WAT and muscle [91]. How is a high-fat diet-related to microbiota? In a four week study, Tomas *et al.* scrutinized the effect of HFD in cecal and fecal microbiota composition [92]. At the phylum level, HFD

led to a lower amount of *Bacteroidetes* and *Verrucomicrobiota* (mostly genus *Akkermansia*) and a significant increase of *Proteobacteria* (family *Desulfovibrionaceae)*. Lam *et al.* also observed an increase of families *Desulfovibrionaceae, Enterococcaceae, Lachnospiraceae* and *Oscillospiraceae* and a decrease of *Lactobacillaceae* (phylum *Firmicutes*) [93, 94]. La Serre *et al.* observed similar growth of the phylum *Proteobacteria* after HFD consumption for eight weeks [95] as well as Shen *et al.,* suggesting the bloom of *Proteobacteria* (*Bilophila wadsworthia*) [36]. The increase of *Firmicutes* and *Proteobacteria* can occur within 24 hours of intervention [24]. Thus, a general consensus is that HFD leads to an increased ratio between *Firmicutes* and *Bacteroidetes*, and an increase in the abundance of *Proteobacteria*. In addition, a HFD is clearly leading to a less diverse microbiota [96].

In 2007, Cani *et al.* hypothesized that bacteria or bacterial products could be connected to metabolic syndrome through a mechanism referred to as endotoxemia. Bacterial lipopolysaccharides (LPS) are present in the gram-negative bacterial membrane and their concentration in plasma has a diurnal cycle associated with feeding patterns. The consumption of HFD disrupted those patterns, keeping the plasma LPS levels continuously elevated. When LPS was infused into the mouse in low concentrations for four weeks, it led to an increase of the adipose tissue weight and the expression of toll-like receptor (TLR)-4 in adipose tissue and pro-inflammatory cytokines (TNF-α, IL-1β and IL-6) in the liver were increased, when compared to the control group. LPS resembled the effects of HFD and it was considered as a possible trigger for metabolic syndrome [97]. To prove the hypothesis, the authors applied the same chronic LPS infusion in CD14 mutant mice. CD14 aids LPS binding to TLR4 and is thus essential for mediating the effects of LPS in target cells. The effects of LPS regarding the deposit of macrophages in adipose tissue, hypersensitivity of insulin, triglycerides in the liver and production of pro-inflammatory cytokines were blunted in CD14 mutant mice [97].

Later, Cani *et al.* also demonstrated that endotoxemia related to HFD was also connected with gut microbiota [98]. First, HFD had a negative effect on gut permeability, translated in lower expression of epithelial tight junctions (ZO-1 and occludin) and higher levels of LPS in plasma. Then, they treated both chow and HFD fed mice with antibiotics for four weeks. There was an obvious change in the microbiota of both

groups and the effects of HFD in permeability were restored. Furthermore, the antibiotic treatment also reduced adipose tissue inflammation and improved metabolic parameters of T2D and obesity in HFD fed mice, similar effects to *ob/ob* CD14 mutant mice. Then, they concluded that HFD-changed microbiota had an influence on permeability and LPS passage instigated metabolic disorders [98].

Bacteria adherence to intestinal mucosa was also evidently increased after HFD consumption. When fluorescent marked *Escherichia coli* was administered through the oral route, the number of bacteria was 5-10 times higher in the submucosa of mice fed HFD for one week than in chow diet fed mice. After four weeks, when the diabetic state was established, *E. coli* was also detected in mesenteric lymph nodes together with a higher expression of TNF-α. Here, they concluded that bacterial translocation happens even before the development of metabolic syndrome-related diseases and that could be the origin of low-grade inflammation during T2D and obesity [99].

Although LPS in plasma is associated with HFD and possibly caused by increased gut permeability [97] neither the mechanism nor site of passage is clearly understood. Tomas *et al.* observed a 30% increase in transepithelial conductance in ileum after eight weeks of HFD consumption, indicating a disruption of barrier integrity due to the decreased amount of TJs claudin-7 in ileal villi [92]. Hamilton *et al.* also studied the effects of HFD in permeability by measuring both paracellular permeability and transcellular flux [100]. After one week, rats fed HFD showed increased paracellular permeability in both the SI and colon and increased transcellular flux in the colon. With a longer duration of feeding, they actually found increased expression of ZO-1 in the ileum by HFD and improved ileal barrier properties. These results suggest that GI tract vulnerability to HFD is time-dependent and region-specific. Interestingly, both studies observed the restoration of barrier function when animals switched to a chow diet, demonstrating that increased permeability is reversible [92, 100].

However, the type of lipids also plays a significant role in determining the outcome of both microbiota and health [101]. For instance by replacing saturated fat with unsaturated fatty acids such as oleic acid or n-3 fatty acids as fat source essentially attenuate many of the negative effects found with SFAs including obesity [102] and low-grade inflammation [103]. Recently, Caesar *et al.* [104] sought to evaluate the effect of different fat sources on gut microbiota and its effect on the immune response. Mice were

fed isocaloric diets with either lard or fish oil as the fat source. Mice fed lard had a significant increase in weight, food consumption, elevated fasting glucose and insulin levels and impaired insulin sensitivity, compared to mice fed fish oil. Although no observed difference in bacterial translocation, mice fed lard presented an enhanced inflammation response, translated in higher levels of TLR2 and TLR4. When TLR adaptor MyD88 was inactivated (MyD88 KO mice), mice presented lower levels of fasting insulin and an improvement in insulin sensitivity. Reduced sizes of adipocytes and less infiltration of macrophages in WAT were also observed compared to WT mice fed the same diet. These effects prevailed after fecal transplantation into GF mice, supporting the hypothesis of WAT inflammation is modulated through the interaction between dietary SFA and gut microbiota [104].

With modulation of microbiota and an increase of LPS, the innate immune system is activated and TLR4 is a key factor for gut inflammation and development of metabolic syndrome [95, 105]. When knocking out TLR4 in the hematopoietic cell lineage, mice fed HFD had improved insulin sensitivity, reduced adipose tissue inflammation markers and reduced macrophages infiltration [106]. These findings were essentially confirmed by Kim *et al.* in global TLR4 KO mice. HFD mediated up-regulation of TNF-α, IL-1β and IL-6, iNOS and COX2 in the colon and decreased expression of occludin and claudin-1 in WT mice were not evident in TLR4-/- mice [105].

In addition, HFD leads to a negative effect on the production of anti-inflammatory cytokines. De Wit *et al.* and Wang *et al.* observed a lower production of IL-18 and IL-22 in ileum and colon, respectively, in mice fed HFD [107, 108], while Garidou *et al.* detected a down-regulation of IL-10 and IL-22 in both ileum and colon [109]. Down-regulation of IL-18 has a pivotal role in the metabolic syndrome. Mice deprived of IL-18 presented an increased food intake and consequent development of obesity and insulin [110]. Moreover, Hamilton *et al.* observed less IL-10 in the ileum of HFD fed rats [100] and Monteiro-Sepulveda *et al.* observed reduced levels of IL-22 in the jejunum of obese individuals and the increase of pro-inflammatory cytokines TNF-α, TGF-β, and IFN-γ in LP [111].

The influence of HFD in cytokines production leads to a subsequent change in cell population in the gut. Johnson *et al.* observed depletion of eosinophils in LP after mice were fed HFD for one week, even before the expected changes in the populations of

macrophages and dendritic cells or development of obesity [112]. Then, they analyzed *ob/ob* mutant mice fed chow diet and compared the cell populations with WT mice. Eosinophils number in ileum did not differ between those groups, suggesting that the cause of depletion of eosinophils after HFD implementation was rather due to the fat intake than to the obesity status. Luck *et al.* observed a decrease in CD4+ Foxp3+ Treg cells in the LP of both SI and colon in mice fed HFD for six weeks [113]. These cells are involved in tolerance responses towards gut microbiota. Tregs suppress Th1 cells through the production of IL-10 and TGF-β [114]. In fact, IFN-γ from Th1 and CD8^{+} T cells was up-regulated and IL-10 expression was diminished in HFD fed mice [114]. Garidou *et al.* also observed an increase of Th1 and a decrease of Th17 cells in ileum after 30 days of HFD dietary trial [109].

However, not all studies have observed detrimental effects on intestinal health and immune responses as a consequence of HFD. Kless *et al.* indeed observed an impairment of glucose metabolism and low-grade inflammation associated with the increased fat mass after four weeks HFD feeding, but no indication of barrier disruption or any significant marks of gut inflammation were found [115]. Also, Ding *et al.* did not observe the up-regulation of TNF-α in the colon caused by HFD [116] and Johnson *et al.* did not observe any effect of HFD in the levels of TNF-α or IL-1β in the ileum [112]. Although Lam *et al.* observed the up-regulation of TNF-α, the same was not observed in the levels IL-6 [94]. Furthermore, Li *et al.* found no up-regulation of either TNF-α or IL-6 after 14 weeks of HFD feeding and observed only the up-regulation of IL-1β both in SI and proximal colon [117].

The differences in observed results between HFD studies could be explained by the dynamic nature of immune response [100] as well as differences in environmental factors such as feed ingredients (different sources and amounts of fat). Some studies have used a low-fat chow diet and compared it to a synthetic HFD. This comparison can be correct if the objective is to compare a normal low-fat mouse diet to an energy-dense diet, but it is difficult to distinguish the effects of a diet with or without excessive fat content. Moreover, animal housing conditions and vendor, genetic background, age of mice, length of the study, analytic methodologies and most likely, different microbiota are also factors that can explain some of the different findings [118, 119].

The small intestine has certainly a lower bacterial diversity compared to the colon, but still, HFD has a relevant impact on microbiota [101, 120]. The environment in the Duodenum changes dramatically during the day due to stomach, bile and pancreatic secretions, but most distal segments have a more stable environment. SI epithelium is less protected to external influences and a stable microbiota may play a relevant role for the intestinal homeostasis and metabolism. Martinez-Guryn *et al.* observed an abundance of Clostridiaceae family in the jejunum and ileum of mice fed HFD and a decrease of Bifidobactericeae and Bacteroidaceae families in all regions of SI when compared to LFD. Interestingly, recent experiments have revealed that small intestinal microbiota is crucial for the lipids uptake. The first hint on this was shown in GF mice that are resistant to HFD-induced obesity. Mice devoid of gut bacteria had impaired digestion and uptake of lipids as shown by others. However, when they compared microbiota from LFD and HFD fed mice, they found that HFD derived jejunal bacteria directly affected proteins involved in fat uptake and digestion [120].

Beneficial dietary modulation of microbiota

Several studies propose diet as an obvious strategy for ameliorating metabolic syndrome-related diseases. Reduced consumption of saturated fatty acids or higher consumption of fiber, and consequent change of gut microbiota, have proven to benefit the host regarding absorption and storage of fatty acids and inflammatory status [92, 100, 104, 113, 118, 121, 122].

Dietary fiber is a polysaccharide or carbohydrate-containing compound that is neither digested nor absorbed by the GI tract, but it represents an important source of energy to gut microbiota [123]. Fiber is the most studied probiotic and it is classified according to their solubility or their susceptibility for degradation by the colonic microbiota. Soluble fibers are usually prone to microbiota digestibility through fermentation, whereas insoluble fibers, such as cellulose, have poor fermentability. Moreover, different soluble fibers present different fermentation potential, which means a distinct capacity to provide energy to microbiota [124]. Soluble fibers can then be considered as prebiotics when these benefit the composition and diversity of microbiota towards the host [125]. In a healthy status, microbiota metabolizes fiber into SCFA such as acetate, propionate and butyrate in the ratio of 60:20:20, respectively. Propionate and acetate are energy substrates for peripheral tissues such as liver and muscle cells [32]. Butyrate, besides being an important energy source for colonic epithelial cells and regulator of its proliferation, differentiation and gene expression, it also participates in the activation of Treg cells, acting as an anti-inflammatory factor. [126-128].

Polyphenols are phytochemicals derived from plant metabolism characterized by hydroxylated phenyl moieties with an indication of several health benefits and prebiotic effects [129, 130]. Polyphenols are commonly referred as antioxidants or scavengers of oxygen radicals due to their electron-donating phenolic groups which interact with reactive oxygen species in the intestinal tract. However, these compounds are poorly absorbed in the SI and they might act mostly at the intestinal level [131-133]. As a matter of fact, they do not need to be absorbed in order to be bioactive. In the colon, simple polyphenols are metabolized by microbiota and converted until non-aromatic compounds, such as SCFA, lactate, oxaloacetate and others [134, 135], and with lower molecular weight, metabolites are possible to be absorbed and act systemically [130].

Anhê *et al.* fed mice for eight weeks with a high-fat/high sucrose diet supplemented with cranberry extract [136] due to its high content of polyphenols. When mice received the cranberry extract, the group observed a reduced weight gain, less visceral fat and insulin sensitivity was enhanced. Oxidative stress in the gut was also alleviated and barrier function was improved. Furthermore, NF-κB activation was reduced and consequent decrease of inflammatory markers, such as TNFα and COX-2. Cranberry extract had also a probiotic effect by increasing the F:B ratio and the amount of *Akkermansia spp.* [136].

Coffee

Coffee is one of the most consumed beverages around the world and large epidemiological studies associate coffee intake with several health effects [137]. Moderate and regular consumption of coffee (3 cups/day) has been inversely associated with obesity and T2D by regulating lipid absorption, insulin sensitivity and glucose tolerance. It is also positively connected with neurologic and cardiovascular diseases and with anti-cancer effects [137-142]. Coffee is composed of hundreds of biologically active compounds and caffeine is by far the most studied one, but not necessarily the most abundant (50-300mg/cup) [137]. Polyphenols such as flavonoids, phenolic acid and chlorogenic acid (CGA) are highly present in coffee beans (200-500mg/cup) [143]. Lastly, coffee contains high amounts of soluble dietary fiber, mainly galactomannans and arabinogalactans, which act as energy sources for colonic bacteria [144]. However, several factors during coffee production play a role in the composition of the final product. Coffee beans come from two different species, *Coffea arabica* and *Coffea canephora* (known as "Robusta") and the origin, genetic traits and the agriculture practice vary between producers. Then, the level of roasting will contribute immensely to the concentration and bioavailability of compounds such as polyphenols and diterpenes [145, 146].

Caffeine is rapidly absorbed in the upper part of the SI before being metabolized in the liver [147]. Long-term frequent coffee consumption is associated with increased insulin sensitivity and glucose tolerance, reducing the risk of developing T2D [148-150]. Similar effects in insulin and glucose were also observed in decaffeinated coffee [151]. A strong candidate for these beneficial effects is the polyphenol CGA. Studies where CGA

was administered, showed improved insulin sensitivity, enhanced glucose tolerance and lower fasting glucose levels [152]. CGA, like other polyphenols, is poorly absorbed in the SI. It acts as an antioxidant during oxidative stress and it contributes positively to the inflammatory homeostasis, mostly in the colon after microbiota metabolism [140, 149, 153, 154]. Metagenomics analysis showed that coffee consumption, associated with a higher concentration of polyphenols, was connected with increased microbial diversity in the intestine [155]. Mills *et al*. incubated human fecal microbiota from the colon with different coffee samples *in vitro* and coffee samples with higher CGA content that benefit the growth of *Bifidobacterium* spp. When used pure CGA it also benefited the growth of *Clostridium coccoides* [156]. The prebiotic effect of phenolic acids towards *Bifidobacteria* was later observed in other *in vitro* and also *in vivo* studies while decreasing hostile microbiota [157, 158]. Still, the underlying mechanism of the beneficial effects of coffee consumption in microbiota remains unclear.

Regarding HFD and coffee, Cowan *et al*. reported that rats fed chow or HFD (60% energy from fat) with or without caffeinated coffee in water for 10 weeks. Mice that received coffee in their water presented reduced body weight and body fat and increased F:B ratio when compared to HFD fed mice that received just water [159]. Nishitsuji *et al.,* besides adding coffee to water for 16 weeks to obese mice that develop spontaneously diabetes, they also administered either caffeine or CGA [160]. A change in SCFA profiles was observed but no significant effects in F:B ratio in fecal samples. Only a few genera related to inflammation presented significant changes, such as *Blautia*, *Coprococcus* and *Provotela* [160]. However, the group suggests, as an improvement of the study, the increase of animals per group, instead of n=3. Lastly, Fukushima *et al.* fed mice for 8 weeks with chow diet and HFD supplemented with either caffeinated or decaffeinated coffee [161]. They observed a reduction of body weight in mice that consumed coffee, as well as a reduction in the expression of the pro-inflammatory cytokine IL-1β in adipose tissue. After observing considerable similarity in the results in both coffee groups, they suggest that coffee consumption prevents the development of severe obesity and caffeine is not a key factor in suppressing the development of the metabolic syndrome.

Aims of the study

In this project, the main objective has been to contribute to the understanding of how diet and reactive oxygen species can affect gut health and microbiota. To do this we have used the mouse as a model, presented in four papers.

- The aim of **paper I** was to understand the effects of a high-fat diet (HFD) when compared to a low-fat diet (LFD) as a control, with fat as the only variable. We studied the different sections in the small intestine (duodenum, jejunum and ileum) since the profile and number of bacteria vary along the gut and it is tightly connected to digestion and absorption of fat. In addition, we aimed to observe the interaction between HFD-modulated microbiota with the immune system.

- In **paper II** the aim was to investigate whether relevant doses of coffee given to mice affected the putative detrimental impact of HFD on obesity, gut health and microbiota composition. Previous studies have observed a positive impact of coffee on health, but the mechanism of action remains unclear. Coffee is composed of hundreds of compounds beneficial to commensal microbiota, such as fibers and phenolic compounds, and the interaction between coffee, microbiota and the immune system has to our knowledge not been scrutinized before.

- In **paper III**, we aimed to study the role of ROS at the distal part of the small intestine. The ileum and the large intestine are separated by the ileocecal valve, which avoids the reflux of large intestine content. However, this valve is not effective in preventing the backflow of cecal bacteria into the ileum. Still, these two adjacent segments harbor distinct groups and amounts of bacteria. We hypothesized that ROS production has a pivotal role in the ileal homeostasis and to test it, we used mice deficient in iNOS and NOX1 to observe the consequences of peroxynitrite absence.

- Lastly, in **paper IV** we aimed to understand the role of NOX1 in the colon following a low-grade inflammation. In a normal situation, NOX1 is highly expressed in the colon but during inflammation iNOS and NOX2 become the main sources for ROS production. It is plausible that in this state, NOX1 remains the main source of superoxide. Therefore, we induced low-grade inflammation in WT and NOX1-KO mice to understand the involvement of NOX1 in intestinal hemostasis, involving both gut microbiota and the immune response.

Main Results and Discussion

PAPER I: Small intestine microbiota and immune status in high-fat dieting mice

In paper I, we study the effects of a HFD feeding after 18 weeks using a LFD diet as a control, where the fat was replaced with corn starch. The HFD fed mice presented characteristics of metabolic syndrome-related diseases such as obesity and type 2 diabetes. There was an increase in body weight, energy intake, adipocyte size and impaired glucose regulation. Moreover, we observed a change in the microbiota composition between the groups. As regards α-diversity, we did not observe significant changes between the groups, which is not surprising considering that the microbiota in this region is overall phylogenetically less diverse than in the large intestine [162]. The HFD group had a change of jejunal and ileal bacteria, translated in increased F:B ratio and increased abundance of *Proteobacteria*, a phylum composed of Gram-negative bacteria with several of them known as pathogens. This shift of the microbiota community is indicative of dysbiosis and low-grade inflammation, commonly related to the consumption of HFD and metabolic syndrome [92, 163, 164]. LPS produced by Gram-negative bacteria is thought to induce endotoxemia that further leads to an inflammatory state in the gut [98]. In our study, the change of microbiota and the increased abundance of *Proteobacteria* can be associated to the observed increase of LPS binding protein (LBP) in the plasma of mice fed HFD, as an indication of leakage of LPS from the gut. Another possible explanation for the increased LBP levels is that LPS can, together with fat, be incorporated into chylomicrons which subsequently facilitates LPS release from the intestinal epithelial cells [165]. In addition, LBP is also induced by pro-inflammatory cytokines originating from adipose tissue as a response to obesity-induced low-grade inflammation [166].

ROS are an integral part of the innate immune system, mostly by the induction of respiratory burst in phagocytic cells to efficiently kill microbes. We observed increased levels of ROS using non-invasive imaging [167]. However, when analyzing the gene expression of ROS-related genes, we observed reduced NOX1 and increased NOX2 expressions, suggesting that the ROS production in HFD fed mice was caused by the

increased presence of NOX2 expressing macrophages, indicating the passage of pathogens into the lamina propria. We found indeed an increased proportion of inflammatory macrophages by assessing the expression of MCHII/CX3CR1[int] as a marker of monocyte-derived immature macrophages. This could also be explained by the reduced Treg cells as mature intestinal macrophages are important for Treg formation [168]. Although other studies have shown a reduction of Treg cells after HFD consumption, it was only observed when used chow diet as LFD control [113]. Our results thus confirm that reduction of Treg cells is indeed due to the increased fat consumption.

We further observed a moderate increase of pro-inflammatory cytokines in the distal segments of the SI, mostly in the jejunum, as well as expression of PRRs and barrier related genes. The PRRs are important signaling molecules to maintain the gut homeostasis [169] and their increased expression has dominantly been linked to increased permeability after HFD consumption [99, 170]. However, we observed an increase in the expression of antimicrobial Reg3γ and tight junctions occluding and zonula occludens. We believe this up-regulation is a compensatory mechanism mediated by the host when challenged by a detrimental microbial environment imposed by HFD, as others suggested [100]. Importantly, many of the studies so far have compared HFD with a low-fat chow diet rich in fiber. In our study, we matched HFD to a LFD varying only with respect to carbohydrate content and fat. Indeed, Kless *et al.* use the same similar diets and observed little or no differences in intestinal barrier properties between the two diets [115].

Overall, paper I demonstrate that the consumption of HFD, when compared to a LFD, affects the host metabolism and it has an important effect in the microbiota, mostly in the ileum, leading to dysbiotic and pro-inflammatory profile. These conditions elicit an adaptive host response resulting in reduced barrier permeability, change in ROS production and more inflammatory immune cells. We believe the reason for stronger effects in previous studies could be explained by the difference of fiber content between the control and target diets. This study also highlights the importance of choosing the correct diet to secure that, in fact, we compare the impact of HFD.

PAPER II: Coffee consumption in moderate doses attenuates microbial dysbiosis and inflammation induced by high-fat feeding in mice.

In paper II we have investigates for the first time the impact of coffee on the microbial composition along the length of intestinal mice fed LF diet, HF diet and HF diet supplemented with different coffee doses. Several studies focused on the effects of HF diet, study the SI as a whole and analyze microbiota composition in feces or in the large intestine [171]. Recently, some studies have shown that changes in the microbiota of the small intestine lead to detrimental consequences in nutrient digestion and transport [92, 120, 172]. Here we analyzed the microbial composition throughout the whole intestine including the three regions of the small intestine (duodenum, jejunum and ileum).

Coffee supplementation was revealed to have a positive dose-dependent influence in energy intake and weight gain in the direction of LFD-like group. Similar indications were also observed by Fukushima *et al.* where HFD supplemented with both caffeinated and decaffeinated coffee were tested. Both coffee types had similar effects and according to the authors, caffeine could not be the main factor for reduced weight gain [161]. Moreover, consumption of caffeine has been shown to positively alter the gut microbiota [173]. Besides caffeine, coffee contains several poly- and oligosaccharides, as well as peptides that could act as a carbon and nitrogen source to bacteria, and therefore alter the microbial composition [174], especially in the small intestine as this is the primary site of absorption. Coffee is also rich in phenolic compounds [175-177], especially, chlorogenic acid, which has been found to modulate positively the gut microbiota in HF diet-fed mice [178]. Lastly, coffee contains high amounts of soluble dietary fiber, mainly galactomannans and arabinogalactans, which act as energy sources for commensal bacteria [179]. Then, it is not surprising that coffee can modulate the microbiota either in the small intestine by polyphenols action or in the colon by their fiber content.

In our study, we observed that coffee consumption in moderate doses attenuated the microbial dysbiosis induced by HF diet. We observed a beneficial decreased of F:B ratio, with higher doses of coffee resembling the LFD fed mice. Moderate coffee consumption also improved the intestinal barrier and led to less pro-inflammatory macrophages in

the lamina propria. In all coffee groups, we observed an increased expression of genes related to pathogens recognition receptors, which might have enhanced expression of genes related with tight junctions, as a mechanism of defense against HFD detrimental effects. Still, it is not clear which compounds from coffee counteract the detrimental effects of HFD. We hypothesize that coffee reduces inflammation in the small intestine by attenuating the microbial dysbiosis but also there are indications that caffeine, CGA and diterpenes kahweol and cafestol can reduce act directly at the cell level and inhibit the activity of NF-κB and consequent reduced inflammatory response and oxidative stress [180-182], also observed in our study.

PAPER III: iNOS-and NOX1-dependent ROS production maintains bacterial homeostasis in the ileum of mice.

In paper III, we observed *in vivo* that ROS was highly produced in the distal part of the small intestine by using L-012, an optical imaging probe specific for peroxynitrite. Gene expression analysis confirmed that iNOS and NOX1 were highly expressed in this segment, which are involved in the production of nitric oxide and superoxide, respectively, to form peroxynitrite. When using iNOS and NOX1 KO mice, they presented a reduction of L-012 signal when compared to WT mice, suggesting the dependency of these molecules to the production of L-012 signal. Similar results were observed after using adequate ROS inhibitors and scavengers. Together, these results proved that L-012 signal is related to iNOS- and NOX1-depended ROS. We then treated WT mice with a cocktail of antibiotics capable to reduce the bacterial load in the SI. Both L-012 signal and gene expression demonstrated a reduction of ROS in ileum when the number of bacteria was dampened, proving the relationship between ROS production and bacterial load.

Although peroxynitrite is likely detected in our experiments, there are other candidates such as hydrogen peroxide and hypochlorous acid, which are involved in the respiratory burst [84], but these molecules are dependent in a high concentration of peroxidase and myeloperoxidase, respectively, and such compounds are not commonly found in the gut under normal conditions. ROS are also commonly produced by the

electron transport chain in mitochondria in connection with intracellular signaling, but their low levels are not detectable *in vivo* imaging.

Then, to study the role of iNOS and NOX1 in the SI homeostasis, we compared the microbiota of iNOS KO and NOX1 KO mice to the microbiota of WT mice. Regarding the composition, both KO groups showed an increase of the F:B ratio in the ileum when compared to WT. The microbiota of KO groups was relatively similar, presenting only minor differences at the lower taxonomic groups. Furthermore, we observed that in the absence of iNOS and NOX1 the bacterial load was increased in the ileum, in fact, similar to the cecum. These results indicated that ROS deriving from epithelial cells contribute to the control of microbiota in the SI and compensate for the inefficiency of the ileocecal valve to avoid the growth of bacteria from the cecum in the ileum. However, the mechanism of action of ROS produced by epithelial cells is not yet fully understood. It does not mean that the bacteria are killed by ROS. Different bacteria can indeed have different tolerance to ROS. Still, we can say that ROS affects bacterial virulence. In addition, ROS could act in the bacterial population indirectly by modifying the mucus structure and therefore affecting their adherence. Nevertheless, ROS-derived from iNOS and NOX1 do have a relevant impact on the number of bacteria in the ileum. Moreover, we also observed a significant increase of bacterial DNA in the liver of KO mice when compared with WT, indicating that ROS also participates in the defense mechanism against bacterial translocation.

Altogether, we observed that ROS, likely peroxynitrite, is highly produced by iNOS and NOX1 in epithelial cells and it participates actively in the regulation of bacteria in the ileum, benefiting nutrient uptake and barrier function of the gut.

PAPER IV: NOX1 regulates colonic microbiota and gut defense following DSS-induced low-grade inflammation in mice

In paper IV we investigated the role of NOX1 in the colon during steady-state and in subclinical low-grade inflammation. The fact that NOX1 is highly expressed during colonic epithelial cells both during non-inflammation conditions and during inflammation, points out the importance of NOX1 for the intestinal homeostasis. Peroxynitrite as been pointed out as a regulator of microbiota in the small intestine [76]

but how NOX1 modulates the colonic microbiota and sequentially affects the course of low-grade colonic inflammation is still unknown.

We started by developing a low-grade inflammation model where mice presented none or few visible signs of disease, together with a moderate up-regulation of inflammation-related genes in the colon. We then concluded that 1% of DSS in drinking water for six days was the most adequate model to induce the expected colonic low-grade inflammation. We applied the developed model to WT and NOX1 KO mice. Surprisingly, animals exposed to DSS revealed reduced stool quality (although not significantly different) and histological analysis revealed changes in the structure of the gut wall and infiltration of immune cells, indicative of more than a mild phenotype, but no obvious structural differences between genotypes.

In vivo imaging revealed that NOX1 KO mice had lower production of peroxynitrite in both conditions, proving the NOX1 dependency for ROS production after DSS treatment. Since gene expression showed that the expression of iNOS and not NOX1 was enhanced by DSS, the increased L-012 signal in WT mice was most likely caused by increased nitric oxide production and not superoxide. In NOX1 KO mice we also observed an increased ROS production after DSS exposure. In this case, other sources such as myeloperoxidase [183] or NOX3 [184] activity could have contributed to L-012 signal.

Regarding inflammation, gene expression revealed a tendency for a higher up-regulation of inflammatory markers after DSS exposure in NOX1 KO mice when compared to WT mice. We further analyzed Lcn-2 protein in fecal samples, which have shown to be a sensitive marker for DSS-induced inflammation [183]. Recently Makhezer *et al.* demonstrated that induction of Lcn-2 by pro-inflammatory cytokines is partly dependent on NOX1 in epithelial cells [185]. In contrast, we saw that Lcn-2 is in fact modestly increased in NOX1 KO mice when compared with WT after DSS exposure. However, we believe that in our low-grade inflammation state the direct effect of NOX1 on Lcn-2 production might be negligible. Instead, the proximity of bacteria to epithelial cells might have promoted the production of Lcn-2, as DSS increases the permeability of the mucus layer [186] and Lcn-2 production is also dependent on the bacterial exposure [187]. An alternative theory is that the absence of NOX1-generated ROS leads to altered microbial composition analogous to observations in the ileum [76]. Indeed, Li *et al.*

showed that DSS induced Lcn-2 levels were dependent on the initial microbial profile [188].

Furthermore, NOX1 revealed to have an influence on the composition of colonic microbiota. We observed an overall decrease in the α-diversity of NOX1 KO mice when compared to mice under normal conditions and the β-diversity of fecal samples analyses revealed that all groups were statistically different from each other. Together, these data suggest that the absence of NOX1 influences microbiota composition, mostly in luminal areas. At the phylum level, NOX1 KO mice presented an increased *Firmicutes/Bacteroidetes* ratio as commonly seen in obese-related inflammation [37]. Moreover, NOX1 KO mice had elevated relative abundance of *Akkermansia* when compared to WT mice*. However, DSS exposure reduced such difference due to a bloom of *Akkermansia* in WT mice. The role of this genus is still discussable but there are several indications of their beneficial effects for intestinal homeostasis [189, 190]. Since NOX1 KO mice are associated with an increased number of goblet cells and consequent mucus production [191], it could explain the increased relative abundance in NOX1 KO mice under normal conditions. The detrimental effects of DSS on the mucus layer [186] could explicate the increase of the relative abundance of *Akkermansia* in WT mice. However, why *Akkermansia* in NOX1 KO mice seems unaffected by DSS remains unclear. At the genus level, we observed that the absence of NOX1 led to changes in microbiota associated with intestinal health. We saw that the abundance of bacteria related to barrier function stability and anti-inflammatory response [192-195] was reduced in NOX1 KO mice and at the same time, genera commonly associated with inflammation and disease had increased relative abundance [188, 196-199]. In fact, the bacterial profile of NOX1 KO mice became more similar to the composition of mice exposed to DSS.

Overall, although we observed a shift of microbiota in NOX1 KO mice towards dysbiosis and inflammatory profile, there was no manifestation of pathological changes even though analyses of inflammatory markers showed an indication of enhanced inflammation status. We, therefore, propose that NOX1 has a role in shaping colonic microbiota, which may have consequences for intestinal health.

Future Perspectives

The research in this thesis provides new knowledge about the interactions between diet, gut microbiota, immune system and host health. The importance of microbiota on the host health is recognized and it has received relevant attention in the last years, but the mechanisms of the interaction between host and microbiota are not yet fully understood. We tried to answer some unsolved questions, focusing on the interaction of diet, microbiota and the immune response, and other factors involved in microbiota modulation, such as the production ROS in both SI and colon and their role in the intestinal homeostasis.

The paper I showed the importance of including SI in dietary studies involving fat, as well as to other nutrients that either modulated microbiota or are digested and/or absorbed in the small intestine. We also emphasize the use of an adequate control diet. Several studies use standard chow diet as a control, but due to its different amounts of soluble dietary fiber, the observed results cannot be associated solely to fat. Still, fiber is important for the intestinal homeostasis. Perhaps would be advantageous to either substitute cellulose by inulin [128] or develop a standard dietary fiber composition in purified diets. However is difficult to study the effects of individual fibers and develop an optimal "standard fiber formula" that responds to general requirements.

Regarding paper II, a recent study suggests CGA as a possible candidate for the beneficial effects of coffee. However, the results were not conclusive, possibly due to the small number of sampled mice (n=3) [160]. For future research, different compounds should be tested, such as CGA or other polyphenols, not only as isolated but also in combinations between them. After identifying which compound/combination has the most beneficial effects on intestinal microbiota and host health, coffee production could be orientated to preserve or potentialize such compounds.

Paper III and IV have shown that the production of ROS is important for the modulation of gut microbiota, both in SI and colon. However, ROS is an umbrella term used to different molecules with different actions and interactions, and they are not exclusively present in the gut. Studies with genetic KO of more than one ROS-related gene could not just prove the importance of ROS but also the dependency on general health. Moreover, it is needed new and easier techniques to analyze ROS *in vivo*. Then,

we could scrutinize the pathways involving ROS and understand in more detail the interaction between microbiota, ROS and the host.

Still, as commonly said, more research is needed. Studies in intestinal microbiota should involve analyzes of the dietary effects in the SI as often as possible. However, sampling methodologies (biopsies) in SI for human studies are difficult to perform. Kastl *et al.* proposed the usage of indwelling catheters or ingested smart capsules in order to collect samples from SI and facilitate the understanding of the dietary effects or other perturbations in the SI microbiota [162]. Tremaroli *et al.* suggest studies in pigs as a model, due to the similarity of their GI tracts to humans. Then it would be easier to understand the function of different bacteria in the GI tract and their interactions with diet and the host [200]. The group also suggests the development of GF mice that can be "humanized" by colonization with human intestinal samples or bacterial profiles that resemble human intestinal microbiota, as demonstrated by Turnbaugh *et al.* [201]. This methodology will also enable us to represent different ethnic origins with different food habits and therefore different bacterial compositions [200].

Supplementation of probiotics and prebiotics should also be a case of study to promote intestinal homeostasis. Several studies suggest that the introduction of probiotics can naturally change the bacterial community in the gut by either promoting the growth of beneficial bacteria or reducing the number of pathogens. The introduction of bacteria belonging to the group *Bifidobacterium* and *Akkermansia* [99, 202, 203] were presented as good candidates to promote the health in individuals with metabolic-related diseases. However, Anhê *et al.* point out that the production of *Akkermansia spp.* at a commercial scale is not just costly but the safety of using it as probiotic is still questionable. They suggest that the usage of a prebiotic that selectively benefit this bacterium could be a better approach [136]. Fortunately, several studies already presented the benefits of plant-based prebiotic consumption, such as pectin, β-glucan, oligofructose or polyphenols [136, 204-206], but the outcome results are always dependent on the present bacteria. The use of probiotics and prebiotics as treatments

still needs further research and validation in a large-scale human trial, including double-blind, placebo-controlled studies [200, 207].

From observations made in mice where microbiota transplantation induced or regulated weight gain [88, 89], there are strong indications that fecal microbiota transplantation in humans could also be a strategy to treat patients with metabolic diseases or disorders related with the intestinal microbiota. Fecal transplantation from healthy patients has shown great success rates in the treatment of *Clostridium difficile* [208] and more studies started using the same methodology for the treatment of obesity with fecal bacteria from lean patients [32, 209]. During fecal microbiome transplantation, the new community would replace or correct the anomalous microbiota in the recipient. Vrieze *et al.* performed small intestine infusions of fecal microbiota from lean donors until obese individuals, leading to improvements in insulin tolerance and beneficial changes in the microbiota in both SI and colon [210]. However, it is difficult to determine who is the most adequate donor for each case, guarantee that transplanted samples are pathogen-free and predict the immune response of the recipient [32, 207].

There is strong evidence that future therapeutics will consider microbiota as a relevant factor in host metabolism and health. Current studies tend to use the concept of "each case is a case", suggesting that future interventions and clinical studies should be leaning with a personalized medicine-oriented view based on the bacterial composition of each patient. However, metagenomic sequencing is expensive, and not always accessible to all patients and clinics. Cheaper sequencing and bioinformatic tools are required to be accessible and more routinely used in research laboratories. Metagenome sequencing could be then complemented with metatranscriptomics and metaproteomics to identify which bacterial genes and proteins are expressed. Then, we could have a better understanding of the bacterial community as a whole and decide which treatment is the most adequate and effective, elevating the concept of personalized nutrition to another level.

References

1. Barrett, K.E., *Gastrointestinal physiology*. 2nd edition. ed. Lange Physiology Series. **2014**, New York: Lange Medical Books/McGraw-Hill Education.

2. Bollinger, R.R., A.S. Barbas*, et al.*, Biofilms in the large bowel suggest an apparent function of the human vermiform appendix. *Journal of theoretical biology*, **2007**. 249(4): p. 826-831.

3. Barker, N., J.H. van Es*, et al.*, Identification of stem cells in small intestine and colon by marker gene Lgr5. *Nature*, **2007**. 449(7165): p. 1003-7.

4. Peterson, L.W. and D. Artis, Intestinal epithelial cells: regulators of barrier function and immune homeostasis. *Nat Rev Immunol*, **2014**. 14(3): p. 141-53.

5. Assimakopoulos, S.F., I. Papageorgiou, and A. Charonis, Enterocytes' tight junctions: From molecules to diseases. *World J Gastrointest Pathophysiol*, **2011**. 2(6): p. 123-37.

6. Lee, B., K.M. Moon, and C.Y. Kim, Tight Junction in the Intestinal Epithelium: Its Association with Diseases and Regulation by Phytochemicals. *J Immunol Res*, **2018**. 2018: p. 2645465.

7. Johansson, M.E., H. Sjovall, and G.C. Hansson, The gastrointestinal mucus system in health and disease. *Nat Rev Gastroenterol Hepatol*, **2013**. 10(6): p. 352-61.

8. Johansson, M.E. and G.C. Hansson, Immunological aspects of intestinal mucus and mucins. *Nat Rev Immunol*, **2016**. 16(10): p. 639-49.

9. Specian, R.D. and M.R. Neutra, Mechanism of rapid mucus secretion in goblet cells stimulated by acetylcholine. *J Cell Biol*, **1980**. 85(3): p. 626-40.

10. Jakobsson, H.E., A.M. Rodriguez-Pineiro*, et al.*, The composition of the gut microbiota shapes the colon mucus barrier. *EMBO Rep*, **2015**. 16(2): p. 164-77.

11. Johansson, M.E., Fast renewal of the distal colonic mucus layers by the surface goblet cells as measured by in vivo labeling of mucin glycoproteins. *PLoS One*, **2012**. 7(7): p. e41009.

12. Birchenough, G.M., E.E. Nystrom*, et al.*, A sentinel goblet cell guards the colonic crypt by triggering Nlrp6-dependent Muc2 secretion. *Science*, **2016**. 352(6293): p. 1535-42.

13. Sender, R., S. Fuchs, and R. Milo, Revised estimates for the number of human and bacteria cells in the body. *PLoS biology*, **2016**. 14(8): p. e1002533.

14. Dominguez-Bello, M.G., E.K. Costello*, et al.*, Delivery mode shapes the acquisition and structure of the initial microbiota across multiple body habitats in newborns. *Proc Natl Acad Sci U S A*, **2010**. 107(26): p. 11971-5.

15. Mueller, N., A. Pizoni*, et al.*, Delivery mode and neonate gut microbiota. *The FASEB Journal*, **2015**. 29: p. 385.7.

16. Rodriguez, J.M., K. Murphy*, et al.*, The composition of the gut microbiota throughout life, with an emphasis on early life. *Microb Ecol Health Dis*, **2015**. 26(1): p. 26050.

17. Tanaka, M. and J. Nakayama, Development of the gut microbiota in infancy and its impact on health in later life. *Allergol Int*, **2017**. 66(4): p. 515-522.

18. Sekirov, I., S.L. Russell, *et al.*, Gut microbiota in health and disease. *Physiol Rev*, **2010**. 90(3): p. 859-904.

19. Rodriguez-Pineiro, A.M., J.H. Bergstrom, *et al.*, Studies of mucus in mouse stomach, small intestine, and colon. II. Gastrointestinal mucus proteome reveals Muc2 and Muc5ac accompanied by a set of core proteins. *Am J Physiol Gastrointest Liver Physiol*, **2013**. 305(5): p. G348-56.

20. Donaldson, G.P., S.M. Lee, and S.K. Mazmanian, Gut biogeography of the bacterial microbiota. *Nat Rev Microbiol*, **2016**. 14(1): p. 20-32.

21. Sender, R., S. Fuchs, and R. Milo, Revised Estimates for the Number of Human and Bacteria Cells in the Body. *PLoS Biol*, **2016**. 14(8): p. e1002533.

22. Brown, E.M., M. Sadarangani, and B.B. Finlay, The role of the immune system in governing host-microbe interactions in the intestine. *Nat Immunol*, **2013**. 14(7): p. 660-7.

23. Arumugam, M., J. Raes, *et al.*, Enterotypes of the human gut microbiome. *Nature*, **2011**. 473(7346): p. 174-80.

24. Turnbaugh, P.J., M. Hamady, *et al.*, A core gut microbiome in obese and lean twins. *Nature*, **2009**. 457(7228): p. 480-4.

25. Thursby, E. and N. Juge, Introduction to the human gut microbiota. *Biochem J*, **2017**. 474(11): p. 1823-1836.

26. Qin, J., R. Li, *et al.*, A human gut microbial gene catalogue established by metagenomic sequencing. *Nature*, **2010**. 464(7285): p. 59-65.

27. Dao, M.C., A. Everard, *et al.*, *Akkermansia muciniphila* and improved metabolic health during a dietary intervention in obesity: relationship with gut microbiome richness and ecology. *Gut*, **2016**. 65(3): p. 426-36.

28. Strachan, D.P., Hay fever, hygiene, and household size. *BMJ*, **1989**. 299(6710): p. 1259-60.

29. Johansson, M.E., H.E. Jakobsson, *et al.*, Normalization of Host Intestinal Mucus Layers Requires Long-Term Microbial Colonization. *Cell Host Microbe*, **2015**. 18(5): p. 582-92.

30. LeBlanc, J.G., C. Milani, *et al.*, Bacteria as vitamin suppliers to their host: a gut microbiota perspective. *Curr Opin Biotechnol*, **2013**. 24(2): p. 160-8.

31. Brandl, K., V. Kumar, and L. Eckmann, Gut-liver axis at the frontier of host-microbial interactions. *Am J Physiol Gastrointest Liver Physiol*, **2017**. 312(5): p. G413-G419.

32. Cani, P.D., M. Van Hul, *et al.*, Microbial regulation of organismal energy homeostasis. *Nat Metab*, **2019**. 1(1): p. 34-46.

33. Desai, M.S., A.M. Seekatz, *et al.*, A dietary fiber-deprived gut microbiota degrades the colonic mucus barrier and enhances pathogen susceptibility. *Cell*, **2016**. 167(5): p. 1339-1353. e21.

34. Tilg, H., N. Zmora, *et al.*, The intestinal microbiota fuelling metabolic inflammation. *Nature Reviews Immunology*, **2019**: p. 1-15.

35. Neis, E.P., H.M. van Eijk, *et al.*, Distal versus proximal intestinal short-chain fatty acid release in man. *Gut*, **2019**. 68(4): p. 764-765.

36. Shin, N.-R., T.W. Whon, and J.-W. Bae, Proteobacteria: microbial signature of dysbiosis in gut microbiota. *Trends in Biotechnology*, **2015**. 33(9): p. 496-503.

37. Ley, R.E., F. Backhed, *et al.*, Obesity alters gut microbial ecology. *Proc Natl Acad Sci U S A*, **2005**. 102(31): p. 11070-5.

38. Levy, M., A.A. Kolodziejczyk, *et al.*, Dysbiosis and the immune system. *Nature Reviews Immunology*, **2017**. 17(4): p. 219-232.

39. Fei, N. and L. Zhao, An opportunistic pathogen isolated from the gut of an obese human causes obesity in germfree mice. *ISME J*, **2013**. 7(4): p. 880-4.

40. Faith, J.J., J.L. Guruge, *et al.*, The long-term stability of the human gut microbiota. *Science*, **2013**. 341(6141): p. 1237439.

41. Mowat, A.M. and W.W. Agace, Regional specialization within the intestinal immune system. *Nat Rev Immunol*, **2014**. 14(10): p. 667-85.

42. Bergstrom, K.S., V. Kissoon-Singh, *et al.*, Muc2 protects against lethal infectious colitis by disassociating pathogenic and commensal bacteria from the colonic mucosa. *PLoS Pathog*, **2010**. 6(5): p. e1000902.

43. Bhullar, K., M. Zarepour, *et al.*, The Serine Protease Autotransporter Pic Modulates *Citrobacter rodentium* Pathogenesis and Its Innate Recognition by the Host. *Infect Immun*, **2015**. 83(7): p. 2636-50.

44. Pabst, O. and E. Slack, IgA and the intestinal microbiota: the importance of being specific. *Mucosal immunology*, **2019**: p. 1-10.

45. Ito, T., PAMPs and DAMPs as triggers for DIC. *J Intensive Care*, **2014**. 2(1): p. 67.

46. Medzhitov, R., Recognition of microorganisms and activation of the immune response. *Nature*, **2007**. 449(7164): p. 819-26.

47. Janeway, C.A., Jr. and R. Medzhitov, Innate immune recognition. *Annu Rev Immunol*, **2002**. 20: p. 197-216.

48. Akira, S. and K. Takeda, Toll-like receptor signalling. *Nat Rev Immunol*, **2004**. 4(7): p. 499-511.

49. Kumar, H., T. Kawai, and S. Akira, Toll-like receptors and innate immunity. *Biochem Biophys Res Commun*, **2009**. 388(4): p. 621-5.

50. Oosting, M., S.-C. Cheng, *et al.*, Human TLR10 is an anti-inflammatory pattern-recognition receptor. *Proceedings of the National Academy of Sciences*, **2014**. 111(42): p. E4478-E4484.

51. Burgueño, J.F. and M.T. Abreu, Epithelial Toll-like receptors and their role in gut homeostasis and disease. *Nature Reviews Gastroenterology & Hepatology*, **2020**: p. 1-16.

52. Poltorak, A., X. He, *et al.*, Defective LPS signaling in C3H/HeJ and C57BL/10ScCr mice: mutations in Tlr4 gene. *Science*, **1998**. 282(5396): p. 2085-8.

53.   Chamaillard, M., M. Hashimoto, *et al.*, An essential role for NOD1 in host recognition of bacterial peptidoglycan containing diaminopimelic acid. *Nat Immunol*, **2003**. 4(7): p. 702-7.

54.   Girardin, S.E., I.G. Boneca, *et al.*, Nod2 is a general sensor of peptidoglycan through muramyl dipeptide (MDP) detection. *Journal of Biological Chemistry*, **2003**. 278(11): p. 8869-8872.

55.   Ogura, Y., S. Lala, *et al.*, Expression of NOD2 in Paneth cells: a possible link to Crohn's ileitis. *Gut*, **2003**. 52(11): p. 1591-7.

56.   Strober, W., P.J. Murray, *et al.*, Signalling pathways and molecular interactions of NOD1 and NOD2. *Nat Rev Immunol*, **2006**. 6(1): p. 9-20.

57.   Rosenstiel, P., M. Fantini, *et al.*, TNF-alpha and IFN-gamma regulate the expression of the NOD2 (CARD15) gene in human intestinal epithelial cells. *Gastroenterology*, **2003**. 124(4): p. 1001-9.

58.   Inohara, N., Nods: a family of cytosolic proteins that regulate the host response to pathogens. *Current Opinion in Microbiology*, **2002**. 5(1): p. 76-80.

59.   McGovern, D.P., P. Hysi, *et al.*, Association between a complex insertion/deletion polymorphism in NOD1 (CARD4) and susceptibility to inflammatory bowel disease. *Human molecular genetics*, **2005**. 14(10): p. 1245-1250.

60.   Pashenkov, M.V., Y.A. Dagil, and B.V. Pinegin, NOD1 and NOD2: Molecular targets in prevention and treatment of infectious diseases. *Int Immunopharmacol*, **2018**. 54: p. 385-400.

61.   Tukhvatulin, A.I., A.S. Dzharullaeva, *et al.*, Powerful complex immunoadjuvant based on synergistic effect of combined TLR4 and NOD2 activation significantly enhances magnitude of humoral and cellular adaptive immune responses. *PloS one*, **2016**. 11(5): p. e0155650.

62.   Cavaillon, J.M., Pro- versus anti-inflammatory cytokines: myth or reality. *Cell Mol Biol (Noisy-le-grand)*, **2001**. 47(4): p. 695-702.

63.   Pabst, O. and A.M. Mowat, Oral tolerance to food protein. *Mucosal Immunol*, **2012**. 5(3): p. 232-9.

64.   Brandtzaeg, P., H. Kiyono, *et al.*, Terminology: nomenclature of mucosa-associated lymphoid tissue. *Mucosal Immunol*, **2008**. 1(1): p. 31-7.

65.   Mabbott, N.A., D.S. Donaldson, *et al.*, Microfold (M) cells: important immunosurveillance posts in the intestinal epithelium. *Mucosal Immunol*, **2013**. 6(4): p. 666-77.

66.   Niess, J.H., S. Brand, *et al.*, CX3CR1-mediated dendritic cell access to the intestinal lumen and bacterial clearance. *Science*, **2005**. 307(5707): p. 254-8.

67.   Rescigno, M., M. Urbano, *et al.*, Dendritic cells express tight junction proteins and penetrate gut epithelial monolayers to sample bacteria. *Nat Immunol*, **2001**. 2(4): p. 361-7.

68.   McDole, J.R., L.W. Wheeler, *et al.*, Goblet cells deliver luminal antigen to CD103+ dendritic cells in the small intestine. *Nature*, **2012**. 483(7389): p. 345-9.

69.   Flannagan, R.S., G. Cosio, and S. Grinstein, Antimicrobial mechanisms of phagocytes and bacterial evasion strategies. *Nat Rev Microbiol*, **2009**. 7(5): p. 355-66.

70. Parham, P., *The immune system*. **2014**: Garland Science.

71. Alexander-Miller, M.A., G.R. Leggatt*, et al.*, Role of antigen, CD8, and cytotoxic T lymphocyte (CTL) avidity in high dose antigen induction of apoptosis of effector CTL. *J Exp Med*, **1996**. 184(2): p. 485-92.

72. Macdonald, T.T. and G. Monteleone, Immunity, inflammation, and allergy in the gut. *Science*, **2005**. 307(5717): p. 1920-5.

73. Aviello, G. and U.G. Knaus, NADPH oxidases and ROS signaling in the gastrointestinal tract. *Mucosal immunology*, **2018**. 11(4): p. 1011-1023.

74. Aviello, G. and U.G. Knaus, ROS in gastrointestinal inflammation: Rescue Or Sabotage? *Br J Pharmacol*, **2017**. 174(12): p. 1704-1718.

75. Hart, B.A., S. Copray, and I. Philippens, Apocynin, a low molecular oral treatment for neurodegenerative disease. *Biomed Res Int*, **2014**. 2014: p. 298020.

76. Matziouridou, C., S.D.C. Rocha*, et al.*, iNOS- and NOX1-dependent ROS production maintains bacterial homeostasis in the ileum of mice. *Mucosal Immunol*, **2018**. 11(3): p. 774-784.

77. Bedard, K. and K.H. Krause, The NOX family of ROS-generating NADPH oxidases: physiology and pathophysiology. *Physiol Rev*, **2007**. 87(1): p. 245-313.

78. Shaked, H., L.J. Hofseth*, et al.*, Chronic epithelial NF-kappaB activation accelerates APC loss and intestinal tumor initiation through iNOS up-regulation. *Proc Natl Acad Sci U S A*, **2012**. 109(35): p. 14007-12.

79. Ha, E.M., C.T. Oh*, et al.*, A direct role for dual oxidase in *Drosophila* gut immunity. *Science*, **2005**. 310(5749): p. 847-50.

80. Chávez, V., A. Mohri-Shiomi, and D.A. Garsin, Ce-Duox1/BLI-3 generates reactive oxygen species as a protective innate immune mechanism in Caenorhabditis elegans. *Infection and immunity*, **2009**. 77(11): p. 4983-4989.

81. Grasberger, H., J. Gao*, et al.*, Increased Expression of DUOX2 Is an Epithelial Response to Mucosal Dysbiosis Required for Immune Homeostasis in Mouse Intestine. *Gastroenterology*, **2015**. 149(7): p. 1849-59.

82. Bedard, K. and K.-H. Krause, The NOX Family of ROS-Generating NADPH Oxidases: Physiology and Pathophysiology. **2007**. 87(1): p. 245-313.

83. Kato, M., M. Marumo*, et al.*, The ROS-generating oxidase Nox1 is required for epithelial restitution following colitis. *Exp Anim*, **2016**. 65(3): p. 197-205.

84. Pircalabioru, G., G. Aviello*, et al.*, Defensive Mutualism Rescues NADPH Oxidase Inactivation in Gut Infection. *Cell Host Microbe*, **2016**. 19(5): p. 651-63.

85. Botteaux, A., C. Hoste*, et al.*, Potential role of Noxes in the protection of mucosae: H2O2 as abacterial repellent. *Microbes and infection*, **2009**. 11(5): p. 537-544.

86. Hayes, P., S. Dhillon*, et al.*, Defects in NADPH Oxidase Genes NOX1 and DUOX2 in Very Early Onset Inflammatory Bowel Disease. *Cell Mol Gastroenterol Hepatol*, **2015**. 1(5): p. 489-502.

87.　Alberti, K.G., R.H. Eckel*, et al.*, Harmonizing the metabolic syndrome: a joint interim statement of the International Diabetes Federation Task Force on Epidemiology and Prevention; National Heart, Lung, and Blood Institute; American Heart Association; World Heart Federation; International Atherosclerosis Society; and International Association for the Study of Obesity. *Circulation*, **2009**. 120(16): p. 1640-5.

88.　Bäckhed, F., H. Ding*, et al.*, The gut microbiota as an environmental factor that regulates fat storage. *Proceedings of the national academy of sciences*, **2004**. 101(44): p. 15718-15723.

89.　Turnbaugh, P.J., R.E. Ley*, et al.*, An obesity-associated gut microbiome with increased capacity for energy harvest. *Nature*, **2006**. 444(7122): p. 1027-31.

90.　Backhed, F., R.E. Ley*, et al.*, Host-bacterial mutualism in the human intestine. *Science*, **2005**. 307(5717): p. 1915-20.

91.　Kennedy, A., K. Martinez*, et al.*, Saturated fatty acid-mediated inflammation and insulin resistance in adipose tissue: mechanisms of action and implications. *J Nutr*, **2009**. 139(1): p. 1-4.

92.　Tomas, J., C. Mulet*, et al.*, High-fat diet modifies the PPAR-gamma pathway leading to disruption of microbial and physiological ecosystem in murine small intestine. *Proc Natl Acad Sci U S A*, **2016**. 113(40): p. E5934-E5943.

93.　Lam, Y.Y., C.W. Ha*, et al.*, Effects of dietary fat profile on gut permeability and microbiota and their relationships with metabolic changes in mice. *Obesity (Silver Spring)*, **2015**. 23(7): p. 1429-39.

94.　Lam, Y.Y., C.W. Ha*, et al.*, Increased gut permeability and microbiota change associate with mesenteric fat inflammation and metabolic dysfunction in diet-induced obese mice. *PLoS One*, **2012**. 7(3): p. e34233.

95.　de La Serre, C.B., C.L. Ellis*, et al.*, Propensity to high-fat diet-induced obesity in rats is associated with changes in the gut microbiota and gut inflammation. *American Journal of Physiology-Gastrointestinal and Liver Physiology*, **2010**. 299(2): p. G440-G448.

96.　Christ, A., M. Lauterbach, and E. Latz, Western diet and the immune system: an inflammatory connection. *Immunity*, **2019**. 51(5): p. 794-811.

97.　Cani, P.D., J. Amar*, et al.*, Metabolic endotoxemia initiates obesity and insulin resistance. *Diabetes*, **2007**. 56(7): p. 1761-72.

98.　Cani, P.D., R. Bibiloni*, et al.*, Changes in gut microbiota control metabolic endotoxemia-induced inflammation in high-fat diet-induced obesity and diabetes in mice. *Diabetes*, **2008**. 57(6): p. 1470-81.

99.　Amar, J., C. Chabo*, et al.*, Intestinal mucosal adherence and translocation of commensal bacteria at the early onset of type 2 diabetes: molecular mechanisms and probiotic treatment. *EMBO Mol Med*, **2011**. 3(9): p. 559-72.

100.　Hamilton, M.K., G. Boudry*, et al.*, Changes in intestinal barrier function and gut microbiota in high-fat diet-fed rats are dynamic and region dependent. *Am J Physiol Gastrointest Liver Physiol*, **2015**. 308(10): p. G840-51.

101. Ko, C.-W., J. Qu, *et al.*, Regulation of intestinal lipid metabolism: current concepts and relevance to disease. *Nature Reviews Gastroenterology & Hepatology*, **2020**: p. 1-15.

102. Buckley, J.D. and P.R. Howe, Anti-obesity effects of long-chain omega-3 polyunsaturated fatty acids. *Obes Rev*, **2009**. 10(6): p. 648-59.

103. Oh, D.Y., S. Talukdar, *et al.*, GPR120 is an omega-3 fatty acid receptor mediating potent anti-inflammatory and insulin-sensitizing effects. *Cell*, **2010**. 142(5): p. 687-98.

104. Caesar, R., V. Tremaroli, *et al.*, Crosstalk between Gut Microbiota and Dietary Lipids Aggravates WAT Inflammation through TLR Signaling. *Cell Metab*, **2015**. 22(4): p. 658-68.

105. Kim, K.A., W. Gu, *et al.*, High fat diet-induced gut microbiota exacerbates inflammation and obesity in mice via the TLR4 signaling pathway. *PLoS One*, **2012**. 7(10): p. e47713.

106. Saberi, M., N.B. Woods, *et al.*, Hematopoietic cell-specific deletion of toll-like receptor 4 ameliorates hepatic and adipose tissue insulin resistance in high-fat-fed mice. *Cell Metab*, **2009**. 10(5): p. 419-29.

107. de Wit, N.J., H. Bosch-Vermeulen, *et al.*, The role of the small intestine in the development of dietary fat-induced obesity and insulin resistance in C57BL/6J mice. *BMC Med Genomics*, **2008**. 1(1): p. 14.

108. Wang, X., N. Ota, *et al.*, Interleukin-22 alleviates metabolic disorders and restores mucosal immunity in diabetes. *Nature*, **2014**. 514(7521): p. 237-41.

109. Garidou, L., C. Pomie, *et al.*, The Gut Microbiota Regulates Intestinal CD4 T Cells Expressing RORgammat and Controls Metabolic Disease. *Cell Metab*, **2015**. 22(1): p. 100-12.

110. Netea, M.G., L.A. Joosten, *et al.*, Deficiency of interleukin-18 in mice leads to hyperphagia, obesity and insulin resistance. *Nat Med*, **2006**. 12(6): p. 650-6.

111. Monteiro-Sepulveda, M., S. Touch, *et al.*, Jejunal T Cell Inflammation in Human Obesity Correlates with Decreased Enterocyte Insulin Signaling. *Cell Metab*, **2015**. 22(1): p. 113-24.

112. Johnson, A.M., A. Costanzo, *et al.*, High fat diet causes depletion of intestinal eosinophils associated with intestinal permeability. *PLoS One*, **2015**. 10(4): p. e0122195.

113. Luck, H., S. Tsai, *et al.*, Regulation of obesity-related insulin resistance with gut anti-inflammatory agents. *Cell Metab*, **2015**. 21(4): p. 527-42.

114. Cong, Y., T. Feng, *et al.*, A dominant, coordinated T regulatory cell-IgA response to the intestinal microbiota. *Proc Natl Acad Sci U S A*, **2009**. 106(46): p. 19256-61.

115. Kless, C., V.M. Muller, *et al.*, Diet-induced obesity causes metabolic impairment independent of alterations in gut barrier integrity. *Mol Nutr Food Res*, **2015**. 59(5): p. 968-78.

116. Ding, S., M.M. Chi, *et al.*, High-fat diet: bacteria interactions promote intestinal inflammation which precedes and correlates with obesity and insulin resistance in mouse. *PloS one*, **2010**. 5(8): p. e12191.

117. Li, H., C. Lelliott, *et al.*, Intestinal, adipose, and liver inflammation in diet-induced obese mice. *Metabolism*, **2008**. 57(12): p. 1704-10.

118.   Winer, D.A., H. Luck*, et al.*, The Intestinal Immune System in Obesity and Insulin Resistance. *Cell Metab*, **2016**. 23(3): p. 413-26.

119.   Araújo, J.R., J. Tomas*, et al.*, Impact of high-fat diet on the intestinal microbiota and small intestinal physiology before and after the onset of obesity. *Biochimie* **2017**. 141: p. 97-106.

120.   Martinez-Guryn, K., N. Hubert*, et al.*, Small Intestine Microbiota Regulate Host Digestive and Absorptive Adaptive Responses to Dietary Lipids. *Cell Host Microbe*, **2018**. 23(4): p. 458-469 e5.

121.   Zhao, L., F. Zhang*, et al.*, Gut bacteria selectively promoted by dietary fibers alleviate type 2 diabetes. *Science*, **2018**. 359(6380): p. 1151-1156.

122.   Singh, R.K., H.W. Chang*, et al.*, Influence of diet on the gut microbiome and implications for human health. *J Transl Med*, **2017**. 15(1): p. 73.

123.   Sonnenburg, E.D. and J.L.J.C.m. Sonnenburg, Starving our microbial self: the deleterious consequences of a diet deficient in microbiota-accessible carbohydrates. *Cell metabolism*, **2014**. 20(5): p. 779-786.

124.   Kuo, S.-M., The interplay between fiber and the intestinal microbiome in the inflammatory response. *Advances in Nutrition*, **2013**. 4(1): p. 16-28.

125.   Roberfroid, M., Prebiotics: the concept revisited. *J Nutr*, **2007**. 137(3 Suppl 2): p. 830S-7S.

126.   Karaki, S.-i., R. Mitsui*, et al.*, Short-chain fatty acid receptor, GPR43, is expressed by enteroendocrine cells and mucosal mast cells in rat intestine. *Cell and tissue research*, **2006**. 324(3): p. 353-360.

127.   Arpaia, N., C. Campbell*, et al.*, Metabolites produced by commensal bacteria promote peripheral regulatory T-cell generation. *Nature*, **2013**. 504(7480): p. 451-455.

128.   Chassaing, B., J. Miles-Brown*, et al.*, Lack of soluble fiber drives diet-induced adiposity in mice. *Am J Physiol Gastrointest Liver Physiol*, **2015**. 309(7): p. G528-41.

129.   Tsao, R., Chemistry and biochemistry of dietary polyphenols. *Nutrients*, **2010**. 2(12): p. 1231-46.

130.   Van Hul, M. and P.D. Cani, Targeting Carbohydrates and Polyphenols for a Healthy Microbiome and Healthy Weight. *Curr Nutr Rep*, **2019**. 8(4): p. 307-316.

131.   Pandey, K.B. and S.I. Rizvi, Plant polyphenols as dietary antioxidants in human health and disease. *Oxidative medicine and cellular longevity*, **2009**. 2(5): p. 270-278.

132.   Scalbert, A., I.T. Johnson, and M. Saltmarsh, Polyphenols: antioxidants and beyond. *Am J Clin Nutr*, **2005**. 81(1 Suppl): p. 215S-217S.

133.   Manach, C., G. Williamson*, et al.*, Bioavailability and bioefficacy of polyphenols in humans. I. Review of 97 bioavailability studies. *Am J Clin Nutr*, **2005**. 81(1 Suppl): p. 230S-242S.

134.   Moco, S., F.P. Martin, and S. Rezzi, Metabolomics view on gut microbiome modulation by polyphenol-rich foods. *J Proteome Res*, **2012**. 11(10): p. 4781-90.

135. Roopchand, D.E., R.N. Carmody, *et al.*, Dietary Polyphenols Promote Growth of the Gut Bacterium *Akkermansia muciniphila* and Attenuate High-Fat Diet-Induced Metabolic Syndrome. *Diabetes*, **2015**. 64(8): p. 2847-58.

136. Anhe, F.F., D. Roy, *et al.*, A polyphenol-rich cranberry extract protects from diet-induced obesity, insulin resistance and intestinal inflammation in association with increased *Akkermansia* spp. population in the gut microbiota of mice. *Gut*, **2015**. 64(6): p. 872-83.

137. O'Keefe, J.H., S.K. Bhatti, *et al.*, Effects of habitual coffee consumption on cardiometabolic disease, cardiovascular health, and all-cause mortality. *J Am Coll Cardiol*, **2013**. 62(12): p. 1043-1051.

138. Akash, M.S., K. Rehman, and S. Chen, Effects of coffee on type 2 diabetes mellitus. *Nutrition*, **2014**. 30(7-8): p. 755-63.

139. de Mejia, E.G. and M.V. Ramirez-Mares, Impact of caffeine and coffee on our health. *Trends in Endocrinology & Metabolism*, **2014**. 25(10): p. 489-492.

140. Bohn, S.K., R. Blomhoff, and I. Paur, Coffee and cancer risk, epidemiological evidence, and molecular mechanisms. *Mol Nutr Food Res*, **2014**. 58(5): p. 915-30.

141. Gunter, M.J., N. Murphy, *et al.*, Coffee Drinking and Mortality in 10 European Countries: A Multinational Cohort Study. *Ann Intern Med*, **2017**. 167(4): p. 236-247.

142. Costabile, A., K. Sarnsamak, and A.C. Hauge-Evans, Coffee, type 2 diabetes and pancreatic islet function–A mini-review. *Journal of Functional Foods*, **2018**. 45: p. 409-416.

143. Kempf, K., C. Herder, *et al.*, Effects of coffee consumption on subclinical inflammation and other risk factors for type 2 diabetes: a clinical trial. *Am J Clin Nutr*, **2010**. 91(4): p. 950-7.

144. Gniechwitz, D., B. Brueckel, *et al.*, Coffee dietary fiber contents and structural characteristics as influenced by coffee type and technological and brewing procedures. *Journal of agricultural and food chemistry*, **2007**. 55(26): p. 11027-11034.

145. Smrke, S., S.E. Opitz, *et al.*, How does roasting affect the antioxidants of a coffee brew? Exploring the antioxidant capacity of coffee via on-line antioxidant assays coupled with size exclusion chromatography. *Food & function*, **2013**. 4(7): p. 1082-1092.

146. Naidoo, N., C. Chen, *et al.*, Cholesterol-raising diterpenes in types of coffee commonly consumed in Singapore, Indonesia and India and associations with blood lipids: a survey and cross sectional study. *Nutr J*, **2011**. 10(1): p. 48.

147. Chvasta, T.E. and A.R. Cooke, Emptying and absorption of caffeine from the human stomach. *Gastroenterology*, **1971**. 61(6): p. 838-43.

148. Keijzers, G.B., B.E. De Galan, *et al.*, Caffeine can decrease insulin sensitivity in humans. *Diabetes care*, **2002**. 25(2): p. 364-369.

149. van Dam, R.M. and E.J. Feskens, Coffee consumption and risk of type 2 diabetes mellitus. *Lancet*, **2002**. 360(9344): p. 1477-8.

150. Huxley, R., C.M. Lee, *et al.*, Coffee, decaffeinated coffee, and tea consumption in relation to incident type 2 diabetes mellitus: a systematic review with meta-analysis. *Arch Intern Med*, **2009**. 169(22): p. 2053-63.

151.   Pereira, M.A., E.D. Parker, and A.R. Folsom, Coffee consumption and risk of type 2 diabetes mellitus: an 11-year prospective study of 28 812 postmenopausal women. *Arch Intern Med*, **2006**. 166(12): p. 1311-6.

152.   de Sotillo, D.V.R. and M. Hadley, Chlorogenic acid modifies plasma and liver concentrations of: cholesterol, triacylglycerol, and minerals in (fa/fa) Zucker rats. *The Journal of nutritional biochemistry*, **2002**. 13(12): p. 717-726.

153.   Kono, Y., K. Kobayashi*, et al.*, Antioxidant activity of polyphenolics in diets. Rate constants of reactions of chlorogenic acid and caffeic acid with reactive species of oxygen and nitrogen. *Biochim Biophys Acta*, **1997**. 1335(3): p. 335-42.

154.   Olthof, M.R., P.C. Hollman*, et al.*, Chlorogenic acid, quercetin-3-rutinoside and black tea phenols are extensively metabolized in humans. *J Nutr*, **2003**. 133(6): p. 1806-14.

155.   Zhernakova, A., A. Kurilshikov*, et al.*, Population-based metagenomics analysis reveals markers for gut microbiome composition and diversity. *Science*, **2016**. 352(6285): p. 565-9.

156.   Mills, C.E., X. Tzounis*, et al.*, In vitro colonic metabolism of coffee and chlorogenic acid results in selective changes in human faecal microbiota growth. *Br J Nutr*, **2015**. 113(8): p. 1220-7.

157.   Chacar, S., T. Itani*, et al.*, The Impact of Long-Term Intake of Phenolic Compounds-Rich Grape Pomace on Rat Gut Microbiota. *J Food Sci*, **2018**. 83(1): p. 246-251.

158.   Xie, M., G. Chen*, et al.*, Modulating Effects of Dicaffeoylquinic Acids from *Ilex kudingcha* on Intestinal Microecology in Vitro. *J Agric Food Chem*, **2017**. 65(47): p. 10185-10196.

159.   Cowan, T.E., M.S. Palmnas*, et al.*, Chronic coffee consumption in the diet-induced obese rat: impact on gut microbiota and serum metabolomics. *J Nutr Biochem*, **2014**. 25(4): p. 489-95.

160.   Nishitsuji, K., S. Watanabe*, et al.*, Effect of coffee or coffee components on gut microbiome and short-chain fatty acids in a mouse model of metabolic syndrome. *Sci Rep*, **2018**. 8(1): p. 16173.

161.   Fukushima, Y., M. Kasuga*, et al.*, Effects of coffee on inflammatory cytokine gene expression in mice fed high-fat diets. *J Agric Food Chem*, **2009**. 57(23): p. 11100-5.

162.   Kastl Jr, A.J., N.A. Terry*, et al.*, The structure and function of the human small intestinal microbiota: current understanding and future directions. *Cellular and molecular gastroenterology and hepatology*, **2020**. 9(1): p. 33-45.

163.   Martinez-Guryn, K., N. Hubert*, et al.*, Small Intestine Microbiota Regulate Host Digestive and Absorptive Adaptive Responses to Dietary Lipids. *Cell Host Microbe*, **2018**. 23(4): p. 458-469.

164.   Rizzatti, G., L.R. Lopetuso*, et al.*, *Proteobacteria*: A Common Factor in Human Diseases. *Biomed Res Int*, **2017**. 2017: p. 9351507.

165.   Ghoshal, S., J. Witta*, et al.*, Chylomicrons promote intestinal absorption of lipopolysaccharides. *J Lipid Res*, **2009**. 50(1): p. 90-7.

166.   Grube, B.J., C.G. Cochane*, et al.*, Lipopolysaccharide binding protein expression in primary human hepatocytes and HepG2 hepatoma cells. *J Biol Chem*, **1994**. 269(11): p. 8477-82.

167.   Kielland, A., T. Blom, *et al.*, In vivo imaging of reactive oxygen and nitrogen species in inflammation using the luminescent probe L-012. *Free Radic Biol Med*, **2009**. 47(6): p. 760-766.

168.   Zigmond, E. and S. Jung, Intestinal macrophages: well educated exceptions from the rule. *Trends Immunol*, **2013**. 34(4): p. 162-8.

169.   Vaishnava, S., C.L. Behrendt, *et al.*, Paneth cells directly sense gut commensals and maintain homeostasis at the intestinal host-microbial interface. *Proc Natl Acad Sci U S A*, **2008**. 105(52): p. 20858-63.

170.   Araújo, J.R., J. Tomas, *et al.*, Impact of high-fat diet on the intestinal microbiota and small intestinal physiology before and after the onset of obesity. *Biochimie*, **2017**. 141: p. 97-106.

171.   Chang, E.B. and K. Martinez-Guryn, Small intestinal microbiota: the neglected stepchild needed for fat digestion and absorption. *Gut Microbes*, **2019**. 10(2): p. 235-240.

172.   Meng, Y., X. Li, *et al.*, Effects of Different Diets on Microbiota in The Small Intestine Mucus and Weight Regulation in Rats. *Sci Rep*, **2019**. 9(1): p. 8500.

173.   Gurwara, S., A. Dai, *et al.*, Caffeine Consumption and the Colonic Mucosa-Associated Gut Microbiota. *The American Journal of Gastroenterology*, **2019**. 114(p): p. 119-120.

174.   Capek, P., E. Paulovicova, *et al.*, Coffea arabica instant coffee--chemical view and immunomodulating properties. *Carbohydr Polym*, **2014**. 103: p. 418-26.

175.   Ozdal, T., D.A. Sela, *et al.*, The Reciprocal Interactions between Polyphenols and Gut Microbiota and Effects on Bioaccessibility. *Nutrients*, **2016**. 8(2): p. 78.

176.   Duda-Chodak, A., T. Tarko, *et al.*, Interaction of dietary compounds, especially polyphenols, with the intestinal microbiota: a review. *Eur J Nutr*, **2015**. 54(3): p. 325-41.

177.   Wu, Y., W. Liu, *et al.*, Dietary chlorogenic acid regulates gut microbiota, serum-free amino acids and colonic serotonin levels in growing pigs. *Int J Food Sci Nutr*, **2018**. 69(5): p. 566-573.

178.   Wang, Z., K.L. Lam, *et al.*, Chlorogenic acid alleviates obesity and modulates gut microbiota in high-fat-fed mice. *Food Sci Nutr*, **2019**. 7(2): p. 579-588.

179.   Gniechwitz, D., B. Brueckel, *et al.*, Coffee dietary fiber contents and structural characteristics as influenced by coffee type and technological and brewing procedures. *J Agric Food Chem*, **2007**. 55(26): p. 11027-34.

180.   Zhao, W., L. Ma, *et al.*, Caffeine Inhibits NLRP3 Inflammasome Activation by Suppressing MAPK/NF-κB and A2aR Signaling in LPS-Induced THP-1 Macrophages. *Int J Biol Sci*, **2019**. 15(8): p. 1571-1581.

181.   Paur, I., T.R. Balstad, and R. Blomhoff, Degree of roasting is the main determinant of the effects of coffee on NF-κB and EpRE. *Free Radical Biology and Medicine*, **2010**. 48(9): p. 1218-1227.

182.   Zhang, P., H. Jiao, *et al.*, Chlorogenic Acid Ameliorates Colitis and Alters Colonic Microbiota in a Mouse Model of Dextran Sulfate Sodium-Induced Colitis. *Frontiers in Physiology*, **2019**. 10: p. 325.

183. Chassaing, B., G. Srinivasan, *et al.*, Fecal lipocalin 2, a sensitive and broadly dynamic non-invasive biomarker for intestinal inflammation. *PLoS One*, **2012**. 7(9): p. e44328.

184. Aviello, G., A.K. Singh, *et al.*, Colitis susceptibility in mice with reactive oxygen species deficiency is mediated by mucus barrier and immune defense defects. *Mucosal Immunology*, **2019**. 12(6): p. 1316-1326.

185. Makhezer, N., M.B. Khemis, *et al.*, NOX1-derived ROS drive the expression of Lipocalin-2 in colonic epithelial cells in inflammatory conditions. *Mucosal Immunology*, **2019**. 12(1): p. 117-131.

186. Johansson, M.E., J.K. Gustafsson, *et al.*, Bacteria penetrate the inner mucus layer before inflammation in the dextran sulfate colitis model. *PloS one*, **2010**. 5(8): p. e12238.

187. Singh, V., B.S. Yeoh, *et al.*, Microbiota-inducible Innate Immune, Siderophore Binding Protein Lipocalin 2 is Critical for Intestinal Homeostasis. *Cell Mol Gastroenterol Hepatol*, **2016**. 2(4): p. 482-498 e6.

188. Li, M., Y. Wu, *et al.*, Initial gut microbiota structure affects sensitivity to DSS-induced colitis in a mouse model. *Science China Life Sciences*, **2018**. 61(7): p. 762-769.

189. Derrien, M., P. Van Baarlen, *et al.*, Modulation of mucosal immune response, tolerance, and proliferation in mice colonized by the mucin-degrader *Akkermansia muciniphila*. *Frontiers in microbiology*, **2011**. 2: p. 166.

190. Derrien, M., M.C. Collado, *et al.*, The Mucin degrader *Akkermansia muciniphila* is an abundant resident of the human intestinal tract. *Appl. Environ. Microbiol.*, **2008**. 74(5): p. 1646-1648.

191. Coant, N., S. Ben Mkaddem, *et al.*, NADPH oxidase 1 modulates WNT and NOTCH1 signaling to control the fate of proliferative progenitor cells in the colon. *Mol Cell Biol*, **2010**. 30(11): p. 2636-50.

192. Liang, Y.-N., J.-G. Yu, *et al.*, Indigo Naturalis Ameliorates Dextran Sulfate Sodium-Induced Colitis in Mice by Modulating the Intestinal Microbiota Community. *Molecules*, **2019**. 24(22): p. 4086.

193. Sokol, H., B. Pigneur, *et al.*, *Faecalibacterium prausnitzii* is an anti-inflammatory commensal bacterium identified by gut microbiota analysis of Crohn disease patients. *Proceedings of the National Academy of Sciences*, **2008**. 105(43): p. 16731-16736.

194. Chen, C., M. Perez de Nanclares, *et al.*, Identification of redox imbalance as a prominent metabolic response elicited by rapeseed feeding in swine metabolome. *Journal of Animal Science*, **2018**. 96(5): p. 1757-1768.

195. Fomenky, B.E., D.N. Do, *et al.*, Direct-fed microbial supplementation influences the bacteria community composition of the gastrointestinal tract of pre-and post-weaned calves. *Scientific Reports*, **2018**. 8(1): p. 1-21.

196. Liu, X.-c., Q. Mei, *et al.*, Balsalazine decreases intestinal mucosal permeability of dextran sulfate sodium-induced colitis in mice. *Acta pharmacologica Sinica*, **2009**. 30(7): p. 987-993.

197. Chun-Sai-Er Wang, W.-B., H.-Y.W. Li, *et al.*, VSL# 3 can prevent ulcerative colitis-associated carcinogenesis in mice. *World journal of gastroenterology*, **2018**. 24(37): p. 4254.

198. Zhao, H., X. Jiang, and W. Chu, Shifts in the gut microbiota of mice in response to dexamethasone administration. *International microbiology: the official journal of the Spanish Society for Microbiology*, **2020**.

199. Parker, B.J., P.A. Wearsch, *et al.*, The Genus *Alistipes*: Gut Bacteria With Emerging Implications to Inflammation, Cancer, and Mental Health. *Frontiers in Immunology*, **2020**. 11.

200. Tremaroli, V. and F. Backhed, Functional interactions between the gut microbiota and host metabolism. *Nature*, **2012**. 489(7415): p. 242-9.

201. Turnbaugh, P.J., V.K. Ridaura, *et al.*, The effect of diet on the human gut microbiome: a metagenomic analysis in humanized gnotobiotic mice. *Sci Transl Med*, **2009**. 1(6): p. 6ra14.

202. Moya-Perez, A., A. Neef, and Y. Sanz, Bifidobacterium pseudocatenulatum CECT 7765 Reduces Obesity-Associated Inflammation by Restoring the Lymphocyte-Macrophage Balance and Gut Microbiota Structure in High-Fat Diet-Fed Mice. *PLoS One*, **2015**. 10(7): p. e0126976.

203. Everard, A., C. Belzer, *et al.*, Cross-talk between *Akkermansia muciniphila* and intestinal epithelium controls diet-induced obesity. *Proc Natl Acad Sci U S A*, **2013**. 110(22): p. 9066-71.

204. Jiang, T., X. Gao, *et al.*, Apple-Derived Pectin Modulates Gut Microbiota, Improves Gut Barrier Function, and Attenuates Metabolic Endotoxemia in Rats with Diet-Induced Obesity. *Nutrients*, **2016**. 8(3): p. 126.

205. Cao, Y., S. Zou, *et al.*, Hypoglycemic activity of the Baker's yeast beta-glucan in obese/type 2 diabetic mice and the underlying mechanism. *Mol Nutr Food Res*, **2016**. 60(12): p. 2678-2690.

206. Everard, A., V. Lazarevic, *et al.*, Responses of gut microbiota and glucose and lipid metabolism to prebiotics in genetic obese and diet-induced leptin-resistant mice. *Diabetes*, **2011**. 60(11): p. 2775-86.

207. Suez, J., H. Shapiro, and E. Elinav, Role of the microbiome in the normal and aberrant glycemic response. *Clinical Nutrition Experimental*, **2016**. 6: p. 59-73.

208. Chapman, B.C., H.B. Moore, *et al.*, Fecal microbiota transplant in patients with *Clostridium difficile* infection: A systematic review. *J Trauma Acute Care Surg*, **2016**. 81(4): p. 756-64.

209. Carlucci, C., E.O. Petrof, and E. Allen-Vercoe, Fecal Microbiota-based Therapeutics for Recurrent *Clostridium difficile* Infection, Ulcerative Colitis and Obesity. *EBioMedicine*, **2016**. 13: p. 37-45.

210. Vrieze, A., E. Van Nood, *et al.*, Transfer of intestinal microbiota from lean donors increases insulin sensitivity in individuals with metabolic syndrome. *Gastroenterology*, **2012**. 143(4): p. 913-6 e7.

Paper I

Small intestine microbiota and immune status in high-fat dieting mice

Sérgio D. C. Rocha[1], Chrysoula Kielland[1], Silje Harvei[1], Harald Carlsen[1], Anders Kielland[1]

[1]*Faculty of Chemistry, Biotechnology and Food Science, Norwegian University of Life Sciences, P. O. Box 5003, N-1432 Ås, Norway*

Abstract

The small intestine's essential role is to secure adequate nutrient uptake from the diet. Importantly, the small intestine is also in intimate contact with microbes which both are formed by the diet and can affect the function and immune state of the small intestinal tissue. Relatively few studies have explored how diet affects the small intestinal microbiota and its interaction with the host. We have here fed mice high-fat diet (HFD) or low-fat control diet (LFD) to explore changes in microbiota composition in different segments of the small intestine and further assessed the intestinal barrier function and immune status. Both diets had the same fiber content and only differed in the amount of fat and corn starch.

Compared to the LFD mice, the HFD group presented an altered gut microbiota towards a dysbiotic profile with a higher *Firmicutes* to *Bacteriodetes* ratio and an increased abundance of proteobacteria as the main features. The amount of T-regulatory cells were reduced and the proportion of pro-inflammatory macrophages assessed by expression of CX3CR1 and MHCII was increased. In line with this, the cytokines TNFa, IL1b, TGFb and CCL5 were elevated and the production of antimicrobial cytotoxic reactive oxygen species was increased. Expressions of the tight junction proteins and Reg3g were increased and FITC dextran 4 influx was decreased, suggesting a strengthened barrier of the small intestinal wall.

In conclusion, we here show that HFD promotes a dysbiotic small intestinal microbiota profile with a resultant defensive host response possibly ameliorating putative detrimental systemic effects.

Introduction

The small intestinal epithelial layer is absorbing most of the food nutrients and has for that purpose a huge surface area in intimate contact with the luminal content of the small intestine (SI). However, the lumen is also the habitat of a vast number of microbes that are ideally kept there by elaborate barriers to prevent leakage into the bloodstream. It is therefore essential with a well-controlled host-microbe interaction in maintaining a healthy homeostatic environment in the SI. Here, we explore the influence of this homeostasis by a high-fat diet (HFD) with respect to microbial composition, barrier permeability and immune activity of the SI. This is of relevance for health as local intestinal conditions are linked to systemic metabolic diseases such as obesity and glucose dysregulation, cardiovascular disease and brain disorders [1-5].

Multiple pathways are suggested regarding the impact of HFD on systemic metabolic pathophysiology, however, induction of chronic low-grade inflammation through a shift in the microbial composition is highly emphasized and it is a likely contributor since diet-induced microbial and immunological changes in the intestine appear to affect immunity in other tissues relevant for metabolic disorders [6-14]. Compared to the large intestine, the SI is subjected to much fewer studies with the aim of scrutinizing the influence of HFD on changes in microbiota [15]. In HFD interventions of one week or shorter, analysis of bacterial changes in ileum has shown a reduction in the *Clostridiales* order [16]. In a four weeks intervention study, ileal *Bacteroidetes (S24-7 family)* and *Clostridia* were both decreased [17]. However, in another four weeks study the *Clostridiaceae* family was decreased in both jejunum and ileum as well as the ileal *Bacteroidetes*. Interestingly, in this study, they showed that the microbiota composition in jejunum shaped by the HFD feeding directly promoted lipid absorption [18]. In two other studies, the effects in the SI of a 12 weeks HFD intervention were examined. One of the studies found no changes in microbiota composition at the phylum level [19], whereas the other described a decrease in the relative abundance of *Bacteroidetes* and *Actinobacteria*, while *Proteobacteria* increased [20]. However, in neither of these studies, they discriminated between the different segments of the SI. In general, it is an unclear picture to what extent HFD changes the small intestinal microbiota, however, a switch in intestinal microbiota to fewer *Bacteroidetes* (mainly

characterized by the *S24-7* and *Bacteroidaceae* families) and more *Firmicutes* and *Proteobacteria* appears to be a relevant hypothesis. Such microbiota composition is referred to as dysbiosis which is regarded as a homeostatic microbial imbalance with potential detrimental influence on immune functions of the gut [3].

Most studies of the immune system and its response to HFD in the SI have characterized the cytokine profiles in mucosal tissue, and for the most, they suggest a pro-inflammatory profile by HFD [7]. This is most prominent in the distal part (ileum) and with longer interventions [15, 21] which also is in accordance with the observed increase in NF-κB activity along the SI during HFD feeding [10]. Furthermore, the T-cell population after long-time HFD feeding appears to shift to a more inflammatory profile as shown by reduced numbers of Foxp3/iTreg cells and increased numbers of Th1 cells, CD8 cells and Th17 cells [6, 22]. This is also most pronounced in the more distal part of the SI. However, eosinophils which normally accumulate during intestinal inflammation, are in fact depleted after only one week of HFD [23]. The effects of HFD on macrophages (MΦ) and dendritic cells (DC) are not thoroughly studied, and in the few studies undertaken in rodents, only minor changes are revealed [22, 23]. However, these studies did not distinguish between the different subsets of mononuclear phagocytic cells that have been reported to exist for both MΦ and DC in the intestine.

We have here selectively analyzed changes in the MΦ phenotype proportion in response to HFD. Macrophages of the SI in the adult stage are entirely of hematopoietic origin and are constantly replenished. When blood monocytes extravasate into the mucosa, they are described to undergo a four-stage differentiation process to mature mucosa resident MΦ [24]. The fully matured MΦ expressing high CX3CR1 and high MHCII lack some of the classical inflammatory response patterns, including secretion of proinflammatory cytokines and oxidative burst, typical for most other MΦ. [25, 26]. This more dampened intestinal MΦ still clear microbes and scavenge degraded cell material from the lamina propria, but without generating inflammatory responses of detrimental character to the surrounding tissue, making them well adapted in maintaining homeostasis and tolerance in the constantly immune challenged environment of the intestine. At the same time, mature MΦ are involved in the regulation of Treg cells and in the production of anti-

inflammatory cytokine IL-10 [26]. However, in intestinal inflammation, the monocytes entering the mucosa apparently do not reach full maturation but instead remain in the intermediate differential stages, presenting intermediate CX3CR1 and low to intermediate MHCII. Thus, these MΦ display typical proinflammatory behavior in response to TLR ligands by producing pro-inflammatory mediators, such as TNFα and IL-1β [25].

Previous studies of the effects of HFD on the SI show substantial variation and also some contradictions [7]. There are multiple potential explanations to this, but which dietary component the fat is substituted for in the control diet is highly relevant as this directly influences the deviation in the microbiota composition. In most studies, chow diet is used as control which differs in multiple components compared to HFD. Here, we have used a control diet that differs in only one component: the fat is substituted with corn starch.

In our study, we have fed mice either HFD or LFD for 18 weeks to better understand the diet-microbiota-host axis of the SI. We analyzed the segmental microbe composition along the SI to correlate this with changes of the host barrier and immune functionality. The HFD group had clearly an altered bacterial community structure in the distal segments where the *Firmicutes*/Bacteroidetes (F:B) ratio was increased accompanied by an increased abundance of *Proteobacteria*, which represents a dysbiotic environment. We further observed that genes involved with barrier function were upregulated as a response to HFD, as well as the upregulation of pro-inflammatory cytokines and increased pro-inflammatory immune cells in the SI of mice fed HFD.

Results

HFD induced obesity and insulin resistance

Eighteen weeks of HFD consumption resulted in increased body weight, increased adipocyte size of epididymal fat depots, and impaired glucose homeostasis compared to the LFD control group. HFD-fed mice gained 45% more weight than LFD-mice, and the difference in body weight became significant from the third week on of the dietary trial (**fig. 1a**). Energy intake in the HFD group was on average 20% higher than LFD mice (**fig. 1b**). We produced paraffin sections of epidydimal fat depots and we observed a significant increase in the average transversal sections, almost double, in mice fed HFD (**fig. 1c-d**). Regarding glucose regulation, the HFD group had higher fasting blood glucose levels and reduced insulin sensibility (**fig. 1e-f**). After insulin injection, glucose levels were always higher in HFD group (**fig. 1e**). During the oral glucose tolerance test, both groups presented a similar glucose peak after 15 minutes of administration (**fig. 1f**) and during the following time points, the HFD group had significantly higher glucose concentrations than the LFD group.
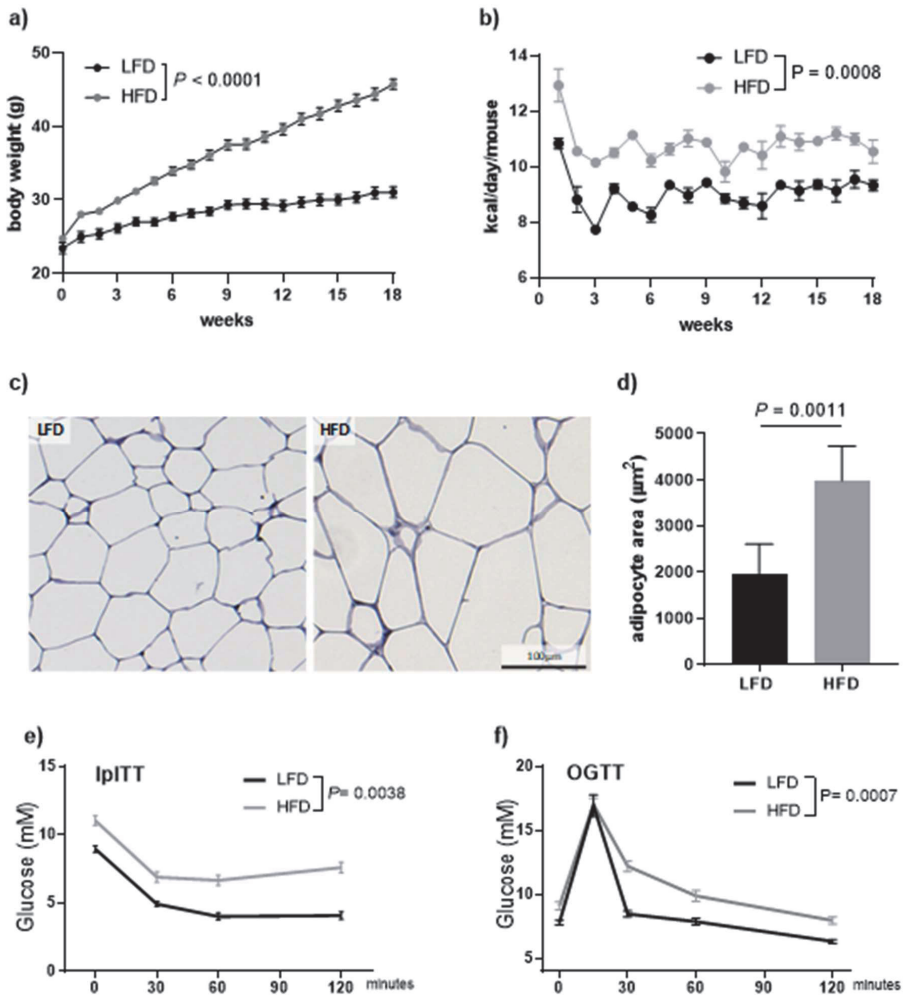
Figure 1. **Bodyweight and glucose regulation during long-term HFD consumption**. (**a**) Bodyweight development through 18 weeks (n=11-12); (**b**) Estimated energy intake (kcal) per mouse and (n=3); (**c**) Paraffin sections adipose tissue stained with H&E representative of the each group; (**d**) Area of transversal section (μm^2) of adipocytes in the epidydimal depot (n=6); (**e**) IpITT after 6 hours of fasting (n=11-12); (**f**) OgTT after 4 hours of fasting (n=11-12); (**a**, **b**, **e**, **f**) Values are presented as mean with s.e.m. Mixed-effect model with Sidak's multiple comparisons test; (**d**) Values are presented as mean with s.e.m. Unpaired t-test. HFD: high-fat diet, LFD: low-fat diet, IpITT: intra-peritoneal insulin tolerance test, OgTT: oral gavage tolerance test, s.e.m: standard error of the mean.

Consumption of HFD promoted a dysbiotic microbiota profile

To determine the impact of the HFD on the composition of the gut microbiota, we compared the 16S rRNA gene profile from intestinal samples of HFD and LFD mice. We observed that at the phylum level, the composition is different between the two diet groups throughout the GI tract (**fig. 2a-b**). Overall, there is a higher F:B ratio in the HFD group (**fig. 2c**). This difference is most pronounced in the ileum. In addition, there is an increase in the relative abundance of *Proteobacteria* in the ileal samples of the mice fed the HFD (**fig. 2b**). At the genus level, mice fed HFD presented an increase of *Peptoclostridium* in both jejunum and ileum, an uncultured genus of the *Lachnospiraceae* family in the jejunum and *Lactobacillus* in the ileum. At the same time, we observed a decrease of *Bacteroidales S24_7* and *Faecalibac*ulum in both jejunum and ileum (**fig. 2d**). The composition of the colon mucosa-associated microbiota appears to be relatively unaltered between the two groups, while the major alterations in the microbial composition of the colonic chyme are similar to the one observed in the ileum, namely increase of *Lactobacilli* and *Peptoclostridium* and decrease of *Bacteroidales S24-7* (**fig. 2d**).

The PCoA plots (**fig. 2e-i**) confirm the different microbial composition in the distal part of the GI tract of the two diet groups. While in the duodenum and jejunum the two groups appear to cluster together, in the ileum, as well as in the colonic chyme samples, the two groups cluster separately. Furthermore, we have evaluated the impact of the HFD on the α-diversity by analyzing the Shannon Index. We found no difference in the small intestinal segments, whereas in the colonic chyme samples the HFD group had a lower total number of different species in comparison to the control (**fig 2j**). In conclusion, these results indicate that the microbial colonization of the whole gut becomes more dysbiotic in mice fed HFD.
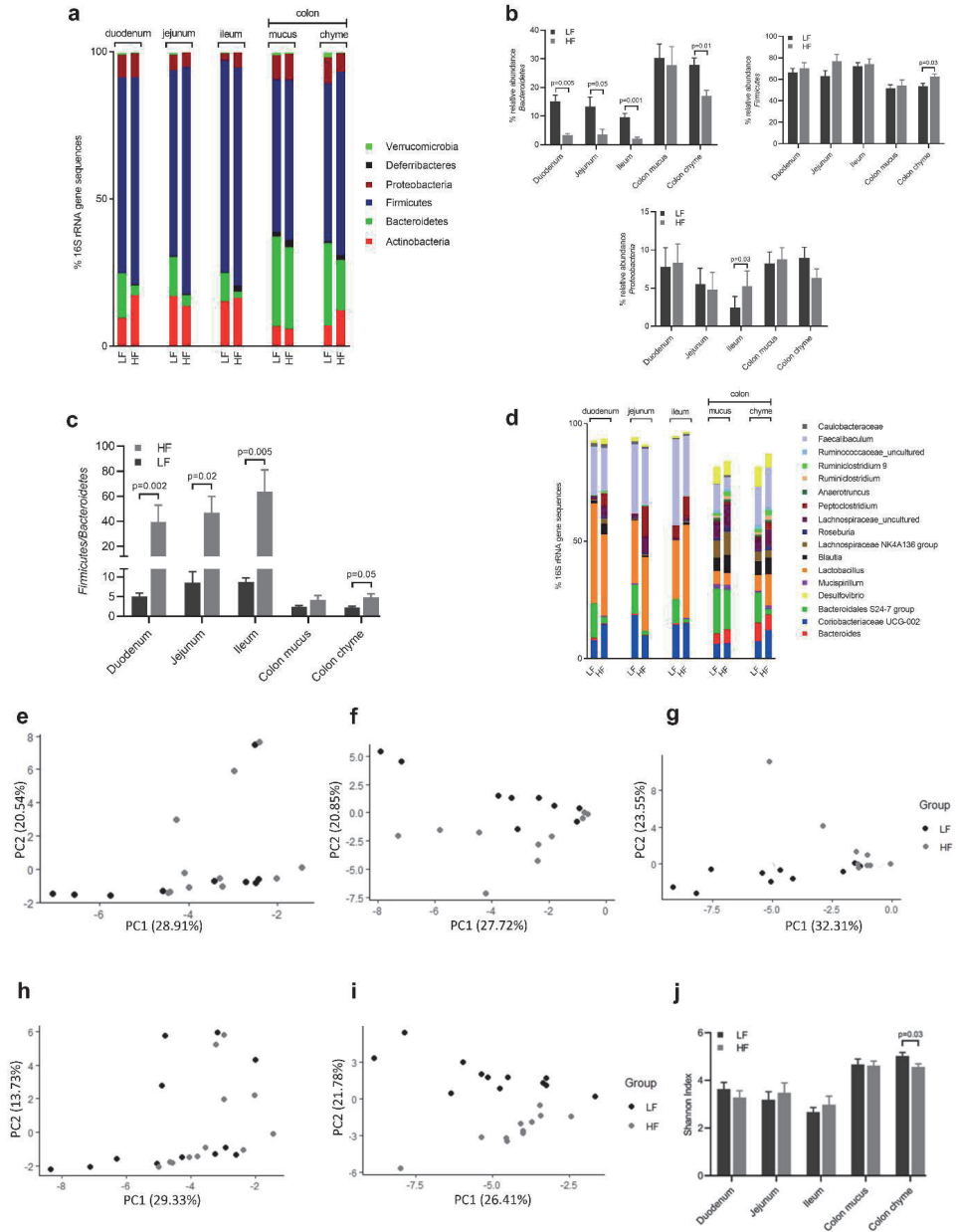
Figure 2 *(legend in the next page)*

←Figure 2. **Microbial composition of the GI tract of mice fed the LF and HFD. (a, d)** Relative abundance of bacterial taxa at the phylum (a) and genus (d) levels based on the 16S rRNA amplicon sequences in the two groups. Only abundances > 1 % are shown (n=9-12); (**b**) Relative abundance of the phyla that significantly changed between the two groups (n=9-12). Values are presented as mean with s.e.m. Brown-Forsythe and Welch ANOVA tests with Tamhane's T2 multiple comparisons test; (**c**) The F:B ratio in all segments of the GI tract in the mice fed the HFD. Values are presented as mean with s.e.m. Kruskal Wallis test with Dunn's correction for multiple comparisons (n=9-12); (**d**) In the HF fed mice the relative amount of *Peptoclostridium* increased in both jejunum and ileum, while *Lachnospiraceae* (uncultured genus) increase in the jejunum (p<0.0001, adj. p=0.03) and *Lactobacillus* increase in the ileum. The relative abundance of *Bacteroidales S24-7* and *Faecalibac*ulum decreased in HFD group in both jejunum and ileum segments. In colon content of the HFD group there is an increase of *Lactobacillus, Coriobacteriaceae UCG-002, Lachnospiraceae* (uncultured genus) (p<0.0001 adj. p=0.0008) and *Peptoclostridium* (p<0.0001 adj.p=0.01). At the same time Bacteroidales S24-7, *Desulfovibrio* (p<0.0001 adj. p=0.0006) and *Clostridiales vadinBB60 group* (p<0.0001 adj. p=0.02) decreased in the colonic content of the HF group. The differences between groups had the significance of p<0.0001, adj. p<0.0001, unless if stated. Multiple *t*-tests with Bonferonni corrections (n=10-12); (**e-i**) PCoA plots based on the Bray Curtis distance of the OTUs of samples taken from duodenum (**e**), jejunum (**f**), ileum (**g**), colon mucus (**h**) and colon luminal chyme (**i**) (n=8-12); (**j**) Species richness using Shannon index (n=10-12). Data are presented as mean with s.e.m. One-way ANOVA with Sidak's multiple comparisons. PCoA: principal coordinate analysis. HFD: high-fat diet, LFD: low-fat diet. OTU: operational taxonomic unit. GI: gastrointestinal, s.e.m: Standard error of the mean.

HFD established a proinflammatory microbial environment in the distal SI characterized by increased colonization of *Peptoclostridium* and multiple taxa belonging to *Proteobacteria*

To expand our understanding of the impact of HF feeding on the gut microbiota alterations we sought to identify the specifically differentiated taxa for the two diets in each of the different gut segments by performing a Linear discriminant analysis effect size (LEfSe) analysis. *Peptoclostridium* was identified for the HFD group in both jejunum and ileum (**fig. 3a - d**). Furthermore, in accordance with our findings related to the elevated relative abundance of *Proteobacteria* in the ileum, we found that 11 out of the 14 identified taxa that were specifically identified for the HFD belonged the *Proteobacteria* phylum. Most of the identified groups belonged to the α- and γ-*Proteobacteria* classes (**fig. 3c** and **3d**). The same pattern as in ileum was observed in the colon mucosal samples, where 6 out of 9 identified taxa belonged to *Proteobacteria* (**fig. 3e** and **3f**). Regarding the colon luminal chyme samples, most of the HFD-identified taxa belonged to the class of *Clostridia* and to the *Actinobacteria* phylum (**fig. 3g** and **3h**). Of these identified taxa, *Peptoclostridium* and the γ-*Proteobacteria* are described to be of proinflammatory nature in the gut suggesting more proinflammatory microbial environment in the distal SI of the HFD group [27].

Figure 3. *(legend in the next page)*

←Figure 3. **LEfSe results of the microbiota of HF and LF fed mice**. (**a, c, e, g**) Histogram of the LDA scores computed for OTUs for the jejunal (**a**), ileal (**c**), colon mucosal (**e**) and colon luminal chyme (**g**) samples. LEfSe scores can be interpreted as the degree of consistent difference in relative abundance between the two groups. The histogram thus identifies which taxa among all those detected as statistically and biologically different explain the greatest differences between the HFD and LFD fed mice [28]. Red colored taxa were identified as specifically increased after the introduction of the HFD, while green colored taxa were associated to the LFD. (**b, d, f, h**) Cladogram displaying the identified taxa for LF and HFD groups for jejunal (**b**), ileal (**d**), colon mucosal (**f**) and colon luminal chyme (**h**) samples. Differences are represented in the color of the most abundant class (red and green indicating LFD and HFD groups, respectively, yellow non-significant). Each circle's diameter is proportional to the taxon's abundance. HF: high-fat diet, LF: low-fat diet.

HFD alters the integrity of the intestinal barrier

To determine whether the dysbiotic microbiota composition of the SI could cause microbes or microbial products to pass the intestinal lining we measured LPS binding protein (LBP) in plasma as a marker of increased LPS flux from the intestinal lumen. The LBP level was on average increased by 27% in HFD mice compared to LFD (**fig. 4a**). We next examined differences in the expression of pattern recognition receptors (PRRs) of the lamina propria as they typically are upregulated in response to the presence of microbial products and are an important link to downstream responses of intestinal translocation [29]. TLR4 expression was consistently higher in all intestinal segments in the HFD group (**fig. 4b**). NOD1 also showed higher expression levels along the different intestinal segments, but only statistically significant in jejunum and colon (**fig. 4c**). NOD2 was solely higher in the jejunum (**fig. 4d**). To elucidate the permeability properties of the SI we assessed the uptake of orally administered Fluorescein Isothiocyanate-dextran 4 (FD4). We observed 34% lower levels of FD4 in the plasma of mice fed HFD compared to the LFD group indicating reduced paracellular passage pathway (**fig. 4e**). Consistently, we observed a clear upregulation of the genes encoding the tight junction proteins occludin and zonula occludens in the HFD group (**fig. 4f-g**), where the expression of both genes was significantly higher all the way from the jejunum to the colon. We also measured the antimicrobial peptide Reg3γ (**fig. 4h**) and observed an increase in the SI of the HFD group when evaluating the SI as a whole. Together, these data suggest that HFD promotes an increased microbial challenge of the gut wall with a responding strengthening of the intestinal barrier.
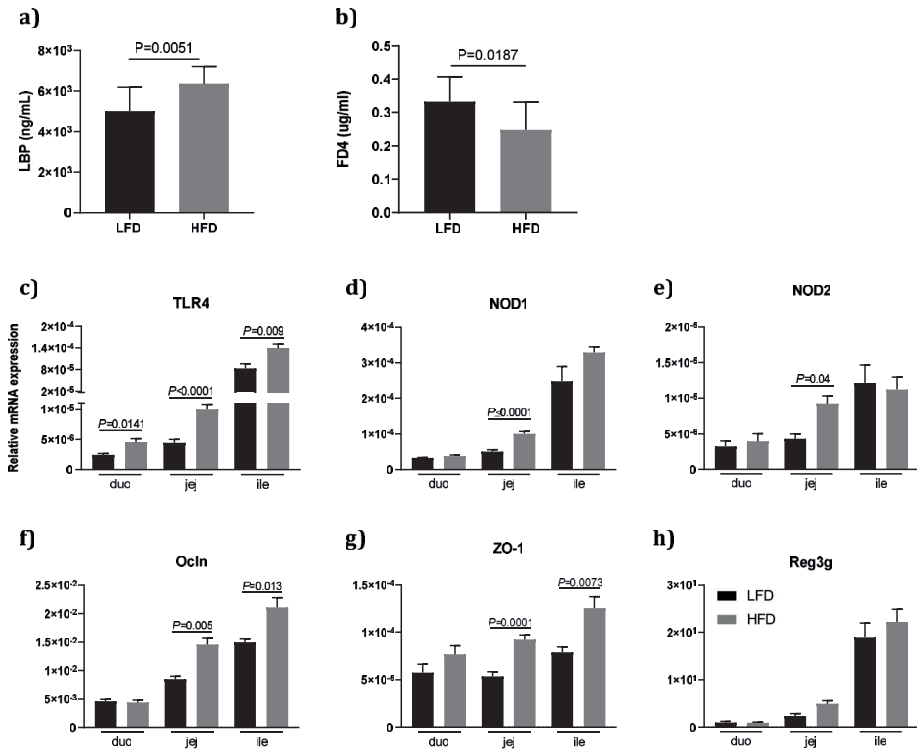
<u>Figure 4</u>. **Barrier function after long- term HFD consumption.** (**a**) LPS binding protein in plasma. (**b**) FD4 in plasma 1.5h after oral gavage. FD4 fixed amount was based on the average weight of the LF group and normalized with body weight. (**a-b**) n=10-12. Values are presented as mean with s.e.m. Unpaired t-test. (**c-h**) mRNA expression of TLR4 (**c**), NOD1 (**d**), NOD2 (**e**), Ocln (**f**), ZO-1 (**g**) and Reg3γ (**h**) in SI and colon. When evaluated Reg3γ expression in the SI as a whole, we observed a significant increase (*p*=0.04). Gene expression normalized by GAPDH (n=10-12). Values are presented as mean with s.e.m. One-way ANOVA with Sidak's multiple comparisons test. HFD: high-fat diet, LFD: low-fat diet, LBP: LPS binding protein, FD4: fluorescein isothiocyanate dextran, TLR4: transmembrane toll-like receptor 4, NOD1/2 nucleotide-binding oligomerization domains 1 and 2, Reg3γ: regenerating islet-derived 3 gamma, Ocln: occluding, ZO-1: zonula occludens, duo: duodenum, jej: jejunum, ile: ileum, col: colon, s.e.m: standard error of the mean.

HFD promote a pro-inflammatory immune cell population of the lamina propria

To examine the effect of HFD and the accompanied microbial dysbiosis to the host immune response we investigated the amount of T regulatory (Tregs) cells and the developmental stage of MΦ of the small intestinal lamina propria by flow cytometry. We observed a significantly lower number of CD4+ Foxp3+ Tregs in the HFD group compared to control. To investigate changes to the MΦ cell population we took advantage of the increased expression of CX3CR1 and MHCII as the intestinal MΦs mature in the lamina propria [25]. We compared the ratio between cells expressing high CX3CR1 and high MHCII which are regarded as fully mature MΦ with cells expressing intermediate CX3CR1 and low to intermediate MHCII (**fig. 5c**). We found a significantly lower ratio in the HFD fed mice compared to LFD fed mice (**fig. 5d**). These immature MΦs are known to be pro-inflammatory [25]. Pro-inflammatory MΦ generally releases cytokines promoting an inflammatory environment [30, 31] and we did observe an increase in TNFα, IL-1β, as well as the MΦ-regulatory cytokines TGF-β and CCL5 [32, 33](**fig. 5e-h**), however, on a segmental level, we only observed statistical significance for TNFα and CCL5 in the jejunum. Nevertheless, evaluating the SI as a whole showed a clear increase for all of the cytokines.

Pro-inflammatory MΦ contributes to antimicrobial activity by the production of cytotoxic reactive oxygen species (ROS) [34]. The production of such ROS is in MΦ NOX2-dependent. Upon measuring NOX2 expression we observed a significant increase in the distal part of the SI (**fig. 5i**). Additionally, we measured abdominal ROS production *in vivo* through non-invasive imaging of the L-012 activity (**fig. 5j-k**). This method is shown to reflect distal SI ROS production [35]. At three different time-points, the signal was consistently higher in the HFD group compared to the control group. At the last time-point, ten weeks of dietary intervention, the L-012 signal was 2.7 times higher in the HFD group (**fig. 5k**). Altogether, these suggest that HFD with accompanied dysbiotic microbiota composition promoted a pro-inflammatory immune cell population of the SI.
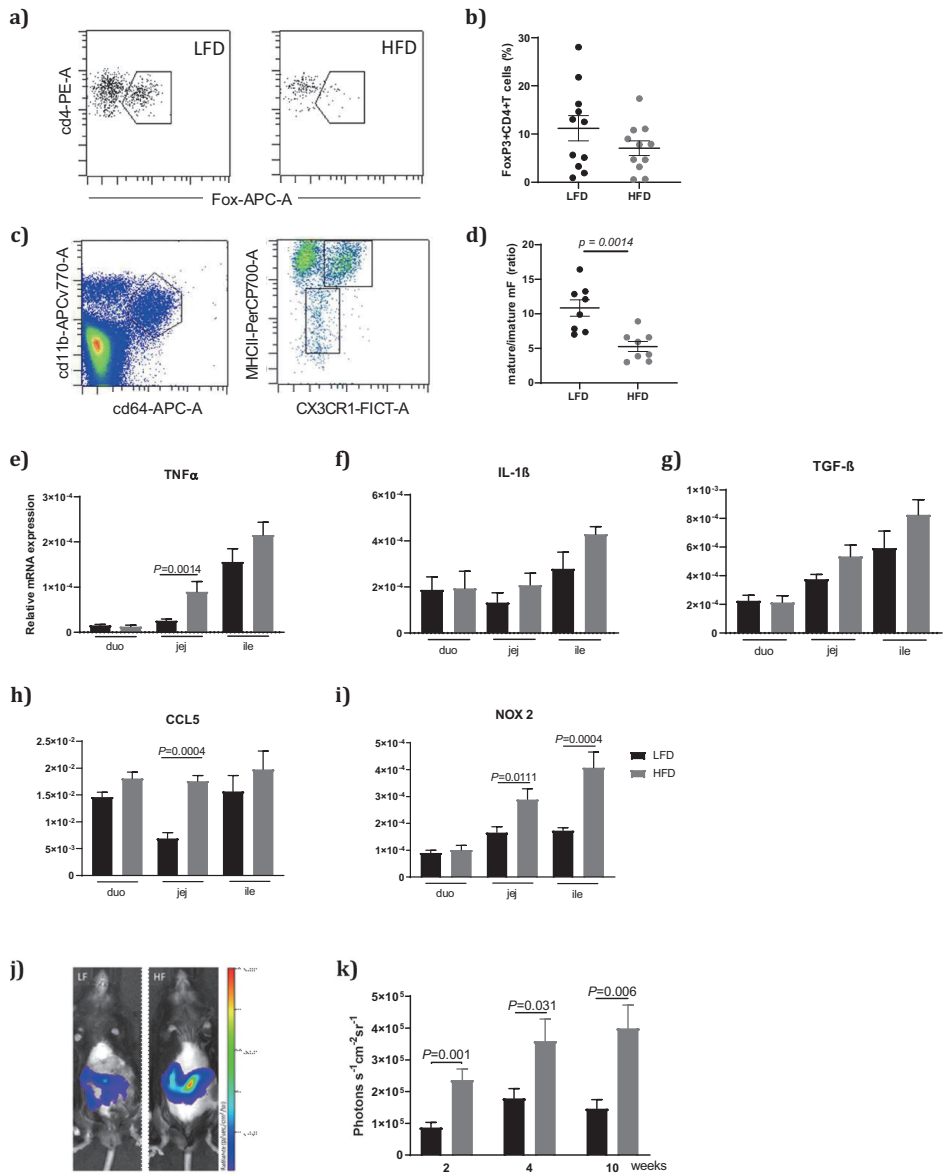
a)

cd4-PE-A (vertical axis), Fox-APC-A (horizontal axis)
LFD / HFD

b)

FoxP3+CD4+T cells (%)
LFD / HFD

c)

cd11b-APCv770-A (vertical axis), cd64-APC-A (horizontal axis)
MHCII-PerCP700-A (vertical axis), CX3CR1-FICT-A (horizontal axis)

d)

mature/imature mF (ratio)
p = 0.0014
LFD / HFD

e) TNFα

Relative mRNA expression
$P=0.0014$
duo / jej / ile

f) IL-1ß

duo / jej / ile

g) TGF-ß

duo / jej / ile

h) CCL5

$P=0.0004$
duo / jej / ile

i) NOX 2

$P=0.0111$ $P=0.0004$
LFD / HFD
duo / jej / ile

j)

LF / HF

k)

Photons s^{-1}cm^{-2}sr^{-1}
$P=0.001$ $P=0.031$ $P=0.006$
2 4 10 weeks

Figure 5 *(legend in the next page)*

17

←Figure 5. **The immune system response in GI mucosa.** (**a, c**) Gating scheme of the FOXP3+CD4+ Tcell (**a**) and CD64+ MHCII+ cells after exclusion of lymphocytes and NK cells (**c**). Polygons indicate gated cells subsets; (**b**) Proportion (%) of FOxP3+CD4+ T cells of total CD4+ gated cells (p=0.1887) (n=11); (**d**) ratio between cells expressing high CX3CR1+ and high MHCII+ with cells expressing intermediate CX3CR1+ and low to intermediate MHCII+ (n=8); (**e-i**) mRNA expression of TNFα (**e**), IL-1β (**f**), TGF-β (**g**), CCL5 (**h**) and NOX2 (**i**) in SI. When evaluating the SI as a whole TNFα (p=0.03), IL-1β (p=0.04), TGF-β (p=0.04), CCL5 (p=0.01). Gene expression normalized by GAPDH (n=8-12). (**j**) L-012 signal of one representative mouse of each group after 10 weeks of dietary trial. The signal is presented in radiance (photons/sec/cm^2/steradian) and was measured 5 minutes after L-012 injection with 3 minutes of exposure time; (**k**) Measurement of L-012-mediated luminescence signal in LF and HFD groups at three different time points (n=12); Values are presented as mean with s.e.m. (e-i, j) One-way ANOVA with Sidak's multiple comparisons test. HFD: high-fat diet, LFD: low-fat diet, TNFα: tumor necrosis factor alpha, IL-1β: interleukin-1 beta, TGF-β: transforming growth factor beta, CCL5: C-C motif chemokine ligand 5, NOX2: NADPH oxidase 2, duo: duodenum, jej: jejunum, ile: ileum, col: colon, s.e.m: standard error of the mean.

Discussion

In the present study, we investigated the effects of long term HFD feeding on microbiota, barrier function and immune status in the SI. We used LFD as control, where the fat was replaced with corn starch. Our main findings were that HFD caused a dysbiotic profile of gut microbiota with concomitant changes in primarily distal SI-segments of innate immune markers including an increased proportion of inflammatory MΦ, decrease in Tregs and increased expression of proinflammatory cytokines, NOX2 and PRRs. Interestingly, we observed that the antibacterial peptide Regγ3 and TJ proteins occludin and ZO-1 were upregulated followed by reduced SI-permeability. These results indicate that host intestinal tissue elicited a defense response to attenuate the detrimental impact of HFD mediated dysbiosis.

Numerous studies have investigated and described gut microbiota and its interaction with diet as a modulator of nutrient uptake and host metabolism in humans and mice [1, 3, 18, 36, 37]. Effects of high-fat diets have been the target of many studies, demonstrating an association with fecal and colonic dysbiosis in most of them [38, 39]. However, the majority of studies have limited their analyses to colon and cecum and largely neglected the impact of HFD on the small intestinal microbiota and its putative effect on SI tissue. The SI is the primary site of nutrient absorption and due to the significant contact between food substrate and commensal bacteria, it is characterized as a site rich in microbe-microbe and host-microbe interactions [40]. We found that the microbial population showed more distinct differences between the two groups in the distal part of the SI (jejunum and ileum) than in duodenum. This is not so surprising considering that duodenum is characterized by low numbers of bacteria that are less diverse and that most of the fat uptake takes place in the jejunum [18]. More specifically, at the phylum level, we observed a shift of the microbiota in the animals fed HFD towards a higher F:B ratio along the GI tract. In addition, in the ileal samples, we observed a significant increase in the relative abundance of *Proteobacteria.* Overall, such alterations are known to be the result after HF feeding in cecal, colonic and fecal microbiota and have been previously reported by others to be associated with obesity and low-grade inflammation [38, 39, 41]. In the few studies analyzing the impact of the HFD on the small intestinal microbiota, a decrease in Bacteroidetes was a

common finding [17, 18, 20], while Meng and co-workers observed an increase in the small intestinal *Proteobacteria* in rats [20]. As regards alpha diversity, we found no significant differences between the two groups in any of the SI-segments. This was not surprising though, considering that the microbiota in this region is overall phylogenetically less diverse than in the large intestine [42]. At the genus level, we found that *Peptoclostridium* increases along all segments of the SI in the HFD fed mice, while *Bacteroidales S24-7* and *Faecalibaculum* decrease. A decrease in ileal *Bacteroidales S24-7* has been previously linked to HFD [17], while its presence in the feces of non-obese diabetic mice has been proposed to protect against diabetes [43]. Bacterial species belonging to the *Peptoclostridium* genus are thought to be pro-inflammatory. One of its members is *Peptoclostridium difficile aka Clostridium difficile* one of the main pathogens that have been associated with infectious diarrhea [44]. Furthermore, we found that in ileum most of the identified taxa associated with the HFD belonged to the *Proteobacteria* phylum. *Proteobacteria* consist of Gram-negative bacteria and are one of the most abundant phyla of the microbiota in the SI consisting of several known pathogens. An increased presence of *Proteobacteria* has been characterized as a microbial signature of disease and a connection between *Proteobacteria* with low-grade inflammation and the metabolic syndrome has been previously described [27]. In this context LPS produced by Gram-negative bacteria is thought to induce endotoxemia that further leads to an inflammatory state in the gut [45]. In recent studies focusing on the identification of bacteria that might be involved in the genesis of endotoxemia, the prevalence of *Proteobacteria* has been found to be increased [27]. Together, our data clearly show that a HFD leads to a dysbiotic microbial environment in jejunum and ileum.

We observed an increase of LBP in the plasma of mice fed HFD, an indication of LPS leakage from the gut. LBP is an acute-phase protein primarily produced by the liver in response to LPS and then secreted into the blood. Its main role is to escort LPS to its target cells with subsequent binding to CD14 and TLR4 signaling induction. Indeed, Cani and coworkers have shown that feeding rats corn oil by oral gavage increases levels of LPS in plasma compared to water controls [46]. A possible explanation is that LPS can, together with fat, be incorporated into chylomicrons which subsequently facilitate LPS released

from intestinal epithelial cells [47]. As we see an upregulation of *Proteobacteria* in the HFD group, this can also explain the increased LPS flux in the intestinal lumen. However, we cannot rule out that LBP is also induced by proinflammatory cytokines originating from adipose tissue as a response to obesity with subsequent low-grade inflammation [48]. We also observed a lower intestinal permeability assessed by FD4 in mice fed HFD. We administered FD4 after 4h fasting and measured its concentration in plasma after 90 minutes, reflecting primarily assessment of the SI barrier. Contrary to most other studies, we administered a fixed amount of FD4 based on the average weight of lean mice, as suggested by McGuinness *et al.* [49].

ROS are an integral part of the innate immune system, foremost by the induction of respiratory burst in phagocytic cells to efficiently kill microbes. In the present study, we observed increased levels of ROS using non-invasive imaging [35] after HFD consumption. Previous studies have shown that the highly reactive peroxynitrite made by the combination of nitric oxide and superoxide produced by iNOS and NOX1/NOX2, respectively is prominent in the SI [35]. NOX1 is expressed in epithelial cells [34] whereas NOX2 is primarily expressed in lamina propria residing MΦ. We demonstrated previously that intestinal ROS production assessed by L-012 in healthy animals is dependent on NOX1 expression [50]. However, here we observed reduced NOX1 expression and increased NOX2 expression suggesting that the increased ROS production in HFD fed mice is caused by the increased presence of NOX2 expressing MΦ. Indeed we found an increased proportion of inflammatory MΦ by assessing the expression of MHCII/CX3CR1[int] as markers of monocyte-derived immature MΦ. To our knowledge, this is not previously described, and the results imply that monocytes are recruited to the SI lamina propria as a consequence of the HFD. The increased proportion of these cells can also explain the reduced number of Treg cells as mature intestinal MΦ are important for Treg formation [26]. A reduction in Treg cells by HFD has been observed by others, but only in the context where the low-fat control diet was a chow diet [6]. Our results thus confirm that reduction in Treg cells is indeed due to the increased fat consumption. We further observed a moderate increase in the expression of proinflammatory cytokines in the distal segments of the SI. The most robust changes in expression were found in the jejunum. Interestingly,

we also found higher relative expressions of PRRs and barrier related genes in this area. As most of the fat is digested and absorbed in the jejunum, and very little fat remains in the ileum, it is fair to suggest that dietary fat is of relevance to these changes seen in the jejunum [7, 51].

The increased expression of the PRRs TLR4, NOD1 and NOD2 by the HFD is line with most other studies [51-54]. The PRRs are crucial for sensing microbiota and critical for eliciting downstream responses that maintain gut homeostasis [55]. However, their increased expression has dominantly been linked to increased permeability in HFD settings [15, 56]. We measured the expression of Reg3γ and the tight junction proteins occludin and ZO-1. Reg3γ is an antimicrobial peptide secreted by Paneth cells into the gut lumen, and dependent on TLRs via MyD88 signaling [55, 57, 58], whereas occludin and ZO-1's functions are to create a seal in the epithelium to avoid paracellular influx. In both cases, we found increased expression by HFD. These observations are contradictory to most other findings with respect to HFD, which find diminished expression of Reg3γ [59] and TJ encoding genes [7, 45]. For instance, increased NOD1 and TLR4 signaling are shown to decrease the expression of TJ proteins in HFD mice [56]. However, NOD2 on the other hand is crucial for maintaining normal TJ expression and maintaining barrier properties. Therefore we believe that the induced expressions of Reg3γ and TJ genes are compensatory responses mediated by the host when challenged by a detrimental microbial environment imposed by HFD. As shown by Hamilton, the adaptation to new dietary regimes is a dynamic process which over time strengthens the intestinal barrier. In their study, rats fed HFD had diminished barrier function during the first week, but after 3 and 6 weeks, the barrier was essentially restored [16]. Importantly, many of the studies so far have compared HFD with a low-fat chow diet rich in fiber. In our study, we used a HFD matched low-fat diet that differed only with respect to carbohydrate content and fat. Indeed, Kless and coworkers demonstrated that HFD with matched LFD controls found little or no differences in intestinal barrier properties between HFD and LFD mice [60].

Overall our results show that HFD compared with a matched LFD control, lead to a dysbiotic profile in the distal segments of the SI, particularly in the ileum. These conditions further elicit an adaptive host response resulting in reduced barrier permeability and shift

in more inflammatory immune cells. This study also highlights the importance of choosing the correct control diet to secure that we, in fact, compare the impact of a high-fat diet.

Material and Methods

Animal housing and diets

Twenty-four male mice, 9 weeks old (C57BL/6J; Envigo, The Netherlands), were housed in individually ventilated cages in a controlled environment (12 hours light-dark cycle; 24 ± 1 °C; 45-55% humidity). Initially, all 24 animals were fed with a LFD (D12540J, 10 E% fat, Research Diets) for 4 weeks to acclimatize. Then, mice were randomized divided into two groups and given a HFD (D12492, 60 E% fat, Research Diets) or LFD for 18 weeks. Mice had *ad libitum* access to food and water. Food and body weight were measured once a week to assess food intake and weight development. Activity wheels were removed at experiment start-up to exclude physical activity as a confounder.

Animals were euthanized by cervical dislocation under anesthesia, composed of Zolezepam (32 mg/kg), Tiletamin (32 mg/kg), Xylazine (4.5 mg/kg), and Fentanyl (26 ug/kg).

Ethical aspects

The animal experiment was performed with permission from The Norwegian Animal Research Authority (Mattilsynet, FOTS #8196), and conducted in compliance with the current guidelines of The Federation of European Laboratory Animal Science Associations (FELASA).

Glucose homeostasis and insulin sensitivity

Mice were subjected to intraperitoneal insulin tolerance test (IpITT) and oral glucose tolerance test (OGTT) to assess glucose homeostasis and insulin sensitivity. Blood was obtained from the tail. Blood glucose levels were measured by a glucometer (Accu-Chek, Roche Diagnostics). The IpITT was conducted at week 9 of the experiment. Human insulin (Sigma-Aldrich) was injected in a fixed-dose (0.75 U/kg) after 4 hours of fasting. The OGTT was performed at week 10 of the experiment. A fixed-dose of D-glucose (Sigma-Aldrich) was administrated (2 g/Kg) after 6 hours of fasting.

Intestinal permeability by FITC-dextran

Intestinal permeability was determined at week 14 of the dietary trial using a protocol adapted from Johnson et al., PlosOne [23]. Briefly, mice were fasted for 4 hours prior to an oral administration of 650 mg/Kg of fluorescein isothiocyanate (FITC) dextran (FD4, Sigma-Aldrich). This dose was based on the average weight of the LF group. Blood was collected 1.5 hours after administration from vena saphena into EDTA-coated tubes to separate plasma through centrifugation. Plasma was diluted with one volume of saline solution and FITC dextran concentration was determined by fluorescence spectroscopy with excitation and emission wavelengths at 490 nm and 520 nm, respectively (Synergy H4 Hybrid microplate reader, Bio Tek instrument).

In vivo imaging of ROS using L-012

Mice were shaved in the ventral side in the day prior to imaging. Immobilized using isoflurane (2.5-3.5%), 200 µl of chemiluminescent probe L-012 (Wako Chemical) was injected intraperitoneally, dissolved in saline (2.5 mg/mL). L-012 which reacts with peroxynitrite originated from the interaction between nitric oxide and superoxide anion [61]. Light emission from the ventral side was measured with IVIS Lumina II (Perkin Elmer) as photons per second per cm^2 per steradian using the Living Imaging software (Perkin Elmer) 5 minutes after injection and with 3 minutes exposure time.

Flow cytometry

Intestinal samples were harvested after animal euthanasia. Mesenteric fat, luminal content and Peyer's patches were removed. The intestine was opened longitudinally, cut into 5 mm long segments and placed in cold RPMI. Isolation of epithelial and lamina propria cells followed Goodyear *et al.* [62] description. Briefly, mucus was removed by incubation in DTT at 37 °C for 20 min with agitation. Epithelial cells were separated by three incubation steps in EDTA solution at 37 °C for 15 min with agitation. Loose connective tissue was removed by adding a digestion step containing collagenases, Liberase and DNases (Sigma-Aldrich), for 15 min at 37 °C with agitation. Cells were stained after several washing steps with protein extraction buffer and then pre-blocked with FcR Block (Miltenyi Biotec). Cells were stained with the following intra- and extracellular antibodies: CD3-APCvio770, CD8-

PEvio770, CD45-PerCPvio700, FoxP3-APC, CD11b-APCv770-A, cd64-AP-A, MHCII-PerCP700-A and CX3CR1-FITC-A (Miltenyi Biotec), following the manufacturer's instructions. For differentiation between live and dead cells, we used the LIVE/DEAD fixable Violet Stain kit (Thermo Fisher). We used MACQuant Analyzer 10 Flow cytometer and MACQuantify software (Miltenyi Biotec) for cell acquisition and analyses.

Small intestinal segmentation

For analysis performed in different segments of the SI, we consistently selected the same areas for sampling. Firstly, we identified the middle point of the SI. The most proximal 5 cm of SI was considered as the duodenum, 6 cm around the middle point was considered as jejunum and the most distal 6 cm was considered as the ileum.

Gene expression and 16S rRNA gene sequencing

The mucosa samples for RNA and DNA extraction were scraped off with a blunted microscope glass slide from the intestine after being open longitudinally. Colon content for DNA extraction was squeezed out with forceps. The segmentation of the SI was performed as described above and the colon mucosa was collected from the proximal half. Mucosal samples for RNA extraction were preserved in RNAlater (Sigma-ALdrich) after sampling. Mucosal samples and intestinal content for DNA extraction were placed in S.T.A.R buffer (Roche), together with <106 Mm acid-washed glass beads (Sigma-Aldrich), immediately after dissection.

Real-Time quantitative PCR (RT-qPCR)

RNA was isolated using the NucluoSpin RNA/Protein Purification kit (Macherye-Nagel). The kit iScript cDNA Synthesis (Bio Rad) was used to produce cDNA and FirePol EvaGreen qPCR Supermix (Solis BioDyne) for the RT-qPCR reaction. Used primers and optimized primer annealing temperature are listed in table 1.

Table1: primers used for RT-qPCR and their annealing temperature

Gene	Forward Primer 5'-3'	Reverse Primer 5'-3'	Tm °C
GAPDH	CTTCAACAGCAACTCCCACTCTT	GCCGTATTCATTGTCATACCAGG	60
CCL5	GCCCACGTCAAGGAGTATTT	CTTCGAGTGACAAACACGAC	59
IL-1β	GCAGCTGGAGAGTGTGGAT	AAACTCCACTTTGCTCTTGACTT	61
NOD1	TGACAGTAATCTGGCTGACC	GTCTGGTTCACTCTCAGCAT	59
NOD2	GCAGAAACTAGCTCTCTTCAAC	CGGCTGTGATGTGATTGTTC	61
NOX2	GGGAACTGGGCTGTGAATGA	CAGTGCTGACCCAAGGAGTT	61
Ocln	CTGTGAAAACCCGAAGAAAGATG	GCAGACACATTTTTAACCCACTC	57
Reg3γ	GTCAAGAGCCTCAGGATTTCT	ACCATGATGTCAATTCTGTACTC	57
TGF-β	GAACCAAGGAGACGGAATACAG	CGTGGAGTTTGTTATCTTTGCTG	65
TLR4	GATCTGAGCTTCAACCCCTT	TGTTTCAATTTCACACCTGGA	61
TNFα	CTGTCTACTGAACTTCGGGGTGAT	GGTCTGGGCCATAGAACTGATG	61
ZO-1	GAGAAAGGTGAAACTCTGCTG	ACGAGGAGTCGGATGATTTTAGA	59

RT-qPCR was performed in LightCycler 480 Instrument II (Roche) with the following parameters: 12 min at 95 °C; 40 cycles of 15 s at 95 °C followed by 20 s at optimized primer annealing temperature (listed above); 20 s at 72 °C. LinReg Software was used to calculate Cq values based on a common threshold and individual efficiencies.

16S rRNA gene sequencing

Samples were lysed in a MagNA Lyser Instrument (Roche) at 6500 rpm twice for 20 s with a cooling step in-between, followed by centrifugation for 5 min at 14000 *g.* The supernatant was collected and DNA extracted using the Mag Mini LGC kit (LGC Genomics), according to the manufacturer's protocol in a KingFisher Flex DNA extraction robot (Thermo Scientific).

We followed the 16S rRNA amplicon sequence analysis workflow previously described by Avershina et al. [63]. Briefly, after DNA extraction we amplified the 16S rRNA gene for 25 cycles using prokaryote targeting primers developed by Yu et al. [64]. We used AMPure XP to purify the PCR product (Beckman-Coulter, Brea, CA) and we performed 10 further PCR cycles. The resulting amplicons were sequenced on Illumina MiSeq V3 platform (Illumina, SanDiego, CA). The resulting 300 bp paired-end reads were further paired-end joined, quality-filtered using QIIME33 and clustered with 97% identity level using closed-reference *usearch v7.0* algorithm [65, 66] against Greengenes database v13.8 [67].

LBP in Plasma

LPS binding protein in plasma was used to measured, indirectly, the amount of LPS in samples through an enzyme immunoassay for determination of mouse LBP (Biometec, Greifswald). Briefly, plasma samples were diluted 1:800 and added to a pre-coated plate. Substrate was read with an absorbance at 450 nm and the amount of LBP was calculated based in a standard curve and dilution in a 4-parameter logistic curve fit.

Histology

After dissection, adipose tissue samples were surrounded with OCT, flash-frozen in liquid nitrogen and stored at -80°C until fixation. Samples were fixed in ice-cold 10% formalin for 1 hour and stored overnight in fresh 10% formalin at 4 ^{o}C. Tissues were dehydrated in ethanol, assembled in paraffin blocks and cut in 5 μm thick sections.

Staining and image analysis.

Adipose tissue sections were stained with Hematoxilin and Eosin as described by Parlee et al. [68]. Adipocytes area was measured using Open Source Adiposoft Image Analysis in ImageJ software [69, 70]. The average transversal adipocyte section area of each sample was calculated from 150-250 cells per sample.

Statistical Analysis

Statistical analyses were done in the GraphPad Prism software (La Jolla, USA). Averages are presented as mean and variances as the standard error of the mean (s.e.m). The homogeneity of variances was tested with Bartlett's test. Normal distributed data from multiple groups were compared by one-way ANOVA with Sidak's correction for multiple comparisons. For non-normal distributed data the non-parametric Kruskal-Wallis one way-ANOVA was performed. When only two independent groups were compared, we used the unpaired *t*-test or the non-parametric Mann-Whitney test. We chose 1.500 sequences per sample as a cut-off value to normalize the sequencing data. To identify taxa associated with either the LFD or the HFD group, we used linear discriminant analysis effect size (LEfSe) with LDA score > 2 [28]. PCoA was performed using R [71]. Only OTUs that were present with more than 10 reads in at least 5% of all samples were included for the PCoA.

References

1. Bäckhed, F., H. Ding, *et al.*, The gut microbiota as an environmental factor that regulates fat storage. *Proceedings of the national academy of sciences*, **2004**. 101(44): p. 15718-15723.

2. Bäckhed, F., J.K. Manchester, *et al.*, Mechanisms underlying the resistance to diet-induced obesity in germ-free mice. *Proc Natl Acad Sci U S A*, **2007**. 104(3): p. 979-84.

3. Turnbaugh, P.J., R.E. Ley, *et al.*, An obesity-associated gut microbiome with increased capacity for energy harvest. *Nature*, **2006**. 444(7122): p. 1027-31.

4. Duan, Y., L. Zeng, *et al.*, Inflammatory Links Between High Fat Diets and Diseases. *Front Immunol*, **2018**. 9(2649): p. 2649.

5. Membrez, M., F. Blancher, *et al.*, Gut microbiota modulation with norfloxacin and ampicillin enhances glucose tolerance in mice. *FASEB J*, **2008**. 22(7): p. 2416-26.

6. Luck, H., S. Tsai, *et al.*, Regulation of obesity-related insulin resistance with gut anti-inflammatory agents. *Cell Metab*, **2015**. 21(4): p. 527-42.

7. Winer, D.A., H. Luck, *et al.*, The Intestinal Immune System in Obesity and Insulin Resistance. *Cell Metab*, **2016**. 23(3): p. 413-26.

8. Winer, D.A., S. Winer, *et al.*, Immunologic impact of the intestine in metabolic disease. *J Clin Invest*, **2017**. 127(1): p. 33-42.

9. de La Serre, C.B., C.L. Ellis, *et al.*, Propensity to high-fat diet-induced obesity in rats is associated with changes in the gut microbiota and gut inflammation. *American Journal of Physiology-Gastrointestinal and Liver Physiology*, **2010**. 299(2): p. 440-448.

10. Ding, S., M.M. Chi, *et al.*, High-fat diet: bacteria interactions promote intestinal inflammation which precedes and correlates with obesity and insulin resistance in mouse. *PLoS One*, **2010**. 5(8): p. e12191.

11. Liu, Z., R.S. Brooks, *et al.*, Diet-induced obesity elevates colonic TNF-α in mice and is accompanied by an activation of Wnt signaling: a mechanism for obesity-associated colorectal cancer. *The Journal of Nutritional Biochemistry*, **2012**. 23(10): p. 1207-1213.

12. Teixeira, L.G., A.J. Leonel, *et al.*, The combination of high-fat diet-induced obesity and chronic ulcerative colitis reciprocally exacerbates adipose tissue and colon inflammation. *Lipids Health Dis*, **2011**. 10(1): p. 204.

13. Lam, Y.Y., C.W. Ha, *et al.*, Increased gut permeability and microbiota change associate with mesenteric fat inflammation and metabolic dysfunction in diet-induced obese mice. *PLoS One*, **2012**. 7(3): p. e34233.

14. Li, H., C. Lelliott, *et al.*, Intestinal, adipose, and liver inflammation in diet-induced obese mice. *Metabolism*, **2008**. 57(12): p. 1704-10.

15.	Araújo, J.R., J. Tomas, *et al.*, Impact of high-fat diet on the intestinal microbiota and small intestinal physiology before and after the onset of obesity. *Biochimie*, **2017**. 141: p. 97-106.

16.	Hamilton, M.K., G. Boudry, *et al.*, Changes in intestinal barrier function and gut microbiota in high-fat diet-fed rats are dynamic and region dependent. *Am J Physiol Gastrointest Liver Physiol*, **2015**. 308(10): p. 840-851.

17.	Tomas, J., C. Mulet, *et al.*, High-fat diet modifies the PPAR-gamma pathway leading to disruption of microbial and physiological ecosystem in murine small intestine. *Proc Natl Acad Sci U S A*, **2016**. 113(40): p. E5934-E5943.

18.	Martinez-Guryn, K., N. Hubert, *et al.*, Small Intestine Microbiota Regulate Host Digestive and Absorptive Adaptive Responses to Dietary Lipids. *Cell Host Microbe*, **2018**. 23(4): p. 458-469.

19.	Onishi, J.C., S. Campbell, *et al.*, Bacterial communities in the small intestine respond differently to those in the caecum and colon in mice fed low- and high-fat diets. *Microbiology*, **2017**. 163(8): p. 1189-1197.

20.	Meng, Y., X. Li, *et al.*, Effects of Different Diets on Microbiota in The Small Intestine Mucus and Weight Regulation in Rats. *Sci Rep*, **2019**. 9(1): p. 8500.

21.	Veilleux, A., S. Mayeur, *et al.*, Altered intestinal functions and increased local inflammation in insulin-resistant obese subjects: a gene-expression profile analysis. *BMC Gastroenterol*, **2015**. 15(1): p. 119.

22.	Garidou, L., C. Pomie, *et al.*, The Gut Microbiota Regulates Intestinal CD4 T Cells Expressing RORgammat and Controls Metabolic Disease. *Cell Metab*, **2015**. 22(1): p. 100-12.

23.	Johnson, A.M., A. Costanzo, *et al.*, High fat diet causes depletion of intestinal eosinophils associated with intestinal permeability. *PloS one*, **2015**. 10(4): p. e0122195.

24.	Tamoutounour, S., S. Henri, *et al.*, CD 64 distinguishes macrophages from dendritic cells in the gut and reveals the T h1-inducing role of mesenteric lymph node macrophages during colitis. *European Journal of Immunology*, **2012**. 42(12): p. 3150-3166.

25.	Joeris, T., K. Muller-Luda, *et al.*, Diversity and functions of intestinal mononuclear phagocytes. *Mucosal Immunol*, **2017**. 10(4): p. 845-864.

26.	Zigmond, E. and S. Jung, Intestinal macrophages: well educated exceptions from the rule. *Trends Immunol*, **2013**. 34(4): p. 162-8.

27.	Rizzatti, G., L.R. Lopetuso, *et al.*, *Proteobacteria*: A Common Factor in Human Diseases. *Biomed Res Int*, **2017**. 2017: p. 9351507.

28.	Segata, N., J. Izard, *et al.*, Metagenomic biomarker discovery and explanation. *Genome Biol*, **2011**. 12(6): p. 1-18.

29.	Burgueño, J.F. and M.T. Abreu, Epithelial Toll-like receptors and their role in gut homeostasis and disease. *Nature Reviews Gastroenterology & Hepatology*, **2020**(17): p. 263-278.

30.	Weber, B., L. Saurer, *et al.*, CX3CR1 defines functionally distinct intestinal mononuclear phagocyte subsets which maintain their respective functions during homeostatic and inflammatory conditions. *European Journal of Immunology*, **2011**. 41(3): p. 773-779.

31.	Grainger, J.R., E.A. Wohlfert, *et al.*, Inflammatory monocytes regulate pathologic responses to commensals during acute gastrointestinal infection. *Nat Med*, **2013**. 19(6): p. 713-21.

32.	Smythies, L.E., A. Maheshwari, *et al.*, Mucosal IL-8 and TGF-β recruit blood monocytes: evidence for cross-talk between the lamina propria stroma and myeloid cells. *Journal of leukocyte biology*, **2006**. 80(3): p. 492-499.

33.	Cavaillon, J.M., Cytokines and macrophages. *Biomed Pharmacother*, **1994**. 48(10): p. 445-53.

34.	Bedard, K. and K.H. Krause, The NOX family of ROS-generating NADPH oxidases: physiology and pathophysiology. *Physiol Rev*, **2007**. 87(1): p. 245-313.

35.	Kielland, A., T. Blom, *et al.*, In vivo imaging of reactive oxygen and nitrogen species in inflammation using the luminescent probe L-012. *Free Radic Biol Med*, **2009**. 47(6): p. 760-766.

36.	Sonnenburg, J.L. and F. Backhed, Diet-microbiota interactions as moderators of human metabolism. *Nature*, **2016**. 535(7610): p. 56-64.

37.	El Aidy, S., C.A. Merrifield, *et al.*, The gut microbiota elicits a profound metabolic reorientation in the mouse jejunal mucosa during conventionalisation. *Gut*, **2013**. 62(9): p. 1306-14.

38.	Hildebrandt, M.A., C. Hoffmann, *et al.*, High-fat diet determines the composition of the murine gut microbiome independently of obesity. *Gastroenterology*, **2009**. 137(5): p. 1716-24.

39.	Murphy, E.A., K.T. Velazquez, and K.M. Herbert, Influence of high-fat diet on gut microbiota: a driving force for chronic disease risk. *Current opinion in clinical nutrition and metabolic care*, **2015**. 18(5): p. 515-520.

40.	Booijink, C.C., E.G. Zoetendal, *et al.*, Microbial communities in the human small intestine: coupling diversity to metagenomics. *Future Microbiol*, **2007**. 2(3): p. 285-95.

41.	Zhang, C., M. Zhang, *et al.*, Structural resilience of the gut microbiota in adult mice under high-fat dietary perturbations. *ISME J*, **2012**. 6(10): p. 1848-57.

42.	Kastl Jr, A.J., N.A. Terry, *et al.*, The structure and function of the human small intestinal microbiota: current understanding and future directions. *Cellular and molecular gastroenterology and hepatology*, **2020**. 9(1): p. 33-45.

43.	Krych, L., D.S. Nielsen, *et al.*, Gut microbial markers are associated with diabetes onset, regulatory imbalance, and IFN-gamma level in NOD mice. *Gut Microbes*, **2015**. 6(2): p. 101-9.

44.	Liu, W., Y. Zhang, *et al.*, Quinoa whole grain diet compromises the changes of gut microbiota and colonic colitis induced by dextran Sulfate sodium in C57BL/6 mice. *Sci Rep*, **2018**. 8(1): p. 14916.

45.   Cani, P.D., R. Bibiloni, *et al.*, Changes in gut microbiota control metabolic endotoxemia-induced inflammation in high-fat diet-induced obesity and diabetes in mice. *Diabetes*, **2008**. 57(6): p. 1470-81.

46.   Cani, P.D., J. Amar, *et al.*, Metabolic endotoxemia initiates obesity and insulin resistance. *Diabetes*, **2007**. 56(7): p. 1761-72.

47.   Ghoshal, S., J. Witta, *et al.*, Chylomicrons promote intestinal absorption of lipopolysaccharides. *J Lipid Res*, **2009**. 50(1): p. 90-7.

48.   Grube, B.J., C.G. Cochane, *et al.*, Lipopolysaccharide binding protein expression in primary human hepatocytes and HepG2 hepatoma cells. *J Biol Chem*, **1994**. 269(11): p. 8477-82.

49.   McGuinness, O.P., J.E. Ayala, *et al.*, NIH experiment in centralized mouse phenotyping: the Vanderbilt experience and recommendations for evaluating glucose homeostasis in the mouse. *Am J Physiol Endocrinol Metab*, **2009**. 297(4): p. E849-55.

50.   Matziouridou, C., S.D.C. Rocha, *et al.*, iNOS- and NOX1-dependent ROS production maintains bacterial homeostasis in the ileum of mice. *Mucosal Immunol*, **2018**. 11(3): p. 774-784.

51.   Jin, C. and R.A. Flavell, Innate sensors of pathogen and stress: linking inflammation to obesity. *J Allergy Clin Immunol*, **2013**. 132(2): p. 287-94.

52.   Schertzer, J.D., A.K. Tamrakar, *et al.*, NOD1 activators link innate immunity to insulin resistance. *Diabetes*, **2011**. 60(9): p. 2206-15.

53.   Tukhvatulin, A.I., A.S. Dzharullaeva, *et al.*, Powerful Complex Immunoadjuvant Based on Synergistic Effect of Combined TLR4 and NOD2 Activation Significantly Enhances Magnitude of Humoral and Cellular Adaptive Immune Responses. *PLoS One*, **2016**. 11(5): p. e0155650.

54.   Pashenkov, M.V., Y.A. Dagil, and B.V. Pinegin, NOD1 and NOD2: Molecular targets in prevention and treatment of infectious diseases. *Int Immunopharmacol*, **2018**. 54: p. 385-400.

55.   Vaishnava, S., C.L. Behrendt, *et al.*, Paneth cells directly sense gut commensals and maintain homeostasis at the intestinal host-microbial interface. *Proc Natl Acad Sci U S A*, **2008**. 105(52): p. 20858-63.

56.   Amar, J., C. Chabo, *et al.*, Intestinal mucosal adherence and translocation of commensal bacteria at the early onset of type 2 diabetes: molecular mechanisms and probiotic treatment. *EMBO Mol Med*, **2011**. 3(9): p. 559-72.

57.   Loonen, L.M., E. Stolte, *et al.*, REG3γ-deficient mice have altered mucus distribution and increased mucosal inflammatory responses to the microbiota and enteric pathogens in the ileum. *Mucosal immunology*, **2014**. 7(4): p. 939-947.

58.   Bluemel, S., L. Wang, *et al.*, The Role of Intestinal C-type Regenerating Islet Derived-3 Lectins for Nonalcoholic Steatohepatitis. *Hepatol Commun*, **2018**. 2(4): p. 393-406.

59.   Guerville, M., A. Leroy, *et al.*, Western-diet consumption induces alteration of barrier function mechanisms in the ileum that correlates with metabolic endotoxemia in rats. *Am J Physiol Endocrinol Metab*, **2017**. 313(2): p. E107-E120.

60.   Kless, C., V.M. Muller, *et al.*, Diet-induced obesity causes metabolic impairment independent of alterations in gut barrier integrity. *Mol Nutr Food Res*, **2015**. 59(5): p. 968-78.

61.   Aviello, G. and U.G. Knaus, ROS in gastrointestinal inflammation: Rescue Or Sabotage? *Br J Pharmacol*, **2017**. 174(12): p. 1704-1718.

62.   Goodyear, A.W., A. Kumar, *et al.*, Optimization of murine small intestine leukocyte isolation for global immune phenotype analysis. *J Immunol Methods*, **2014**. 405: p. 97-108.

63.   Avershina, E., K. Lundgard, *et al.*, Transition from infant- to adult-like gut microbiota. *Environ Microbiol*, **2016**. 18(7): p. 2226-36.

64.   Yu, Y., C. Lee, *et al.*, Group-specific primer and probe sets to detect methanogenic communities using quantitative real-time polymerase chain reaction. *Biotechnology and Bioengineering*, **2005**. 89(6): p. 670-679.

65.   Edgar, R.C., Search and clustering orders of magnitude faster than BLAST. *Bioinformatics*, **2010**. 26(19): p. 2460-1.

66.   Edgar, R.C., UPARSE: highly accurate OTU sequences from microbial amplicon reads. *Nat Methods*, **2013**. 10(10): p. 996-8.

67.   DeSantis, T.Z., P. Hugenholtz, *et al.*, Greengenes, a chimera-checked 16S rRNA gene database and workbench compatible with ARB. *Appl Environ Microbiol*, **2006**. 72(7): p. 5069-72.

68.   Parlee, S.D., S.I. Lentz, *et al.*, *Quantifying size and number of adipocytes in adipose tissue*, in *Methods in enzymology*. 2014, Elsevier. p. 93-122.

69.   Rueden, C.T., J. Schindelin, *et al.*, ImageJ2: ImageJ for the next generation of scientific image data. *BMC Bioinformatics*, **2017**. 18(1): p. 529.

70.   Schindelin, J., I. Arganda-Carreras, *et al.*, Fiji: an open-source platform for biological-image analysis. *Nat Methods*, **2012**. 9(7): p. 676-82.

71.   Team, R.C., R: A language and environment for statistical computing. **2013**.

Paper II

Coffee consumption in moderate doses attenuates microbial dysbiosis and inflammation induced by high-fat feeding in mice

Sérgio D. C. Rocha[1]*, Chrysoula Kielland[1]*, Silje Harvei[1], Harald Carlsen[1], Anders Kielland[1]

[1]Faculty of Chemistry, Biotechnology and Food Science, Norwegian University of Life Sciences, P. O. Box 5003, N-1432 Ås, Norway

* Shared first author

Abstract

An impaired balance in the gut microbes has been linked to the deterioration of health. Consumption of a high-fat (HF) diet leads to intestinal dysbiosis and inflammation in the small intestine. Coffee is widely consumed and it contains several bioactive compounds. Although several studies have reported a positive correlation between health and coffee consumption, its impact on gut health remains rather unexplored. Here we show that dietary supplementation of coffee attenuates HF diet caused microbial dysbiosis and pro-inflammatory macrophages in the small intestine.

The microbial profile of mice consuming coffee in a dose-dependent manner showed a shift into a more low-fat diet-like profile characterized by a decrease in *Firmicutes/Bacteroidetes* ratio, decrease in *Peptoclostridium* and increase in *Bacteroidales S24_7* family. Coffee restored the levels of the circulating LPS binding protein and the expression of intestinal TLR4 and NOD1. Coffee consumption decreased the intestinal expression of TNF-α, TGF-β and NOX2, and reduced reactive oxygen species content. Furthermore, the surface marker MHCII and CX3CR1 were increased, suggesting a reduced amount of pro-inflammatory macrophages by coffee intake.

Our data show that consumption of coffee can have a positive impact on gut health characterized by the presence of a symbiotic microbial environment, improved barrier function and homeostasis of the immune system.

Introduction

Coffee is the second most consumed beverage worldwide, after water, [1] and its daily consumption is estimated to be approximately 2,25 billion cups [2]. Coffee contains numerous bioactive compounds including phenolic polymers, chlorogenic acid, minerals and caffeine [3]. Due to its high consumption, coffee may have a substantial effect on public health [2]. Numerous studies have focused on the impact of coffee consumption on health but sometimes the results are conflicting. However, in research over the past years, the benefits of coffee appear to outgrow the risks linked with its consumption. Daily coffee consumption is suggested to prevent several metabolic, liver and neurological conditions as well as certain cancer types (Nieber, 2017; Poole et al., 2017). The strongest correlation was observed when the consumption was moderate, 3-4 cups per day, rather than when only 1 cup was consumed [2, 4]. Despite the increased interest in coffee and health, the relationship between coffee and the gut microbiota as well as whether downstream host-microbial interactions could be one of the mechanisms for the health claims of coffee, remain still rather unexplored.

The intestinal microbiota consists of approximately a hundred trillion microorganisms that form a complex ecological community. Although the gut microbiota composition is stable over time in healthy subjects, dietary modifications have a strong impact on its community structure [5]. More specifically, the consumption of HF diet has been associated with the establishment of a dysbiotic profile that is characterized by higher *Firmicutes/Bacteroidetes* ratio as well as an increased prevalence of *Proteobacteria* [6]. Such a profile can be characterized as pro-inflammatory and a bloom of *Proteobacteria* has been linked with intestinal bowel disease and in general the presence of an inflammatory state in the intestine [7, 8].

Although coffee is the second most consumed beverage worldwide [1] and several studies have analyzed its impact on health focusing among others, on metabolic disorders [2, 4], there have not been many studies on the correlation of coffee with gut microbiota and whether this might possess a causal role in the observed health benefits of coffee.

Jaquet *et al.* analyzed the microbial composition in human fecal samples after coffee consumption and found that, although the dominant bacteria were not altered, coffee led to an increase of the probiotic *Bifidobacterium spp.* [9]. Nakayama *et al.* also reported an increase in fecal *Bifidobacteria* as a result of the colonic fermentation of the oligosaccharides present in coffee [10]. Nishitsuji *et al.* reported that although the liver lobular inflammation decreased after diet supplementation with coffee in a diabetes-prone mouse model, the microbial dysbiosis that has been established with a HF diet did not improve after coffee consumption [3]. However, only fecal or colonic bacteria were analyzed in these studies. It is well known that the community structure of microbes along the GI tract is different [11, 12]. The composition of fecal samples differs not only in comparison to the one in the small intestine but also that in the large intestine [13-15]. Therefore, although convenient, using fecal samples can result in "false negatives" when screening for microbiota effects and results should be interpreted with caution when fecal samples are used as a proxy [11, 16].

Apart from changing the composition of the gut microbiota, the HF diet has been linked with alterations in the innate and adaptive immune responses in the small intestine [17]. Coffee has been shown to affect the inflammatory status in various tissues, such as liver and blood, however with contradictory findings [18-21]. Furthermore, a couple of studies have analyzed the impact of polyphenols, chlorogenic acid and caffeine on intestinal inflammation [22-24].

The lack of evidence on the interplay among coffee, gut microbiota and intestinal inflammation becomes even more important, considering that the few reports on coffee and bacteria focus either on *in vitro* fermentation experiments based on fecal slurries [25] or on the composition of the fecal bacteria after coffee consumption [3, 9, 26]. In addition, many of these studies base their analyses on real-time quantitative PCR and analyze only a selection of bacteria that are thought to be of relevance, neglecting possible differences of the whole gut microbial population [10, 26].

The objective of this study was to examine the impact of coffee on gut health by examining whether coffee consumption would attenuate the negative effects caused by HF feeding. We have subjected mice to the HF diet together with different amounts of coffee,

representing the human consumption of 1 and 5 cups per day (HFC1 and HFC5 respectively). We found that coffee attenuated the HF diet-induced dysbiosis in a dose-dependent manner, resulting in a very similar microbial composition as in low fat (LF) fed mice. Coffee additionally led to lower levels of circulating lipopolysaccharide-binding protein (LBP), increased expression of the intestinal tight junction protein occludin and zonula occludens (ZO-1), and reduced expression of intestinal NOD1 and TLR4, suggesting an enhanced gut wall barrier. Furthermore, the macrophage (Mɸ) population of the lamina propria showed higher expression of CX3CR1 and MHCII and lower production of reactive oxygen species (ROS), suggesting the presence of less pro-inflammatory and more homeostatic Mɸ [27]. In conclusion, our data support a positive impact of coffee on gut health.

Results

Coffee counteracted the weight gain caused by HF diet consumption

Mice fed the HF diet had an increase in body weight in comparison to the LF diet-fed mice. Mice fed the HFC1 diet had similar weight gain as the HF diet group. In fact, HFC1 was the group with the highest weight gain by the end of the experiment, gaining three times more weight than the LF diet group. On the other hand, mice fed the HFC5 diet showed a decreased body weight gain in comparison to the HF diet group **(Fig. 1a)**. The HF diet group had higher energy intake per cage than the LF diet group. Mice fed HFC1 diet had the highest energy intake, being 31.9% and 10.6% higher than the LF and HF diet groups, respectively. From the HF diets, HFC5 diet group had a more similar energy intake when compared to LF diet **(Fig. 1b)**.
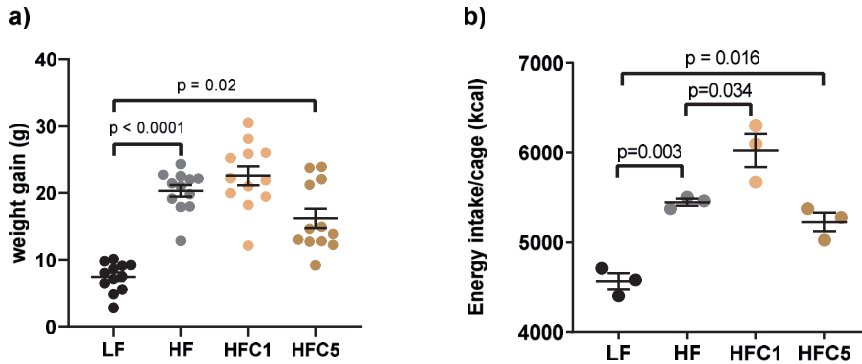
Figure 1. **Weight gain and energy intake**. **(a)** Weight gain after 18 weeks of dietary trial. n=12. **(b)** Energy intake (kcal) per cage (4 mice per cage) after 18 weeks. n=3. Values are presented as mean with s.e.m. One-way ANOVA with Sidak's correction for multiple comparisons.

Coffee supplementation decreases HF diet-induced dysbiosis

To evaluate the impact of coffee on the gut microbial composition we performed a 16S rRNA gene-based sequencing approach. Consumption of the HF diet led to a dysbiotic environment characterized by an increase in *Firmicutes* and a decrease in *Bacteroidetes,* both in the small and in the large intestine. Diet supplementation with coffee resulted in a concentration-dependent shift to a profile resembling the one seen in the LF diet, namely, a decrease in *Firmicutes* and an increase in *Bacteroidetes* **(Fig. 2a, 2c-d)**. In addition, there was an increase in *Actinobacteria* observed only in the mice supplemented with coffee **(Fig. 2e)**. On a genus level, the coffee groups had again a concentration-dependent composition similar to the LF diet-induced profile **(Fig. 2b).** In the distal small intestine, the HF diet led to an increase in *Peptoclostridium* and *Lachnospiraceae (uncultured bacterium)* in the jejunum (p < 0.0001, adj. p = 0.03), and *Lactobacillus* in the ileum. Regarding the coffee supplemented groups, HFC1 had the least effect. In the jejunum, HFC1 decreased *Peptoclostridium* and increased *Lachnospiraceae*, while *Lactobacillus* and *Coriobacteriaceae UCG-002* increased in both ileum and jejunum. HFC5 led to a decrease of *Peptoclostridium* and *Lactobacillus* with a concurrent increase of *Bacteroidales S24_7 family (uncultured bacterium)*, *Coriobacteriaceae UCG-002* and *Faecalibaculum* in both jejunum and ileum. In colon chyme *Coriobacteriaceae UCG-002, Lachnospiraceae, Peptoclostridium* and *Lactobacillus* increased in the HF diet group, while *Bacteroidales S24_7 family, Desulfovibrio* and *Clostridiales vadin BB60* decreased. HFC1 led to an increase in *Bacteroidales S24_7 family, Coriobacteriaceae UCG-002* and *Bacteroides*. HFC5 reduced the levels of *Lactobacillus, Blautia* (p < 0.0001, adj. p < 0.001), *Faecalibaculum* and *Peptoclostridium* (p < 0.001, adj. p = 0.002), while it led to increased abundance of *Coriobacteriaceae UCG-002, Bacteroidales S24-7 family, Bacteroides* and *Alistipes*. For all comparisons, unless stated otherwise, p < 0.0001, adj. p < 0.0001. Summing up, we observed a correlation between the increased dose of coffee and the relative abundance of *Bacteroidales S24-7 family, Peptoclostridium* and *Faecalibaculum,* both in the small as well as in the large intestine **(Fig. 2f-k)**.
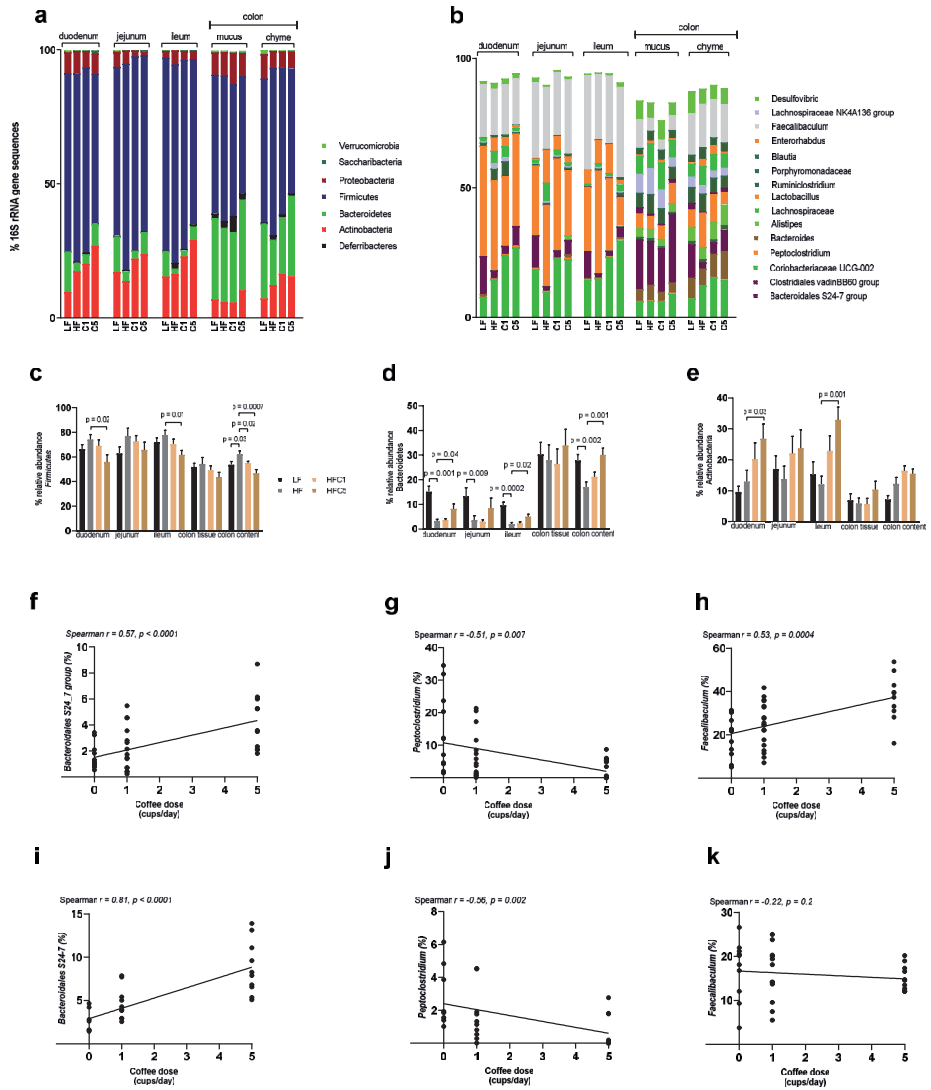
Figure 2 *(legend in the next page)*

← Figure 2 – Gut microbiota composition of mice on coffee diets. **(a)** Relative abundance of bacterial taxa at the phylum **(b)** and genus level based on the 16S rRNA amplicon sequences. Only abundances > 1 % are shown. **(c-e)** Relative abundance of *Firmicutes (c)*, *Bacteroidetes* **(d)** and *Actinobacteria* **(e)**. These phyla are the ones that showed significant differences among the different diet groups. Values are presented as mean with s.e.m. One-way ANOVA with Sidak's multiple comparisons test. **(f-k)** Significant associations between coffee dosage and changes in genus abundance in the small intestine **(f-h)** of *Bacteroidales S24-7 family (uncultured bacterium)* **(f)**, *Peptoclostridium* **(g)**, and *Faecalibaculum* **(h)** and the colonic chyme **(i-k)** *Bacteroidales S24-7 family (uncultured bacterium)* **(i)**, *Peptoclostridium* **(j)**, and *Faecalibaculum* **(k)** as measured by the Spearman's correlation. n = 9-12.

The microbial population after coffee supplementation shows a higher level of overlap with the LF group in ileum and colon

Regarding β-diversity, the principal coordinate analysis (PCoA) plots based on Bray Curtis distance **(Fig. 3a-e)** showed that in the small intestine **(Fig. 3a-c)** there was a more spread clustering of all groups than in colon chyme **(Fig. 3e).** However, we did see that in jejunum and ileum the HF and LF diet groups cluster separately **(Fig. 3b-c)**, indicating a high level of diversity in terms of bacterial composition, while the coffee groups, especially HFC5, clustered closer to the LF group. In colon chyme **(Fig. 3e)** we saw that HFC1 clustered in between the HF and LF groups, while HFC5 showed a higher level of overlap with the LF group indicating similar composition. For duodenum **(Fig. 3a)** and colon mucus **(Fig. 3d)** we observed a higher degree of co-clustering among all groups. It has been previously shown that consumption of a HF diet leads to decreased α-diversity in the distal gut (cecal and fecal samples) [28, 29]. We used Shannon Index as a measure to estimate the α-diversity and we saw that, indeed, it decreased in the colon chymal content in the HF fed mice (**Fig. 3f**). Regarding the coffee groups, the HFC5 diet group showed an increase in the Shannon Index in colon chyme. No significant changes were observed in the small intestine.
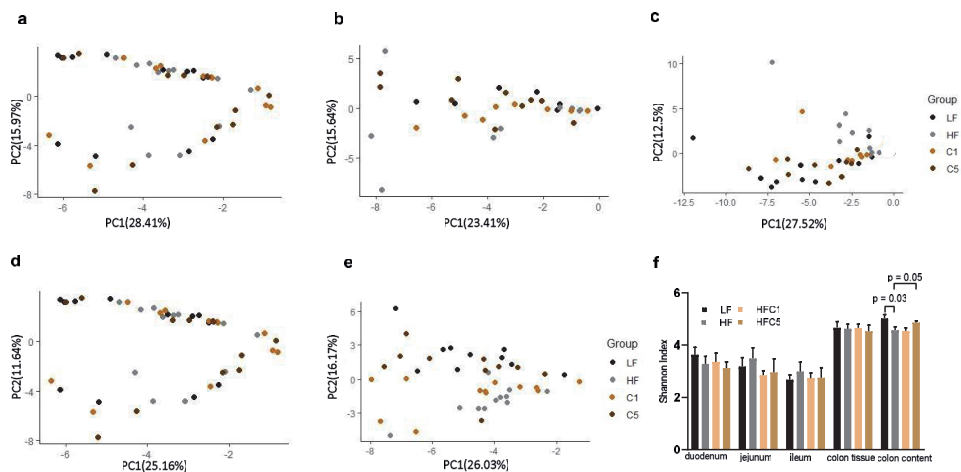
<u>Figure 3</u> – **Beta and alpha diversity of the HF, LF and the HF supplemented with different doses of coffee. (a-e)** PCoA plots using Bray Curtis distances of the OTUs of samples taken from the duodenum **(a)**, jejunum **(b)**, ileum **(c)**, colon mucus **(d)**, and colon chyme **(e)**. **(f)** Alpha diversity shown by Shannon Index for the different diets, n = 9-12. Values are presented as mean with s.e.m. One-way ANOVA with Dunnett's multiple comparisons.

The microbiota composition of mice fed coffee resembles the LF diet-associated taxa

As we observed similarities in the affected taxa at both the phylum and genus level among the LF and the coffee groups, we then identified the genera that were significantly different between the LF diet and the HF diet groups in the ileum and colon chyme. Further, we wished to examine how the presence of coffee in the HF diet influences these LF-associated genera. We have clustered the different diet groups based on the relative abundance of the LF-associated genera. **Figure 4** consists of two heatmaps; one deriving from ileal samples **(Fig. 4a)** and one from colonic chyme samples **(Fig. 4b)** and it shows that most of the HFC5 fed mice cluster together with the LF group, while HFC1 cluster with HF fed mice. This indicates that supplementation of HF diet with coffee at moderate doses changes the relative abundance of the LF-associated genera to a LF-like profile.
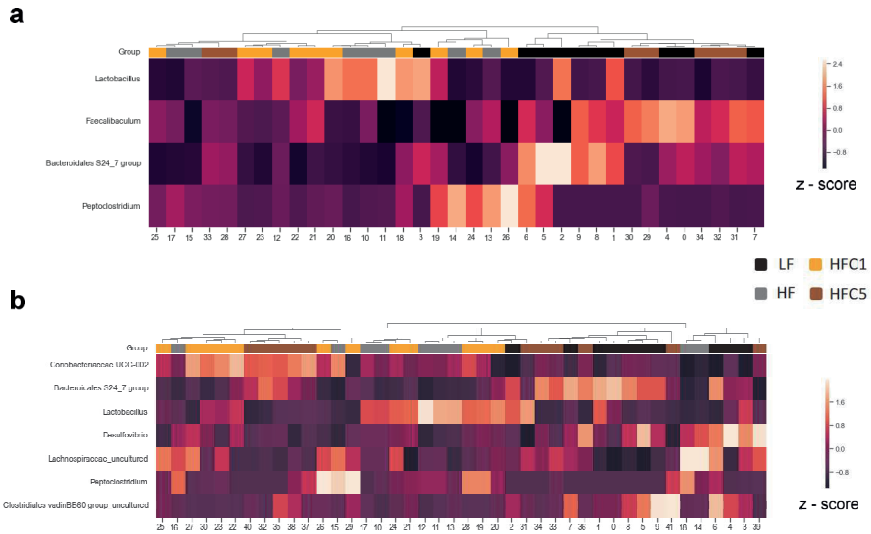
Figure 4. **Group clustering is based on the relative abundance of microbial genera associated with the LF diet in the ileum and colon chyme.** Clustering of mice according to relative abundance at genus level in the ileum **(a)** and colon chyme **(b)**. Heatmap visualization is based on the relative abundance of the selected genera. Rows are clustered by Euclidean distance and ward linkage hierarchical clustering. Row-bar is color-coded by the diet group. The color scale represents the scaled abundance of each genus, denoted as Z-score, with red indicating high abundance and blue indicating low abundance. n = 9-12.

Coffee protects against HF mediated endotoxemia

HF diet-induced dysbiosis is known to increase intestinal translocation of bacteria or bacterial products such as LPS [17]. HF diet increased the levels of plasma LBP and HFC5 was able to reverse this. HFC1 had no impact on the plasma LBP levels **(Fig. 5a)**. We have additionally measured the levels of circulating FD4 and the expression of tight junction protein genes. We found no change in plasma FD4 **(Fig. 5b-c)**. Regarding tight junctions, the expression of ocludin and zonula occludens was upregulated by HF diet in jejunum, ileum and colon and this effect were even more pronounced in the HFC5 group **(Fig. 5d-e)**.

In addition, we measured the expression of the pattern recognition receptors TLR4 and NOD1. TLR4 is upregulated when LPS passes through the intestinal barrier [30]. Furthermore, it has been shown that bacterium-related leakage after the HF diet is dependent on NOD1 [17]. We observed that the HF diet caused the upregulation of TLR4 and NOD1 throughout the whole intestine. Both receptors were downregulated by coffee supplementation with either dose in jejunum and ileum. Regarding the large intestine, the HFC1 had an impact on both receptors, while the HFC5 downregulated only the expression of NOD1 **(Fig. 5f-g)**. In summary, these data suggest that supplementation of HF diet with coffee can prevent bacteria and microbial products from passing through the gut wall.
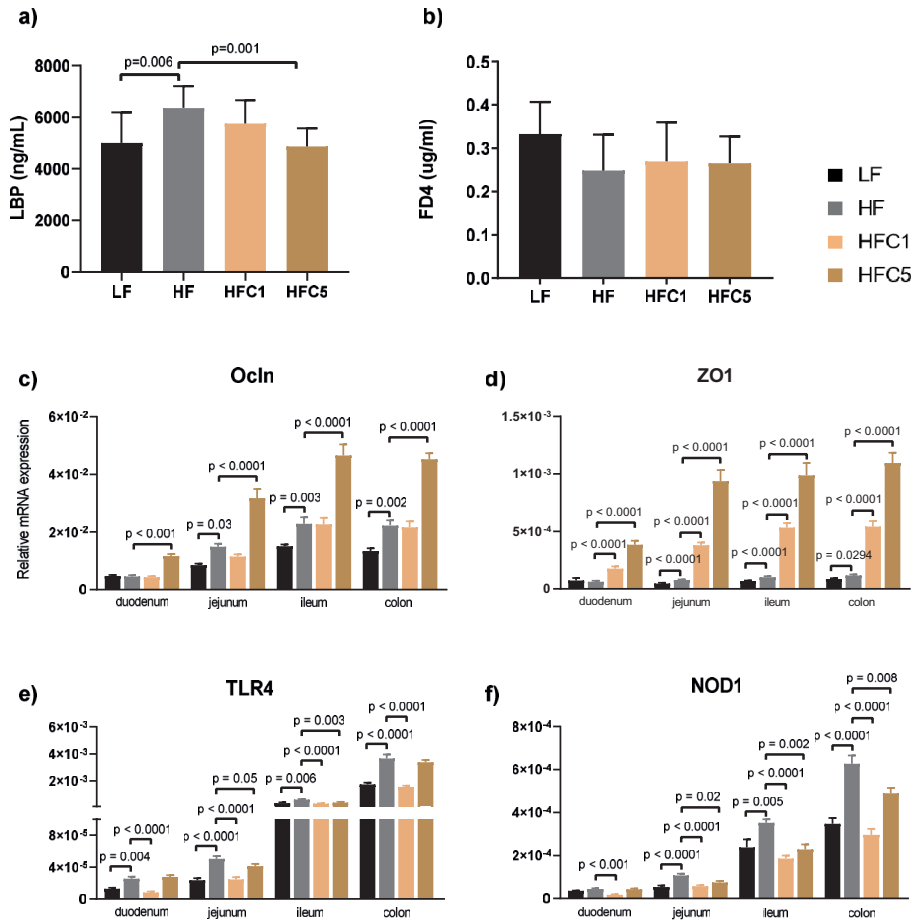
<u>Figure 5</u> – **Intestinal barrier function in the LF, HF, and coffee supplemented HF diets.**
(a) LBP protein in plasma. **(b)** FD4 in plasma 1.5h after oral gavage. **(c-f)** mRNA expression
of Ocln **(c)**, ZO-1 **(d)**, TLR4 **(e)** and NOD1 **(f)** in the intestinal mucosa. n=10-12. Relative
quantification by RT-qPCR normalized to GAPDH. Values are presented as mean with s.e.m.
One-way ANOVA with Sidak's correction for multiple comparisons test.

Dietary coffee consumption dampens the intestinal inflammation caused by HF diet

It has been previously shown that the HF diet leads to a more inflammatory profile of the intestinal immune system [17]. Since mice fed coffee show a healthier microbial composition, we investigated whether supplementation of the HF diet with coffee would impact the Mφ cell population of small intestinal lamina propria. We took advantage of the increased expression of CX3CR1 and MHCII as the intestinal Mφ mature in the lamina propria and the fact that the non-fully maturated Mφ are pro-inflammatory [27]. Evaluating the ratio between cells expressing high CX3CR1 and high MHCII with cells expressing intermediate CX3CR1 and low to intermediate MHCII showed a dose-dependent relationship between the amount of coffee in the diet and the relative amount of Mφ with high CX3CR1 and MHCII expression **(Fig. 6a-b)**.

Furthermore, we investigated whether the changes in the Mφ population is reflected in the release of typical pro-inflammatory cytokines. We saw that the HF diet led to increased mRNA expression of TGF-β in the ileum, and TNF-α and IL-1β in both jejunum and ileum **(Fig. 6c-e)**. HFC1 led to a decrease of the TNF- α levels and IL-1β in the ileum but did not influence the TGF-β expression. HFC5 led to a decrease of TGF-β, TNF-α and IL-1β in the ileum, while only for TNF-a in the jejunum **(Fig. 6c-e).** Pro-inflammatory Mφ use cytotoxic ROS in their antimicrobial respiratory burst to combat microbes [31]. The production of these ROS in Mφ are NOX2-dependent [32-35]. We observed that mice fed the HF diet showed increased expression of NOX2 in jejunum and ileum and both HFC1 and HFC5 reduced the expression of these genes to a similar level observed in the LF diet group **(Fig. 6f)**. Furthermore, we recorded *in vivo* ROS production by non-invasive imaging using the ROS probe L-012. We saw abdominal increased ROS content by HF consumption after two weeks, which continued to the final measuring time point of 10 weeks **(Fig. 6g)**. This L-012 dependent in vivo signal was previously shown to originate from the distal small intestine [32]. Coffee consumption decreased significantly the production of ROS in the gut to a similar level as in the LF diet group at all time points **(Fig. 6g)**. Taken together, our data indicate that coffee at moderate doses (HFC5) partly dampens the intestinal inflammatory response caused by the consumption of a HF diet.
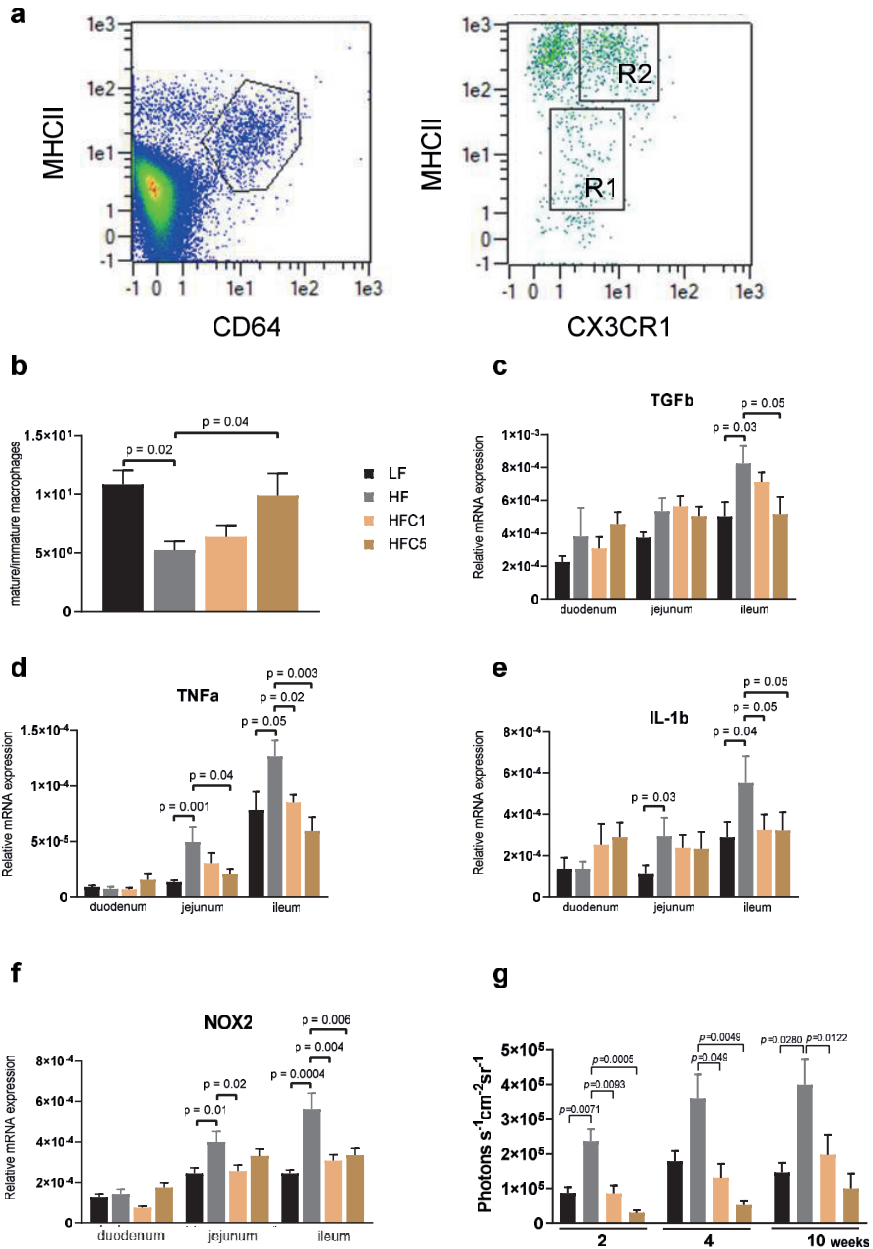
Figure 6 *(legend in the next page)*

←Figure 6 – **Intestinal immune response to HF diet supplemented with coffee.** **(a)** Following the exclusion of lymphocytes and NK-cells, Mφ was identified as CD64+/MHCII+ cells. Mφ was further subdivided into mature/homeostatic and immature/pro-inflammatory Mφ based on the expression level of CX3CR1 and MHCII. Pro-inflammatory was identified as intermediate CX3CR1 and low to intermediate MHCII (R1), while mature was identified as CX3CR1 high/MHCII high (R2). **(b)** The ratio of mature to pro-inflammatory Mφ showed a dose-dependent increase in response to coffee intake (linear regression, p=0.02). **(c-f)** mRNA expression of TGF-β **(c)**, TNF-α **(d)**, IL-1β **(e)** and NOX2 **(f)** mRNA expression in the intestinal mucosa, n = 8-12. Relative quantification by RT-qPCR normalized to GAPDH. **(g)** Measurement of L-012-mediated luminescence signal in all dietary groups at three different time points, n=12. Values are presented as mean with s.e.m. One-way ANOVA with Sidak's correction for multiple comparisons for all apart from **(g)** where Kruskal-Wallis with Dunn's correction for multiple comparisons was used instead.

Discussion

In the present study, we have investigated for the first time the impact of coffee on the microbial composition along the length of the intestine in mice fed a LF diet, a HF diet and HF diet supplemented with different coffee doses. Our results indicate that the consumption of coffee in moderate doses attenuated the microbial dysbiosis that was induced by a HF diet. This was accompanied by an improved barrier function and less pro-inflammatory Mφ in the lamina propria.

Several previous rodent studies have shown that consumption of HF diet might unbalance the gut microbiota composition [6, 28, 29, 36-38]. However, the majority of these studies have investigated the microbial composition in faeces and in the large intestine [39]. Here, we analyzed the microbial composition throughout the whole intestine including the three regions of the small intestine; duodenum, jejunum, ileum. The small intestine is the primary site of nutrient absorption and the terminal small intestine, the ileum, possesses the most abundant immune tissue of the whole GI. Additionally, the small intestine has been characterized as a site rich in microbe-microbe and host-microbe interactions that affect metabolic, immune and endocrine functions [40, 41]. Recently, some studies have shown that the small intestinal microbiota is subject to dietary changes and that it plays a role in nutrient digestion and transport [36, 42, 43]. The changes we observed in the gut microbial community of the HF diet-fed mice, namely lower levels of Firmicutes/Bacteroidetes, higher amounts of Actinobacteria and Bacteroidales S24_7 family with a concurrent decrease in Peptoclostridium, are in accordance with some of the previous findings on HF diet-induced microbiota alterations. Firmicutes and Bacteroidetes are the major phyla in the intestinal tract and an imbalance between them has been associated with HF diet-induced dysbiosis and disease [6, 28, 29, 38, 42, 44]. A decrease in S24_7 family has been previously correlated to HF diet, while Faecalibaculum (which was decreased in the HF diet group) has been proposed to promote body weight loss as a result of its ability to produce lactic acid as a metabolic end product [45, 46].

We saw that the supplementation of coffee attenuated the dysbiosis caused by the HF diet. With about 1500 chemical compounds present in coffee it is difficult to pinpoint the responsible molecule for the observed changes, it might also be a synergistic action of multiple compounds. Coffee contains several poly- and oligosaccharides, as well as peptides that could act as a carbon and nitrogen source and therefore alter the microbial composition [47], especially in the small intestine as this is the primary site of absorption. Coffee is also rich in phenolic compounds that could also alter the microbial composition [48-50], especially, chlorogenic acid, which has been found to modulate positively the gut microbiota in HF diet-fed mice [51]. Additionally, consumption of caffeine has been also shown to positively alter the gut microbiota [52]. Lastly, coffee contains high amounts of soluble dietary fiber, mainly galactomannans and arabinogalactans, which act as energy sources for commensal bacteria [53].

The establishment of a dysbiotic environment as a result of HF feeding has been associated with impairment in the gut barrier function, leading to leakage of bacteria or bacterial compounds dependent on the NOD1 microbial pattern recognition receptors. Furthermore, it was also observed an increased inflammatory status in the small intestinal mucosa after HF diet feeding [17]. Previous studies have analyzed the impact of coffee on inflammation in liver and blood with contradictory results [18-20]. A recently published study has shown that coffee exhibits anti-inflammatory properties via the inhibition of inflammatory mediator release and enhances the barrier function in a cell model of the intestinal mucosa [54], suggesting that our observed beneficial impact of coffee on the barrier function and the inflammatory status can be a direct response.

It is not clear whether one or many bioactive compounds present in coffee mediates the observed inflammatory response directly or whether it is a cascade effect. There are indications that caffeine, chlorogenic acid and diterpenes kahweol and cafestol can act directly at the cell level and thus inhibit the activity of NF-κB and consequent reduced inflammatory response and oxidative stress [55-57]. However, it has been previously shown that a change in the small intestinal microbial environment can reduce the inflammation on this site [58, 59]. Therefore, we hypothesize that inflammation in the small intestine is attenuated after coffee beneficial modulation of microbiota.

In conclusion, our results show that coffee consumption ameliorates the negative effects that accompany a high-fat diet in terms of gut. In addition, the barrier function is enhanced, and the intestinal inflammatory status is decreased.

Material and Methods

Animal housing and diets

Nine-week-old (n = 12/group) male mice (C57BL/6J background, Envigo, The Netherlands) were housed in individually ventilated cages (4 mice per cage) in a controlled environment (12h-light-dark cycle; temperature, 24 ± 1 °C; humidity, 45-55%). Animals were acclimatized for 4 weeks with a LF diet (D12540J, 10 E% fat, Research Diets). Thereafter 12 mice/group were fed HF diet (D12492, 60 E% fat, Research Diets), HF diet supplemented with coffee equivalent to 1 cup/day (HFC1) or 5 cups/day (HFC5). Diets were obtained from Research Diets (New Brunswick, NJ, USA) by adding freeze-dried coffee to the D12492 diet. The conversion of estimated cups/day into the actual amount of coffee in feed was done by relating intake to body mass/body surface area (kg/m^2). Therefore, HFC1 and HFC5 had 5 and 25 g of coffee per kg of food. Mice had *ad libitum* access to food and water and weight measurements were performed weekly to assess food intake and weight development. To exclude physical activity as a confounder, we removed running wheels after acclimatization. Animals were euthanized by cervical dislocation under anesthesia (100 µL/10 g mouse), by Zolezepam (32 mg/Kg), Tiletamin (32 mg/Kg), Xylazine (4.5 mg/Kg) and Fentanyl (26 ug/Kg).

Ethical aspects

The animal experiment was performed with permission from The Norwegian Animal Research Authority and was conducted in compliance with the current guidelines of The Federation of European Laboratory Animal Science Associations (FELASA).

Intestinal permeability by FITC-dextran

Intestinal permeability was determined at week 14 using a protocol adopted from Johnson et al., [60]. Briefly, mice that have previously fasted for 4h received orally 650mg/Kg of fluorescein isothiocyanate (FITC) dextran (FD4, Sigma-Aldrich) and blood was collected after 1.5 hours. Concentration of FITC dextran in plasma was determined by fluorescence spectroscopy with excitation and emission wavelengths at 490 nm and 520 nm, respectively (Synergy H4 Hybrid microplate reader, Bio Tek instrument).

LBP measurement

LBP in plasma was measured through an enzyme immunoassay for the determination of mouse LBP (Biometec, Greifswald). Briefly, plasma samples were diluted 1:800 and loaded into a precoated plate. Subtracts were read with an absorbance at 450 nm and the amount of LBP was estimated based on a standard curve constructed in a 4-parameter logistic curve fit.

Flow cytometry

After isolating the small intestine, mesenteric fat, lumen content and Peyer's patches were removed. Then, it was opened longitudinally, cut into 5 mm long segments and placed immediately in cold RPMI. Isolation of epithelial and lamina propria cells followed the description by Goodyear and coworkers [61]. Briefly, mucus was removed after incubation in DTT at 37 °C/20min, epithelial cells were separated by three incubation steps in EDTA solution at 37 °C/15min and loose connective tissue was removed by adding a digestion step containing collagenases, liberase and DNases (Sigma-Aldrich), at 37 °C/15min. All incubation steps were performed together with agitation. Cells were washed with PEB buffer (Miltenyi Biotec) and pre-blocked with FcR Block reagent (Miltenyi Biotec). Cells were stained with the following intra- and extracellular antibodies: CD3-APCvio770, CD4-PE, CD8-PEvio770, CD45-PerCPvio700, FoxP3-APC, Mouse IgG1-APC, and CD11b-APCv770-A and MHCII-PerCP700-A (Miltenyi Biotec). Live cells were identified with the use of propidium iodide or LIVE/DEAD fixable Violet Stain kit (Thermo Fisher). Cell acquisition and analysis were performed with MACQuant Analyzer 10 Flow cytometer and MACQuantify software (Miltenyi Biotec) for cell acquisition and analyses..

Gene expression and 16S rRNA gene sequencing

Mucosal samples for RNA and DNA extraction were scraped off from longitudinally opened intestine with a glass slide. The small intestine was divided as: duodenum (most proximal 5 cm), jejunum (6 cm around the center) and ileum (most distal 6 cm). Mucosal samples for RNA extraction were preserved in RNAlater (Sigma-ALdrich) after sampling. RT-qPCR was performed in LightCycler 480 Instrument II (Roche). Used primers and

optimized primer annealing temperature are listed in **table 1**. LinReg Software was used to calculate Cq values based with a common threshold and individual efficiencies.

Mucosal samples and intestinal content for DNA extraction were placed in S.T.A.R buffer (Roche), together with <106 Mm acid-washed glass beads (Sigma-Aldrich), immediately after dissection.

Table1: primers used for RT-qPCR and their annealing temperature

Gene	Forward Primer 5'-3'	Reverse Primer 5'-3'	Tm °C
GAPDH	CTTCAACAGCAACTCCCACTCTT	GCCGTATTCATTGTCATACCAGG	60
IL-1β	GCAGCTGGAGAGTGTGGAT	AAACTCCACTTTGCTCTTGACTT	61
NOD1	TGACAGTAATCTGGCTGACC	GTCTGGTTCACTCTCAGCAT	59
NOX2	GGGAACTGGGCTGTGAATGA	CAGTGCTGACCCAAGGAGTT	61
Ocln	CTGTGAAAACCCGAAGAAAGATG	GCAGACACATTTTTAACCCACTC	57
TGF-β	GAACCAAGGAGACGGAATACAG	CGTGGAGTTTGTTATCTTTGCTG	65
TLR4	GATCTGAGCTTCAACCCCTT	TGTTTCAATTTCACACCTGGA	61
TNFα	CTGTCTACTGAACTTCGGGGTGAT	GGTCTGGGCCATAGAACTGATG	61
ZO-1	GAGAAAGGTGAAACTCTGCTG	ACGAGGAGTCGGATGATTTTAGA	59

16S rRNA based gut microbiota sequencing

The 16S rRNA amplicon sequence analysis protocol was previously described by Avershina et al. [62]. Briefly, after DNA extraction the 16S rRNA gene was amplified for 25 cycles using prokaryote targeting primers developed by Yu et al. [63]. AMPure XP was used for purification of the PCR product (Beckman-Coulter, Brea, CA) and 10 further PCR cycles followed. The resulting amplicons were sequenced on Illumina MiSeq V3 platform (Illumina, SanDiego, CA). The resulting 300 bp paired-end reads were further paired-end joined, quality-filtered using QIIME33 and clustered with 97% identity level using closed-reference *usearch v7.0* algorithm [64, 65] against Greengenes database v13.8 [66].

In vivo imaging ROS using L-012 probe

In vivo imaging was performed with IVIS Lumina II (Perkin Elmer). During the 2nd, 4th and 10th week of the experiment, 200μl of luminescence probe L-012 (Wako Chemical) was injected intraperitoneally in a concentration of 2.5mg/mL. Light emission from the ventral

side was measured as photons per second per cm^2 per steradian, 5 minutes after injection, using Living Imaging software (Perkin Elmer).

Statistical Analysis

Statistical analyses were done in the GraphPad Prism software (La Jolla, USA). Averages are presented as mean and variances as the standard error of the mean (s.e.m). The homogeneity of variances was tested with Bartlett's test. Normal distributed data from multiple groups were compared by one-way ANOVA with Sidak's correction for multiple comparisons. For non-normal distributed data the non-parametric Kruskal-Wallis one way-ANOVA was performed. When only two independent groups were compared, we used the unpaired *t* test or the non-parametric Mann-Whitney test.

To identify the LF associated taxa students t-test adjusted for multiple comparisons with Bonferonni correction were performed between the LF and HF fed mice. Genera with adj. p < 0.05 were selected. The PCoA plots were performed in R by plotting the Bray-Curtis distance matrix using *vegan* and *ggplot*. Heatmaps and hierarchical clustering were created in Python using *seaborn* where rows were clustered by the Euclidean distance matrix and ward linkage hierarchical clustering.

References

1. Butt, M.S. and M.T. Sultan, Coffee and its consumption: benefits and risks. *Crit Rev Food Sci Nutr*, **2011**. 51(4): p. 363-73.

2. Nieber, K., The Impact of Coffee on Health. *Planta Med*, **2017**. 83(16): p. 1256-1263.

3. Nishitsuji, K., S. Watanabe, *et al.*, Effect of coffee or coffee components on gut microbiome and short-chain fatty acids in a mouse model of metabolic syndrome. *Sci Rep*, **2018**. 8(1): p. 16173.

4. Poole, R., O.J. Kennedy, *et al.*, Coffee consumption and health: umbrella review of meta-analyses of multiple health outcomes. *BMJ*, **2017**. 359: p. j5024.

5. Lozupone, C.A., J.I. Stombaugh, *et al.*, Diversity, stability and resilience of the human gut microbiota. *Nature*, **2012**. 489(7415): p. 220-30.

6. Murphy, E.A., K.T. Velazquez, and K.M. Herbert, Influence of high-fat diet on gut microbiota: a driving force for chronic disease risk. *Curr Opin Clin Nutr Metab Care*, **2015**. 18(5): p. 515-20.

7. Rizzatti, G., L.R. Lopetuso, *et al.*, *Proteobacteria*: A Common Factor in Human Diseases. *Biomed Res Int*, **2017**. 2017: p. 9351507.

8. Marchesi, J.R., D.H. Adams, *et al.*, The gut microbiota and host health: a new clinical frontier. *Gut*, **2016**. 65(2): p. 330-9.

9. Jaquet, M., I. Rochat, *et al.*, Impact of coffee consumption on the gut microbiota: a human volunteer study. *Int J Food Microbiol*, **2009**. 130(2): p. 117-21.

10. Nakayama, T. and K. Oishi, Influence of coffee (Coffea arabica) and galacto-oligosaccharide consumption on intestinal microbiota and the host responses. *FEMS Microbiol Lett*, **2013**. 343(2): p. 161-8.

11. Ericsson, A.C., J. Gagliardi, *et al.*, The influence of caging, bedding, and diet on the composition of the microbiota in different regions of the mouse gut. *Sci Rep*, **2018**. 8(1): p. 4065.

12. Pereira, F.C. and D. Berry, Microbial nutrient niches in the gut. *Environ Microbiol*, **2017**. 19(4): p. 1366-1378.

13. Gu, S., D. Chen, *et al.*, Bacterial community mapping of the mouse gastrointestinal tract. *PLoS One*, **2013**. 8(10): p. e74957.

14. Pang, W., F.K. Vogensen, *et al.*, Faecal and caecal microbiota profiles of mice do not cluster in the same way. *Lab Anim*, **2012**. 46(3): p. 231-6.

15. Tanca, A., V. Manghina, *et al.*, Metaproteogenomics Reveals Taxonomic and Functional Changes between Cecal and Fecal Microbiota in Mouse. *Front Microbiol*, **2017**. 8: p. 391.

16. Yan, W., C. Sun, *et al.*, Efficacy of Fecal Sampling as a Gut Proxy in the Study of Chicken Gut Microbiota. *Front Microbiol*, **2019**. 10: p. 2126.

17. Winer, D.A., H. Luck, *et al.*, The Intestinal Immune System in Obesity and Insulin Resistance. *Cell Metab*, **2016**. 23(3): p. 413-26.

18. Gavrieli, A., M. Yannakoulia, *et al.*, Caffeinated coffee does not acutely affect energy intake, appetite, or inflammation but prevents serum cortisol concentrations from falling in healthy men. *J Nutr*, **2011**. 141(4): p. 703-7.

19. Loftfield, E., M.C. Cornelis, *et al.*, Association of Coffee Drinking With Mortality by Genetic Variation in Caffeine Metabolism: Findings From the UK Biobank. *JAMA Intern Med*, **2018**. 178(8): p. 1086-1097.

20. Zampelas, A., D.B. Panagiotakos, *et al.*, Associations between coffee consumption and inflammatory markers in healthy persons: the ATTICA study. *Am J Clin Nutr*, **2004**. 80(4): p. 862-7.

21. Vitaglione, P., F. Morisco, *et al.*, Coffee reduces liver damage in a rat model of steatohepatitis: the underlying mechanisms and the role of polyphenols and melanoidins. *Hepatology*, **2010**. 52(5): p. 1652-61.

22. Liang, N. and D.D. Kitts, Role of Chlorogenic Acids in Controlling Oxidative and Inflammatory Stress Conditions. *Nutrients*, **2015**. 8(1): p. 16.

23. Shimizu, M., Multifunctions of dietary polyphenols in the regulation of intestinal inflammation. *J Food Drug Anal*, **2017**. 25(1): p. 93-99.

24. Lee, I.A., D. Low, *et al.*, Oral caffeine administration ameliorates acute colitis by suppressing chitinase 3-like 1 expression in intestinal epithelial cells. *J Gastroenterol*, **2014**. 49(8): p. 1206-16.

25. Gniechwitz, D., N. Reichardt, *et al.*, Dietary fiber from coffee beverage: degradation by human fecal microbiota. *J Agric Food Chem*, **2007**. 55(17): p. 6989-96.

26. Cowan, T.E., M.S. Palmnas, *et al.*, Chronic coffee consumption in the diet-induced obese rat: impact on gut microbiota and serum metabolomics. *J Nutr Biochem*, **2014**. 25(4): p. 489-95.

27. Joeris, T., K. Muller-Luda, *et al.*, Diversity and functions of intestinal mononuclear phagocytes. *Mucosal Immunol*, **2017**. 10(4): p. 845-864.

28. Zhang, C., M. Zhang, *et al.*, Structural resilience of the gut microbiota in adult mice under high-fat dietary perturbations. *ISME J*, **2012**. 6(10): p. 1848-57.

29. Turnbaugh, P.J., F. Backhed, *et al.*, Diet-induced obesity is linked to marked but reversible alterations in the mouse distal gut microbiome. *Cell Host Microbe*, **2008**. 3(4): p. 213-23.

30. Park, B.S. and J.O. Lee, Recognition of lipopolysaccharide pattern by TLR4 complexes. *Exp Mol Med*, **2013**. 45: p. e66.

31. Bedard, K. and K.H. Krause, The NOX family of ROS-generating NADPH oxidases: physiology and pathophysiology. *Physiol Rev*, **2007**. 87(1): p. 245-313.

32. Matziouridou, C., S.D.C. Rocha, *et al.*, iNOS- and NOX1-dependent ROS production maintains bacterial homeostasis in the ileum of mice. *Mucosal Immunol*, **2018**. 11(3): p. 774-784.

33. Babior, B.M., NADPH oxidase: an update. *Blood*, **1999**. 93(5): p. 1464-76.

34. Larsson, E., V. Tremaroli, *et al.*, Analysis of gut microbial regulation of host gene expression along the length of the gut and regulation of gut microbial ecology through MyD88. *Gut*, **2012**. 61(8): p. 1124-31.

35. Schwerd, T., R.V. Bryant, *et al.*, NOX1 loss-of-function genetic variants in patients with inflammatory bowel disease. *Mucosal Immunol*, **2018**. 11(2): p. 562-574.

36. Martinez-Guryn, K., N. Hubert, *et al.*, Small Intestine Microbiota Regulate Host Digestive and Absorptive Adaptive Responses to Dietary Lipids. *Cell Host Microbe*, **2018**. 23(4): p. 458-469 e5.

37. Xiao, S., N. Fei, *et al.*, A gut microbiota-targeted dietary intervention for amelioration of chronic inflammation underlying metabolic syndrome. *FEMS Microbiol Ecol*, **2014**. 87(2): p. 357-67.

38. Hildebrandt, M.A., C. Hoffmann, *et al.*, High-fat diet determines the composition of the murine gut microbiome independently of obesity. *Gastroenterology*, **2009**. 137(5): p. 1716-24 e1-2.

39. Chang, E.B. and K. Martinez-Guryn, Small intestinal microbiota: the neglected stepchild needed for fat digestion and absorption. *Gut Microbes*, **2019**. 10(2): p. 235-240.

40. Kastl, A.J., Jr., N.A. Terry, *et al.*, The Structure and Function of the Human Small Intestinal Microbiota: Current Understanding and Future Directions. *Cell Mol Gastroenterol Hepatol*, **2020**. 9(1): p. 33-45.

41. El Aidy, S., B. van den Bogert, and M. Kleerebezem, The small intestine microbiota, nutritional modulation and relevance for health. *Curr Opin Biotechnol*, **2015**. 32: p. 14-20.

42. Meng, Y., X. Li, *et al.*, Effects of Different Diets on Microbiota in The Small Intestine Mucus and Weight Regulation in Rats. *Sci Rep*, **2019**. 9(1): p. 8500.

43. Tomas, J., C. Mulet, *et al.*, High-fat diet modifies the PPAR-gamma pathway leading to disruption of microbial and physiological ecosystem in murine small intestine. *Proc Natl Acad Sci U S A*, **2016**. 113(40): p. E5934-E5943.

44. Turnbaugh, P.J., V.K. Ridaura, *et al.*, The effect of diet on the human gut microbiome: a metagenomic analysis in humanized gnotobiotic mice. *Sci Transl Med*, **2009**. 1(6): p. 6ra14.

45. Evans, C.C., K.J. LePard, *et al.*, Exercise prevents weight gain and alters the gut microbiota in a mouse model of high fat diet-induced obesity. *PLoS One*, **2014**. 9(3): p. e92193.

46. Wang, S., M. Huang, *et al.*, Gut microbiota mediates the anti-obesity effect of calorie restriction in mice. *Sci Rep*, **2018**. 8(1): p. 13037.

47. Capek, P., E. Paulovicova, *et al.*, Coffea arabica instant coffee--chemical view and immunomodulating properties. *Carbohydr Polym*, **2014**. 103: p. 418-26.

48. Ozdal, T., D.A. Sela, *et al.*, The Reciprocal Interactions between Polyphenols and Gut Microbiota and Effects on Bioaccessibility. *Nutrients*, **2016**. 8(2): p. 78.

49. Duda-Chodak, A., T. Tarko, *et al.*, Interaction of dietary compounds, especially polyphenols, with the intestinal microbiota: a review. *Eur J Nutr*, **2015**. 54(3): p. 325-41.

50. Wu, Y., W. Liu, *et al.*, Dietary chlorogenic acid regulates gut microbiota, serum-free amino acids and colonic serotonin levels in growing pigs. *Int J Food Sci Nutr*, **2018**. 69(5): p. 566-573.

51. Wang, Z., K.L. Lam, *et al.*, Chlorogenic acid alleviates obesity and modulates gut microbiota in high-fat-fed mice. *Food Sci Nutr*, **2019**. 7(2): p. 579-588.

52. Gurwara, S., A. Dai, *et al.*, Caffeine Consumption and the Colonic Mucosa-Associated Gut Microbiota. *The American Journal of Gastroenterology*, **2019**. 114(p): p. 119-120.

53. Gniechwitz, D., B. Brueckel, *et al.*, Coffee dietary fiber contents and structural characteristics as influenced by coffee type and technological and brewing procedures. *J Agric Food Chem*, **2007**. 55(26): p. 11027-34.

54. Weber, L., K. Kuck, *et al.*, Anti-Inflammatory and Barrier-Stabilising Effects of Myrrh, Coffee Charcoal and Chamomile Flower Extract in a Co-Culture Cell Model of the Intestinal Mucosa. *Biomolecules*, **2020**. 10(7): p. 1033.

55. Zhao, W., L. Ma, *et al.*, Caffeine Inhibits NLRP3 Inflammasome Activation by Suppressing MAPK/NF-κB and A2aR Signaling in LPS-Induced THP-1 Macrophages. *Int J Biol Sci*, **2019**. 15(8): p. 1571-1581.

56. Paur, I., T.R. Balstad, and R. Blomhoff, Degree of roasting is the main determinant of the effects of coffee on NF-κB and EpRE. *Free Radical Biology and Medicine*, **2010**. 48(9): p. 1218-1227.

57. Zhang, P., H. Jiao, *et al.*, Chlorogenic Acid Ameliorates Colitis and Alters Colonic Microbiota in a Mouse Model of Dextran Sulfate Sodium-Induced Colitis. *Frontiers in Physiology*, **2019**. 10: p. 325.

58. Nishida, A., R. Inoue, *et al.*, Gut microbiota in the pathogenesis of inflammatory bowel disease. *Clin J Gastroenterol*, **2018**. 11(1): p. 1-10.

59. Khan, I., N. Ullah, *et al.*, Alteration of Gut Microbiota in Inflammatory Bowel Disease (IBD): Cause or Consequence? IBD Treatment Targeting the Gut Microbiome. *Pathogens*, **2019**. 8(3): p. 126.

60. Johnson, A.M., A. Costanzo, *et al.*, High fat diet causes depletion of intestinal eosinophils associated with intestinal permeability. *PLoS One*, **2015**. 10(4): p. e0122195.

61. Goodyear, A.W., A. Kumar, *et al.*, Optimization of murine small intestine leukocyte isolation for global immune phenotype analysis. *J Immunol Methods*, **2014**. 405: p. 97-108.

62. Avershina, E., K. Lundgard, *et al.*, Transition from infant- to adult-like gut microbiota. *Environ Microbiol*, **2016**. 18(7): p. 2226-36.

63.   Yu, Y., C. Lee*, et al.*, Group-specific primer and probe sets to detect methanogenic communities using quantitative real-time polymerase chain reaction. *Biotechnology and bioengineering*, **2005**. 89(6): p. 670-679.

64.   Edgar, R.C., Search and clustering orders of magnitude faster than BLAST. *Bioinformatics*, **2010**. 26(19): p. 2460-2461.

65.   Edgar, R.C., UPARSE: highly accurate OTU sequences from microbial amplicon reads. *Nat Methods*, **2013**. 10(10): p. 996-8.

66.   DeSantis, T.Z., P. Hugenholtz*, et al.*, Greengenes, a chimera-checked 16S rRNA gene database and workbench compatible with ARB. *Appl Environ Microbiol*, **2006**. 72(7): p. 5069-72.

Paper III

iNOS- and NOX1-dependent ROS production maintains bacterial homeostasis in the ileum of mice

C Matziouridou[1], SD C Rocha[1], OA Haabeth[2,3], K Rudi[1], H Carlsen[1] and A Kielland[1]

The intestinal epithelial cells constitute the first line of defense against gut microbes, which includes secretion of various antimicrobial substances. Reactive oxygen species (ROS) are well characterized as part of the innate phagocytic immunity; however, a role in controlling microorganisms in the gut lumen is less clear. Here, we show a role for nitric oxide synthase (iNOS)- and NOX1-produced ROS in maintaining homeostasis of the gut microbiota. In vivo imaging revealed distinctly high levels of ROS in the ileum of normal healthy mice, regulated in accordance with the amount of gut bacteria. The ROS level was dependent on the nitric oxide and superoxide producers iNOS and NOX1, respectively, suggesting peroxynitrite as the effector molecule. In the ileum of iNOS- and NOX1-deficient mice, the bacterial load is increased and the composition is more cecum like. Our data suggest a unique role of ileum in maintaining homeostasis of gut microbes through production of ROS with potential importance for preventing reflux from the large intestine, bacterial overgrowth, and translocation.

INTRODUCTION

The small intestine possesses a dual role: on the one hand, it is responsible for uptake of nutrients, which requires a large absorptive surface, whereas on the other hand it must prevent the gut lumen microbiota from entering this same surface. The gut lumen is separated from the host interior by only one cell layer, which is ideal for its absorptive role. However, this creates a challenge for its role as a barrier. As part of the barrier function, the epithelial cells interact with the microbes in the gut lumen. Several secretory molecules, such as mucins that make up the mucus layer, antimicrobial peptides, and secretory IgA participate in controlling the gut microbes. Reactive oxygen species (ROS) are universally accepted to be an essential component of the innate immune system through the respiratory burst in neutrophils, macrophages, and dendritic cells; however, an antimicrobial role of ROS in the gut is less determined. Here, we have explored a role of ROS production in maintaining bacterial homeostasis in the small intestine at the border with the large intestine.

The ROS producing enzymes, Dual oxidase (DUOX) and NADPH oxidase (NOX), are expressed in the intestinal epithelial cells in correlation with microbial content, indicating a role of these enzymes in ROS-based immune homeostasis of the gut.[1] In Drosophila, it is shown that DUOX produces ROS in the gut, which is directly bactericidal, and necessary to control gut bacteria and prevent infections. The DUOX in Drosophila contains two enzymatic domains: one oxidase domain that produces hydrogen peroxide and one peroxidase domain that converts the hydrogen peroxide to hypochlorous acid.[2] In C. elegans, DUOX-dependent ROS production in the gut was shown to improve survival during bacterial infections; however, no direct bactericidal effect was determined.[3] Hydrogen peroxide is suggested as the effector molecule, but this is a less bactericidal molecule than hypochlorous acid. In mammals, DUOX2 is reported to have an anti-bacterial role in cultured primary airway epithelial cells[4] and in defense against Helicobacter felis infection in gastric epithelium.[5] In these systems, it was suggested that DUOX2 produced hydrogen peroxide as a substrate for lactoperoxidase, with a subsequent formation of the bactericidal hypothiocyanous acid. In a DUOX2-deficient mouse, bacterial translocation was increased and expression of a ROS-inducible gene was downregulated in

the mucosal-segmented filamentous bacteria.[6] NOX1 is highly expressed in epithelial cells, particularly, in colon and ileum. Most studies have focused on NOX1's role in redox modifications of signaling pathways involved in cell division and differentiation, particularly, with respect to wound healing in colon.[7] However, its role in controlling gut microbes is elusive. In one study of NOX1 knockout (KO) mice inoculated with *Salmonella typhimurium*, no effect on cecal concentration of the bacterium and changes in overall protection were observed.[8] In another study with *Citrobacter rodentium* infection, reduced cecal numbers and lower disease status were found in NOX1 KO mice.[9] They further provided evidence suggesting NOX1 to operate through regulation of DUOX2. The NOX enzymes generate superoxide, which does not kill microbes directly, but is precursor of other ROS with bactericidal activity such as hydrogen peroxide, hydroxyl radicals, hypochlorous acid, and peroxynitrite. Superoxide combines with nitric oxide (NO) to form peroxynitrite, which is regarded as one of the crucial bactericidal ROS in the respiratory burst of the innate immune system. NO is produced by inducible nitric oxide synthase (iNOS), which is expressed by epithelial cells of the small intestine in association with the amount of bacterial content.[1,10] Furthermore, NO is found in the gut lumen.[11] This raises the question whether peroxynitrite produced in the intestine can affect the luminal gut bacteria and thus participate in maintaining homeostasis of gut microbes.

Here, we have found evidence for a high NOX1- and iNOS-dependent ROS production in the ileum of normal healthy mice. We furthermore observed a strong impact of this ROS production on the microbial load and composition in the ileum. This suggests a unique role of ileum in maintaining homeostasis of gut microbes through production of peroxynitrite with potential importance for preventing reflux from the large intestine, bacterial overgrowth, and invasion.

RESULTS

iNOS- and NOX1-dependent production of ileal ROS

To determine whether ROS are present in the small intestine, we used the optical imaging probe L-012, which has high specificity for ROS, particularly, peroxynitrite.[12] *In vivo* imaging of L-012-dependent luminescence showed a strong signal coming from the abdominal region of the mice (**Figure 1a**). Dissection and imaging of individual organs *ex vivo* showed that the signal originated from the distal small intestine, the ileum (**Figure 1b**). This overlaps with the particularly high expression of iNOS in ileum in comparison to the rest of the intestine and the relatively high expression of NOX1 in ileum compared to more proximal parts (**Figure 1c**). As these enzymes catalyze the production of superoxide anion and NO, which rapidly react to form peroxynitrite we wanted to determine their involvement in the ROS production. We injected the NOS inhibitor L-NAME i.v. ($50\,mg\,kg^{-1}$) and imaged the L-012-mediated luminescence, which was reduced by 70% (**Figure 1d**). To elucidate the involvement of superoxide, we added the superoxide scavenger TEMPOL

in the drinking water ($2.5\,g\,l^{-1}$) (**Figure 1e**). After 2 days, the L-012 signal was reduced by more than 60%. To assess the presence of peroxynitrite, we administrated the peroxynitrite scavenger MnTBAP chloride i.v ($20\,mg\,kg^{-1}$), and we here observed around 60% reduction in the L-012 signal (**Figure 1f**). Furthermore, we explored the ROS production in KO mice of iNOS and NOX1. We first imaged the L-012 signal in KO mice cohoused with wild type (WT) mice and then 4 weeks after being separated and housed as single genotypes (**Figure 1g**). The signal was reduced by around 60% in the iNOS KO mice and almost abolished in the NOX1 KO mice. We did not observe any significant difference between the mice during and after cohousing. Furthermore, as peroxynitrite is a strong oxidant, we gave the antioxidants vitamin C ($10\,g\,l^{-1}$) and tannic acid ($5\,g\,l^{-1}$) in the drinking water of WT mice. We measured the L-012 signal over 3 weeks (**Figure 1h**). The signal went gradually down reaching 70% reduction for both antioxidants. To determine whether the epithelial cells could be responsible for the peroxynitrite production, we measured the NO content in these cells with the probe DAF-FM using flow cytometry (**Figure 2a, b**). We observed in the cells staining positively for the epithelial cell marker CD326, a significantly larger fraction of cells with DAF-FM labeling in the distal small intestine compared with the proximal region. Furthermore, the distal cells showed higher mean fluorescent intensity indicating more NO production in the distal cells compared to the proximal. As innate immune cells in the lamina propria can mount a respiratory burst, we also determined the NO content in cells stained with CD11b, a marker for monocytes, dendritic cells, and macrophages. There was significantly higher signal from the epithelial cells in comparison to CD11b stained cells. Taken together, these observations support an iNOS- and NOX1-dependent ROS production in epithelial cells of ileum.

The amount of gut bacteria is associated with the ROS production

To elucidate whether gut bacteria can induce ROS production in ileum, we manipulated the amount of bacteria. To decrease the bacterial load, we first used an antibiotics treatment proven to almost fully deplete the gut microbiota ($1\,g\,l^{-1}$ neomycin, $0.5\,g\,l^{-1}$ vancomycin, $1\,g\,l^{-1}$ metronidazole, and $1\,g\,l^{-1}$ ampicillin, oral gavage daily for a week).[13] As this is a harsh treatment with potential unforeseen physiological effects and depletion of ileal microbiota is sufficient here, we also exposed the mice to a milder antibiotic treatment ($0.5\,g\,l^{-1}$ neomycin and $0.25\,g\,l^{-1}$ vancomycin through the drinking water over 4 weeks) (**Figure 3a, b**). In both cases, the L-012-mediated signal went down by $\sim 80\%$. As expected, the bacterial load went down in ileum (**Figure 3c**). Consistent with these observations, the mRNA expression of both iNOS and NOX1 was decreased in the ileum (**Figure 3d, e**). We also decreased the bacterial content in the intestine by 15 h fasting (**Figure 3f**). This caused a reduction in the L-012 signal from the mice by 70%. To study the ROS production during an increase in the bacterial load, we imaged mice before, during and after weaning, as this is a period where massive increase of intestinal bacteria occurs.[14] Here, we observed a large increase in
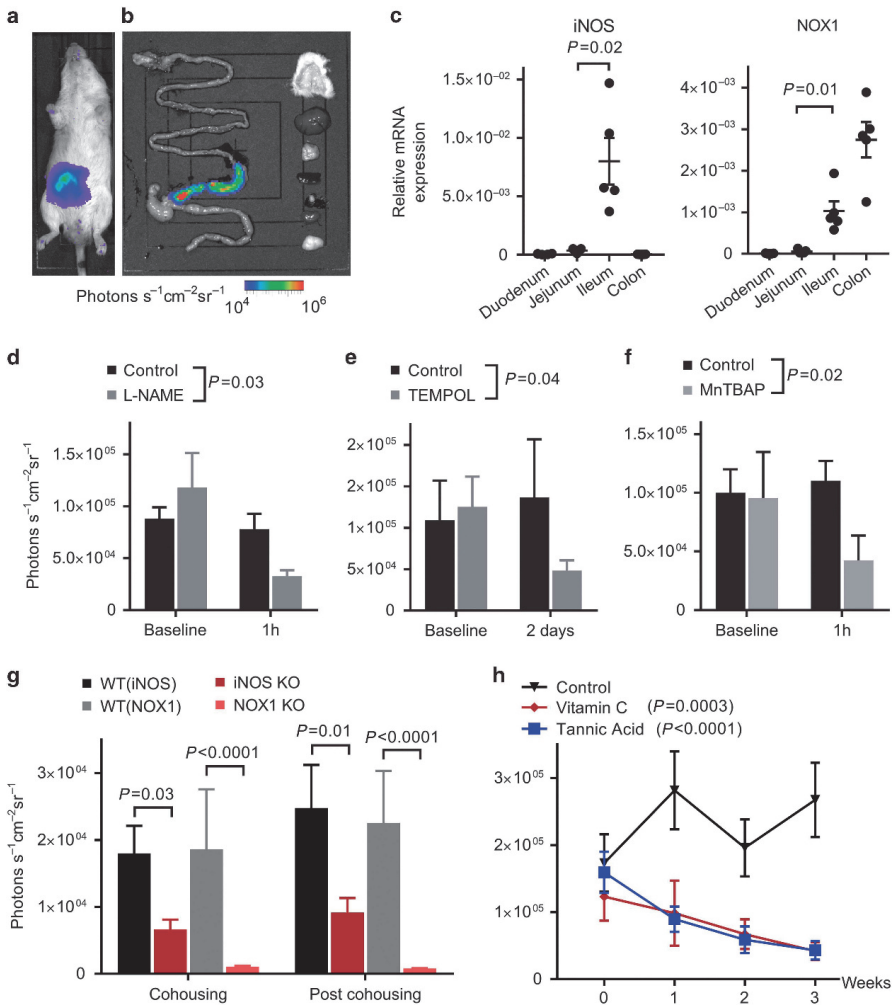
Figure 1 iNOS- and NOX1-dependent production of ileal ROS. (**a**, **b**) L-012-mediated luminescence signal (**a**) *in vivo* and (**b**) *ex vivo* indicating high ROS production in the terminal part of the small intestine, the ileum. Dissected organs displayed to the right in the panel illustrates low L-012 signal (from top to bottom: skin, liver, pancreas, spleen, inguinal lymph node, kidney and mesenteric fat). The pseudo colors represent photons s^{-1} cm^2 sr. (**c**) mRNA expression of iNOS and NOX1 in the small intestine and colon of WT mice. GADPH is used for normalization. Both of the genes are highly expressed in ileum, $n = 5$. (**d**–**h**) The following conditions reduced the L-012-mediated signal: (**d**) L-NAME provided i.p., $n = 6$; (**e**) TEMPOL in the drinking water, $n = 8$–10; (**f**) MnTBAP provided i.v., $n = 8$ (**g**) iNOS and NOX1 KO mice compared to WT that were imaged both during cohousing with WT mice and 4 weeks after separation to individual cages, $n = 15$–30; (**h**) Vitamin C or tannic acid in the drinking water, $n = 15$. Values are mean with s.e.m. (**c**) Student's *t*-test. (**d**–**f**) Student's *t*-test of the difference in reduction between control and treatment groups. (**g**) Kruskal–Wallis test with Dunn's correction for multiple comparisons. (**h**) One-way ANOVA. iNOS, nitric oxide synthase; ROS, reactive oxygen species; WT, wild type.

the L-012 signal the first week after separating the mice from their mother, which thereafter stabilized (**Figure 3g**). In conclusion, these finding suggest that the intestinal ROS production is dependent on the presence of bacteria in the gut.

iNOS and NOX1 KO mice had higher bacterial load in the distal small intestine

As we observed that iNOS and NOX1 are necessary for the ROS production, we sought to determine whether the

bacterial content in the gut of iNOS and NOX1 KO mice is increased compared to WT mice. To balance the environmental influence, the KO and WT mice were cohoused for 3 to 4 weeks directly after weaning. The mice were then allocated to separate cages based on genotype for 4 weeks before sampling. We estimated the amount of bacteria in the luminal chyme by colony-forming units (CFU) counting (**Figure 4a**) and in the mucus by RT-qPCR against the 16S rRNA gene (**Figure 4b**).). In both KO
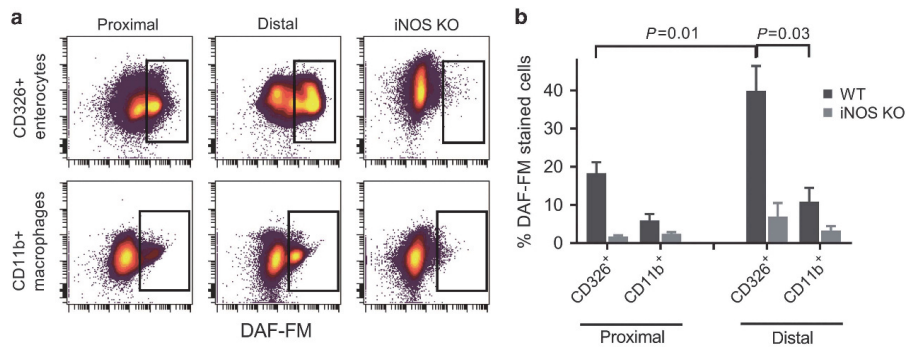
Figure 2 Flow cytometry analysis of NO content in cells of proximal and distal part of the small intestine. (**a**) Scatter plots of the NO probe DAF-FM staining combined with the epithelial cell marker CD326 and the phagocyte cell marker CD11b in cells isolated from the epithelial layer and lamina propria. Labeling of cells from iNOS KO is consistent with the absence of NO production (**b**) WT and iNOS KO mice show higher NO production in epithelial cells of distal intestine compared to both proximal intestine and macrophages of the lamina propria Mann–Whitney test. Furthermore, in all the corresponding cell populations of the iNOS KO and WT mice, the iNOS KOs showed significantly reduced NO production ($P < 0.03$ for all comparisons) Kruskal–Wallis test with Dunn's correction for multiple comparisons. Values are mean with s.e.m. iNOS, nitric oxide synthase; NO, nitric oxide; WT, wild type.

types, the amount of bacteria was higher in ileum and jejunum in comparison to the WT mice for the luminal samples. For the mucosal samples, we did observe higher bacterial load in the ileum of the two KOs, but it was only statistically significant for the NOX1. We also estimated the bacterial content in cecum samples by CFU counting (**Figure 4a**). Here, we found no significant difference between either of the KO with the WT mice. Interestingly, we observed that in the KOs the bacterial amount reached cecum-like numbers in ileum, consistent with potential bacterial overgrowth. In conclusion, the amount of bacteria in the distal small intestine is dependent on both iNOS and NOX1 suggesting involvement of a converging effect, possibly the formation of peroxynitrite.

The microbial composition in the small intestine is altered in a similar manner for the iNOS and NOX1 KO mice

To determine the impact of ROS production on potential alterations in the composition of the gut microbiota, we performed 16S rRNA gene sequencing of DNA extracted from mucosa and luminal chyme samples of the WTs and the iNOS and NOX1 KO mice. We observed that at phylum level, there is a similar shift in the microbial composition in jejunum and ileum for both KO mice (**Figure 5a**). Firmicutes increase and Bacteroidetes concurrently decrease. This can be seen for both mucosa and luminal chyme samples; however, it is more pronounced in the former. In cecum, the microbial composition appears to be unaltered between the KO and the WT mice. To investigate whether the gut microbiota is also altered at finer taxonomic levels, we performed a Principal component analysis (PCA) using the relative abundance of the taxa classified at family level (**Figure 5b–e**). Families that were present in at least five mice with relative abundance higher than 0.5% were included in the analysis. The PCA distinguished the ileal samples of the WT and KO, whereas the two KO types co-clustered. The results were

similar for the mucus and chyme samples; however, the chyme samples show some degree of overlap with the WT. All cecum samples showed co-clustering. In addition, we sought to determine whether there is an overlap between the specifically differentiated taxa for each of the two KO mice. We performed a LEfSE analysis on the ileal mucosal samples to identify the taxa that were associated with the iNOS and the NOX1 KO mice. Five taxa were identified for the iNOS KO mice: four increasing (Actinobacteria, Actinomycetales, *Sporosarcina*, *Allobaculum*) and one decreasing (S24_7). For the NOX1 KO mice, nine taxa were identified: eight increasing (Actinobacteria, Bacillaceae, Coriobacteriaceae, *Dietzia*, *Turicibacter*, *Bifidobacterium*, *Sporosarcina*, *Allobaculum*) and one decreasing (*Lactobacillus*). We next compared the relative abundance of the enriched identified taxa in each of the KOs to the WT (**Figure 6**). Six out of the eight taxa associated with the NOX1 KO mice show a statistically significant increase in the iNOS KO mice, whereas three out of the four taxa associated with the iNOS KO mice increase in the NOX1 KO mice. However, the taxa that decreased in each of the KOs did not change significantly in the other KO type. Taken together, these findings suggest that iNOS- and NOX1-dependent production of ROS in the small intestine alters the gut microbial composition. The observed alterations appear to be similar for both KOs indicating a synergistic effect of NO and superoxide.

iNOS and NOX1 KO mice show a shift in ileal microbiota resembling more cecal composition

We observed a higher ratio of Firmicutes to Bacteroidetes for the two KOs (**Figure 7a**). Interestingly, this moves the microbiota composition in a direction resembling more the one in cecum. Furthermore, the increased Firmicutes/Bacteroidetes ratio is most pronounced in the ileum and becomes gradually less in more proximal parts of the small intestine. To elucidate whether this could be caused by
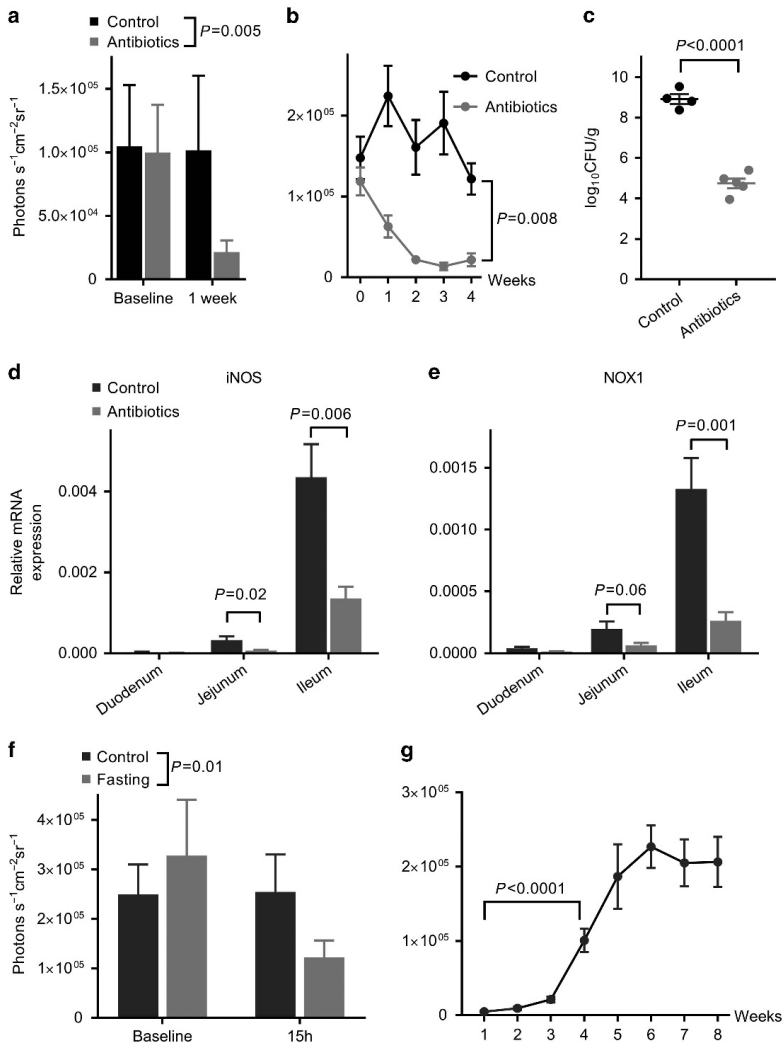
Figure 3 Effect of bacterial luminal load on ROS production. (**a**, **b**) The L-012-mediated signal is reduced in mice receiving antibiotics concoctions either by (**a**) daily oral gavage, $n = 5–6$ or (**b**) via the drinking water, $n = 10$. (**c**) The amount of cultivable luminal chyme bacteria in ileum is reduced in mice receiving antibiotics via gavage over 1 week, $n = 4–5$. (**d**, **e**) The mRNA expression of iNOS and NOX1 decreases in jejunum and ileum in mice receiving antibiotics in the drinking water over 4 weeks, $n = 10$. (**f**) The L-012-mediated signal goes down in mice after 15 h of fasting $n = 10$. (**g**) The L-012 signal is minimal in the 3 weeks prior to weaning and increases severely after separation from mother $n = 11–16$. Values are mean with s.e.m. (**a**, **f**) Student's t-test of the difference in reduction between control and treatment groups. (**c**) Student's t-test (**b**, **g**) one-way ANOVA. (**d**, **e**) One-way ANOVA with Sidak's correction for multiple comparisons. iNOS, nitric oxide synthase; ROS, reactive oxygen species.

migration of bacteria from cecum to ileum, we identified all genera that were significantly more abundant in cecum than in ileum of WT mice and determined if they were increased in the KO mice (**Figure 7b**). We observed the abundance in ileum of most of these genera to be higher in both of the two KO mouse types compared to WT. In conclusion, these results may imply that ROS production in ileum has a role in prevention of cecal microbiota reflux.

Bacterial DNA is higher in the liver of the KO mice
To evaluate potential implications of the intestinal ROS production on bacterial translocation, we determined the content of bacterial DNA in liver by RT-qPCR against the 16S rRNA gene. We found an increase in bacterial DNA of 56% ($n = 6–10$, $P = 0.02$, Kruskal–Wallis test with Dunn's correction for multiple comparisons) for iNOS KO mice and of 112% ($n = 10–13$, $P = 0.009$) for NOX1 KO mice compared to WT

mice, indicating a role for intestinal ROS production in defense against bacterial translocation.

DISCUSSION

In the present study, we have demonstrated that ROS, possibly peroxynitrite, are highly produced by iNOS and NOX1 in the ileum of normal healthy mice. Furthermore, the amount, composition and translocation of intestinal bacteria appear to be regulated by this ROS production.

To address temporal and spatial *in vivo* ROS production, we exploited the luminescent probe L-012 as an imaging marker for ROS.[15–18] We observed a strong L-012-mediated signal in ileum that we believe is the result of epithelial cell secretion of superoxide and NO, with a resultant peroxynitrite formation. This is supported by the following: firstly, L-012 is recognized to act extracellularly, and with a high specificity and sensitivity to peroxynitrite.[12] NOX1 together with iNOS are responsible for the signal and the major substrate of superoxide, in terms of reaction kinetics, is NO, which together form peroxynitrite.[19] Both L-NAME, a NOS inhibitor, and using iNOS KO mice reduced the signal, whereas the superoxide quencher TEMPOL and particularly knocking out NOX1 nearly abolished the L-012-generated signal. Secondly, NOX1 and iNOS are co-expressed in the small intestine, with a particularly high expression in the ileum. In addition, the L-012 signal is not present in the colon where NOX1 has high expression, but where iNOS is not detectable. Finally, we demonstrated that NO production is more abundant in ileal epithelial cells compared to more proximal intestinal regions and immune cells of the lamina propria. Others have reported that iNOS expression in the healthy gut is confined to the ileal villi.[10] We regard these data as convincing evidence of NO and superoxide production by epithelial cells of ileum, which may join to form peroxynitrite in the gut lumen.

Although peroxynitrite is likely detected in our experiments, there are other candidates such as hydrogen peroxide and hypochlorous acid, which both have prominent roles in respiratory burst.[9] However, hydrogen peroxide is in itself a poor activator of L-012 and requires the presence of high concentrations of peroxidase,[20] which to our knowledge is not expressed at high levels in the ileum of normal healthy mice. Hypochlorous acid can activate L-012, but its production is dependent on myeloperoxidase.[21] Hydrogen peroxide can also be converted to hydroxyl radicals in the presence of Fe^{2+} through the Fenton reaction. Hydroxyl radicals can activate L-012, but the concentration of Fe^{2+} in the intestine is low. However, superoxide can through the Haber–Weiss reaction generate Fe^{2+} suggesting that a combination of NOX1 and DUOX2 could generate part of the intestinal ROS responsible for the L-012 signal. Indeed, when eliminating the iNOS activity not all the signal is abolished. In addition to ROS production related to immune defense, ROS are also produced by the electron transport chain inside the mitochondria and in connection with intracellular signaling, but this is a global phenomenon and comprise only low levels of ROS concentrations, and hence cannot be imaged *in vivo*.

The strength of the L-012-mediated signal is exceptionally high, which implies that the amount of ROS produced in the ileum is high. This is in accordance with previous studies where L-012 is used to image ROS during various conditions of acute inflammation.[15,17] Interestingly, the signal strength generated by L-012 in models of arthritis and skin inflammation is lower than the signal we observe in a healthy ileum. However, it resembles the amount of signal in models of colonic inflammation.[17,18] This raises the interesting question if a large amount of ROS production only is consistent with secretion in non-host tissue, such as the intestinal lumen. Certainly, constant exposure to an extensive oxidative environment can be detrimental to the host tissue.
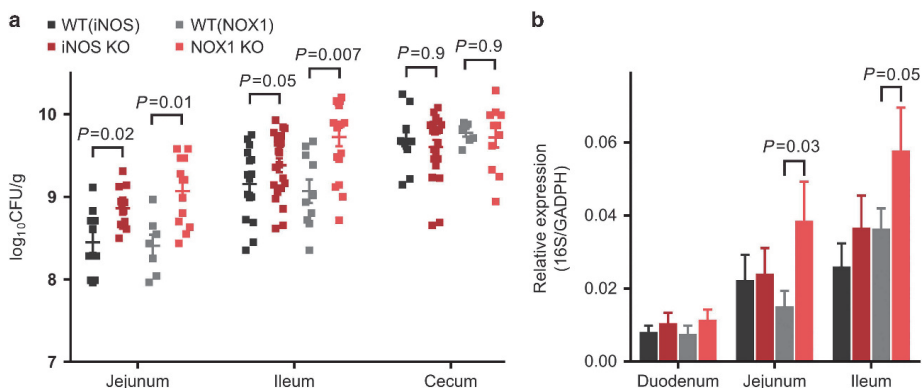

Figure 4 ROS production in the distal part of the small intestine affects the amount of mucosal and luminal bacteria. (**a**) Amount of cultivable bacteria in the luminal chyme of iNOS and NOX1 KO mice. In both jejunum and ileum, the amount of bacteria is increased in the KO mice in comparison to their, respectively, cohoused WT mice. In cecum, no such difference could be detected, $n=10–16$. (**b**) Amount of bacteria in the mucus layer as determined by RT-qPCR of 16S rRNA. GADPH is used for normalization. The bacterial load is increased in the jejunum and ileum of the NOX1 KO mice, $n=9–15$. Values are mean with s.e.m. (**a**) One-way ANOVA with Sidak's correction for multiple comparisons. (**b**) Kruskal–Wallis test with Dunn's correction for multiple comparisons. iNOS, nitric oxide synthase; ROS, reactive oxygen species; WT, wild type.

We found that in the ileum of iNOS and NOX1 KO mice the bacterial load was increased, suggesting an antimicrobial role for the epithelium-deriving ROS. This could be seen overall in ileum, both in the luminal content and in the mucosa. However,

the approach used for the assessment of the bacteria in the luminal content was based on CFU counting, which only assesses the cultivable bacteria, and thus gives an underestimate of the total bacteria that are present. In addition, the microbial
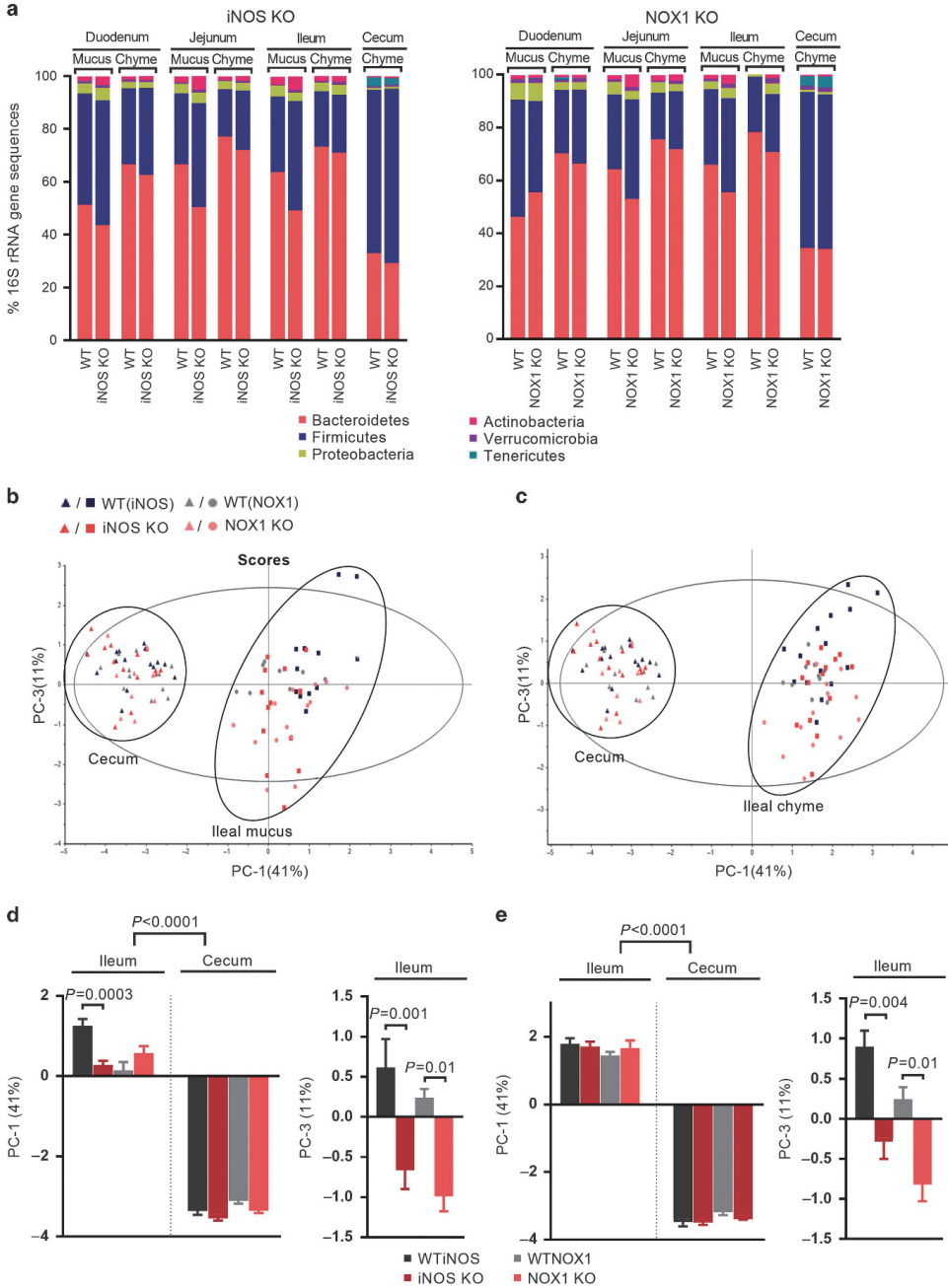
composition of both KO mice was altered. The changes in bacterial composition were similar between NOX1 and iNOS KO mice and to some extent more evident in mucus compared to lumen samples, supporting a cooperative effect of superoxide and nitric oxide originating from the epithelium, as discussed above possibly through the secretion of peroxynitrite. The strong reduction of L-012-mediated signal following administration of broad-spectrum antibiotics, concurred with a

downregulation of iNOS and NOX1. This observation fits well with comparable data showing that germ-free mice have four- and sevenfold lower expression of NOX1 and iNOS, respectively, than conventional mice.[1] Furthermore, intestinal ROS production is lower in germ-free mice, as detected by a broad range *ex vivo* ROS probe.[22] L-012 signals were also influenced by other conditions that change the bacterial load such as after introduction of solid food in weaned mice and during a fasting
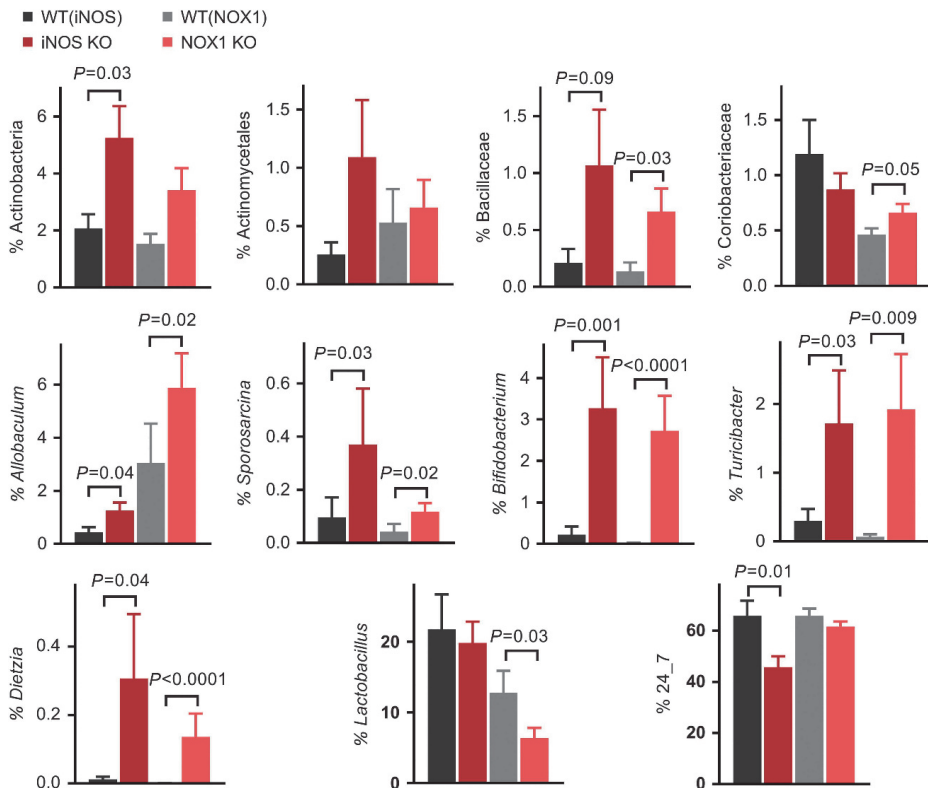
Figure 6 Overlap in identified taxa between iNOS and NOX1 KO mice. Relative abundance of the taxa that either increased or decreased in each of the KO mice as identified by LEfSE. The two KO types show a similar increase for most of these taxa, $n = 10$–14. Values are mean with s.e.m. For each taxon after logarithmic data transformation, one-way ANOVA with Sidak's correction for multiple comparisons. iNOS, nitric oxide synthase; LEfSE, linear discriminant analysis effect size.

Figure 5 Gut microbial composition of the iNOS and NOX1 KO mice shows overlap. (**a**) Relative abundance of phyla in iNOS and NOX1 KO mice and their, respectively, cohoused WT mice. In the two KO mice, Firmicutes are increased in the mucus layer of both jejunum ($P < 0.0001$ for both KO) and ileum ($P < 0.0001$ for iNOS KO and $P = 0.01$ for NOX1 KO), whereas Bacteroidetes decrease (jejunum $P < 0.0001$ for both KO, ileum $P < 0.0001$ for iNOS KO and $P = 0.006$ for NOX1 KO). For the ileal chyme samples, Firmicutes are statistically increased only in NOX1 KO ($P = 0.004$), whereas Bacteroidetes increase only in jejunum in iNOS KO ($P = 0.02$) and in ileum in NOX1 KO ($P = 0.0002$). No differences could be detected in the cecum samples, $n = 10$–16. Values are mean with s.e.m. One-way ANOVA with Tukey's *post hoc*. (**b, c**) PCA plot of the taxa at family level of the ileum and cecum samples. After examining all possible principal components, we found that PC-1 and PC-3 could best explain the variation among the groups. All of the cecum samples were co-clustered regardless of mouse groups. (**b**) The ileal mucosa samples of the two KO mice cluster together and the two WT mice cluster together with minimal overlap between the KOs and the WTs, $n = 8$–15. For the ileal chyme samples (**c**) a similar pattern is observed; however, more overlap can be seen between the iNOS and the WT, $n = 10$–15. (**d, e**) Loading scores of cecum, ileal mucosa (**d**), and ileal chyme (**e**) samples presented in PCA plots in **b** and **c**. In accordance with the above findings, both KO mice for both of the ileal compartments differ from their respective WT on PC3, whereas the iNOS mucosal samples are also separated in PC1, $n = 8$–15. Values are mean with s.e.m. One-way ANOVA with Sidak's corrections for multiple comparisons. iNOS, nitric oxide synthase; PCA, principal component analysis; ROS, reactive oxygen species; WT, wild type.
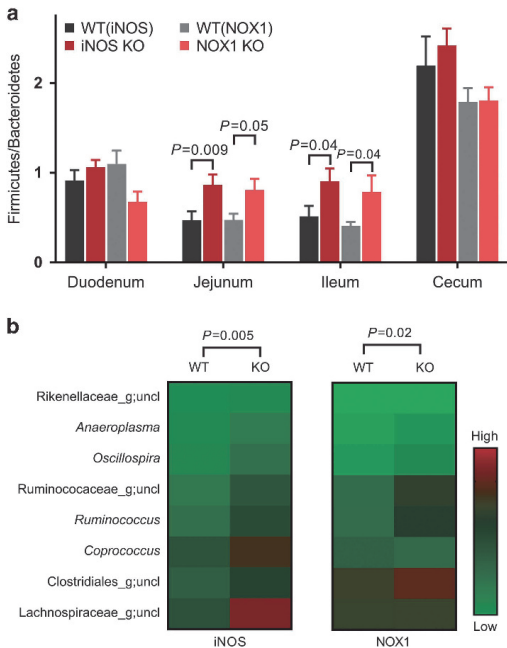
Figure 7 The gut microbial composition of the iNOS and NOX1 KO mice shifts in the direction of cecum. (**a**) Ratio of relative abundance of Firmicutes and Bacteroidetes in different mucosa gut segments. The ratio increases for both KO mice in jejunum and in ileum. No difference was observed for duodenum, $n = 11–16$. Values are mean with s.e.m. One-way ANOVA with Sidak's correction for multiple comparisons for jejunum and duodenum samples, Kruskal–Wallis test with Dunn's correction for multiple comparisons for ileum samples. (**b**) Shift in the relative abundance of the eight genera that were higher in cecum compared to the small intestine. The heat map shows the ratio of ileum to cecum. Columns represent the mean value of each group. In general, in both KOs the mice showed warmer colors compared to the WTs, indicating an ileal shift in these genera to a cecum-like profile, $n = 8–12$. One-way ANOVA. iNOS, nitric oxide synthase; WT, wild type.

period.[14,23] It has been known for some time that ROS affect the luminal bacteria directly. It is reported that during an infectious state DUOX-dependent ROS exert antimicrobial properties in the gut of *Drosophila*.[2] In addition, hydrogen peroxide through the activity of DUOX2 is reported to directly influence the virulence of *Campylobacter jejuni* in an organ culture.[24] In a DUOX2 KO mouse, a ROS-inducible gene was lowered in mucosal associated bacteria suggesting a role of hydrogen peroxide against microbes close to the epithelial surface.[6] ROS through the action of NOX1 has foremost been associated with intracellular signaling related to tissue-wound repair in the colon.[7,25] Pircalabioru *et al.*[9] showed reduced DUOX2 expression in a NOX1 KO mouse during infection suggesting a regulatory role of NOX1 in relation to luminal bacteria. They further observed, in accordance with our results, that microbiota in cecum of the KO had the same distribution of the main phyla as in the WT mice. However, they found an increase in certain species of *Lactobacilli*. It is difficult to compare their

data directly with ours as they did not assess the microbiota composition in ileum. Nevertheless, we found that *Lactobacilli* are reduced in the ileum of NOX1 KO mice. As *Lactobacilli* are known to harbor a strong defense against ROS,[26,27] we believe that the reduction of ROS rather removes a competitive advantage that can explain the decrease in *Lactobacilli*. Our data contribute to the knowledge about NOX1 by showing a direct role in controlling the gut microbiota.

The microbiota content in ileum is much higher than in the rest of the small intestine. This is likely caused by microbial reflux from the large load of microbes in cecum and colon. This suggests a unique role for ileum in preventing bacterial overgrowth and maintaining homeostasis of microbes in the small intestine. This is reflected by the higher density of lymphoid tissue in ileum compared to the rest of the gut. We believe that secretion of ROS, potentially peroxynitrite, from the ileal epithelial cells is an integral part of a defense system controlling the small intestinal microbiota and thus important for the nutrient uptake and barrier role of the gut. These insights may have implications for understanding the pathogenic mechanisms that underlie conditions or diseases often found in the ileum such as SIBO, Crohn's disease, and ileitis.

METHODS

Animals. Animal procedures were approved by the Norwegian Animal Research Authority (Mattilsynet). All experiments apart from the experiments with KO mice were performed on NMRI mice of both genders up to 3 months of age from Janvier Labs. In experiments where both genders were used, we could not observe any gender-specific differences. Breeding stocks of C57BL/6J, and the following KO mice: iNOS$^{-/-}$ and NOX1$^{-/-, y/-}$ on C57BL/6J background were purchased from The Jackson Laboratory. As the largest impact of environmental influence on gut microbiota composition occurs during weaning, we cohoused the KO mice for 3–4 weeks together with WT mice directly after separation from mother.[14,28] All mice used for the analysis of the gut microbiota composition were supplied by the same provider (The Jackson Laboratory, Bar Harbor, ME). The diet was RM1 diet (SDS Diet, Essex, UK) and mice were housed in humidity, temperature and by 12 h night/day light cycle controlled environment in individually ventilated cages (Innovive, San Diego, CA).

Imaging. Imaging was done with IVIS Lumina II (Perkin Elmer, Walthamn, MA). The luminescent probe L-012 (Wako Chemical, Neuss, Germany) was dissolved in saline and injected intraperitoneally (i.p.) at 10 mg kg^{-1}. During *in vivo* imaging the mice were immobilized using isoflurane (2.5–3.5%). *Ex vivo* imaging on dissected organs was performed within 5 min of L-012 injection. Data acquisition were done with the Living Image software (Perkin Elmer). Light emission from the region of interest was quantified as photons s^{-1} cm^{-2} steradian^{-1}.

Flow cytometry. Isolation of an epithelial cell fraction and a lamina propria cell fraction was done as previously described by Goodyear *et al.*[29] Briefly, after killing the mouse, the small intestine was dissected and divided into a proximal and a distal part to be analyzed separately. Peyers patches were removed, the intestine was opened longitudinally and cut into 5 mm long pieces and placed in ice-cold RPMI. The tissue successively went through a three-step process removing mucus, isolating epithelial cells, and isolating lamina propria cells. Mucus was removed by incubation in HBSS/5 mM DTT/2% FBS for 20 min at 37 °C with agitation. Epithelial cells were isolated by three incubation steps each in HBSS/5 mM EDTA/2% FBS for 15 min at 37 °C with agitation. Lamina propria cells were isolated by digestion in HBSS/

Liberase (Roche, Basel, Switzerland)/DNAse (Sigma Aldrich, St Louis, MO) for 30 min at 37 °C. The epithelial cell fraction and lamina propria cell fraction were further enriched for/or depleted-off epithelial cells using magnetic EpCam microbeads in accordance with the manufacturer's protocol (Miltenyi Biotech, Bergisch Gladbach, Germany). Cells were pre-blocked in 60% inactivated rat sera and 10 µg ml^{-1} of anti-CD16/32 (HB2.4) in PBS/2%FBS/2 mM EDTA for 10 min on ice. Cells where washed and stained in PBS/2%FBS/2 mM EDTA for 30 min on ice with 5 µl per test of the following antibodies: CD326 Pacific blue (Biolegend, San Diego, CA), CD11b PE-Cy7 (BD Bioscience, San Jose, CA), CD3-APC (BD Bioscience), and CD24-PE (Biolegend). NO was detected with the florescent probe 4-amino-5-methylamino-2′,7′-difluorofluorescein (DAF-FM) in accordance with the manufacturer's protocol (Thermo Fisher Scientific, Waltham, MA). The labeled cells were acquired on a LSR II flow cytometer (BD Bioscience). Flow data were analyzed in Cytobank.

Sampling. Biological samples were collected under sterile conditions after killing the mice by neck dislocation. The small intestine was divided in three: duodenum (most proximal 5 cm), jejunum (6 cm around the center), and ileum (most distal 6 cm). Cecum samples were taken directly opposite to the ileocecal valve to collect samples close to the valve that additionally are easy to anatomically identify to avoid sampling error. Luminal chyme for DNA extraction or microbe cultivation was squeezed out. The intestinal fragments were cut longitudinally and mucosal samples for RNA or DNA extraction were scraped off with a glass slide.

Counting of cultivable microbes. Luminal chyme samples were weighed, suspended in 1:10 sterile PBS (Sigma Aldrich) and homogenized by brief vortexing. The suspensions were serially diluted in the range of 10^{-1} to 10^{-8} and 100 µl of each dilution factor were plated on 7% freshly prepared horse blood agar plates (Oxoid, Basingstoke, UK). The procedure was performed in duplicates and the plates were incubated at 37 °C under anaerobic conditions for 48 h before counting CFU.

DNA extraction. Luminal chyme and mucosal samples were placed in S.T.A.R buffer (Roche) complimented with acid-washed glass beads (size < 106 µm, Sigma-Aldrich) directly after dissection. Cells were lysed by homogenization in a MagnaLyser (Roche) at 6500 rpm for 2×20 s with a cooling step in-between. Samples were centrifuged at 14,000 g for 5 min. The supernatants were transferred to 96-well plates and DNA was extracted using the Mag Mini LGC kit (LGC Genomics, Teddington, UK) according to the manufacturer's protocol in a KingFisher Flex DNA extraction robot (Thermo Fisher Scientific).

Real-time quantitative. Mucosal samples were placed in RNAlater (Sigma-Aldrich) directly after dissection. mRNA was isolated with NucleoSpin RNA/Protein Purification kit (Macherey-Nagel, Düren, Germany) according to the manufacturer's protocol and cDNA was synthesized with the iScript cDNA Synthesis kit (Bio-Rad, Hercules, CA). The primers used for mRNA expression were as follows: Gapdh, forward 5′-CTTCAACAGCAACTCCCACTCTT-3′ and reverse 5′-GCCGTATTCATTGTCATACCAGG-3′ (T_m 60 °C); iNOS, forward 5′-GACATTACGACCCCTCCCAC-3′ and reverse 5′-ACTC TGAGGGCTGACACAAG-3′ (T_m 62 °C); NOX1, forward 5′-GTGATTACCAAGGTTGTCATGC-3′ and reverse 5′-AAGCCTC GCTTCCTCATCTG-3′ (T_m 64 °C). The primer used for genomic quantification were as follows: 16S rRNA gene (modified from ref. 30) forward 5′-TAGCTATTACCGCGGCTGCT-3′, and reverse 5′-AC TCCTACGGGAGGCAGCAGT-3′ (T_m 64 °C). Gapdh forward 5′-AATACGGCTACAGCAACAGG-3′ and reverse 5′-TCTCTTGC TCAGTGTCCTTG-3′ (T_m = 56 °C). The RT-qPCR was performed with FirePol EvaGreen qPCR Supermix (Solis BioDyne, Tartu, Estonia) in accordance with the manufacturer's protocol in a LightCycler 480 Instrument II (Roche). The thermal cycle parameters were as follows: 12 min at 95 °C; 40 cycles of 15 s at 95 °C followed by 20 s at T_m

(primer optimized); 20 s at 72 °C. LinReg Software was used to calculate Cq values and primer efficiency. The exact efficiency was used for the comparative C_q values analyzes.

16S rRNA gene sequencing. The analysis of the composition of the gut microbiota was performed on iNOS and NOX1 KO and their respective WT mice. The 16S rRNA gene sequence workflow analysis has previously been reported.[31] Briefly, after DNA extraction the 16S rRNA gene was PCR amplified for 25 cycles using prokaryotes-targeting primers developed by Yu et al.[32] The PCR product was purified with AMPure XP (Beckman-Coulter, Brea, CA) and 10 further PCR cycles were performed. The resulting amplicons were sequenced on Illumina MiSeq V3 platform (Illumina, San Diego, CA). Resulting 300 bp paired-end reads were further paired-end joined, quality-filtered using QIIME[33] and clustered with 97% identity level using closed-reference *usearch v7.0* algorithm[34,35] against Greengenes database v13.8.[36]

Statistical analyses. Statistical significance values were calculated in the GraphPad Prism software (La Jolla, CA). Averages are presented as mean and variances as standard error of the mean (s.e.m.). Statistical significance level was set as $\alpha = 0.05$. We chose 3,000 sequences per sample as a cut-off to normalize the sequencing data. Linear discriminant analysis effect size (LefSe) with LDA score > 2 was used to identify taxa associated with the KO groups.[37] PCA were performed in Unscrambler 14.1 (Camo software, Oslo, Norway).

AUTHOR CONTRIBUTIONS
A.K. conceived and designed the study. C.M. and A.K. performed most of the experiments and analyzed data. S.D.C.R. and O.A.H. performed experiments. K.R. provided equipment and reagents. C.M., H.C., and A.K. wrote the paper. All authors reviewed and provided comments to the paper.

DISCLOSURE
The authors declare no conflict of interest.

REFERENCES
1. Larsson, E. *et al.* Analysis of gut microbial regulation of host gene expression along the length of the gut and regulation of gut microbial ecology through MyD88. *Gut* **61**, 1124–1131 (2012).
2. Ha, E.M., Oh, C.T., Bae, Y.S. & Lee, W.J. A direct role for dual oxidase in Drosophila gut immunity. *Science* **310**, 847–850 (2005).
3. Chavez, V., Mohri-Shiomi, A. & Garsin, D.A. Ce-Duox1/BLI-3 generates reactive oxygen species as a protective innate immune mechanism in *Caenorhabditis elegans*. *Infect. Immun.* **77**, 4983–4989 (2009).
4. Moskwa, P. *et al.* A novel host defense system of airways is defective in cystic fibrosis. *Am. J. Respir. Crit. Care Med.* **175**, 174–183 (2007).
5. Grasberger, H., El-Zaatari, M., Dang, D.T. & Merchant, J.L. Dual oxidases control release of hydrogen peroxide by the gastric epithelium to prevent *Helicobacter felis* infection and inflammation in mice. *Gastroenterology* **145**, 1045–1054 (2013).
6. Grasberger, H. *et al.* Increased Expression of DUOX2 Is an Epithelial Response to Mucosal Dysbiosis Required for Immune Homeostasis in Mouse Intestine. *Gastroenterology* **149**, 1849–1859 (2015).
7. Jones, R.M. & Neish, A.S. Redox signaling mediated by the gut microbiota. *Free Radic. Biol. Med.* **105**, 41–47 (2017).
8. Chu, F.F., Esworthy, R.S., Doroshow, J.H. & Shen, B. NADPH oxidase-1 deficiency offers little protection in *Salmonella typhimurium*-induced typhlitis in mice. *World J. Gastroenterol.* **22**, 10158–10165 (2016).

9. Pircalabioru, G. *et al.* Defensive mutualism rescues NADPH oxidase inactivation in gut infection. *Cell Host Microbe* **19**, 651–663 (2016).

10. Shaked, H. *et al.* Chronic epithelial NF-kappaB activation accelerates APC loss and intestinal tumor initiation through iNOS up-regulation. *Proc. Natl Acad. Sci. USA* **109**, 14007–14012 (2012).

11. Lundberg, J.O. & Weitzberg, E. Biology of nitrogen oxides in the gastrointestinal tract. *Gut* **62**, 616–629 (2013).

12. Daiber, A., Oelze, M., Steven, S., Kroller-Schon, S. & Munzel, T. Taking up the cudgels for the traditional reactive oxygen and nitrogen species detection assays and their use in the cardiovascular system. *Redox Biol.* **12**, 35–49 (2017).

13. Reikvam, D.H. *et al.* Depletion of murine intestinal microbiota: effects on gut mucosa and epithelial gene expression. *PLoS ONE* **6**, e17996 (2011).

14. Laukens, D., Brinkman, B.M., Raes, J., De Vos, M. & Vandenabeele, P. Heterogeneity of the gut microbiome in mice: guidelines for optimizing experimental design. *FEMS Microbiol. Rev.* **40**, 117–132 (2016).

15. Asghar, M.N. *et al.* In vivo imaging of reactive oxygen and nitrogen species in murine colitis. *Inflamm. Bowel Dis.* **20**, 1435–1447 (2014).

16. Han, W., Li, H., Segal, B.H. & Blackwell, T.S. Bioluminescence Imaging of NADPH Oxidase Activity in Different Animal Models. *J. Vis. Exp.* **68**, e3925 (2012).

17. Kielland, A., Blom, T., Nandakumar, K.S., Holmdahl, R., Blomhoff, R. & Carlsen, H. *In vivo* imaging of reactive oxygen and nitrogen species in inflammation using the luminescent probe L-012. *Free Radic. Biol. Med.* **47**, 760–766 (2009).

18. Zangani, M. *et al.* Tracking early autoimmune disease by bioluminescent imaging of NF-kappaB activation reveals pathology in multiple organ systems. *Am. J. Pathol.* **174**, 1358–1367 (2009).

19. Radi, R. Peroxynitrite a stealthy biological oxidant. *J. Biol. Chem.* **288**, 26464–26472 (2013).

20. Zielonka, J., Lambeth, J.D. & Kalyanaraman, B. On the use of L-012, a luminol-based chemiluminescent probe, for detecting superoxide and identifying inhibitors of NADPH oxidase: a reevaluation. *Free Radic. Biol. Med.* **65**, 1310–1314 (2013).

21. Goiffon, R.J., Martinez, S.C. & Piwnica-Worms, D. A rapid bioluminescence assay for measuring myeloperoxidase activity in human plasma. *Nat. Commun.* **6**, 6271 (2015).

22. Jones, R.M. *et al.* Symbiotic lactobacilli stimulate gut epithelial proliferation via Nox-mediated generation of reactive oxygen species. *EMBO J.* **32**, 3017–3028 (2013).

23. Sonoyama, K. *et al.* Response of gut microbiota to fasting and hibernation in Syrian hamsters. *Appl. Environ. Microbiol.* **75**, 6451–6456 (2009).

24. Corcionivoschi, N. *et al.* Mucosal reactive oxygen species decrease virulence by disrupting *Campylobacter jejuni* phosphotyrosine signaling. *Cell Host Microbe* **12**, 47–59 (2012).

25. Leoni, G. *et al.* Annexin A1, formyl peptide receptor, and NOX1 orchestrate epithelial repair. *J. Clin. Investig.* **123**, 443–454 (2013).

26. Chooruk, A., Piwat, S. & Teanpaisan, R. Antioxidant activity of various oral Lactobacillus strains. *J. Appl. Microbiol.* **123**, 271–279 (2017).

27. Miyoshi, A. *et al.* Oxidative stress in *Lactococcus lactis*. *Genet. Mol. Res.* **2**, 348–359 (2003).

28. Deloris Alexander, A., Orcutt, R.P., Henry, J.C., Baker, J. Jr., Bissahoyo, A.C. & Threadgill, D.W. Quantitative PCR assays for mouse enteric flora reveal strain-dependent differences in composition that are influenced by the microenvironment. *Mamm. Genome* **17**, 1093–1104 (2006).

29. Goodyear, A.W., Kumar, A., Dow, S. & Ryan, E.P. Optimization of murine small intestine leukocyte isolation for global immune phenotype analysis. *J. Immunol. Methods* **405**, 97–108 (2014).

30. Brukner, I., Longtin, Y., Oughton, M., Forgetta, V. & Dascal, A. Assay for estimating total bacterial load: relative qPCR normalisation of bacterial load with associated clinical implications. *Diagn. Microbiol. Infect. Dis.* **83**, 1–6 (2015).

31. Avershina, E. *et al.* Transition from infant- to adult-like gut microbiota. *Environ. Microbiol.* **18**, 2226–2236 (2016).

32. Yu, Y., Lee, C., Kim, J. & Hwang, S. Group-specific primer and probe sets to detect methanogenic communities using quantitative real-time polymerase chain reaction. *Biotechnol. Bioeng.* **89**, 670–679 (2005).

33. Caporaso, J.G. *et al.* QIIME allows analysis of high-throughput community sequencing data. *Nat. Methods* **7**, 335–336 (2010).

34. Edgar, R.C. UPARSE: highly accurate OTU sequences from microbial amplicon reads. *Nat. Methods* **10**, 996–998 (2013).

35. Edgar, R.C. Search and clustering orders of magnitude faster than BLAST. *Bioinformatics* **26**, 2460–2461 (2010).

36. DeSantis, T.Z. *et al.* Greengenes, a chimera-checked 16S rRNA gene database and workbench compatible with ARB. *Appl. Environ. Microbiol.* **72**, 5069–5072 (2006).

37. Segata, N. *et al.* Metagenomic biomarker discovery and explanation. *Genome Biol.* **12**, R60 (2011).

Paper IV

NOX1 regulates colonic microbiota and gut defense following DSS-induced low-grade inflammation in mice

Herfindal A.M.[1]*, Rocha S.D.C.[1]*, Papoutsis D.[1], Bøhn S.K.[1], Carlsen H.[1]

[1]*Faculty of Chemistry, Biotechnology and Food Science, Norwegian University of Life Sciences, P. O. Box 5003, N-1432 Ås, Norway*
* Shared first author

Abstract

Reactive oxygen species (ROS) have diverse physiological roles including cellular signaling and antimicrobial effects in the innate immune system. ROS are also shown to modulate small intestinal microbiota in healthy mice. Peroxynitrite, a type of ROS, is a product of nitric oxide and superoxide produced by the enzymes iNOS and NOX1, respectively. In the colon, less is known about the role of ROS in modulating microbiota and host response. In a healthy situation, NOX1 is highly expressed in the colon. However, during inflammation, a number of new players may enhance ROS production such as iNOS and NOX2. In subclinical states, the colon more likely experiences episodes of low-grade inflammation. It is therefore plausible that in low-grade inflammation, NOX1 remains the main source of superoxide. To explore the role of NOX1 we exposed WT and NOX1 KO mice to 1% DSS in water for six days to induce colonic low-grade inflammation, and assessed effects on ROS production, colon structure, inflammation markers and colonic microbiota. 1% DSS induced iNOS strongly in colonic tissue but not NOX2, and a marked up-regulation of peroxynitrite was observed. In the absence of NOX1, mice had reduced peroxynitrite production in colon and a microbiota profile indicative of dysbiosis. NOX1 KO mice were also more prone to inflammation suggesting NOX1 involvement in colonic homeostasis.

Introduction

The human gut is the host of trillions of bacteria with up to 1000 different species and for most parts, they live in a mutualistic relationship with the host. Both parts benefit from a balanced gut ecosystem, which reduces the chances of the establishment of pathogens. The host immune system plays an important role in such stability by controlling the commensal bacteria and keeping the gut immunity in a tolerant mode. However, the gut microbiota is continually challenged and is also challenging the host. In the case of unbalanced microbiota (dysbiosis) or presence of pathogens, both the innate and adaptive immune system mounts various responses such as increased mucus production, the release of antimicrobial factors and immune cell activation [1].

Reactive oxygen species (ROS) are important mediators of the innate immune system, particularly when released during the respiratory burst in neutrophils, macrophages and dendritic cells. However, ROS can also exert detrimental effects if present in too high concentrations and create what is known as oxidative stress, potentially leading to cellular stress and DNA mutations. Cells also have a battery of ROS producing enzymes in place to produce ROS for intentional purposes. These include different types of nicotinamide adenine dinucleotide phosphate (NADPH) oxidases (NOX), dual oxidases (DUOX) and nitric oxide synthase (NOS), transmembrane proteins found in virtually every tissue and is largely present in the mucosal layers of the gut [2, 3].

In the intestine, ROS are important for bacterial defense [4]. In addition, ROS possess other roles related to intestinal homeostasis affecting signaling pathways and cell proliferation regulating the number of goblet cells and the production of mucin [2, 5-10]. ROS are versatile compounds and they can interact with different molecules and their roles can vary with location, concentration and inflammatory environment [2, 11]. DUOX2 and NOX1 are the main NADPH oxidases and ROS producers in the gut epithelium [3], while NOX2 is mostly activated under infection or during inflammation [12], and is predominantly expressed in phagocytic cells in lamina propria as a response to bacterial encounters [13]. In the absence of inflammation or infections, NOX1 regulates microbiota in the ileum together with iNOS, presumably through the production of superoxide ($O_2^{\bullet-}$) and nitric oxide ($NO^{\bullet}$), and their consequent production of the ROS peroxynitrite ($ONOO^-$) [14].

In the colon, the role of NOX1 has been studied under conditions of chronic inflammation induced by high concentrations of dextran sodium sulfate (DSS) [7, 8, 15, 16]. These studies show that NOX1 deficient mice exposed to high concentrations (2-4%) of DSS exhibit overall small differences in colitis pathology compared to wild type mice, but wild type mice appear to recover faster after the withdrawal of DSS, which is also in line with NOX1's beneficial role in wound healing [17]. However, chronic inflammation is an extreme situation with a massive release of inflammatory cytokines and high production of ROS, which may mask the effects of the absence or presence of NOX1 in the DSS models mentioned. A situation of low-grade inflammation may be more relevant.

Low-grade inflammation is regarded as a condition with no overt signs of tissue damage in the intestine but with a moderate increased expression of pro-inflammatory mediators [18]. Low-grade inflammation is present in patients with inflammatory bowel disease with remission [19]. It may also be present in patients with irritable bowel syndrome [20] and can be caused by dietary exposures such as Western diet high in fat and low in fiber [21], or high in food additives such as emulsifiers [22]. Low-grade inflammation is connected to weakened barrier function including thinner mucus layer and impaired tight junction expression and can precede inflammatory bowel disease and colon cancer [23]. The use of a low dose DSS was therefore regarded as a relevant model since DSS exposure is associated with degradation of the mucus, making the mucosa more susceptible to bacterial exposure leading to an inflammatory response [24, 25].

A previous study has demonstrated that 1% DSS did not lead to any clinical signs in the colon of exposed mice. However, the authors found nitrotyrosine staining in the epithelial layers of the colon, which indicates enhanced peroxynitrite production in the colon [26]. That 1% DSS increase nitrotyrosine-staining has also been observed by others [27]. Seril and coworkers did however also observe symptoms of mild colitis [27]. Regardless, increased peroxynitrite may therefore indicate that iNOS is up-regulated under these conditions and that nitric oxide produced can combine with superoxide to form peroxynitrite. Since NOX2 is mostly activated under more severe inflammation [12] and NOX1 is highly expressed in the colonic cells in healthy mice, it is plausible that NOX1 is the primary source of superoxide during low-grade inflammation

induced by 1% DSS. Thus, we evaluated this to be a relevant model to study the impact of NOX1 in the colon.

Our first aim was to induce a mild and subclinical inflammation model relevant to a situation where the gut barrier is weakened. To obtain a low-grade inflammation model we exposed WT mice to low doses (0.5-2%) of DSS in water for 8 days applying a strategy commonly used to induce colitis [28]. Based on the results from the establishment experiment we then exposed WT and NOX1 KO mice to 1% DSS for 6 days, where we hypothesized that NOX1 has a protective role both in regulating the steady-state colonic homeostasis and in response to a low-grade inflammation. More specifically, that the lack of superoxide produced by NOX1 may modulate colonic microbiota and sequentially affect the course of low-grade colonic inflammation, especially since the development of DSS induced inflammation is highly affected by the initial microbial profile [29-31].

RESULTS

Establishment of the low-grade inflammation model

The criteria set for a relevant low-grade inflammation model were none or only a few visible signs of disease together with a moderate up-regulation of inflammation-related genes. To find the optimal time-dose for inducing low-grade inflammation, we exposed mice to 0, 0.5, 1 or 2% DSS for eight days. Animals exposed to the highest dose, 2% DSS, had significant weight loss after six days of exposure **(Supplementary Figure 1A)**. Animals exposed to 1% or 0.5% DSS showed only marginal or no weight loss and did not differ significantly from the controls. From day four, the 2% DSS group presented poorer stool quality translated in loose consistency and traces of blood. Groups exposed to 1% and 0.5% DSS revealed milder symptoms by day six and eight, respectively, as compared to animals receiving 2% DSS.

At termination day, the 2% DSS group also had a significantly shorter colon when compared to the other groups **(Supplementary Figure 1B)**, while the lower doses did not lead to shortening of the colon compared to no DSS treatment.

DSS caused a dose-dependent up-regulation of the pro-inflammatory genes TNFα, Ptgs2, IL-6, IL-1β and Lcn-2 and in ROS related genes **(Supplementary Figure 2A-H)**. Importantly, iNOS was up-regulated 10-15-fold with 1% DSS whereas DUOX2 and NOX2 were moderately to marginally increased with the same dose. Apart from TNFα, 0.5% DSS dose did not induce any of the inflammatory or ROS related genes. NOX1 expression was not affected by any of the DSS concentrations **(Supplementary Figure 2I)**.

From this, we conclude that 1% DSS was a suitable dose to induce low-grade subclinical inflammation due to lack of marked clinical signs, while high enough to significantly up-regulate inflammatory and ROS related genes. In the following knockout experiment, the timeframe was set to six days because with 8 days of treatment with 1% DSS the mice started showing a decline in stool quality.

NOX1 is important for peroxynitrite production in the colon

Since we found increased expressions of ROS related genes, in particular iNOS, in the colon of 1% DSS exposed mice, we wanted to examine whether ROS production was increased accordingly. We therefore imaged excised colons by the use of L-012, a sensitive bioluminescent probe for the detection of ROS, in particular peroxynitrite [32-34]. As shown in **Figure 1A-B**, WT mice exposed to 1% DSS had a marked up-regulation of light emitted from the colon. Because peroxynitrite is produced by combining superoxide and nitric oxide, we hypothesized that the absence of NOX1 would lead to a reduced light emission. Indeed, the L-012 signal from NOX1 KO mice was strongly reduced compared to WT mice.

To test if the absence of NOX1 activity would affect the other ROS related genes (NOX2, iNOS, DUOX2), we assessed the mRNA levels of these genes in the colon **(Figure 1C-E)**. iNOS was strongly up-regulated by 1% DSS, whereas DUOX2 was only moderately elevated and NOX2 was not affected. However, neither NOX2, DUOX2 nor iNOS mRNA levels were different in NOX1 KO mice when compared to WT. These data therefore indicate that in these conditions there are no evident compensatory mechanisms to restore ROS production.
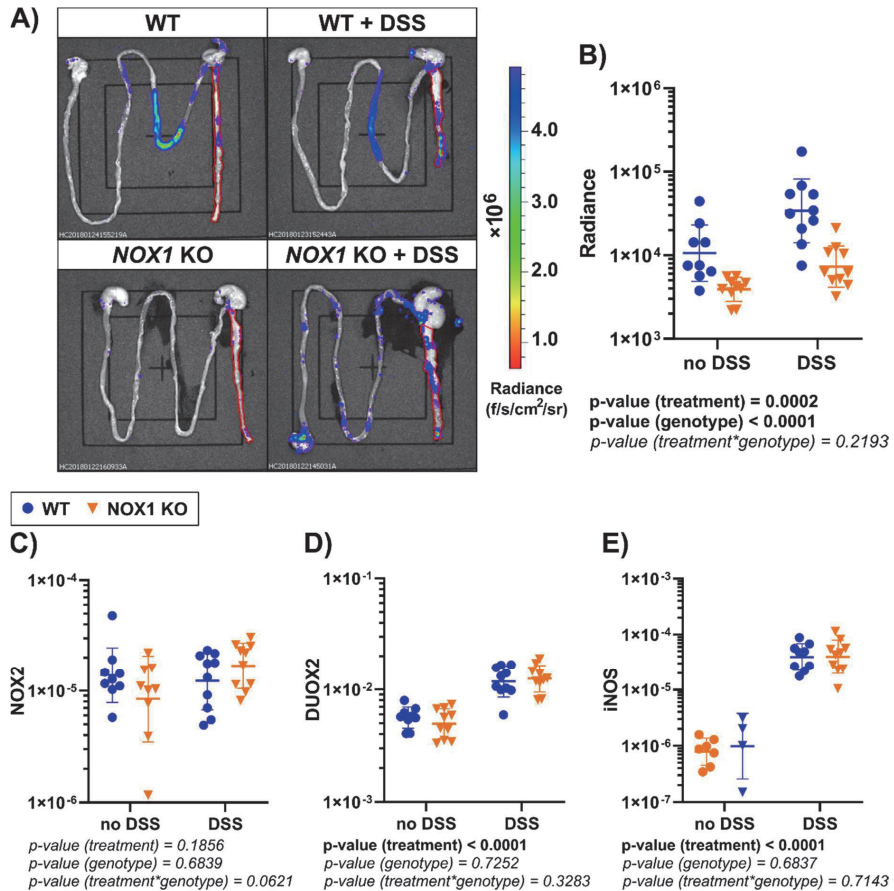
Figure 1: ROS production in the colon of WT and NOX1 KO mice with or without 6-days 1% DSS treatment. (A) Representative *ex vivo* images of one animal from each of the four groups in the knockout experiment after injection with L-012. The injection was done before dissection. Pseudo colors represent photons/sec/cm2/steradian, with minimum and maximum values of 8.71e[3] and 4.37e[5] respectively. Red markings show the region of interest. **(B)** L-012-induced chemiluminescence from the colon expressed as average radiance (photons/sec/cm^2/steradian). N=9-10 in each group. **(C-E)** Relative mRNA expression of (C) NOX2 (D), DUOX2 and (E) iNOS in mucosa from the proximal colon. N=4-10 in each group. (B-E) P-values below graphs from 2-way ANOVA (main effects and interaction effect) on log10-transformed data. Horizontal lines and whiskers are geometric group mean *÷ geometric SD factor. (C) The interaction trend is highly affected by the two extreme values in groups not exposed to DSS. If excluded, the interaction is no longer borderline significant (p=0.2352). WT, wild type; KO, knockout; DSS, dextran sulfate sodium.

Assessing the role of NOX1 by analyzing biomarkers of inflammation

As expected, from the initial experiment establishing the low-grade inflammation model, six days of 1% DSS exposure did not result in a significant change in body weight **(Supplementary Figure 3A)**. Unexpectedly, in most of the animals DSS treatment displayed changes in stool quality from day four and reduced colon length at termination **(Supplementary Figure 3B)**. These changes were however not different between NOX1 KO mice and WT.

Histological analyses of colon tissue revealed no obvious structural differences between the WT and the NOX1 KO mice, neither without nor with DSS treatment **(Figure 2)**. When mice were exposed to 1% DSS, both gebotypes showed characteristic signs of colonic translated in the infiltration of immune cells in lamina propria and increased space between epithelial cell bases and muscularis mucosa.

We next measured the expression of inflammatory genes. These included TNFα, IL-1β, Ptgs2, IL-6 and Lcn-2 **(Figure 3A-E)**. With DSS exposure, all genes were up-regulated in both genotypes. However, the only effects of genotype were a higher up-regulation of TNFα and an overall tendency towards higher levels of IL-6 in NOX1 KO mice **(Figure 3A-B)**.

Although only minor effects on inflammatory genes were observed between the genotypes, other inflammation-induced mechanisms might be differently regulated. Chassaing et al. reported that Lcn-2 in feces is a sensitive marker for colonic inflammation [35]. Lcn-2 is a protein released by colonic epithelial cells in response to inflammation and may also be released by neutrophil granulocytes [36]. Lcn-2 is important in the defense against pathogenic bacteria and to prevent overgrowth in the intestinal lumen. We observed significantly increased levels of Lcn-2 in mice exposed to 1% DSS **(Figure 3F)**. There was also a trend for an interaction effect between treatment and genotype, with higher levels of Lcn-2 in NOX1 KO mice after DSS treatment when compared to WT. Further, it should be mentioned that two animals in the groups exposed to DSS differed greatly from the other animals in the same group. When these data points were excluded from the analysis, the significance of the interaction effect is strengthened (p=0.0189), which indicates that the effect of DSS on Lcn-2 is dependent on the genotype, with a higher increase in NOX1 KO mice. Although NOX1 KO mice showed considerable variation upon DSS treatment, these data indicated an increased vulnerability to DSS-induced low-grade inflammation in NOX1 KO mice.

Colonic inflammation is commonly associated with a breach in barrier function and consequent leak of bacteria or bacterial compounds [37]. Following the leakage of LPS through the gut wall this will induce the release of the LPS binding protein (LBP) into the circulation. We examined whether the absence of NOX1 activity would impair intestinal barrier integrity, both with and without DSS treatment, by measuring the LBP plasma levels **(Figure 3G)**. LBP was increased by the DSS treatment, but no effect of NOX1 ablation was observed.
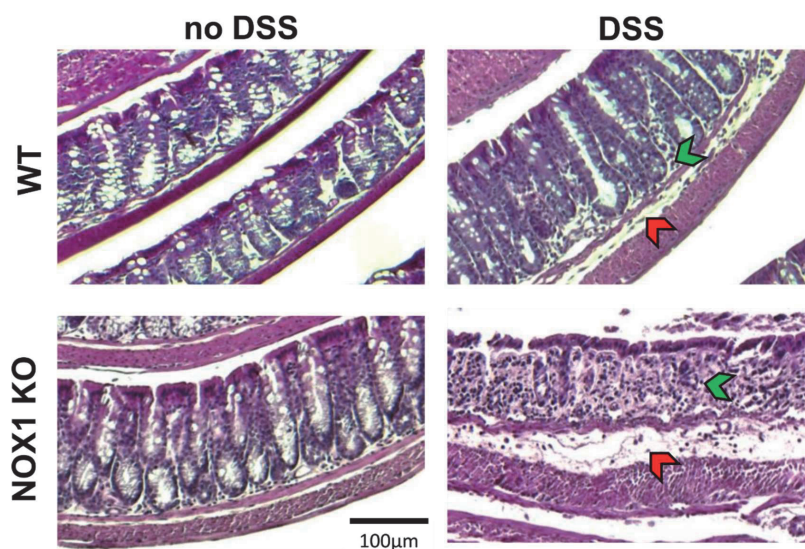
Figure 2: **Colon tissue on day 6 in WT and NOX1 KO mice with or without 6-days 1% DSS treatment.** Representative images of colon (n=3) with the exception of the picture from NOX1 KO mouse after DSS treatment. In this case, we present the most severe observed case as an indication of the lack of symptoms similar to chronic inflammation. Other KO mice exposed to DSS could not be distinguished from WT mice after DSS treatment. Green arrows indicate the infiltration of immune cells into the lamina propria. Red arrows indicate increased space between epithelial cell bases and muscularis mucosa. Colon sections (5μm) were stained with hematoxylin and eosin. WT, wild type; KO, knockout; DSS, dextran sulfate sodium.
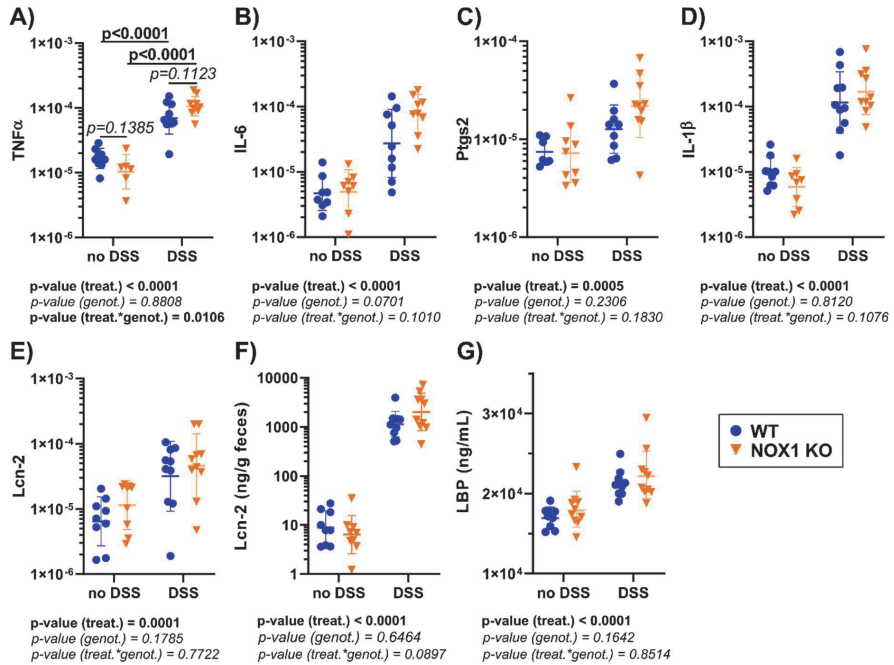
Figure 3: Mucosal inflammation and intestinal barrier integrity of WT and NOX1 KO mice with or without 6-days 1% DSS treatment. (A-E) Relative mRNA expression of (A)TNFα, (B) IL-6, (C) Ptgs2, (D) IL-1β and (E) Lcn-2 in mucosa from the proximal colon. N=6-10 in each group. **(F)** Concentration of lipocalin-2 in feces. N=9-10 in each group. **(G)** Concentration of LBP in plasma. N=9-10 in each group. (A-G) P-values below graphs from 2-way ANOVA (main effects and interaction effect) on log10-transformed data. P-values in graph for simple main effects with Bonferroni correction for multiple comparisons. Horizontal lines and whiskers are geometric group mean *÷ geometric SD factor. (C) The significance of the interaction effect is highly affected by the extreme value in the NOX1 KO group exposed to DSS. If excluded, the interaction effect becomes borderline significant (p=0.0536), translated in significant difference between genotypes after DSS exposure (p=0.0166) and only significant effect of DSS for NOX1 KO mice (p<0.0001). (F) The significance of the interaction effect is highly affected by two extreme value in the groups exposed to DSS. If excluded, the interaction effect becomes significant (p=0.0189), where there is a significant difference between genotypes after DSS exposure (p=0.0325). Treat., treatment. Genot., genotype. WT, wild type; KO, knockout; DSS, dextran sulfate sodium.

Alpha-diversity in colonic bacteria is reduced in NOX1 KO mice

To evaluate the potential effect of NOX1 absence on the colonic microbiota during steady-state conditions and during DSS-induced colonic inflammation, we performed a 16S rRNA gene-based sequencing approach. With normalization cut-off of 6,500 sequences per sample, we identified 538 OUTs in total. From this we first examined the potential effects NOX1 KO could have on the microbial diversity in the colon.

The within-sample diversity (α-diversity) was investigated using different measures. In feces, the Shannon-Wiener index was affected by both treatment and genotype, where DSS exposure led to increased index in both genotypes, and NOX1 KO mice had a lower index **(Figure 4A)**. For colon tissue, potential differences in the Shannon-Wiener index were only evaluated between genotypes within each treatment, which also revealed a significant decrease in NOX1 KO compared to WT when not exposed to DSS **(Figure 4D)**.

Since the Shannon-Wiener index increase with increased richness (number of species) and evenness (species distribution), additional information can be obtained when these two characteristics are examined separately. The observed number of species in feces was lower for NOX1 KO compared to WT mice **(Figure 4B)**, while neither treatment nor genotype had a significant effect in colon tissue **(Figure 4E)**. The evenness of the fecal samples was highly affected by an interaction effect between treatment and genotype **(Figure 4C)**. With no DSS, evenness was lower in NOX1 KO mice compared to WT, while there was no difference between genotypes after DSS treatment, only a trend towards lower evenness in NOX1 KO mice. The effect of DSS was however significant for both NOX1 KO and WT. In colon tissue, we only compared genotypes within each treatment and found that NOX1 KO mice presented a reduced evenness compared to WT when not exposed to DSS **(Figure 4F)**.

In summary, these results indicate that lack of NOX1 causes decreased species richness and evenness in luminal areas of the colon, and that the same patterns are found at mucosal surfaces. Additionally, DSS had only marginal effects on the richness and induced only a minor increase in evenness in WT mice when compared to NOX1 KO.
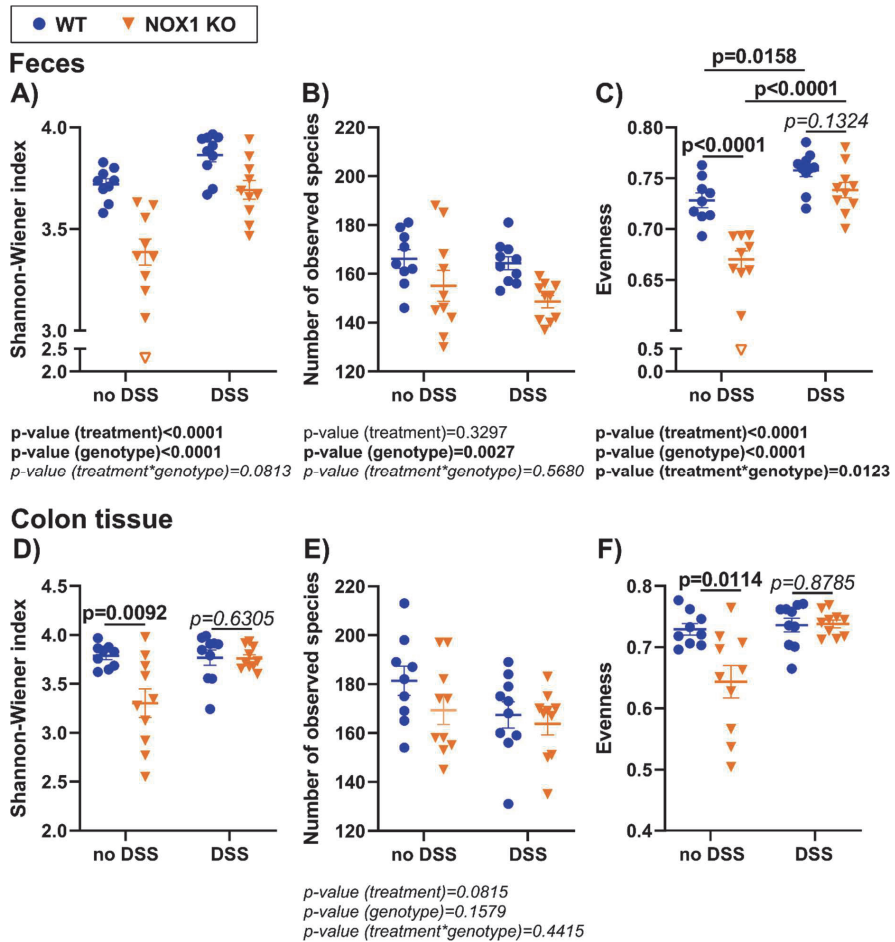
Figure 4: α-diversity of colonic bacterial communities in WT and NOX1 KO mice with or without 6-days 1% DSS treatment. (A,D) Shannon-Wiener index, **(B,E)** observed number of species (OTUs) and (C,F) evenness (equitability) of bacterial communities in (A, B, C) feces and (D, E, F) colon tissue. (A, B, C, E) P-values below graphs from 2-way ANOVA (main effects and interaction effect). (C) P-values in the graph for simple main effects with Bonferroni correction for multiple comparisons. (A, C) One extreme value was excluded from statistical analysis (unfilled triangle). When included, the significance of the interaction increased for the Shannon-Wiener index (p=0.0640) and decreased for evenness (p=0.0235), but for these models, the assumption of normality was violated, with no improvement using log-transformation of the data. (D) 2-way ANOVA could not be performed due to heteroskedasticity and violation of normality assumption. P-values in the graph from Welch's t-test (no DSS condition) and Mann-Whitney test (DSS condition). (F) 2-way ANOVA could not be performed due to heteroskedasticity and violation of normality assumption. P-values in the graph from Welch's t-test (no DSS) and t-test (DSS). (A-F) N=9-10 in each group. Horizontal lines and whiskers are group mean ± SEM. WT, wild type; KO, knockout; DSS, dextran sulfate sodium.

Beta-diversity in feces and colon tissue

In addition to microbial α-diversity, we also examined the between-sample diversity (β-diversity). PCoA of weighted UniFrac distances, a measure of β-diversity, shows that bacterial communities in feces were significantly different between all groups examined **(Figure 5A)**. Still, NOX1 KO and NOX1 KO+DSS are clustered closer together than samples from WT and WT+DSS. For colon tissue, samples significantly clustered according to treatment **(Figure 5B)**. Similar clusters for both feces and colon tissue were obtained using NMDS **(Supplementary Figure 4)**. No differences in within-cluster distances between groups were observed **(Figure 5C-D)**, meaning that the apparent higher dispersion in the NOX1 KO and WT+DSS group is mostly a result of some extreme values.
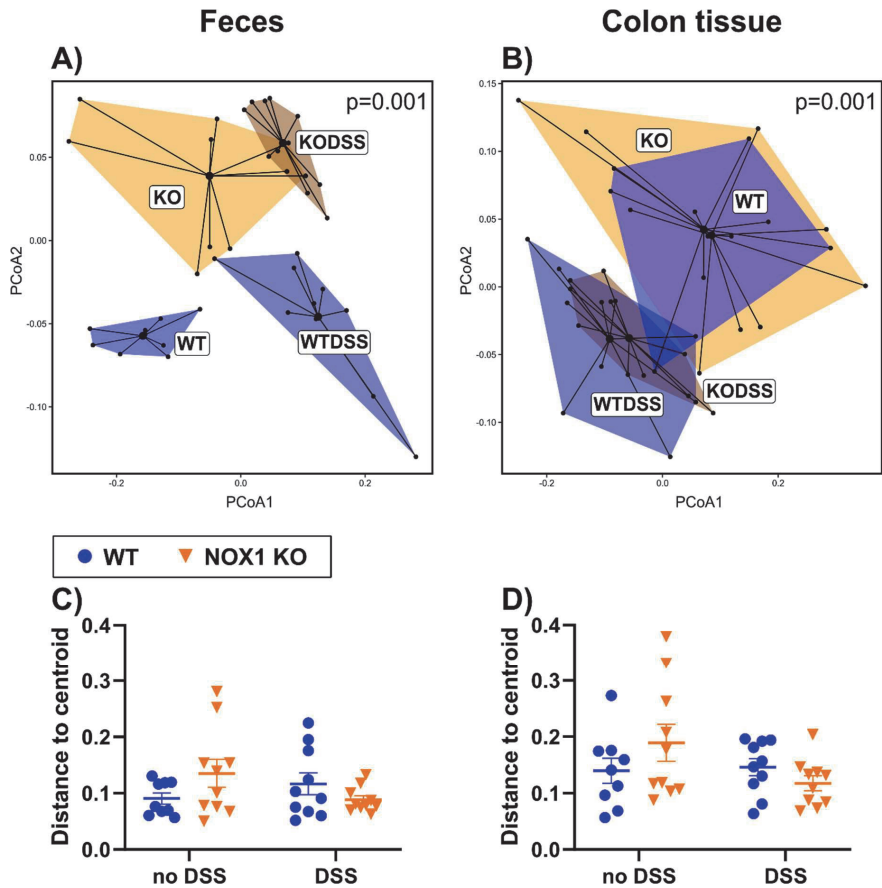
Figure 5: β-diversity of WT and NOX1 KO mice with or without 6-days 1% DSS treatment. Principal coordinate analysis (PCoA) of weighted UniFrac distances between samples in **(A)** feces and **(B)** colon tissue samples. Colors indicate which group individual samples belong to (WT, NOX1 KO (KO), WT with DSS (WTDSS), NOX1 KO with DSS (KODSS)). N=9-10 in each group. P-values in the plot from global PERMANOVA. Pairwise PERMANOVA showed in feces a significant difference between all groups (all p's≤0.01). In colon tissue, no statistical difference was found between KO and WT (p>0.2), or between KODSS and WTDSS (p>0.07), only across treatment (all p's<0.04). **(C,B)** Distances from centroids in PCoA plots from (C) feces and (D) colon tissue. 2-way ANOVA revealed no main effects or interaction effects between treatment and genotype. For feces, statistical analysis was performed on log10-transformed data. WT, wild type; KO, knockout; DSS, dextran sulfate sodium.

Increased *Firmicutes/Bacteroidetes* ratio and *Verrucomicrobia* in NOX1 KO mice

Based on the assessment of α- and β-diversity, it was clear that NOX1 KO causes shifts in the bacterial communities colonizing the colon, especially in luminal areas. To obtain a more detailed understanding of these shifts, we first examined the 10 phyla identified from the 538 OTUs **(Figure 6A-B)**. Potential effects on relative abundance at the phylum level were assessed for feces and colon tissue separately **(Supplementary Figure 5 and 6)**. Only phyla with average abundance above 1% in at least one group were here considered.

In both feces and colon tissue, the main effect of DSS on relative abundance was an increase in *Firmicutes* and *Tenericutes* while *Bacteroidetes* and *Proteobacteria* decreased. No overall effect of genotype was found for any of the mentioned phyla.

In feces, a significant interaction between treatment and genotype was found for *Firmicutes* and *Bacteroidetes*. These phyla were dominated by the orders *Clostridiales* (40-70%) and *Bacteroidales* (20-50%), respectively. With no DSS treatment, the relative abundance of *Bacteroidetes* was lower in NOX1 KO mice compared to WT, while there was no difference between the genotypes after DSS treatment. For *Firmicutes*, no significant difference was found between genotypes neither without nor with DSS treatment, but a tendency towards higher abundance in NOX1 KO mice compared to WT when not exposed to DSS.

Verrucomicrobia was the only phylum to show pronounced differences between NOX1 KO and WT mice in both feces and colon tissue. In feces, *Verrucomicrobia* was only present in three out of nine samples from the WT animals, while NOX1 KO had an average abundance of 3%. In colon tissue, the NOX1 KO mice had a geometric average of about 100 times higher than WT, with a maximum abundance of almost 6%. Further, the DSS only affected the abundance in WT animals.

In summary, these results show that mice with the NOX1 KO genotype have an inflammation-like profile at the phylum level, even without DSS treatment, characterized by a higher *Firmicutes/Bacteroidetes* ratio in feces **(Figure 6C)**. Interestingly we observed a much higher abundance of *Verrucomicrobia* in both feces and colon tissue in NOX1 KO mice without DSS but with DSS this difference is less pronounced. In general, we observed that DSS induced only minor shifts in feces from NOX1 KO mice when compared to WT.
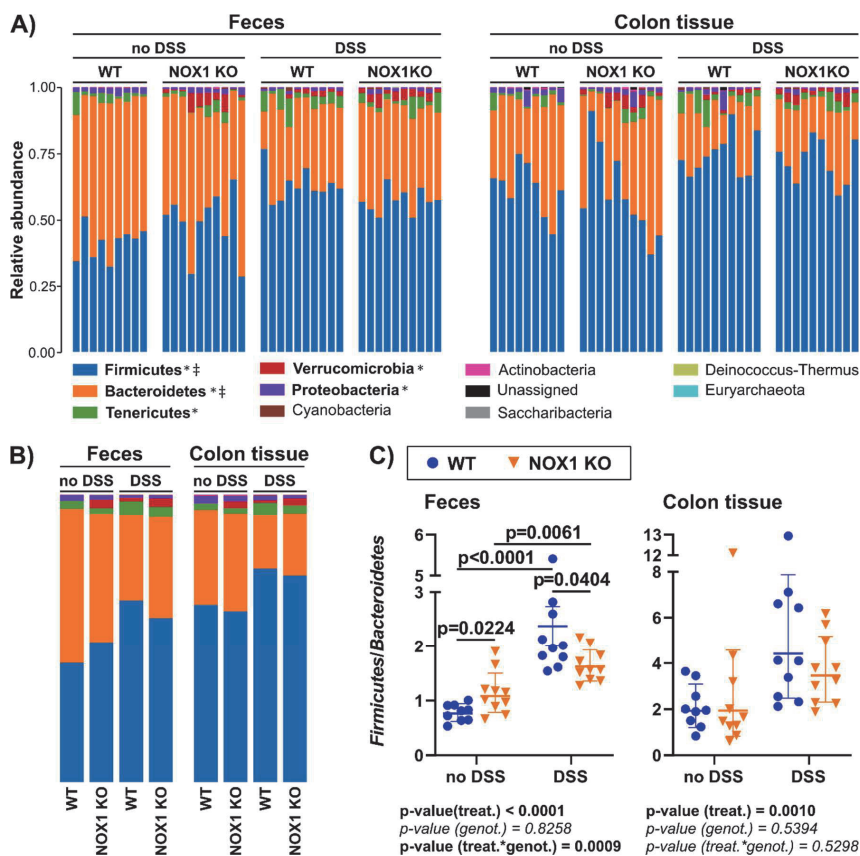
Figure 6: Phyla characteristics of WT and NOX1 KO mice with or without 6-days 1% DSS treatment. (A) The relative abundance of all detected phyla in individual fecal and colon tissue samples from mice in the knockout experiment. Phyla are sorted according to average abundance across all groups. All bars sum to 1. Phyla in bold have an average abundance above 1 % in at least one group. * indicates significant effect of DSS exposure in both feces and colon tissue, while ‡ indicates significant interaction effect between genotype and treatment in feces. See the main text and Supplementary Figure X-X for details on statistics. **(B)** Average relative abundance for all detected phyla for each group in feces and colon tissue. See (A) for color codes. **(C)** Firmicutes/Bacteroidetes ratio in feces and colon tissue. P-values below graph from 2-way ANOVA (main effects and interaction effect) on log10-transformed data. P-values in the graph for simple main effects with Bonferroni correction for multiple comparisons. For fecal samples, the difference between genotypes within the DSS condition is mostly caused by the extreme value in the WT group. If excluded, the difference is no longer significant (p=0.1282), while significance of the interaction is unaffected (p=0.001). Horizontal lines and whiskers are geometric group mean *÷ geometric SD factor. Treat., treatment. Genot., genotype. DSS, dextran sulfate sodium. WT, wild type; KO, knockout.

NOX1 KO mice presented a pro-inflammatory microbiota

To identify specifically differentiated taxa between genotypes within each treatment (no DSS, DSS), we performed linear discriminant analysis (LDA) effect size (LEfSe) **(Supplementary Figures 7-8)**. Here, *Firmicutes* was the only phylum with genera identified by LEfSe analyses in both genotypes and in both treatments. The differences within this phylum were observed mostly in the families *Lachnospiraceae* and *Ruminococcaceae* (order *Clostridiales*).

We then compared the relative abundance of some genera identified by LEfSe commonly associated with intestinal health or inflammation **(Figures 7-8)**.

Analyses of feces revealed that genera commonly associated with good intestinal health were decreased in NOX1 KO mice when compared to WT (*Faecalibaculum, Rumiococcaceae_UCG_009*), and in some cases even absent (*Lachonospiraceae_UCG_010 and Peptococcus*) **(Figure 7A-C, E)**. Similar patterns were also observed in colon tissue **(Figure 8A-C, E)**. Moreover, there was a general tendency for a higher relative abundance of genera associated with inflammation and disease, including *Tyzzerella, Ruminiclostridium* and *Oscillibacter*, in both feces and colon tissue from NOX1 KO mice (**Figures 7F, H and 8F, H**). These differences were mostly persistent after DSS treatment.
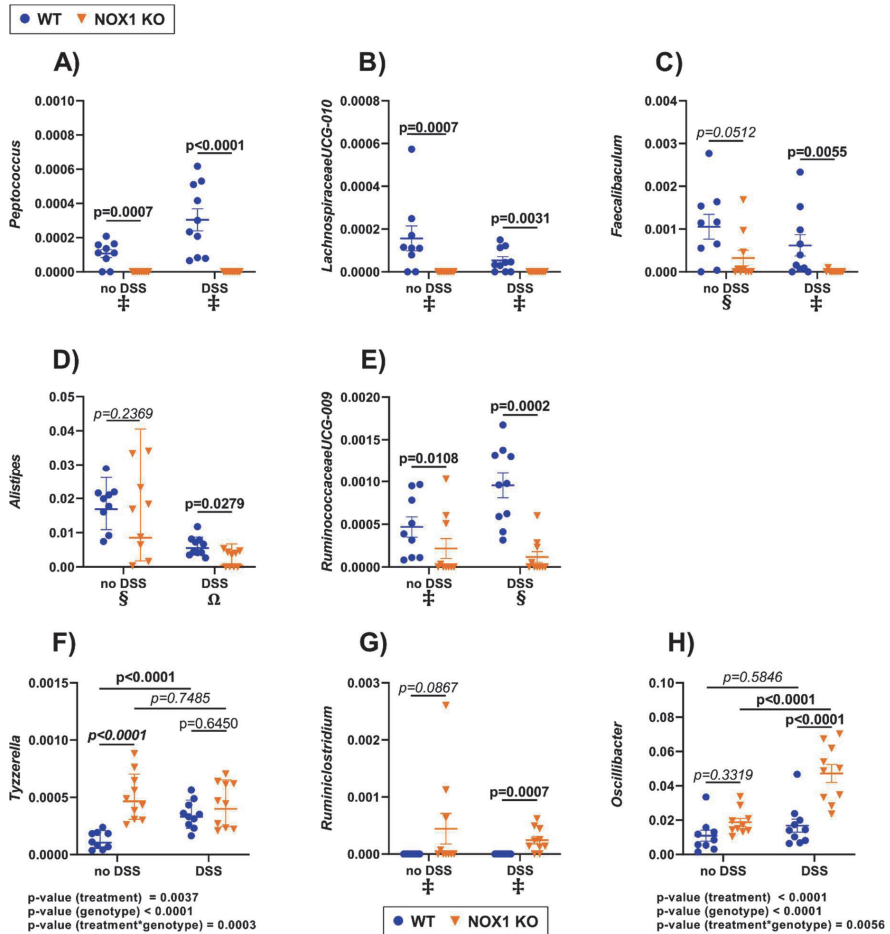
Figure 7: Genus relative abundance in feces from WT and NOX1 KO mice with or without 6-days 1% DSS treatment. (A) *Peptococcus*, **(B)** *Lachnospiraceae_UCG_010*, **(C)** *Faecalibaculum*, **(D)** *Alistipes*, **(E)** *Ruminococcaceae_UCG_009*, **(F)** *Tyzzerella*, **(G)** *Ruminiclostridium1*, **(H)** *Oscillibacter*. (F, H) P-values below graph from 2-way ANOVA (main effects and interaction effect). P-values in the graph for simple main effects with Bonferroni correction for multiple comparisons. (A, B, C, D, E, G) 2-way ANOVA could not be performed due to the violation of normality and/or homoskedasticity. Instead, comparisons of genotypes were performed within each treatment using the model suitable to each case. Specific test is indicated by different symbols: (**§**) Welch's t-test, (**Ω**) Mann-Whitney test and (**‡**) Fisher's exact test. (A, B, C, G, H) Horizontal lines and whiskers are group mean ± SEM. (D, E, F) Statistical analyses were performed on log10-transformed data. Horizontal lines and whiskers are geometric group mean ± geometric SD factor. WT, wild type; KO, knockout; DSS, dextran sulfate sodium.
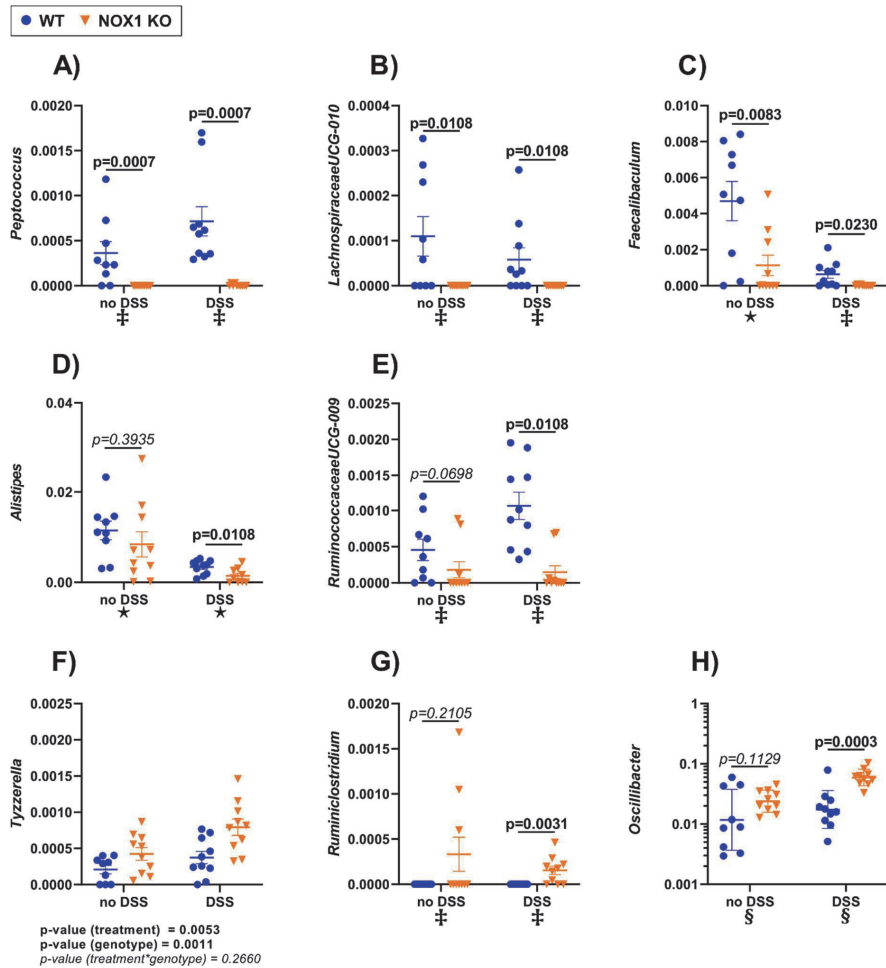
Figure 8: Genus relative abundance in colon tissue from WT and NOX1 KO mice with or without 6-days 1% DSS treatment. (A) *Peptococcus*, **(B)** *Lachnospiraceae_UCG_010*, **(C)** *Faecalibaculum*, **(D)** *Alistipes*, **(E)** *Ruminococcaceae_UCG_009*, **(F)** *Tyzzerella*, **(G)** *Ruminiclostridium1*, **(H)** *Oscillibacter*. (F) P-values below graph from 2-way ANOVA (main effects and interaction effect). P-values in the graph for simple main effects with Bonferroni correction for multiple comparisons.(A, B, C, D, E, H, I) 2-way ANOVA could not be performed due to the violation of normality and/or homoskedasticity. Instead, comparisons of genotypes were performed within each treatment using the model suitable to each case. Specific test is indicated by different symbols: (§) Welch's t-test, (‡) Fisher's exact test and (⋆) unpaired t-test. (A-G) Horizontal lines and whiskers are group mean ± SEM. (H) Statistical analyses were performed on log10-transformed data. Horizontal lines and whiskers are geometric group mean ± geometric SD factor. WT, wild type; KO, knockout; DSS, dextran sulfate sodium.

Discussion

In the present study, we investigated the role of NOX1 in the colon during steady-state and in subclinical low-grade inflammation since the importance of ROS for intestinal homeostasis has become more evident in recent years. The fact that NOX1 is highly expressed in colonic epithelial cells both during non-inflammatory conditions and during inflammation, points in the direction that NOX1 is important for the intestinal homeostasis [5-10, 38]. How superoxide production by NOX1 modulates colonic microbiota and sequentially affects the course of low-grade colonic inflammation is to our knowledge not known.

For the establishment of the low-grade inflammation model, we set the criteria of few or no visible signs of disease (weight loss, and lower stool quality) together with a moderate up-regulation of inflammation-related genes in the colon. Overall, the results indicated that exposing mice to 1% DSS in drinking water for six days would lead to no or only moderate pathology. When this model was applied to WT and NOX1KO animals, we did unexpectedly observe both shortening of the colon and moderate changes in stool quality. In addition, histological analyses revealed immune cell infiltration and changes in cell structure, indicative of more than a mild phenotype. However, we did not observe in any of the analyzed tissues signs of chronic inflammation [39]. Still, to have better control of the severity of the inflammation it might be advisable to include different DSS doses in the experiments since the outcome of DSS exposure in drinking water *ad libitum* can vary between experiments.

As already described, 1% DSS led to certain pathological signs, but no differences were observed between genotypes. In contrast, 1% DSS did increase ROS production in the colon of both genotypes, but with lower levels in NOX1 KO mice. We also observed that NOX1 KO mice exposed to DSS tended to have higher levels of inflammatory markers, although there was no difference in the intestinal barrier integrity. Lastly, NOX1 KO mice had a shift in the microbiota composition characteristic of dysbiosis and pro-inflammatory profile.

The attenuated ROS signal in NOX1 KO mice demonstrates a strong dependency on NOX1 for ROS production after DSS treatment. Since iNOS but not NOX1 was enhanced by DSS, the increased L-012 signal in WT mice is most likely caused by increased nitric oxide production and not superoxide. Further, since the signal in NOX1 KO mice was

sharply reduced, this means that both iNOS and NOX1 must be present to strongly induce ROS. However, we also found an increased ROS production in NOX1 KO mice by DSS, which indicates that other ROS contribute to the signal. It has been shown that 1% DSS can increase myeloperoxidase activity [35], which catalyzes the production of hypochlorous acid. This ROS is shown to activate L-012 [40], and we can therefore not rule it out as a source for the L-012 signal. In the case of NOX1 KO, there could also be some contribution from NOX3, which is shown to be up-regulated in NOX1 KO mice [16].

Based on the gene expression analyses, we only saw a tendency of increased inflammation in the NOX1 KO mice. We further evaluated the production of Lcn-2 protein in fecal samples. Lcn-2 is shown to be a relevant and highly sensitive marker of DSS induced inflammation [35]. Lcn-2 could therefore reveal subtle differences between the genotypes. Recently Makhezer and coworkers demonstrated that induction of Lcn-2 by pro-inflammatory cytokines is partly dependent on NOX1 in epithelial cells [41]. In contrast, we saw that Lcn-2 is in fact modestly increased in NOX1 KO mice compared with WT after DSS exposure, while in non-DSS conditions no difference was observed. In Makhezer's study, they demonstrated that only after the use of high concentrations of TNFα and IL-17 was necessary to reveal that absence of NOX1 reduced the Lcn-2 expression [41]. Since we have a low-grade inflammatory condition, we believe that the direct effect of NOX1 on Lcn-2 production might not be relevant in our case. It appears more likely that the increase in Lcn-2 in NOX1 KO mice is mediated by bacteria from the colon. Lcn-2 induction is dependent on bacterial exposure [36] and our results might thus suggest that epithelial cells expressing Lcn-2 are getting in closer contact with the intestinal microbes. An alternative theory is that the absence of NOX1 generated ROS leads to altered microbial composition analogous to observations of the ileum [38]. Indeed, Li and coworkers showed that DSS induced Lcn-2 levels were dependent on the initial microbial profile [29].

We observed a decrease of overall α-diversity (Shannon-Wiener index) in NOX1 KO mice when compared to WT mice under normal conditions. More specifically, both the number of species and evenness was decreased in NOX1 KO mice. The biological relevance of a 7-10% reduction in species richness is however not clear. To our knowledge, no other studies have examined the microbial α-diversity in NOX1 KO mice, only bacterial load in cecum content which was unaffected [38]. The DSS exposure

mainly affected the evenness, where the increase in NOX1 KO diminished the difference between the genotypes.

Regarding the β-diversity of the fecal samples, all groups were statistically different from each other. That the overall microbial community of epithelial-specific NOX1 KO mice differ from WT have been reported previously [4]. Still, the partial overlap between the groups of NOX1 KO mice which were not observed for the WT groups, indicating that that DSS treatment provokes greater change in the bacterial community of WT than of NOX1 KO animals. One could also argue that the closer proximity of NOX1 KO mice to WT mice exposed to DSS suggests an inflammation-like microbiota of the NOX1 KO mice also without DSS treatment. Together, the analyses of α-and β-diversity suggest that the absence of NOX1 influences microbiota composition, mostly in luminal areas.

At the phylum level, NOX1 KO mice presented an increased *Firmicutes*/*Bacteroidetes* ratio in feces, mostly due to the decrease of *Bacteroidetes* relative amounts. A similar change in the ratio is commonly observed in obese-related inflammation [42]. When exposed to DSS, the ratio increased in both genotypes, but to a lesser extent in the NOX1 KO mice.

Moreover, the genotypes differed immensely in the relative abundance of *Verrucomicrobia (genus Akkermansia)*, with higher abundance in NOX1 KO mice. However, the DSS treatment reduced the difference between the genotypes due to a bloom of *Akkermansia* in WT mice, as also observed in previous studies [31, 43, 44]. *Akkermansia spp.* are anaerobic commensal bacteria that adhere to the intestinal mucus layer and it is reported to have a beneficial role in intestinal homeostasis [45, 46]. With respect to inflammation, some studies have shown that *Akkermansia* supplementation reduces inflammation induced by a high-fat diet [47, 48], while others have in fact shown that *Akkermansia* contributes to enhancing colitis [31]. Since DSS is known to cause structural changes of the inner mucus layer making it more available for bacterial penetration [49], this could explain the increase of *Akkermansia* after DSS treatment in WT animals. Coant *et al.* observed that NOX1 KO mice had an increased number of goblet cells, and consequent higher mucus production [5]. This could explain their increase in *Akkermansia*, although increased mucus production was not observed in more recent studies [4, 50]. Still, why *Akkermansia* in NOX1 KO mice seems unaffected by DSS remains unclear.

When comparing fecal samples of WT and NOX1 KO at lower taxonomic levels, we observed several changes in the genera associated with intestinal health. More specifically we saw a reduction of *Peptococcus, Lachonospiraceae_UCG_010, Faecalibaculum, Alistipes and Ruminococcacea_UCG_009 in* NOX1 KO mice suggesting compromised barrier function and anti-inflammatory response [51-54]. Interestingly, NOX1 KO also showed an increased abundance of the genera commonly associated with inflammation and disease, including *Oscilibacter, Tyzzerella* and *Ruminiclostridium* [29, 55-58]. These data support the earlier observations regarding β-diversity analyses in fecal samples, where the cluster of NOX1 KO mice was closer to WT mice exposed DSS.

To summarize, in the absence of DSS, NOX1 deficient mice had an overall bacterial structure resembling the structure of wild type exposed to DSS. This tendency was confirmed at the phylum level, where NOX1 KO mice had an increase *Firmicutes/Bacteroidetes* ratio, and at lower taxonomic levels with lower levels of putatively beneficial genera and an increase in disease-promoting genera. We therefore conclude that the microbiota composition was shifted in the direction of a dysbiotic profile. This was not manifested in pathological changes. However, analyses of inflammation-associated genes were indicative of an enhanced inflammatory status in NOX1 KO mice. This was further supported by the increment of Lcn-2. We therefore propose that NOX1 has a role in shaping the colonic microbiota, which may have a consequence for intestinal health.

Material and Methods

Animal experiments

Mice were bred in our facility with C57BL/6J background from The Jackson Laboratory (Bar Harbor, ME). NOX1 knockout (KO) strain was confirmed by standard PCR with specific primer-pairs suggested by The Jackson Laboratory. Two experiments were performed.

First, "the establishment experiment", where different concentrations of DSS were tested in order to find the optimal dose and the length of the exposure needed to induce low-grade inflammation in the colon. In our study, colonic low-grade inflammation refers to the presence of none or only a few visible signs of disease together with a moderate up-regulation of inflammation-related genes. For this purpose, 24 wild type (WT) mice (10-14 weeks old) were divided into four groups (n=6) and given 0, 0.5, 1 or 2% DSS in water for 8 days.

Second, the "knockout experiment", where NOX1 KO mice were used to investigate the effect of NOX1 KO on ROS production and colonic low-grade inflammation. Twenty NOX1 KO mice and 19 WT mice were used (eight males, 31 females, 14-17 weeks old) for this purpose. Animals of each genotype were divided into two groups (n=9-10), each of which were given water with 0 or 1% DSS for six days.

In both experiments, mice were housed in individually ventilated cages in a controlled environment (12h-light-dark cycle, 24 ± 1°C, 45-55% humidity), with standard chow (RM1, SDS Diet) and water *ad libitum*. Fresh DSS solutions in new bottles were prepared every second day as suggested by Chassaing *et al.* [28]. Water from the control animals was changed accordingly. Mice were also weighed and inspected for any visible signs of the disease every second day.

The animal experiment was performed with permission from The Norwegian Animal Research Authority (FOTS #7519) and it was conducted in compliance with the current guidelines of The Federation of European Laboratory Animal Science Associations.

Sampling

At the termination day, feces were collected for ELISA. Then, animals were anesthetized by intraperitoneal injection with ZRF cocktail (10µl/g mouse). ZRF is a mixture of Zoletil Forte (Virbac), Rompun (Bayer) and Fentadon (Eurovet) with the active substances Zolezepam (32 mg/kg), Tiletamin (32 mg/kg), Xylazine (4.5 mg/kg), and Fentanyl (26 µg/kg). Blood for ELISA was collected through cardiac puncture with syringes coated with disodium EDTA (0.05 M). After termination by cervical dislocation, the intestine was isolated and *ex vivo* imaging was performed. The length of the colon was measured. Colon was opened longitudinally, 2 cm from both sides. From these sections, 10-30 mg of lamina propria was scraped off with a glass slide for RNA extraction. The remained middle section was fixated for histological observations. In addition, in the knockout experiment, 1 cm of the colon (referred to as "colon tissue") and fecal pellets were collected from the proximal-middle section for DNA extraction.

***Ex vivo* imaging of ROS using L-012 luminescence probe**

Ex vivo imaging in the knockout experiment was performed with IVIS Lumina II (Perkin Elmer). At termination day, L-012 luminescence probe (Wako Chemical) was injected intraperitoneally (10mg/kg mouse). Light emission from intestine was measured as photons/s/cm^2/steradian, 3min after injection with 5min of exposure time, using the Living Imaging software (Perkin Elmer).

Quantification of LBP in plasma and Lcn-2 in feces using ELISA

ELISA was performed on plasma and fecal samples from the knockout experiment. Plasmatic lipopolysaccharide (LPS) was estimated by measuring the concentration of lipopolysaccharide binding protein (LBP) in plasma [59]. Mouse LBP Quantification ELISA kit (Biometec) was used after diluting plasma samples 800 times and load them to the supplied pre-coated plate. Lipocalin-2 (Lcn-2) in fecal samples was used as an indicator of DSS-induced colonic inflammation. To do so, Mouse Lipocalin-2 NGAL DuoSet ELISA and DuoSet ELISA Ancillary Reagent Kit 2 (R&D Systems) was used following the manufacturer's protocol. Fecal samples were prepared as described by Chassaing et al. [35] and supernatants were diluted between 20 and 20,000 times prior

to the assay procedure. For both assays, the level of the target proteins was estimated using standard curves created using 4-parameter logistic curve fit.

Histology

Histological analyses were performed in three animals per group from the knockout experiment. Colon sections were fixated as a *swiss-roll* [60]. Briefly, the colon lumen was washed out with modified Bouin's fixative (50% ethanol, 5% acetic acid in dH$_2$O) and then opened longitudinally. Segments were rolled into *swiss-roll* arrangement, with the luminal side facing inwards. The samples were kept in 10% buffered formalin overnight at room temperature and then stored in 70% ethanol at 4°C until ethanol dehydration and paraffin embedding. Samples were cut with 5µm thickness and stained with hematoxylin and eosin to be analyzed under an optical light microscope. We based our histological analyzes in the infiltration of immune cells in the lamina propria, space between epithelial cells bases and muscularis mucosa and crypts structure, parameters commonly observed during DSS-induced inflammation [15, 28].

RNA isolation and RT-qPCR in lamina propria

Lamina propria samples were placed in RNAlater directly after sampling. For RNA extraction, NucluoSpin RNA/Protein Purification kit (Macherye-Nagel) was used. It was previously shown that DSS might act as an inhibitor in both reverse transcriptase and PCR reactions [61, 62]. We also observed a dose-dependent effect of DSS in the RT-qPCR signal. Therefore, extracted RNA was cleaned following the lithium chloride method described by Viennois *et al.* [62], where RNA precipitates and polysaccharides (including DSS) stay in solution.

RNA was then converted to cDNA using the iScript cDNA Synthesis kit (Bio Rad). For the RT-qPCR reaction, we used HOT FirePol EvaGreen qPCR Supermix (Solis BioDyne) and measured fluorescence in LightCycler480 Instrument II (Roche). LinRegPCR Software (version 2018.0) [63] was used to calculate Cq values based on a common threshold and individual efficiencies. See **Supplementary Tables 1-5** for reagents, primers and temperature cycles.

DNA extraction from fecal material

Fecal material (approximately 0.05 g) and colon tissue from the knockout experiment was placed in S.T.A.R buffer (300 uL, Roche) with acid-washed glass beads (app. 0.2g <106 μm, Sigma-Aldrich) directly after dissection and stored at -80C until further processing. Later, fecal samples were added an additional 300 μL S.T.A.R buffer to obtain the same volumes as were used during method testing. All samples were processed twice on FastPrep 96 (1800 rpm, 40 sec, 5 min cooling step in-between, MP BioMedicals) to obtain cell lysis. Processed samples were centrifuged (13 000 rpm, 10 min) and 50 μL supernatant were transferred to 96-well plates for protease treatment followed by DNA extraction using Mag Midi LGC kit (LGC Genomics) according to the manufacturer's protocol on a KingFisher Flex DNA extraction robot (Thermo Fisher Scientific).

Library preparation and gene sequencing of 16S rRNA

A similar workflow of 16S rRNA gene sequencing has been reported by others [64]. After DNA extraction, 16S rRNA was amplified by PCR ("amplicon PCR") using prokaryote-targeting primers **(Supplementary Table 6-7)**. As DSS from fecal samples has inhibitory effects on PCR (identified through dilution series on qPCR), we diluted the extracted DNA from fecal samples 1:4 prior to amplicon PCR (total dilution of 1:100 in the PCR reaction) to prevent the inhibitory effects of DSS. PCR product (app. 466 bp) was purified with AMPure XP (Beckman-Coulter) and 10 further PCR cycles ("index PCR") were performed **(Supplementary Table 8-10)**, resulting in PCR product of app. 594 bp. All PCR products were qualitatively confirmed by gel electrophoresis. Quantification, normalization and pooling of individual libraries were followed by purification by AMPure XP and quantification of the pooled library. The pooled library was diluted to 6 pM and sequenced with the MiSeq Reagent Kit V3 (cat. nr. MS-102-3003) on the Illumina MiSeq following Illumina's protocol (16S Metagenomic Sequencing Library Preparation Part# 15044223 Rev. B), except we used nuclease free-water instead of Tris for PhiX library dilution. 20 % PhiX served as an internal control. Resulting 300 bp paired-end reads were further paired-end joined and split into their respective samples, quality-filtered using QIIME [65] and clustered with 97 % identity

and higher using closed-reference *usearch* algorithm (version 8) [66, 67] against SILVA database (version 128) [68]. The resulting dataset included 2,392,173 high-quality and chimera-checked sequences from 78 samples (8,644 to 61,079 per sample). 6,500 sequences per sample were chosen as a cut-off to normalize the sequencing data, from which 538 operational taxonomic units (OUTs) were identified in total. See **Supplementary Figure 9** for rarefaction curves.

Alpha- and beta-diversity analyses

Measures of diversity within (α-diversity; number of observed species, Shannon-Wiener index, equitability) and between (β-diversity; weighted UniFrac distances [69]) bacterial communities (samples) were calculated based on the normalized OTU table.

Number of observed species in one sample equals number of OTUs with sequence count > 0. The Shannon-Wiener index for a sample is defined as $H = -\sum_{i=1}^{s}(p_i ln(p_i))$, where *s* is the number of OTUs with sequence count > 0 and p_i is the proportion of the community represented by OTU number *i*. Equitability (evenness) for one sample is defined as $E = \frac{H}{H_{max}}$ where $H_{max} = \ln$ (number of OTUs with sequence count > 0).

Analysis of β-diversity was conducted in R [70] (version 4.0.0). Weighted UniFrac distances were calculated using QIIME default scripts (core_diversity_analyses.py). Principal coordinate analyses (PCoA) of weighted UniFrac distances was performed using the cmdscale() function from the stats package [70] (version 4.0.0) with k=2. Non-metric multidimensional scaling (NMDS) was performed using the metaMDS() function from the vegan package [71] (version 2.5-6), with autotransform=FALSE and try=100. Global PERMANOVA (four groups: WT, WT with DSS, NOX1 KO and NOX1 KO with DSS) on weighted UniFrac distances was performed using the adonis() function from the vegan package with 999 permutations. Pairwise PERMANOVA was performed by applying the adonis() function on each of the six pairs, followed by p-value adjustment using p.adjust() function with method="BH" (Benjamini-Hochberg) from the stats package. Dispersion homogeneity between groups was performed using the function betadisper() from the vegan package. PERMANOVA was performed for fecal and colon tissue samples separately.

Statistics

All statistical analyses, except PERMANOVA, were performed using GraphPad Prism (version 8.3.1 for Windows, GraphPad Software, San Diego, California USA). Briefly, results from the establishment experiment (effects of DSS dose on WT mice) were analyzed using one-way ANOVA (repeated measures two-way ANOVA on change in body weight), while results from the knockout experiment (effects of treatment and genotype) were analyzed preferably using 2-way ANOVA (repeated measures 3-way ANOVA on change in body weight). If not possible, comparisons of genotypes were performed within each treatment using a model suitable for each case (t-test, Welch's t-test, Mann-Whitney test or Fisher's exact test). Significant interactions were followed by the assessment of simple main effects (effect of DSS within each genotype and the effect of genotype within each treatment) with Bonferroni correction for multiple comparisons. Normality was evaluated using Q-Q plot and Shapiro and homoscedasticity were evaluated using residual plots and Brown-Forsythe test. All reported p-values are two-tailed, where $p<0.05$ was considered significant. Data are presented as individual values (with some exceptions) with group means ± standard error of the mean (SEM) or geometric group mean *÷ geometric SD factor in cases where statistical analyses were performed on log10-transformed data. To identify differentiated taxa between groups, we used LEfSe [72] available at https://huttenhower.sph.harvard.edu/galaxy/, with $P < 0.05$ and the linear discriminant analysis (LDA) effect size 2.0 to explain differences between groups. Relative abundance from the taxonomic levels phylum to genus was used for these analyses.

References

1. Tilg, H., N. Zmora, *et al.*, The intestinal microbiota fuelling metabolic inflammation. *Nat Rev Immunol*, **2020**. 20(1): p. 40-54.

2. Bedard, K. and K.-H. Krause, The NOX Family of ROS-Generating NADPH Oxidases: Physiology and Pathophysiology. **2007**. 87(1): p. 245-313.

3. Aviello, G. and U.G. Knaus, NADPH oxidases and ROS signaling in the gastrointestinal tract. *Mucosal immunology*, **2018**. 11(4): p. 1011-1023.

4. Pircalabioru, G., G. Aviello, *et al.*, Defensive Mutualism Rescues NADPH Oxidase Inactivation in Gut Infection. *Cell Host Microbe*, **2016**. 19(5): p. 651-63.

5. Coant, N., S. Ben Mkaddem, *et al.*, NADPH oxidase 1 modulates WNT and NOTCH1 signaling to control the fate of proliferative progenitor cells in the colon. *Mol Cell Biol*, **2010**. 30(11): p. 2636-50.

6. Jones, R.M., L. Luo, *et al.*, Symbiotic *lactobacilli* stimulate gut epithelial proliferation via Nox-mediated generation of reactive oxygen species. *The EMBO journal*, **2013**. 32(23): p. 3017-3028.

7. Leoni, G., A. Alam, *et al.*, Annexin A1, formyl peptide receptor, and NOX1 orchestrate epithelial repair. *J Clin Invest*, **2013**. 123(1): p. 443-54.

8. Tréton, X., E. Pedruzzi, *et al.*, Combined NADPH oxidase 1 and interleukin 10 deficiency induces chronic endoplasmic reticulum stress and causes ulcerative colitis-like disease in mice. *PLoS One*, **2014**. 9(7): p. e101669.

9. Yeligar, S.M., F.L. Harris, *et al.*, Ethanol induces oxidative stress in alveolar macrophages via upregulation of NADPH oxidases. *The Journal of Immunology*, **2012**. 188(8): p. 3648-3657.

10. Lee, A.-J., K.-J. Cho, and J.-H. Kim, MyD88–BLT2-dependent cascade contributes to LPS-induced interleukin-6 production in mouse macrophage. *Experimental & Molecular Medicine*, **2015**. 47(4): p. e156-e156.

11. Mittal, M., M.R. Siddiqui, *et al.*, Reactive oxygen species in inflammation and tissue injury. *Antioxidants & redox signaling*, **2014**. 20(7): p. 1126-1167.

12. Yokota, H., A. Tsuzuki, *et al.*, NOX1/NADPH Oxidase Expressed in Colonic Macrophages Contributes to the Pathogenesis of Colonic Inflammation in Trinitrobenzene Sulfonic Acid-Induced Murine Colitis. *J Pharmacol Exp Ther*, **2017**. 360(1): p. 192-200.

13. Bedard, K. and K.H. Krause, The NOX family of ROS-generating NADPH oxidases: physiology and pathophysiology. *Physiol Rev*, **2007**. 87(1): p. 245-313.

14. Radi, R., Peroxynitrite, a stealthy biological oxidant. *J Biol Chem*, **2013**. 288(37): p. 26464-72.

15. Kato, M., M. Marumo, *et al.*, The ROS-generating oxidase Nox1 is required for epithelial restitution following colitis. *Exp Anim*, **2016**. 65(3): p. 197-205.

16. Aviello, G., A.K. Singh*, et al.*, Colitis susceptibility in mice with reactive oxygen species deficiency is mediated by mucus barrier and immune defense defects. *Mucosal Immunology*, **2019**. 12(6): p. 1316-1326.

17. Alam, A., G. Leoni*, et al.*, The microenvironment of injured murine gut elicits a local pro-restitutive microbiota. *Nat Microbiol*, **2016**. 1: p. 15021.

18. Chassaing, B. and A.T. Gewirtz, Gut microbiota, low-grade inflammation, and metabolic syndrome. *Toxicol Pathol*, **2014**. 42(1): p. 49-53.

19. Moss, A.C., The meaning of low-grade inflammation in clinically quiescent inflammatory bowel disease. *Current opinion in gastroenterology*, **2014**. 30(4): p. 365-369.

20. Barbara, G., C. Cremon, and V. Stanghellini, Inflammatory bowel disease and irritable bowel syndrome: similarities and differences. *Current opinion in gastroenterology*, **2014**. 30(4): p. 352-358.

21. Agus, A., J. Denizot*, et al.*, Western diet induces a shift in microbiota composition enhancing susceptibility to Adherent-Invasive *E. coli* infection and intestinal inflammation. *Scientific reports*, **2016**. 6: p. 19032.

22. Chassaing, B., O. Koren*, et al.*, Dietary emulsifiers impact the mouse gut microbiota promoting colitis and metabolic syndrome. *Nature*, **2015**. 519(7541): p. 92-96.

23. Christ, A., M. Lauterbach, and E. Latz, Western diet and the immune system: an inflammatory connection. *Immunity*, **2019**. 51(5): p. 794-811.

24. Johansson, M.E., J.K. Gustafsson*, et al.*, Bacteria penetrate the normally impenetrable inner colon mucus layer in both murine colitis models and patients with ulcerative colitis. *Gut*, **2014**. 63(2): p. 281-291.

25. Johansson, M.E., J.K. Gustafsson*, et al.*, Bacteria penetrate the inner mucus layer before inflammation in the dextran sulfate colitis model. *PloS one*, **2010**. 5(8): p. e12238.

26. Suzuki, R., H. Kohno*, et al.*, Strain differences in the susceptibility to azoxymethane and dextran sodium sulfate-induced colon carcinogenesis in mice. *Carcinogenesis*, **2006**. 27(1): p. 162-9.

27. Seril, D.N., J. Liao*, et al.*, Dietary iron supplementation enhances DSS-induced colitis and associated colorectal carcinoma development in mice. *Digestive diseases and sciences*, **2002**. 47(6): p. 1266-1278.

28. Chassaing, B., J.D. Aitken*, et al.*, Dextran sulfate sodium (DSS)-induced colitis in mice. *Curr Protoc Immunol*, **2014**. 104: p. Unit 15 25.

29. Li, M., Y. Wu*, et al.*, Initial gut microbiota structure affects sensitivity to DSS-induced colitis in a mouse model. *Science China Life Sciences*, **2018**. 61(7): p. 762-769.

30. Roy, U., E.J.C. Galvez*, et al.*, Distinct Microbial Communities Trigger Colitis Development upon Intestinal Barrier Damage via Innate or Adaptive Immune Cells. *Cell Rep*, **2017**. 21(4): p. 994-1008.

31. Zhang, Q., Y. Wu, *et al.*, Accelerated dysbiosis of gut microbiota during aggravation of DSS-induced colitis by a butyrate-producing bacterium. *Scientific reports*, **2016**. 6(1): p. 1-11.

32. Daiber, A., M. Oelze, *et al.*, Taking up the cudgels for the traditional reactive oxygen and nitrogen species detection assays and their use in the cardiovascular system. *Redox biology*, **2017**. 12: p. 35-49.

33. Van Dyke, K., E. Ghareeb, *et al.*, Luminescence experiments involved in the mechanism of streptozotocin diabetes and cataract formation. *Luminescence*, **2008**. 23(6): p. 386-391.

34. Kielland, A., T. Blom, *et al.*, In vivo imaging of reactive oxygen and nitrogen species in inflammation using the luminescent probe L-012. *Free Radic Biol Med*, **2009**. 47(6): p. 760-6.

35. Chassaing, B., G. Srinivasan, *et al.*, Fecal lipocalin 2, a sensitive and broadly dynamic non-invasive biomarker for intestinal inflammation. *PLoS One*, **2012**. 7(9): p. e44328.

36. Singh, V., B.S. Yeoh, *et al.*, Microbiota-inducible Innate Immune, Siderophore Binding Protein Lipocalin 2 is Critical for Intestinal Homeostasis. *Cell Mol Gastroenterol Hepatol*, **2016**. 2(4): p. 482-498 e6.

37. Cani, P.D., R. Bibiloni, *et al.*, Changes in gut microbiota control metabolic endotoxemia-induced inflammation in high-fat diet-induced obesity and diabetes in mice. *Diabetes*, **2008**. 57(6): p. 1470-81.

38. Matziouridou, C., S.D.C. Rocha, *et al.*, iNOS- and NOX1-dependent ROS production maintains bacterial homeostasis in the ileum of mice. *Mucosal Immunol*, **2018**. 11(3): p. 774-784.

39. Perse, M. and A. Cerar, Dextran sodium sulphate colitis mouse model: traps and tricks. *J Biomed Biotechnol*, **2012**. 2012: p. 718617.

40. Gross, S., S.T. Gammon, *et al.*, Bioluminescence imaging of myeloperoxidase activity in vivo. *Nat Med*, **2009**. 15(4): p. 455-61.

41. Makhezer, N., M.B. Khemis, *et al.*, NOX1-derived ROS drive the expression of Lipocalin-2 in colonic epithelial cells in inflammatory conditions. *Mucosal Immunology*, **2019**. 12(1): p. 117-131.

42. Ley, R.E., F. Backhed, *et al.*, Obesity alters gut microbial ecology. *Proc Natl Acad Sci U S A*, **2005**. 102(31): p. 11070-5.

43. Schwab, C., D. Berry, *et al.*, Longitudinal study of murine microbiota activity and interactions with the host during acute inflammation and recovery. *The ISME journal*, **2014**. 8(5): p. 1101-1114.

44. Berry, D., C. Schwab, *et al.*, Phylotype-level 16S rRNA analysis reveals new bacterial indicators of health state in acute murine colitis. *The ISME journal*, **2012**. 6(11): p. 2091-2106.

45. Derrien, M., P. Van Baarlen, *et al.*, Modulation of mucosal immune response, tolerance, and proliferation in mice colonized by the mucin-degrader *Akkermansia muciniphila*. *Frontiers in microbiology*, **2011**. 2: p. 166.

46. Derrien, M., M.C. Collado, *et al.*, The Mucin degrader *Akkermansia muciniphila* is an abundant resident of the human intestinal tract. *Appl. Environ. Microbiol.*, **2008**. 74(5): p. 1646-1648.

47. Everard, A., C. Belzer, *et al.*, Cross-talk between *Akkermansia muciniphila* and intestinal epithelium controls diet-induced obesity. *Proc Natl Acad Sci U S A*, **2013**. 110(22): p. 9066-71.

48. Shin, N.R., J.C. Lee, *et al.*, An increase in the Akkermansia spp. population induced by metformin treatment improves glucose homeostasis in diet-induced obese mice. *Gut*, **2014**. 63(5): p. 727-35.

49. Johansson, M.E., J.K. Gustafsson, *et al.*, Bacteria penetrate the inner mucus layer before inflammation in the dextran sulfate colitis model. *PLoS One*, **2010**. 5(8): p. e12238.

50. Aviello, G., A.K. Singh, *et al.*, Colitis susceptibility in mice with reactive oxygen species deficiency is mediated by mucus barrier and immune defense defects. *Mucosal Immunol*, **2019**. 12(6): p. 1316-1326.

51. Liang, Y.-N., J.-G. Yu, *et al.*, Indigo Naturalis Ameliorates Dextran Sulfate Sodium-Induced Colitis in Mice by Modulating the Intestinal Microbiota Community. *Molecules*, **2019**. 24(22): p. 4086.

52. Sokol, H., B. Pigneur, *et al.*, *Faecalibacterium prausnitzii* is an anti-inflammatory commensal bacterium identified by gut microbiota analysis of Crohn disease patients. *Proceedings of the National Academy of Sciences*, **2008**. 105(43): p. 16731-16736.

53. Chen, C., M. Perez de Nanclares, *et al.*, Identification of redox imbalance as a prominent metabolic response elicited by rapeseed feeding in swine metabolome. *Journal of Animal Science*, **2018**. 96(5): p. 1757-1768.

54. Fomenky, B.E., D.N. Do, *et al.*, Direct-fed microbial supplementation influences the bacteria community composition of the gastrointestinal tract of pre-and post-weaned calves. *Scientific Reports*, **2018**. 8(1): p. 1-21.

55. Liu, X.-c., Q. Mei, *et al.*, Balsalazine decreases intestinal mucosal permeability of dextran sulfate sodium-induced colitis in mice. *Acta pharmacologica Sinica*, **2009**. 30(7): p. 987-993.

56. Chun-Sai-Er Wang, W.-B., H.-Y.W. Li, *et al.*, VSL# 3 can prevent ulcerative colitis-associated carcinogenesis in mice. *World journal of gastroenterology*, **2018**. 24(37): p. 4254.

57. Zhao, H., X. Jiang, and W. Chu, Shifts in the gut microbiota of mice in response to dexamethasone administration. *International microbiology: the official journal of the Spanish Society for Microbiology*, **2020**.

58. Parker, B.J., P.A. Wearsch, *et al.*, The Genus *Alistipes*: Gut Bacteria With Emerging Implications to Inflammation, Cancer, and Mental Health. *Frontiers in Immunology*, **2020**. 11.

59. Umoh, F.I., I. Kato, *et al.*, Markers of systemic exposures to products of intestinal bacteria in a dietary intervention study. *European journal of nutrition*, **2016**. 55(2): p. 793-798.

60. Bialkowska, A.B., A.M. Ghaleb, *et al.*, Improved Swiss-rolling technique for intestinal tissue preparation for immunohistochemical and immunofluorescent analyses. *JoVE (Journal of Visualized Experiments)*, **2016**(113): e54161.

61. Kerr, T., M. Ciorba, *et al.*, Dextran sodium sulfate inhibition of real-time polymerase chain reaction amplification: a poly-A purification solution. *Inflammatory bowel diseases*, **2012**. 18(2): p. 344-348.

62. Viennois, E., F. Chen, *et al.*, Dextran sodium sulfate inhibits the activities of both polymerase and reverse transcriptase: lithium chloride purification, a rapid and efficient technique to purify RNA. *BMC research notes*, **2013**. 6(1): p. 1-8.

63. Ruijter, J.M., C. Ramakers, *et al.*, Amplification efficiency: linking baseline and bias in the analysis of quantitative PCR data. *Nucleic Acids Res*, **2009**. 37(6): p. e45.

64. Avershina, E., K. Lundgard, *et al.*, Transition from infant- to adult-like gut microbiota. *Environ Microbiol*, **2016**. 18(7): p. 2226-36.

65. Caporaso, J.G., J. Kuczynski, *et al.*, QIIME allows analysis of high-throughput community sequencing data. *Nat Methods*, **2010**. 7(5): p. 335-6.

66. Edgar, R.C., Search and clustering orders of magnitude faster than BLAST. *Bioinformatics*, **2010**. 26(19): p. 2460-1.

67. Edgar, R.C., UPARSE: highly accurate OTU sequences from microbial amplicon reads. *Nat Methods*, **2013**. 10(10): p. 996-8.

68. Pruesse, E., C. Quast, *et al.*, SILVA: a comprehensive online resource for quality checked and aligned ribosomal RNA sequence data compatible with ARB. *Nucleic Acids Res*, **2007**. 35(21): p. 7188-96.

69. Lozupone, C.A., M. Hamady, *et al.*, Quantitative and qualitative beta diversity measures lead to different insights into factors that structure microbial communities. *Appl Environ Microbiol*, **2007**. 73(5): p. 1576-85.

70. Team, R.C., R: A language and environment for statistical computing. **2013**.

71. Oksanen, J., F.G. Blanchet, *et al.*, Community ecology package. *R package version*, **2013**: p. 2.0-2.

72. Segata, N., J. Izard, *et al.*, Metagenomic biomarker discovery and explanation. *Genome Biol*, **2011**. 12(6): p. 1-18.

Supplementary Results
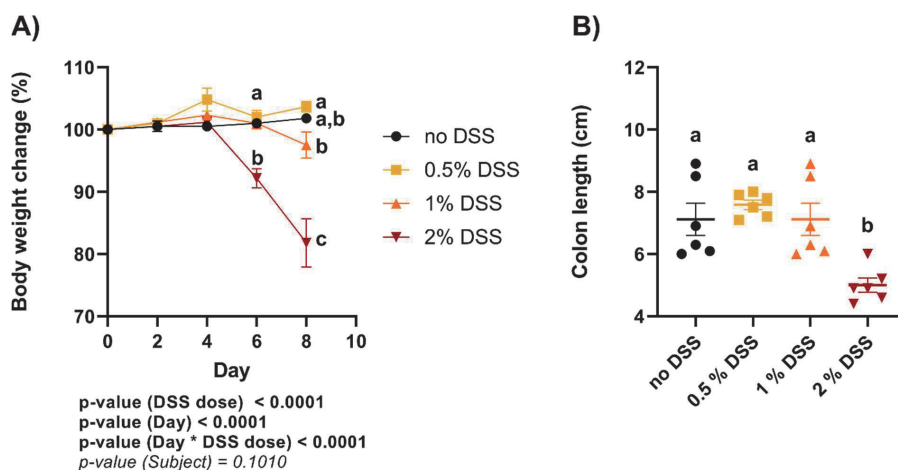
Supplementary Figure 1: Disease evaluation of WT mice after 8-days exposure of DSS in different concentrations. (**A**) Change in bodyweight (%) for mice in the establishment experiment. P-values below graph from repeated measures two-way ANOVA. Characters in the graph (a, b, c) indicate significant differences between DSS dose within each day, with Tukey correction for multiple comparisons. (**B**) Colon length (cm) of animals on day 8 of the establishment experiment. One-way ANOVA revealed a significant effect of DSS dose (p=0.0007). Characters in the graph (a, b, c) indicate significant differences between DSS dose, with Tukey correction for multiple comparisons. (A,B) Horizontal lines and whiskers are group mean ± SEM. N=6 in each group. DSS, dextran sulfate sodium.
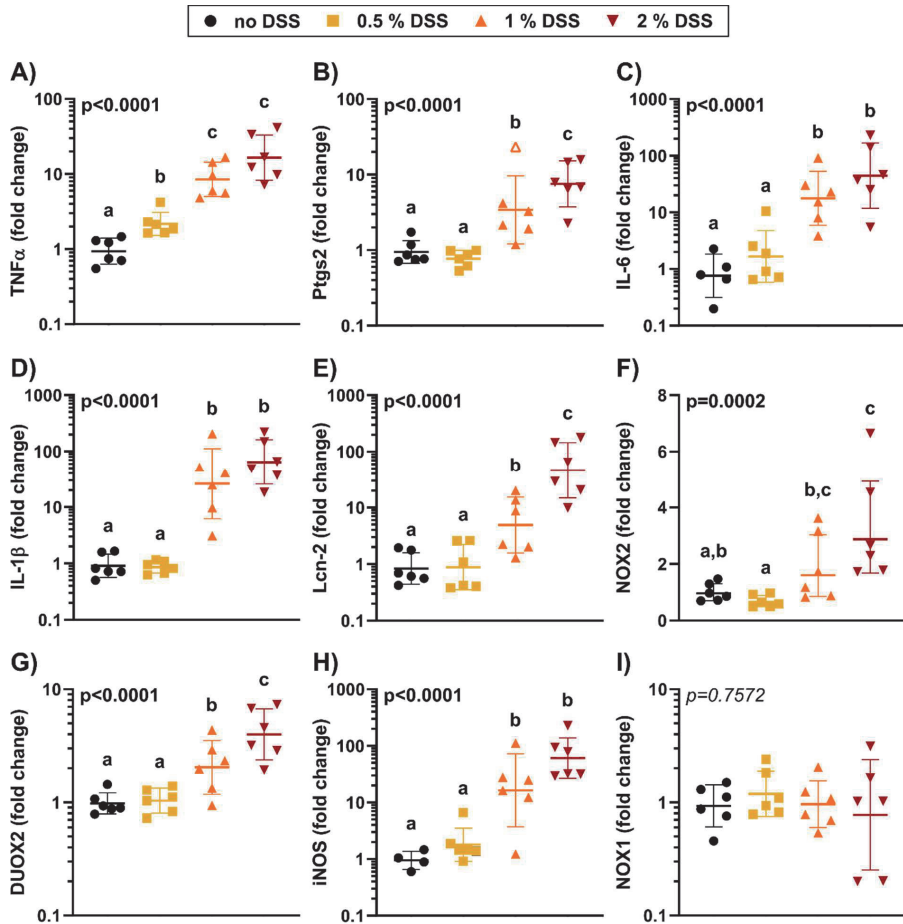
Supplementary Figure 2: Expression of inflammation and ROS associated genes in WT mice after 8-days exposure of DSS in different concentrations. Fold change in gene expression in mucosa from the proximal colon. **(A)** TNFα, **(B)** Ptgs2, **(C)** IL-6, **(D)** IL-1β (n=6 in each group), **(E)** Lcn-2, **(F)** NOX2, **(G)** DUOX2, **(H)** iNOS and **(I)** NOX. Data of animals exposed to DSS were normalized by the mean expression of the group without DSS exposure. P-value in the graph from one-way ANOVA on log10-transformed data. Characters in the graph (a, b, c) indicate significant differences between DSS dose, with Tukey correction for multiple comparisons. Horizontal lines and whiskers are geometric group mean *÷ geometric SD factor. N=4-6 in each group. (B) One extreme value was excluded from statistical analysis (unfilled triangle). When included, the DSS effect was significant (P<0.0001) but letters "a, a, b, c" would be exchanged for "a, a, b, b". For this model however, the assumption of normality was violated. DSS, dextran sulfate sodium.

A)
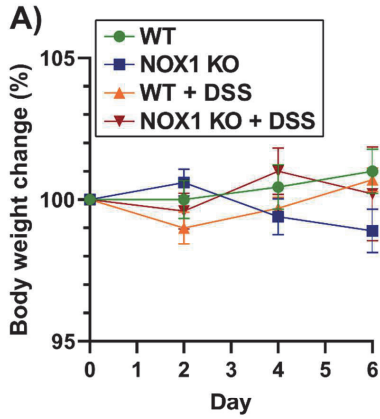
p-value (day) = 0.6921
p-value (treatment) = 0.9699
p-value (genotype) = 0.7652
p-value (day*treatment) = 0.2180
p-value (day*genotype) = 0.1068
p-value (treatment*genotype) = 0.3067
p-value (day*treatment*genotype) = 0.3552

B)
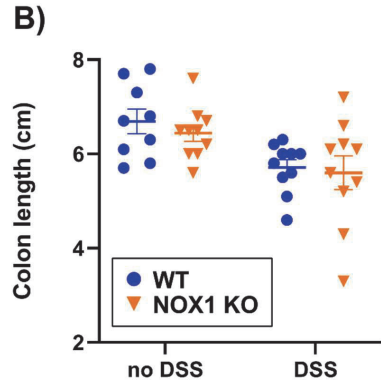
p-value (treatment) = 0.0010
p-value (genotype) = 0.4821
p-value (treatment*genotype) = 0.7850

Supplementary Figure 3: Disease evaluation of WT and NOX1 KO mice with and without 6-days 1% DSS treatment. (A) Change in bodyweight (%) measured on day 0, 2, 4 and 6. P-values below graph from repeated measures 3-way ANOVA. Symbols and whiskers are group mean ± SEM. N=6 in each group. **(B)** Colon length (cm). P-values below graph from 2-way ANOVA (main effects and interaction effect). Horizontal lines and whiskers are group mean ± SEM. N=9-10 in each group. WT, wild type; KO, knockout; DSS, dextran sulfate sodium.
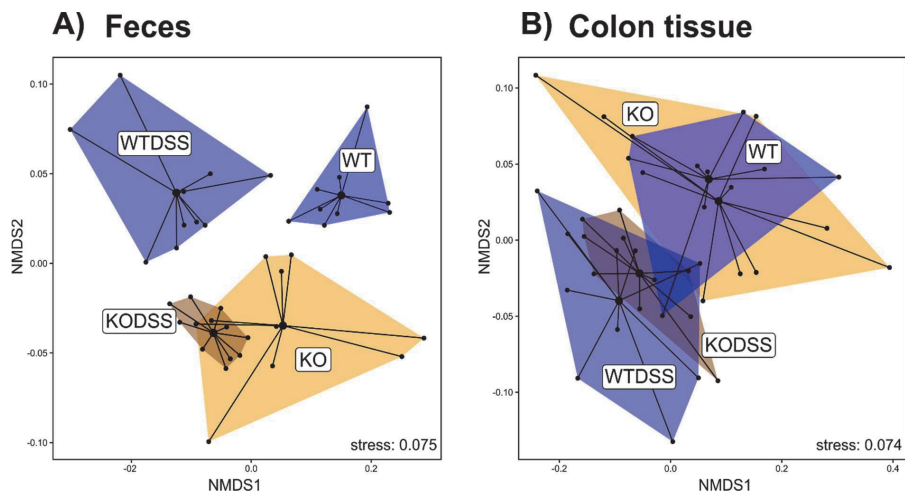
Supplementary Figure 4: Non-metric multidimensional scaling (NMDS) of weighted UniFrac distances between samples in **(A)** feces and **(B)** colon tissue samples in NOX1 KO and WT mice with and without 6-days 1% DSS treatment. N=9-10 in each group. Colors indicate which group individual samples belong to (WT, NOX1 KO (KO), WT with DSS (WTDSS), NOX1 KO with DSS (KODSS). 2D representation in these NMDS plots are in accordance with the pairwise PERMANOVA and the PCoA plot also based on the weighted UniFrac distances (see Figure 5). WT, wild type; KO, knockout; DSS, dextran sulfate sodium.
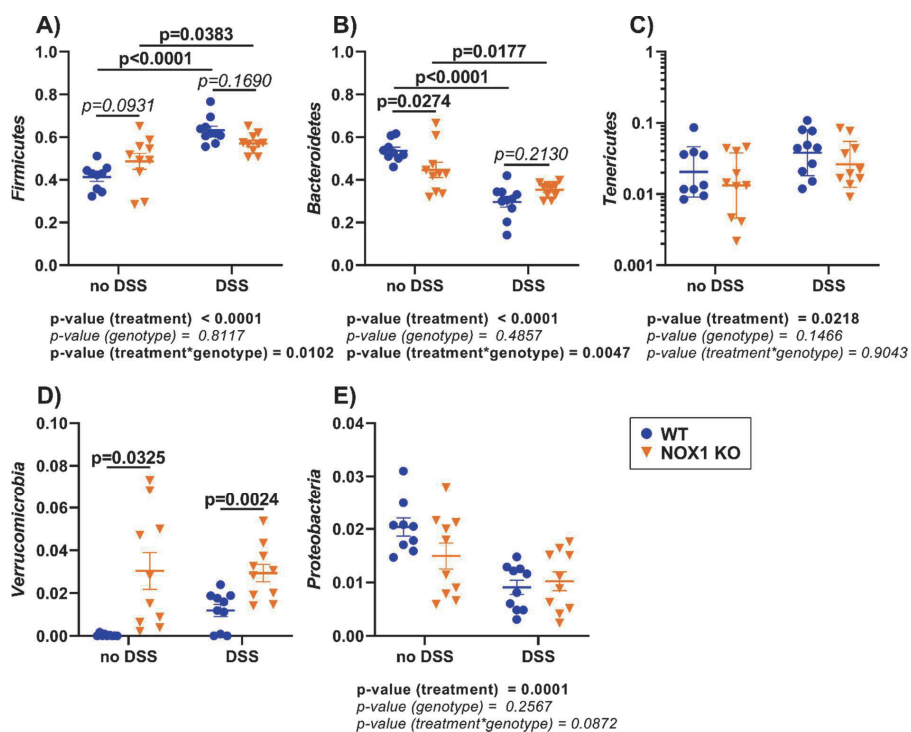
Supplementary Figure 5: Bacterial phyla in fecal samples from NOX1 KO and WT mice with or without 6-days 1% DSS treatment. (A) The relative abundance of bacterial phyla with an average abundance above 1 % in at least one group. **(A)** *Firmicutes*, **(B)** *Bacteroidetes*, **(C)** *Tenericutes*, **(D)** *Verrucomicrobia* and **(E)** *Proteobacteria*. (A, B, C, E) P-values below graph from 2-way ANOVA (main effects and interaction effect). (A, B) P-values in the graph for simple main effects with Bonferroni correction for multiple comparisons. (D) 2-way ANOVA could not be performed due to heteroskedasticity (low/zero abundance in WT group with no DSS). P-values from Fisher's exact test (no DSS condition) and two-sided t-test (DSS condition). (C) Statistical analyses were performed on log10-transformed data. Horizontal lines and whiskers are geometric group mean *÷ geometric SD factor. N=9, 10, 10, 10. (A, B, D, E) Horizontal lines and whiskers are group mean ± SEM. N = 9-10. WT, wild type; KO, knockout; DSS, dextran sulfate sodium.
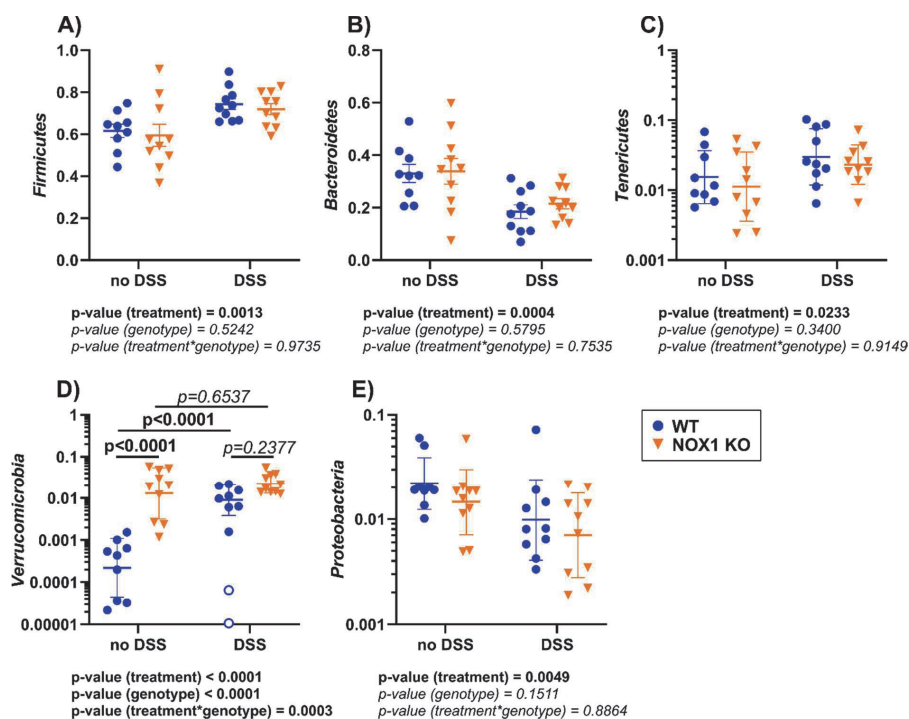
Supplementary Figure 6: Relative abundance of bacterial phyla in colon tissue samples from the knockout experiment with average abundance above 1 % in at least one group. (A) *Firmicutes*, **(B)** *Bacteroidetes*, **(C)** *Tenericutes*, **(D)** *Verrucomicrobia* and **(E)** *Proteobacteria*. (A-E) P-values below graph from 2-way ANOVA (main effects and interaction effect). (C, D, E) Statistical analyses were performed on log10-transformed data. Horizontal lines and whiskers are geometric group mean *÷ geometric SD factor. (A, B) Horizontal lines and whiskers are group mean ± SEM. (D) P-values in the graph for simple main effects with Bonferroni correction for multiple comparisons. One zero-value and one extreme value were excluded from the statistical analysis (unfilled circles). When the extreme value is included, the significance of the interaction decreases (p=0.0069), but for this model, the assumption of normality and homoskedasticity is violated. WT, wild type; KO, knockout; DSS, dextran sulfate sodium.
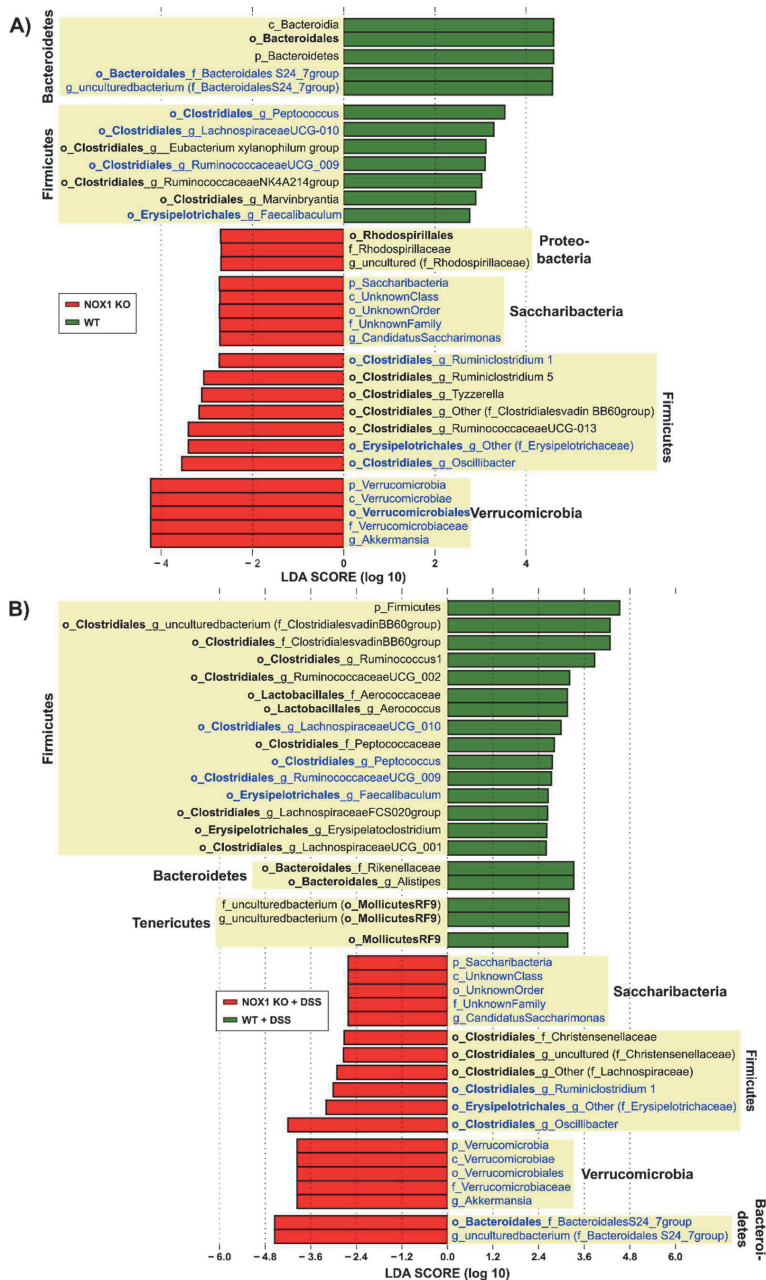
Supplementary Figure 7: LEfSe analysis of the microbiota feces from NOX1 KO and WT mice with or without 6-days 1% DSS treatment. LEfSe results from the analyses of NOX1 KO mice versus WT mice **(A)** without and with **(B)** DSS exposure. Red and green colors indicate higher or lower relative abundance in NOX1 KO and WT mice, respectively. Taxa in blue indicate their presence in both treatment conditions.
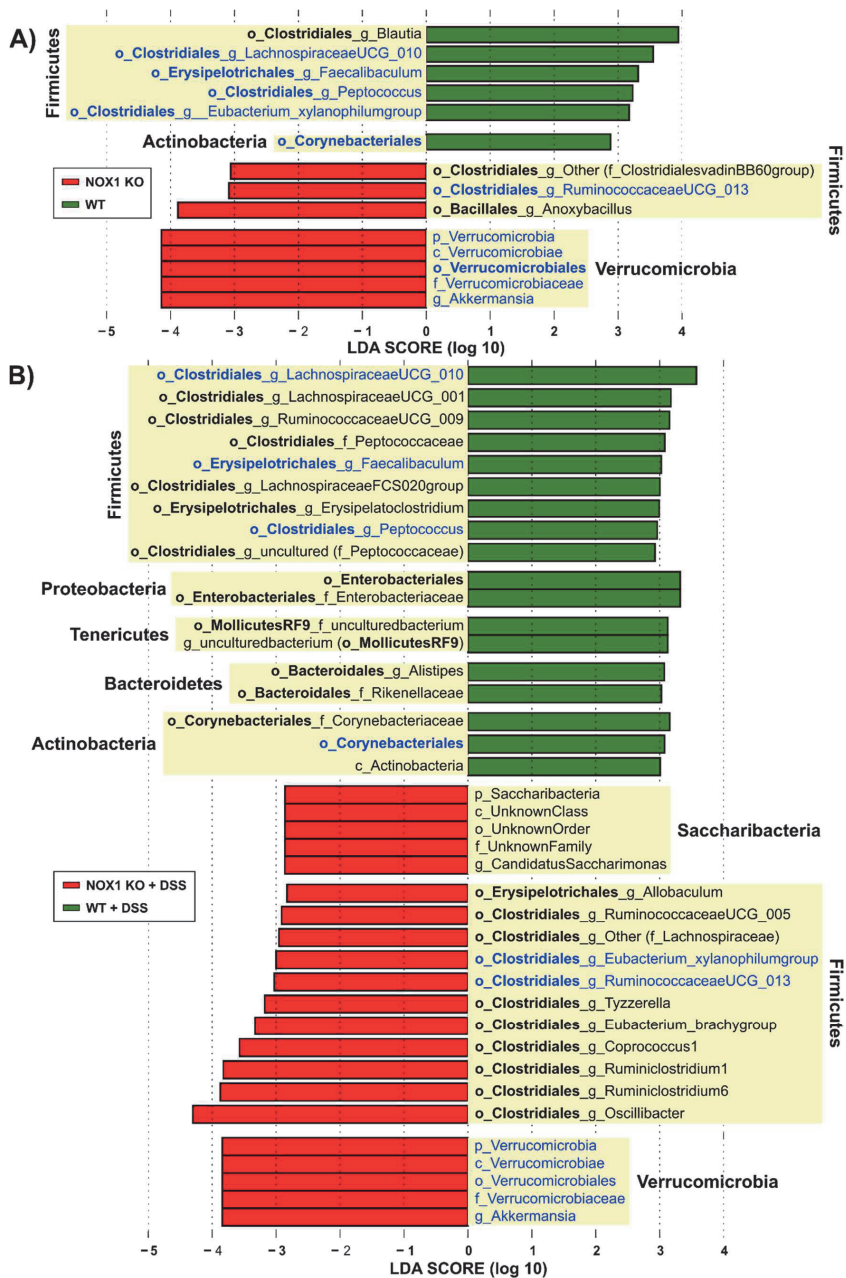
Supplementary Figure 8: LEfSe analysis of the microbiota in colon tissue from NOX1 KO and WT mice with or without 6-days 1% DSS treatment. LEfSe results from analyses of NOX1 KO mice versus WT mice **(A)** without and with **(B)** DSS exposure. Red and green colors indicate higher or lower relative abundance in NOX1 KO and WT mice, respectively. Taxa in blue indicate their presence in both treatment conditions.

Supplementary Methods

Supplementary Table 1: Reaction mixture for cDNA synthesis using the iScript cDNA Synthesis kit (Bio Rad)

Component	Per reaction
5x iScript reaction mix	4 µL
iScript reverse transcriptase	1 µL
Nuclease-free water	11 µL
RNA template (200ng/µL)	4 µL

Supplementary Table 2: Temperature program used for cDNA synthesis.

Operation	Temperature (°C)	Duration
Primer annealing	25	5 min
cDNA synthesis	42	30 min
cDNA synthesis termination	85	5 min
-	4	∞

Supplementary Table 3: Reaction mixture for RT-qPCR.

Component	Per reaction
HOT FirePol EvaGreen qPCR Supermix (Solis BioDyne)	2 µL
Forward primer (10 pmol/µL)*	0.2 µL
Reverse primer(10 pmol/µL)*	0.2 µL
Nuclease-free water	4.6 µL
cDNA template (8ng/µL)	3 µL

* See Supplementary Table 5.

Supplementary Table 4: Temperature program used for RT-qPCR.

Operation	Temperature (°C)	Duration	Cycles
Initial activation	95	12 min	1
Denaturation	95	15 sec	
Annealing	See Supplementary Table X	20 sec	40×
Elongation	72	20 sec	
Final elongation	72	7 min	1
	95	1 min	
Melting curve	45	1 min	1
	60-90(+0.02/sec)	25 min	

Supplementary Table 5: Primers (Solis BioDyne) used for RT-qPCR and their annealing temperature (Tm)

Gene	Forward Primer	Reverse Primer	Tm (°C)
GAPDH	CTTCAACAGCAACTCCCACTCTT	GCCGTATTCATTGTCATACCAGG	60
Doux2	TGTGAATGACGGGTCCAAGT	GGAGGCGAAGACGTACATGA	59
IL-1β	GCAGCTGGAGAGTGTGGAT	AAACTCCACTTTGCTCTTGACTT	61
IL-6	CGTGGAAATGAGAAAAGAGTTGT	AGTGCATCATCGTTGTTCATACA	61
iNOS	GACATTACGACCCCTCCCAC	ACTCTGAGGGCTGACACAAG	62
Lcn-2	CACCACGGACTACAACCAG	TGGTTCTTCCATACAGGGTAAT	59
NOX2	GGGAACTGGGCTGTGAATGA	CAGTGCTGACCCAAGGAGTT	61
Ptgs2	AATATCAGGTCATTGGTGGAGA	TCTACCTGAGTGTCTTTGACTG	61
TNFα	CTGTCTACTGAACTTCGGGGTGAT	GGTCTGGGCCATAGAACTGATG	61

Supplementary Table 6: Reaction mixture for amplicon PCR during library preparation for gene sequencing of 16S rRNA.

Component	Per reaction
5x HOT FIREPol® Blend Master Mix Ready to Load (Solis BioDyne)	5 μL
Forward primer, PRK341F (1 μM)*	0.5 μL
Reverse primer, PRK806R (1 μM)*	0.5 μL
Nuclease-free water	18 μL
Template DNA (0.003-2 ng/μL*)	1 μL

* Forward 5'- CCTACGGGRBGCASCAG-3', reverse 5'- GGACTACYVGGGTATCTAAT-3' [1].

** Measured by Qubit.

Supplementary Table 7: Temperature cycles used for amplicon PCR during library preparation for gene sequencing of 16S rRNA.

Operation	Temperature (°C)	Duration	Cycles
Initial activation	95	15 min	1
Denaturation	95	30 sec	
Annealing	55	30 sec	25/30×
Elongation	72	45 sec	
Final elongation	72	7 min	1
-	4	∞	-

*25 for fecal samples and 30 for colon tissue samples

Supplementary Table 8: Reaction mixture for index PCR during library preparation for gene sequencing of 16S rRNA.

| Component	Per reaction
5x FIREPol® Master Mix Ready to Load (Solis BioDyne)	5 µL
Forward primer (1 µM)*	5 µL
Reverse primer (1 µM)*	5 µL
Nuclease-free water	8 µL
Template DNA	2 µL

* See Supplementary Table 10

Supplementary Table 9: Temperature cycles used for index PCR during library preparation for gene sequencing of 16S rRNA.

Operation	Temperature (°C)	Duration	Cycles
Initial activation	95	5 min	1
Denaturation	95	30 sec	
Annealing	55	1 min	10
Elongation	72	45 sec	
Final elongation	72	7 min	1
-	4	∞	-

Supplementary Table 10: Primers modified with Illumina adapters used for index PCR during library preparation for gene sequencing of 16S rRNA [2]. Unique combination of forward and reverse primer was used for each sample.

Primer name	Sequence, 5' -> 3'	Target region/gene	Direction
F1	aatgatacggcgaccaccgagatctacactctttccctacacgacgctcttccgatctagtcaaCCTACGGGRBGCASCAG	16S rRNA (V3-V4)	Forward
F2	aatgatacggcgaccaccgagatctacactctttccctacacgacgctcttccgatctagttccCCTACGGGRBGCASCAG	16S rRNA (V3-V4)	Forward
F3	aatgatacggcgaccaccgagatctacactctttccctacacgacgctcttccgatctatgtcaCCTACGGGRBGCASCAG	16S rRNA (V3-V4)	Forward
F4	aatgatacggcgaccaccgagatctacactctttccctacacgacgctcttccgatctccgtccCCTACGGGRBGCASCAG	16S rRNA (V3-V4)	Forward
F5	aatgatacggcgaccaccgagatctacactctttccctacacgacgctcttccgatctgtagagCCTACGGGRBGCASCAG	16S rRNA (V3-V4)	Forward
F6	aatgatacggcgaccaccgagatctacactctttccctacacgacgctcttccgatctgtccgcCCTACGGGRBGCASCAG	16S rRNA (V3-V4)	Forward
F7	aatgatacggcgaccaccgagatctacactctttccctacacgacgctcttccgatctgtgaaaCCTACGGGRBGCASCAG	16S rRNA (V3-V4)	Forward

F8	aatgatacggcgaccaccgagatctacactctttccctacacgacgc tcttccgatctgtggccCCTACGGGRBGCASCAG	16S rRNA (V3-V4)	Forwa rd
R1	caagcagaagacggcatacgagatCGTGATgtgactggagttca gacgtgtgctcttccgatctGGACTACYVGGGTATCTAAT	16S rRNA (V3-V4)	Rever se
R2	caagcagaagacggcatacgagatACATCGgtgactggagttca gacgtgtgctcttccgatctGGACTACYVGGGTATCTAAT	16S rRNA (V3-V4)	Rever se
R3	caagcagaagacggcatacgagatGCCTAAgtgactggagttca gacgtgtgctcttccgatctGGACTACYVGGGTATCTAAT	16S rRNA (V3-V4)	Rever se
R4	caagcagaagacggcatacgagatTGGTCAgtgactggagttca gacgtgtgctcttccgatctGGACTACYVGGGTATCTAAT	16S rRNA (V3-V4)	Rever se
R5	caagcagaagacggcatacgagatCACTCTgtgactggagttca gacgtgtgctcttccgatctGGACTACYVGGGTATCTAAT	16S rRNA (V3-V4)	Rever se
R6	caagcagaagacggcatacgagatATTGGCgtgactggagttca gacgtgtgctcttccgatctGGACTACYVGGGTATCTAAT	16S rRNA (V3-V4)	Rever se
R7	caagcagaagacggcatacgagatGATCTGgtgactggagttca gacgtgtgctcttccgatctGGACTACYVGGGTATCTAAT	16S rRNA (V3-V4)	Rever se
R8	caagcagaagacggcatacgagatTCAAGTgtgactggagttca gacgtgtgctcttccgatctGGACTACYVGGGTATCTAAT	16S rRNA (V3-V4)	Rever se
R9	caagcagaagacggcatacgagatCTGATCgtgactggagttca gacgtgtgctcttccgatctGGACTACYVGGGTATCTAAT	16S rRNA (V3-V4)	Rever se
R10	caagcagaagacggcatacgagatAAGCTAgtgactggagttca gacgtgtgctcttccgatctGGACTACYVGGGTATCTAAT	16S rRNA (V3-V4)	Rever se
R11	caagcagaagacggcatacgagatGTAGCCgtgactggagttca gacgtgtgctcttccgatctGGACTACYVGGGTATCTAAT	16S rRNA (V3-V4)	Rever se
R12	caagcagaagacggcatacgagatTACAAGgtgactggagttca gacgtgtgctcttccgatctGGACTACYVGGGTATCTAAT	16S rRNA (V3-V4)	Rever se
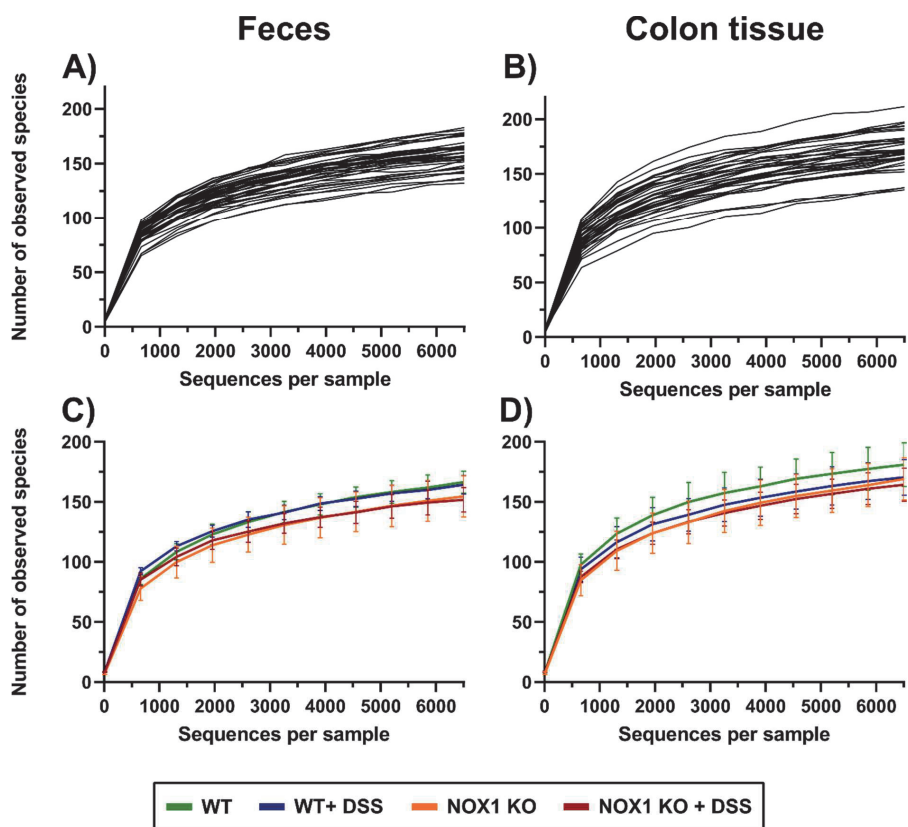
Supplementary Figure 9: Rarefaction curves for the number of observed species (OTUs) in **(A, C)** fecal and **(B, D)** colon tissue samples. (A, B) Shows individual samples while (C, D) shows group mean ± SD for each experimental group for each sequencing depth (10, 659, 1308, 1957, 2606, 3255, 3904, 4553, 5202, 5851 and 6500 sequences per sample). X-axis' show number of sequences per sample and y-axis' show the number of observed species. Based on ten rarefaction iterations

Supplementary References

1.   Yu, Y., C. Lee*, et al.*, Group-specific primer and probe sets to detect methanogenic communities using quantitative real-time polymerase chain reaction*. Biotechnol Bioeng*, **2005**. 89(6): p. 670-9.
2.   Avershina, E., K. Lundgard*, et al.*, Transition from infant- to adult-like gut microbiota*. Environ Microbiol*, **2016**. 18(7): p. 2226-36.

Norwegian University
of Life Sciences